2026

Final Report SPR-FY24(031)

# Characterization of Sediment Loads and Size Distribution in Nebraska Roadway Runoff

**Bruce I. Dvorak, Ph.D.**
Professor
Department of Civil and Environmental Engineering
University of Nebraska-Lincoln

**David M. Admiraal, Ph.D.**
Associate Professor
Department of Civil and Environmental Engineering
University of Nebraska-Lincoln

**Pavel Shrestha**
Graduate Research Assistant
Department of Civil and Environmental Engineering
University of Nebraska-Lincoln

**Nebraska Department of Transportation Research**
Headquarters Address
1400 Nebraska Parkway
Lincoln, NE 68509
ndot.research@nebraska.gov
(402) 479-4697
https://dot.nebraska.gov/business-center/research/

**Nebraska Transportation Center**
262 Prem S. Paul Research Center at Whittier School
2200 Vine Street
Lincoln, NE 68583-0851
(402) 472-1932
http://ntc.unl.edu

This report was funded in part through grant from the U.S. Department of Transportation Federal Highway Administration. The views and opinions of the authors expressed herein do not necessarily state or reflect those of the U.S. Department of Transportation.

# Characterization of Sediment Loads and Size Distribution of Nebraska Roadway Runoff

Bruce I. Dvorak, Ph.D.
Professor
Department of Civil and Environmental Engineering
University of Nebraska-Lincoln

David M. Admiraal, Ph.D.
Associate Professor
Department of Civil and Environmental Engineering
University of Nebraska-Lincoln

Pavel Shrestha
Graduate Research Assistant
Department of Civil and Environmental Engineering
University of Nebraska-Lincoln

Sponsored By

Nebraska Department of Transportation and U.S. Department of Transportation Federal Highway Administration

February 2026

## TECHNICAL REPORT DOCUMENTATION PAGE

| | | |
|---|---|---|
| **1. Report No.**<br>FY24(031) | **2. Government Accession No.** | **3. Recipient's Catalog No.** |
| **4. Title and Subtitle**<br>Characterization Of Sediment Loads and Size Distribution in Nebraska Roadway Runoff | | **5. Report Date**<br>February 2026 |
| | | **6. Performing Organization Code** |
| **7. Author(s)**<br>Bruce I. Dvorak<br>David M. Admiraal<br>Pavel Shrestha | | **8. Performing Organization Report No.** |
| **9. Performing Organization Name and Address**<br>Department of Civil and Environmental Engineering<br>University of Nebraska—Lincoln<br>Lincoln, NE 68588-0531 | | **10. Work Unit No.** |
| | | **11. Contract**<br>FY24(031) |
| **12. Sponsoring Agency Name and Address**<br>Nebraska Department of Transportation<br>Research Section<br>1400 Hwy 2<br>Lincoln, NE 68502 | | **13. Type of Report and Period Covered**<br>Final Report<br>July 2023 – October 2025 |
| | | **14. Sponsoring Agency Code** |
| **15. Supplementary Notes** | | |

**16. Abstract**

The Nebraska Department of Transportation (NDOT) must manage sediment, and pollutant loads from roadway runoff to meet stormwater regulations. The SAFL Baffle, a hydrodynamic separator used by NDOT, depends on reliable estimates of total suspended solids (TSS) and particle size distribution (PSD). However, limited data exists for Nebraska roadways. In this study stormwater runoff was monitored at four NDOT-maintained sites, two in Lincoln and two in Beatrice, over 1.5 years to characterize TSS and PSD and to evaluate SAFL Baffle performance using the SHSAM model. Results showed large variability across sites and seasons. Median TSS ranged from 158 to 580 mg/L, and median particle size (d50) from 16 to 322 µm. Finer particles dominated at most sites, likely due to runoff from gravel or exposed soils off the roadway and especially outside of the NDOT right of way. Higher TSS in spring was observed and reflected low vegetation cover and winter sediment buildup. SHSAM modeling showed that the SAFL Baffle alone may not achieve 80 percent TSS removal, as it is less effective for fine particles. However, if off-site sediment loads are credited toward compliance, performance goals could be met. The study highlights the need for local sediment data and for accounting for off-site sources in NDOT stormwater design.

| | | | |
|---|---|---|---|
| **17. Key Words** | | **18. Distribution Statement**<br>No restrictions. This document is available through the National Technical Information Service.<br>5285 Port Royal Road<br>Springfield, VA 22161 | |
| **19. Security Classification (of this report)**<br>Unclassified | **20. Security Classification (of this page)**<br>Unclassified | **21. No. of Pages**<br>228 | **22. Price** |

**Form DOT F 1700.7** (8-72) Reproduction of completed page authorized

Table of Contents

# List of Tables

## List of Figures

# List of Acronyms

- AADT – Average Annual Daily Traffic
- ADP – Antecedent Dry Period
- APHA – American Public Health Association
- ASTM – American Society for Testing and Materials
- AV – Area-Velocity (flow module)
- BMP – Best Management Practice
- BS – Beal Slough (site code)
- BTN – Beatrice North (site code)
- BTW – Beatrice West (site code)
- CH – Cornhusker (site code)
- CN – Curve Number
- CWA – Clean Water Act
- DEM – Digital Elevation Model
- EMC – Event Mean Concentration
- EPA – Environmental Protection Agency
- GIS – Geographic Information System
- HEC-HMS – Hydrologic Engineering Center – Hydrologic Modeling System
- HEC-RAS – Hydrologic Engineering Center – River Analysis System
- HSG – Hydrologic Soil Group
- ISCO – Teledyne ISCO (samplers/AV modules)
- MnDOT – Minnesota Department of Transportation
- MPCA – Minnesota Pollution Control Agency
- MS4 – Municipal Separate Storm Sewer System

- NDEE – Nebraska Department of Environment and Energy
- NDOT – Nebraska Department of Transportation
- NE – Nebraska
- NJCAT – New Jersey Corporation for Advanced Technology
- NOAA – National Oceanic and Atmospheric Administration
- NPDES – National Pollutant Discharge Elimination System
- NRCS – Natural Resources Conservation Service
- NWS – National Weather Service
- PSD – Particle Size Distribution
- ROW – Right-of-Way
- SAFL – St. Anthony Falls Laboratory
- SCS – Soil Conservation Service (former name of NRCS)
- SHSAM – Sizing Hydrodynamic Separators and Manholes (model)
- SOP – Standard Operating Procedure
- SSC – Suspended Sediment Concentration
- STF – Stormwater Treatment Facility
- TMDL – Total Maximum Daily Load
- TSS – Total Suspended Solids
- ULM – Universal Liquid Module (laser diffraction)
- USDA – United States Department of Agriculture
- VIF – Variance Inflation Factor
- WQV – Water Quality Volume

# Disclaimer

The contents of this report reflect the views of the authors, who are responsible for the facts and the accuracy of the information presented herein. The contents do not necessarily reflect the official views or policies neither of the Nebraska Department of Transportations nor the University of Nebraska-Lincoln. This report does not constitute a standard, specification, or regulation. Trade or manufacturers' names, which may appear in this report, are cited only because they are considered essential to the objectives of the report.

The United States (U.S.) government and the State of Nebraska do not endorse products or manufacturers. This material is based upon work supported by the Federal Highway Administration under SPR-FY24(031). Any opinions, findings and conclusions or recommendations expressed in this publication are those of the author(s) and do not necessarily reflect the views of the Federal Highway Administration.

This report has been reviewed by the Nebraska Transportation Center for grammar and context, formatting, and compliance with Section 508 of the Rehabilitation Act of 1973.

# Abstract

The Nebraska Department of Transportation (NDOT) is required to manage sediment and pollutant loads from roadway runoff to comply with stormwater regulations for discharges into impaired waters. The SAFL Baffle, a hydrodynamic separator used by NDOT, relies on accurate estimates of total suspended solids (TSS) and particle size distribution (PSD). However, existing studies show wide variability in these sediment characteristics, limiting their applicability to Nebraska roadways.

This study addresses this gap by monitoring stormwater runoff at four historically NDOT-maintained sites, with two located in Lincoln and two in Beatrice, over a 1.5-year period. These sites received significant runoff from areas outside the roadway right-of-way, which is typical of many NDOT roadway catchments. The SAFL Baffle was evaluated at each site using the SHSAM (Sizing Hydrodynamic Separators and Manholes) model, following NDOT permit requirements.

Results showed high variability in sediment characteristics across both sites and seasons. Median TSS concentrations ranged from 158 mg/L to 580 mg/L, while median particle size (d50) varied widely, from 16 to 322 µm. Three sites had a higher fraction of finer particles compared to other studies on roadway runoff. Gravel surfaces and exposed soils, often outside the NDOT right-of-way, contributed to increased fine sediment loads, while coarse sediment at one site was linked to impervious cover and steeper roadway slope. Seasonality was observed at all sites, with higher TSS concentrations in spring, which could be explained by slow vegetation development and sediment accumulation from winter applications.

Modeling in SHSAM indicated that the SAFL Baffle alone is unlikely to achieve the 80% TSS removal target due to limited efficiency in capturing fine particles for any of the four sites. However, a substantial portion of sediment originated from off-site areas. If off-site treatment is credited toward compliance under NDOT’s permit, the SAFL Baffle could meet performance goals in many cases. These findings highlight the need for region-specific sediment data and consideration of off-site contributions when designing best management practices for Nebraska roadway runoff.

# Chapter 1 Introduction

## 1.1 Background

Stormwater runoff is a primary pathway through which sediment and associated pollutants are transported into receiving water bodies, leading to harmful effects on aquatic ecosystems. Sediment transport in runoff contributes to elevated turbidity, which reduces light penetration, lowers dissolved oxygen levels, and ultimately degrades aquatic habitat (Zhang et al. 2013). Urban impervious surfaces, such as highways, parking lots, and rooftops, are major sources of pollutants, and total suspended solids (TSS) often carry attached contaminants, including nutrients, metals, and hydrocarbons (Beck and Birch 2011).

To mitigate these impacts, stormwater discharges from roadways and other urban infrastructure are regulated under the National Pollutant Discharge Elimination System (NPDES), authorized under the Clean Water Act (U.S. EPA 1972). The Nebraska Department of Transportation (NDOT) is required to follow Municipal Separate Storm Sewer System (MS4) regulations enforced by the Nebraska Department of Environment and Energy (NDEE) (NDOT 2024). These requirements include the implementation of best management practices (BMPs) to reduce pollutant loads from construction and post-construction runoff, particularly for projects discharging to impaired waters identified under Section 303(d) of the Clean Water Act.

Among structural BMPs, a specific type of inline hydrodynamic separator developed at the University of Minnesota known as the St. Anthony Falls Laboratory (SAFL) Baffle has been used by NDOT due to its space efficiency and cost-effectiveness (Minnesota DNR 2023; Upstream Technologies 2016). However, the performance and sizing of the SAFL Baffle are sensitive to sediment characteristics in the runoff, particularly total suspended solids (TSS) concentration and particle size distribution (PSD). For effective and economical implementation, accurate TSS and PSD data are needed that often vary by region and are influenced by local site conditions.

## 1.2 Purpose for the study

Although numerous studies have examined sediment characteristics in roadway stormwater runoff, the reported values of TSS and PSD vary significantly. This variation reflects differences in climate, catchment characteristics, traffic patterns, off-site contributions, and sampling methods. As a result, the applicability of such datasets for designing BMPs in a specific region or location is limited. In Nebraska, no known studies have quantified sediment characteristics from roadway runoff, posing challenges for accurately sizing and evaluating the performance of BMPs under local conditions.

This study seeks to address that gap by collecting sediment data and identifying potential sources at selected sites representative of NDOT-maintained roadway catchments. The goal is to provide reliable TSS and PSD measurements and to explore how these parameters can be predicted based on specific site conditions. These findings aim to support the design and evaluate the suitability of stormwater treatment systems such as the SAFL Baffle under Nebraska-specific conditions.

## 1.3 Objectives

The primary objective of this study is to characterize sediment in stormwater runoff from roadway catchments maintained by the NDOT. To achieve this, stormwater samples were collected and analyzed over a period of approximately 1.5 years across multiple sites representing varied land use characteristics.

Specifically, the study aims to:

1. Develop a thorough understanding of existing roadway sediment runoff data including concentrations and sediment distributions,

2. Establish a rigorous and defensible methodology for collecting roadway runoff sediment data that is representative of MS4 communities in Nebraska,
3. Collect a complete set of roadway sediment runoff data for a two-year period that includes multiple seasons, and
4. Produce a model and guidelines for extending the data to represent MS4 communities throughout Nebraska.

## 1.4 Report Overview:

This report presents the findings of a collaborative research effort between the University of Nebraska–Lincoln Civil Engineering Department and the NDOT. The study focuses on the characterization of sediment loads and particle size distributions in Nebraska roadway runoff. The report is organized into seven chapters and multiple appendices. Chapter 2 presents a review of relevant studies on sediment characterization. Chapter 3 describes the study sites and outlines regulatory requirements. Chapter 4 details the methods used for field monitoring, sampling, and laboratory analysis. Chapter 5 summarizes the results and discusses trends in sediment characteristics and the performance of the SAFL Baffle at the monitored sites. Chapter 6 provides recommendations for SAFL Baffle sizing, and Chapter 7 presents the conclusions of the study.

# Chapter 2 Literature Review

## 2.1 Introduction

This chapter introduces key concepts and reviews previous research related to stormwater runoff and sediment characterization. It introduces important terms and concepts relevant to understanding sediment behavior in runoff. Sampling and laboratory methods used in previous studies are discussed, followed by a summary of reported sediment concentrations and particle size distributions across different land uses. Lastly, key factors influencing TSS and PSD are highlighted, providing context for the present study.

## 2.2 Key Stormwater Quality Concepts

This section defines key concepts relevant to this report.

### *2.2.1 Total suspended solids*

TSS refers to the dry weight of suspended particles in a sample per unit volume, both organic and inorganic particles that are not dissolved in water. These particles originate from many sources, including erosion, particles deposited on impervious surfaces by vehicles, and atmospheric deposition, which are transportable by water. TSS provides a medium for transport and storage of other pollutants and disturbs aquatic ecosystems (U.S. EPA 1999; Minnesota Pollution Control Agency 2023).

TSS is a key indicator in stormwater analysis because many pollutants, such as heavy metals and nutrients, attach to these particles (Yan et al. 2024), making TSS a practical measure of overall water quality. However, measuring TSS can be challenging. Sampling methods and laboratory methods may not capture all particle sizes, as explained in more detail in Section 2.4 (Selbig and Bannerman 2011; ASTM 2013).

### *2.2.2 Particle size distribution*

PSD refers to a list of values or a mathematical function that defines the relative amount, typically by mass, of particles present according to size (Jillavenkatesa et al. 2001). Particle size distribution can be represented either as percent finer by particle size or as mass fraction across different size ranges, as shown in Figure 2.1. In this report, particle size is represented by percentage finer for a range of sediment sizes.

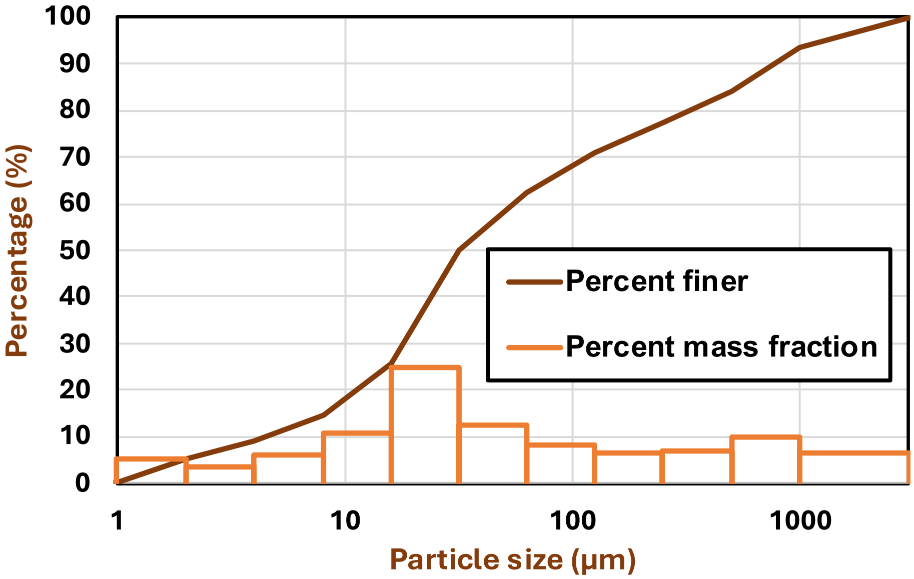

Figure 2.1 Method of representing particle size distribution

Alongside TSS, PSD is a critical factor in sediment characterization, particularly when designing best management practices (BMPs). Fine and coarse particles differ in their physical properties, which influences how they interact with various BMPs. Coarse particles are more effectively captured by sumps or hydrodynamic separators compared to fine particles (Andral et al. 1999). Furthermore, fine particles, especially those smaller than 63 µm, have been found to carry higher concentrations of pollutants compared to coarse particles (Hilliges et al. 2016).

### *2.2.3 Event Mean Concentration*

The event mean concentration (EMC) is defined as “the total constituent mass discharge divided by the total runoff volume” (U.S. EPA 1983). It is a flow-weighted average concentration of a pollutant during a storm event, given by Equation 2.1. Figure 2.2 illustrates a conceptual hydrograph used to calculate EMC, showing discharge volume and pollutant concentration at different time intervals. If the time intervals are equal, the method is referred to as time-paced sampling; if the discharge volumes between samples are equal, it is called flow-weighted sampling.

$$Event\ mean\ concentration\ (EMC) = \frac{\Sigma(C_i.V_i)}{\Sigma V_i} \qquad (2.1)$$

where:

$C_i$ = Concentration at time step, $t_i$ (mg/L)

$V_i$= Discharge volume during time step, $t_i$ (L)

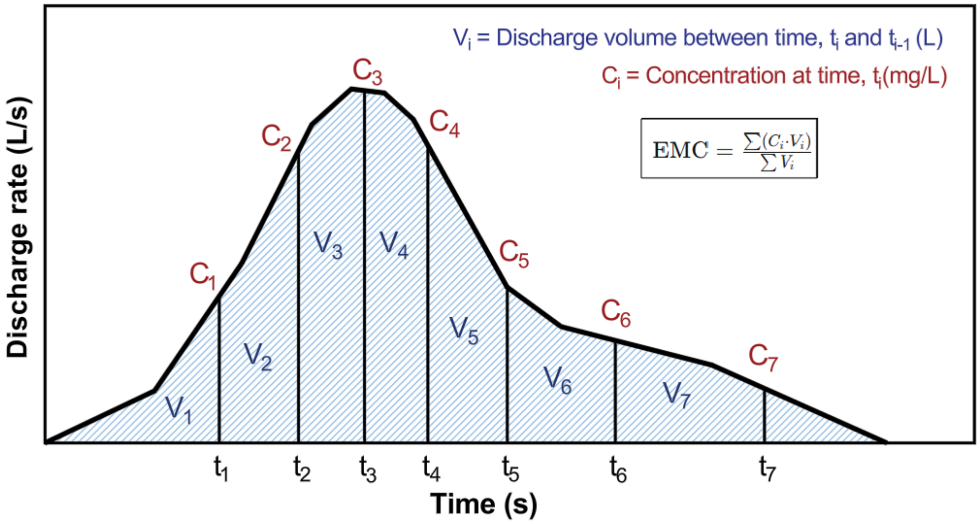

Figure 2.2 Conceptual hydrograph showing discharge volume and concentration between different time intervals

### *2.2.4 First flush*

The “first flush” phenomenon, originally defined by Thornton and Saul (1986), refers to the initial portion of stormwater runoff during a rainfall event that carries a higher concentration of pollutants compared to the later stages of runoff (Gupta and Saul 1996). This occurs because pollutants such as sediments accumulate on impervious surfaces during dry periods and are rapidly washed off at the onset of rainfall. Another way to define first flush is through the relationship between the percentage of total pollutant load and the percentage of cumulative runoff volume. As shown in Figure 2.3, when the cumulative load rises more steeply than a 45° reference line at the beginning of the event, this portion is identified as the first flush (Gupta and Saul 1996). The 45° line represents the condition where the concentration of pollutants remains constant throughout the storm event. The percentage deviation of the cumulative load curve from the 45° line is used to measure the strength of first flush.

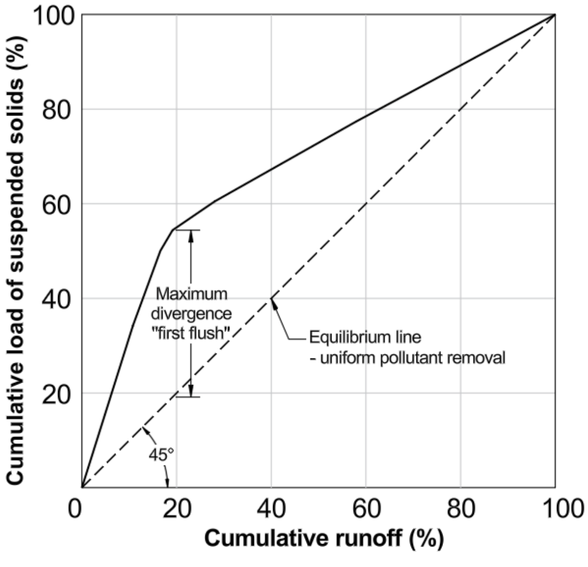

Figure 2.3 First flush shown as the difference between cumulative load and cumulative runoff (Gupta and Saul 1996)

## 2.3 Best management practices

Best management practices (BMPs) are strategies and systems designed to manage stormwater runoff, aiming to improve water quality by reducing pollutant loads (U.S. EPA, 2004). BMPs can be categorized into non-structural and structural types.

### *2.3.1 Non-structural best management practices*

The non-structural BMPs require little to no construction and focus on preventing the generation and transport of pollutants into stormwater systems (U.S. EPA 2004). These practices often involve policy, education and maintenance strategies. Examples include policies and ordinances, protection of sensitive areas, and maintaining and increasing open spaces along water bodies (NDOT 2024).

### *2.3.2 Structural best management practices*

Structural BMPs involve physical construction of devices and structures that aim to reduce and control pollutant loads in stormwater (U.S. EPA 2004). Examples of structural BMPs include detention ponds, infiltration basins, bioretention cells, and hydrodynamic separators.

### *2.3.3 SAFL Baffle and SHSAM*

The SAFL Baffle, as shown in Figure 2.4 is a specific type of hydrodynamic separator that fits into sump manholes to capture sediment, especially coarse sediment, through settling while preventing resuspension during high flow events. It enhances the performance of a standard sump by minimizing sediment washout and increasing sediment retention during storm events. It is a patented stormwater pretreatment device developed by the University of Minnesota’s St. Anthony Falls Laboratory (Minnesota DNR 2023; Upstream Technologies 2019).

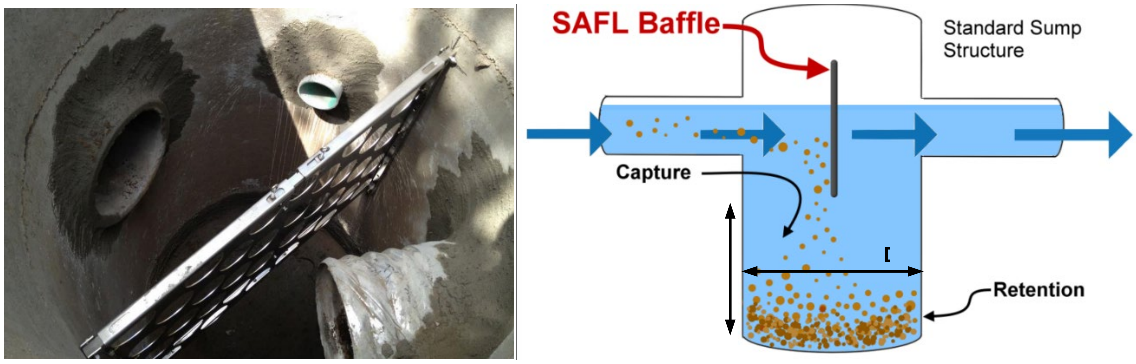

Figure 2.4 (a) SAFL Baffle installed within a sump manhole (b) Schematic view of the operation of the SAFL Baffle. *Source: Adapted from Upstream Technologies 2019*

The SHSAM (Sizing Hydrodynamic Separators and Manholes) software is a tool designed to estimate the TSS removal efficiency of stormwater treatment devices, including the SAFL Baffle. The software simulates seven different sump manhole models of various sizes for designing the SAFL Baffle, as listed in Table 2.1. It enables engineers to model various configurations by inputting site-specific parameters such as sump dimensions, watershed parameters, rainfall data, and sediment characteristics (Upstream Technologies 2016).

Table 2.1 Available sump manhole sizes in SHSAM for SAFL Baffle modeling

| Model | Sump diameter | | Sump height | |
|---|---|---|---|---|
| | ft | m | ft | m |
| 42 | 4 | 1.22 | 2 | 0.61 |
| 44 | 4 | 1.22 | 4 | 1.22 |
| 55 | 5 | 1.52 | 5 | 1.52 |
| 63 | 6 | 1.83 | 3 | 0.91 |
| 66 | 6 | 1.83 | 6 | 1.83 |
| 86 | 8 | 2.44 | 6 | 1.83 |
| 106 | 10 | 3.05 | 6 | 1.83 |

### 2.4 Method of sample collection

Different sampling methods have been used in past studies to measure sediment in stormwater runoff, depending on site conditions and study goals. Flow-paced sampling and time-paced sampling, mentioned in Section 2.2.3, are the common methods of automatic sampling using equipment like ISCO samplers. In flow-paced automatic sampling, samples are collected based on equal volume of runoff (Winston et al. 2019; Gorska et al., 2020). Time-paced sampling, where samples are taken at regular time intervals, has also been used, especially during early storm periods when changes happen quickly (Huang et al. 2007). Grab sampling, which involves collecting water manually, has been used either during dry weather conditions (Characklis and Wiesner 1997; Beck and Birch, 2012) or along with automatic samplers during storm events (Charters et al. 2015). While flow-paced composite sampling is preferred for estimating TSS loads, automatic samplers often under-represent larger particles like gravel or debris, since heavier particles stay near the bottom of pipes (Selbig and Bannerman 2011; Sandoval and Bertrand-Krajewski 2016). Some studies have addressed this by using mesh filters (Winston and Hunt 2017) or depth-integrated samplers (Selbig and Bannerman 2011). Overall, flow-paced automatic sampling remains the most widely used and practical method for TSS monitoring in stormwater studies.

Flow has been measured using weirs (Hathaway and Hunt 2011) or sensors like AV (area and velocity) modules and bubblers (Poudel et al. 2010). AV sensors estimate flow by combining water level and velocity measurements, typically using Doppler technology. Bubblers measure water depth through air pressure and are particularly useful in silty or debris-prone environments (Teledyne ISCO 2013). Other common methods, such as weirs and flumes, rely on established level–discharge relationships but require stable hydraulic conditions and are often unsuitable for retrofitting in existing systems. In partially full pipes, AV modules are generally preferred, as installing weirs or flumes in such configurations is often impractical.

## 2.5 Laboratory techniques or methods

TSS analysis in past studies has commonly followed gravimetric procedures outlined in APHA Standard Method 2540D, which involves filtering a known volume of water through a glass fiber filter and drying it to determine the mass of suspended solids (Characklis and Wiesner 1997; Hathaway and Hunt, 2011; Winston et al., 2019). Filter pore sizes used across studies vary, with most ranging from 0.45 µm to 1.5 µm (Beck and Birch 2012; Nayeb Yazdi et al. 2021). While this method is widely used, it may underestimate solids if larger particles are removed or if only a portion of the sample is filtered (Karamalegos et al. 2005; Nayeb Yazdi et al. 2021). Alternatively, ASTM Method D3977-97 recommends measuring Suspended Sediment Concentration (SSC) using the entire unfiltered sample, allowing both fine and coarse particles to be included (Pitt et al. 2017). Both TSS and SSC analysis methods involve collecting a water sample of known volume and filtering it through a glass fiber filter paper. The filter is dried and weighed before and after filtration, with drying typically done at around 105°C until a constant weight is reached. The concentration of solids is then calculated and reported in milligrams per liter (mg/L). The main difference between the two methods is that SSC uses the entire collected sample, while TSS analysis typically uses only a small subsample (APHA 2540D 2022; ASTM D3977-97 2013). SSC is generally preferred in stormwater studies, especially runoff with larger sediments, as it provides a more complete estimate of sediment load for BMP design.

Various methods have been employed across studies to analyze particle size distribution in stormwater runoff. Laser diffraction was commonly used, with some studies analyzing the full sample directly (Charters et al. 2015; Winston et al. 2023; Lin et al. 2009). Others separated coarse and fine fractions prior to analysis. For example, Kim and Sansalone (2008) distinguished coarse particles using sieve classes and fine particles using laser diffraction, with a 75 µm cutoff. Similarly, Mrowiec (2020) and Selbig and Bannerman (2011) applied cutoffs at 63 µm and 32 µm, respectively, using laser diffraction for finer fractions. Jartun et al. (2008) analyzed dried samples using laser diffraction, while Li et al. (2005) used light scattering techniques.

### 2.6 Previous studies on Sediment characteristics

This section summarizes findings from previous studies on TSS and PSD values across various land use types, as defined in Sections 2.2.1 and 2.2.2.

TSS concentrations in stormwater runoff vary widely across studies, depending on land use type. Studies focused on highway or roadway runoff reported TSS concentrations ranging from 35 to 400 mg/L (Charters et al. 2015; Furumai et al. 2002; Huang et al. 2007; Kayhanian et al. 2007; Kayhanian et al. 2012; Mrowiec 2020; Winston et al. 2023). In catchments with mixed land uses, reported TSS values ranged from 40 to 1089 mg/L (Gorska et al. 2020; Hathaway and Hunt 2011; Huang et al. 2007; Yan et al. 2024). Roof runoff showed variable results, with TSS concentrations ranging from 78 to 107 mg/L in one study (Mrowiec 2020), while Charters et al. (2015) reported much lower values between 3.3 and 4.1 mg/L. Similarly, studies on parking lots found TSS concentrations between 42 and 233 mg/L (Mrowiec 2020; Neary et al. 2012). TSS concentrations in rural or undeveloped watersheds ranged from 30 to 87 mg/L (Graczyk et al. 2011; Poudel et al. 2010), though Poudel et al. (2010) also observed that some agricultural fields exhibited high erosion potential, with TSS levels reaching up to 1845 mg/L.

PSD shows a broad range of values, as indicated by the d90 (µm), d50 (µm), and d10 (µm) parameters from multiple sources in Table 2.2. The d50 parameter represents the median particle size, with 50% of particles finer than this size. Similarly, d10 and d90 indicate the sizes below which 10% and 90% of particles are finer, respectively. These PSD parameters are presented in the table alongside roadway type and Annual Average Daily Traffic (AADT), defined as the average number of vehicles using a roadway per day over a year. Likewise, the PSD data included in SHSAM also reflects a wide distribution, as shown in Table 2.3.

Table 2.2 Particle size distribution parameters from previous studies

| **Study** | **d90 (µm)** | **d50 (µm)** | **d10 (µm)** | **Site characteristics** | **AADT** |
|---|---|---|---|---|---|
| Charters et al., 2015 | 177 | 72 | 23 | Asphalt road | 11,000 |
| Kayhanian et al., 2012 | 125 - 250 | < 38 | - | Interstates/ highways | 5,000 - 130,000 |
| Lin et al., 2009 | 2000 | 600 | 100 | Highway | ~100,000 |
| Lin et al., 2009 | 500 | 200 - 250 | 80 | Highway | ~80,000 |
| Mrowiec 2020 | 1000 | 130 - 180 | 8 | Freeways | 23,000 - 55,000 |
| Mrowiec 2020 | 1000 | 100 | 8 | Local streets | 4,000 |
| Sansalone et al., 1998 | 3500 | 555 | 117 | Interstate | - |
| Selbig and Bannerman, 2011 | 400 | 50 | 2 | Parking | - |
| Selbig and Bannerman, 2011 | 300 | 70 | 2 | Collector | - |
| Selbig and Bannerman, 2011 | 500 | 200 | 2 | Feeder | - |
| Selbig and Bannerman, 2011 | 300 | 100 | 5 | Arterial | - |
| Selbig and Bannerman, 2011 | 200 | 50 | 1 | Mixed use | - |
| Winston et al., 2023 | 145 | 53 | 22 | Interstates/ highways | 7,000 - 131,000 |
| Yan et al. 2024 | 500 | 80 | 10 | Paved residential | - |
| Yan et al. 2024 | 500 | 55 | 5 | Gravel residential | - |
| Yan et al. 2024 | 500 | 32 | 2 | Roads | - |
| Yan et al. 2024 | 450 | 42 | 5 | Mixed use | - |

Table 2.3 Particle size distribution parameters provided in SHSAM

| PSD | Source | d90 (µm) | d50 (µm) | d10 (µm) | Description |
|---|---|---|---|---|---|
| NURP | U.S. EPA 1983 | 90 | 8 | 2 | Based on a combination of data from 28 catch basins around US |
| NJCAT-PSD | NJCAT 2023 | 250 | 67 | 4 | Prepared by NJDEP to test treatment devices |
| Janna-Omid | Mohseni, pers. comm. 2024 | 250 | 135 | 34 | PSD developed at Barr Engineering based on their judgement and experience |
| OK 110 | Minnesota P.C.A | 142 | 116 | 92 | Commercial PSD |
| MnDOT Road Sand | Mohseni, pers. comm. 2024 | 300 | 345 | 273 | Particles encountered by MnDOT during cleaning of roads |

## 2.7 Review of factors affecting sediment characteristics

Sediment characteristics in urban stormwater are influenced by a combination of environmental and anthropogenic factors. Among the most studied are rainfall characteristics and land use type, which directly influence detachment and mobilization. These factors often interact in complex ways, leading to high variability in the type and amount of sediment found at different sites. However, fully understanding sediment behavior also requires consideration of other factors that may be just as important.

### *2.7.1 Impact of rainfall characteristics on sediment properties*

Rainfall characteristics play an important role in shaping both the concentration of TSS and the PSD in urban stormwater runoff. High-intensity storms, especially those with peak 5-minute intensities exceeding 20 mm/h, have been shown to trigger first-flush effects (Li et al. 2015), and sharp TSS peaks are frequently observed following intense rainfall (Murphy et al. 2015a; Zhang et al. 2015), but the relationship is not always straightforward. For example, Farmer (2017) conducted a stormwater monitoring study in a watershed to examine how rainfall and land cover influence TSS during storm events. The study found that rainfall intensity was the strongest predictor of TSS in tributary areas, whereas total rainfall depth was more influential at mainstem sites. In contrast, Schiff et al. (2016) showed that higher rainfall intensity was associated with lower event mean concentrations, as larger volumes of water reduced the overall concentration of pollutants in the runoff. Many studies report that a longer antecedent dry period (ADP) allows more solids to accumulate, increasing TSS when rainfall resumes (Li et al. 2015; Yan et al. 2024). But studies (Li et al. 2008; Barret 1995) observed that TSS concentrations decreased with increasing ADP which was attributed to vehicle-induced pollutant removal, where passing vehicles gradually displaced sediment from road surfaces during dry periods. ADP also influences the PSD by allowing finer particles to settle on surfaces, which are then mobilized during runoff, with their transport behavior strongly influenced by flow intensity (Sansalone et al., 1998). While some studies report that higher rainfall intensity primarily mobilizes finer particles (Zhao et al. 2022), others have observed that a greater proportion of coarse particles can also be transported during high-intensity events, especially when combined with longer durations (Yan et al. 2024). These conflicting results highlight that rainfall's effects on sediment quantity and quality vary widely and often depend on interactions among rainfall parameters, land cover, and site-specific conditions (Yan et al. 2024).

### *2.7.2 Effects of land use type on sediment characteristics*

Land use plays a major role in determining the quantity and characteristics of sediment in stormwater runoff. Urban areas tend to produce the highest TSS concentrations due to impervious surfaces, traffic, and construction, while rural areas generally show lower levels, with occasional spikes from agricultural erosion (Mallin et al., 2008; Coulter et al., 2004). Sub-urban or mixed-use zones typically exhibit TSS levels between those of urban and rural areas. However, a global meta-analysis of 360 urban catchments by Simpson et al. (2022) found no consistent differences in TSS across land use and land cover classification types, attributing the variation instead to other factors. PSD also varies with land use: low-density residential roads tend to produce coarser particles than high-density residential, commercial, or agricultural areas (Winston et al. 2019). Paved residential and commercial areas often yield coarser sediment than gravel roads or mixed-use surfaces (Yan et al. 2024). Still, high variability within the same land use category suggests that relying on a single representative PSD may not always be appropriate (Mrowiec 2020; Selbig et al. 2016).

Beyond land use classification, surface conditions within those areas further influence sediment behavior. Bare soil areas—even when limited to about 10% of a catchment—can significantly increase TSS loads during rainfall events, with finer particles making up more than half of the sediment mobilized (Brodie & Young 2007). Some construction sites have been shown to exceed 1000 mg/L TSS (Minnesota Pollution Control Agency n.d.). In contrast, vegetated surfaces help reduce sediment transport. Grass-lined channels and filter strips along highways have shown TSS removal rates up to 91% (Characklis & Wiesner 1997; Barrett et al. 2004). Similarly, Li et al. (2008) found that vegetated roadsides with over 90% grass cover effectively removed most TSS and metals within 4 m of the pavement edge. Even the type of paved surface plays a role—concrete roads were found to produce higher suspended solids and coarser particles during the early stages of runoff compared to asphalt surfaces (Kim et al. 2021). While these findings illustrate that land use and surface conditions are major contributors, other site-specific factors—such as traffic patterns, road slope, and seasonal variation—further complicate the behavior of sediment in urban runoff.

### *2.7.3 Other factors that influence sediment behavior in stormwater runoff*

Seasonal changes affect both TSS concentrations and PSD. Storm events in spring and summer often result in higher TSS levels, attributed to factors such as salt residue from winter deicing, reduced vegetation cover in early spring, and more intense summer rainfall (Smith et al. 2020; Yan et al. 2024). PSD also shifts with the seasons—coarser particles are typically observed in summer, while spring and fall tend to produce finer sediment fractions, possibly due to changes in rainfall energy and the effectiveness of street sweeping (Winston et al. 2019; Niu et al. 2019; Yan et al. 2024). These patterns highlight the importance of considering temporal variability when interpreting water quality data or designing control measures.

Traffic volume, expressed as Average Annual Daily Traffic (AADT), is another key factor influencing sediment characteristics in roadway runoff. Several studies have observed that TSS concentrations increase with AADT, with high-traffic roads producing significantly more solids than low-traffic roads (Winston et al. 2023; Kayhanian 2007; Mrowiec et al. 2020). Some studies observed that roads with very high AADT tend to yield finer particles, possibly due to increased movement of lighter vehicles (Lin et al. 2009; Winston et al. 2023). In contrast, moderate AADT ranges have been associated with coarser particles, likely due to the influence of heavy vehicle abrasion (Mrowiec 2020). However, not all studies agree—some report no consistent relationship between traffic volume and PSD (Winston & Hunt 2017), indicating that traffic interacts with other conditions. For example: topographic slope is one such factor that contributes to variability in sediment transport. On unpaved roads, steeper slopes have been shown to increase both sediment yield and the proportion of coarse particles due to greater runoff velocity and shear stress (Macdonald et al. 2001; Bilby et al. 1989).

Sampling methods can also influence the observed characteristics of stormwater sediment. Auto-samplers, which are now widely used, tend to capture finer and more consistent PSDs compared to grab or vacuum sampling, which often collect coarser material (Winston et al.

2019). Direct sediment collection from road surfaces or sedimentation basins has also been shown to yield coarser particles (Lin et al. 2009; Sansalone et al. 1998; Jartun et al. 2008).

TSS and PSD in stormwater runoff result from complex interaction of rainfall, land use, surface conditions, traffic flow, seasonality, and sampling methods. Recognizing these influences is crucial for interpreting monitoring data and designing site-specific stormwater treatment facilities.

### 2.8 Knowledge gap and research need

Numerous studies have reported high variability in both TSS and PSD, due to a range of environmental and site-specific factors. This variability, combined with the lack of sediment studies conducted specifically in Nebraska for both roadway-only sites as well as sites with combined right-of-way, roadway, and nearby outside of the right-of-way contributions, limits the applicability of existing data to Nebraska highway catchments. Applying external data may lead to either over-design or under-design of BMPs, potentially affecting their performance and cost-effectiveness. To address this gap, the following chapters present 1.5 years of field monitoring and offer recommendations for selecting representative TSS and PSD values to support BMP design specific to Nebraska conditions.

# Chapter 3 Site Description and Regulatory Background

## 3.1 Introduction

This chapter provides an overview of the study sites and the regulatory context relevant to stormwater treatment in Nebraska. It begins with the criteria used for selecting the four monitoring locations and presents detailed characteristics of each site, including drainage area, land use, roadway features, and hydrologic conditions. The chapter also includes supporting maps and data used to estimate flow paths and catchment boundaries. Finally, it explains important permit requirements used to evaluate stormwater treatment facilities (STFs) in this study.

## 3.2 Study Site Selection

The study sites were selected based on several criteria to ensure reliable data collection and analysis. First, all sites should be located within the thirteen regulated MS4 districts in Nebraska. Second, each site should include a highway or roadway maintained by the NDOT within its drainage area, focusing on sediment contributions from the roadway and the surrounding infrastructure. To allow effective monitoring, the selected sites should have a drainage area size that can generate measurable water flow and sediment runoff. Another key requirement was that the sites should discharge into a natural stream or waterway. Lastly, accessible storm sewer outlets free from excessive sediment buildup, steep slopes, or structural irregularities were selected to ensure convenient and consistent sampling.

Efforts were made to identify sites that met the above criteria. After an extensive review of possible sites using as-builts, Google Maps, and site visits, four sites were selected and are described subsequently. During this process, numerous candidate sites within MS4 communities were examined. Among those with multiple storm inlets, nearly all were found to receive a significant portion of runoff from areas outside the NDOT right-of-way. Thus, it is expected that many NDOT roadways receive significant stormwater contributions runoff and sediment from outside of the NDOT right-of-way.

### 3.3 Site Characteristics

Figure 3.1 shows the four monitoring sites selected to sample TSS and PSD for the study, with two located in Lincoln and two in Beatrice, Nebraska. In Lincoln, one site was along Cornhusker Highway and discharged into Deadman's Run, while the other was on N 14th Street and drained into Beal Slough. The two Beatrice sites were positioned on opposite sides of Highway 77 as shown in Figure 3.1. These locations represent busy roadways with flat to gently sloping terrain, along with adjacent areas that are primarily commercial development. Throughout the study period, the drainage areas at all four sites remained undisturbed, with no construction activity, grading, or intentional clearing of vegetation. Detailed characteristics of sites shown in Table 3.1 and a more detailed description of each site is provided subsequently. HEC-HMS modeling was also conducted for each site to estimate catchment response; input details and simulation results are provided in Appendix A: HEC-HMS analysis of all four sites.

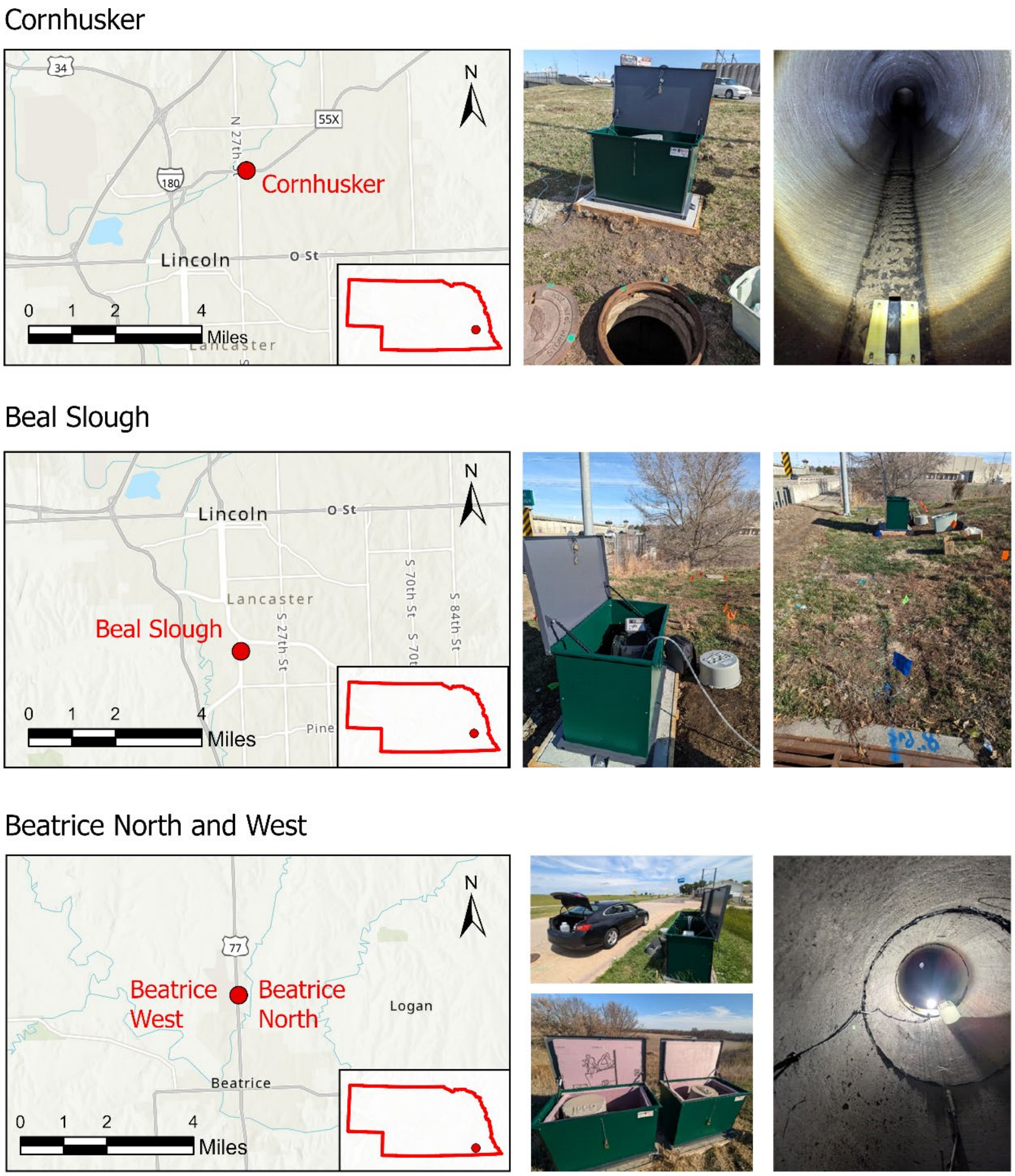

Figure 3.1 Sampling sites in Nebraska

Table 3.1 Comparison of site characteristics

| **Description** | **Beal Slough** | **Beatrice West** | **Cornhusker** | **Beatrice North** |
|---|---|---|---|---|
| Latitude, longitude | 40.7674, -96.7013 | 40.2973, -96.7464 | 40.8428, -96.6787 | 40.2973, -96.7464 |
| ***General site characteristics*** | | | | |
| Pavement type | Concrete | Concrete | Concrete | Concrete |
| Functional class | Other arterial | Expressway | Major arterial | Expressway |
| No. of travel lanes | 4 | 2 | 5 | 2 |
| No. of shoulder lanes | 1 | 1 | 0 | 0 |
| No. of turning lanes | 1 | 0 | 3 | 0 |
| AADT | 10,000 | 4,000 | 30,000 | 4,000 |
| Posted speed limit, mph | 45 | 50 | 45 | 50 |
| Sidewalk | No | No | Yes | No |
| Adjacent land use | Commercial | Commercial/ open area | Commercial | Commercial |
| Development density | Medium | Low | High | Medium |
| ***Hydrologic characteristics*** | | | | |
| Catchment area, ac | 27.6 | 39.8 | 19.5 | 13.2 |
| Percent impervious area, % | 60 | 34 | 45 | 77 |
| Connected impervious area, ac | 15.1 | - | 15 | 10.2 |
| Disconnected impervious area, ac | 1.5 | 13.6 | - | - |
| Longest flow path, ft | 2620 | 4388 | 2111 | 3395 |
| Average Basin slope, % | 2.9 | 0.75 | 0.74 | 0.48 |
| Curve number of pervious surfaces | 81 | 75 | 74 | 84 |
| ***Additional site characteristics*** | | | | |
| Area in NDOT ROW, ac | 4.45 | 4.4 | 4.67 | 2.63 |
| Impervious are in ROW, ac | 3.13 | 4.31 | 4.67 | 2.58 |
| Impervious % in ROW area | 70.3 | 98.0 | 100.0 | 98.1 |
| Area outside NDOT ROW, ac | 23.2 | 35.4 | 14.8 | 10.6 |
| Impervious area outside of ROW, ac | 13.5 | 9.3 | 10.3 | 7.6 |
| Impervious % in non-ROW area | 58.2 | 26.2 | 69.7 | 72.1 |
| Ratio of runoff contribution based on impervious area (ROW vs non-ROW) | 19% : 81% | 32% : 68% | 31% : 69% | 25% : 75% |
| No. of processed samples | 29 | 22 | 31 | 30 |

Figures 3.2 through 3.5 provide maps that highlight the characteristics of each site and show potential contributions of flow and sediment from areas outside the NDOT right-of-way. Within each map, the red line indicates the estimated drainage boundary, while the yellow line outlines the NDOT right-of-way. The contributing drainage area and land cover types for each site were estimated using a one-meter digital elevation model (USDA NRCS 2024), drainage maps, Google Maps, and site visits. The curve number (CN) was determined using the TR-55 manual (USDA SCS 1986). The purple and blue shaded areas represent impervious surfaces connected to storm sewer and unconnected impervious surfaces, respectively. Similarly, pervious areas such as grass are shown in green These maps clearly indicate that a significant portion of the impervious area contributing to runoff lies outside the NDOT right-of-way.

The **Beal Slough** site, shown in Figure 3.2, had a drainage area of 27.6 acres and a relatively steep average slope of 1.5% compared to the other sites. It was located along S 14th Street in Lincoln, an urban road with concrete pavement with approximately 10,000 annual average daily traffic (AADT). Figure 3.2 shows the estimated catchment area for the outfall, including land surface types and the NDOT right-of-way. The surrounding land was primarily commercial buildings and parking lots, with access roads and side streets connecting to the main roadway. Soil erosion potential was considered minimal due to the stable land cover. A notable feature of this site was the presence of curb cuts with a buffer in the middle of the highway, which help partially filter roadway runoff before it enters the drainage system. The drainage from this site flows into Beal Slough through a 24" to 30" straight drainage pipe running along the highway.

The **Beatrice West** site was the largest among the four, covering 39.8 acres. It had very flat terrain and was located on the west side of U.S. Highway 77 in Beatrice. It experienced an

AADT of approximately 4,000 vehicles and did not receive winter maintenance (NDOT 2025). At this site, the area outside NDOT right-of-way primarily consisted of pervious land with some commercial development, as shown in Figure 3.3. Soil erosion potential was minimal, as the entire area drained into an open, grass-lined channel running parallel to the highway, which acted as a natural filter for roadway runoff.

The **Cornhusker** site covered 19.5 acres and featured mostly flat terrain. It was situated along Cornhusker Highway, which ran west to east, and N 27th Street, which extends in a northwest direction—both among the busiest roads in Lincoln, as presented in Figure 3.4. The site experienced heavy traffic, with an approximate AADT of 30,000 vehicles on Cornhusker Highway. Runoff from this area drained into Deadman's Run. The area outside of NDOT right-of-way was highly impervious, dominated by commercial development. During the spring, exposed soil surfaces in the lawns showed noticeable potential for erosion, and relatively lower erosion potential during dry weather in the summer. The site was well-drained, with infrastructure designed to manage stormwater efficiently

The **Beatrice North** site covered 13.22 acres and had a flat slope. It was located on the east side of U.S. Highway 77 in Beatrice, with an estimated AADT of 4,000 vehicles. A detailed GIS map is provided in Figure 3.5. Runoff from this site drained into Indian Creek, which ultimately flowed into the Big Blue River. The surrounding land consisted of commercial development, with gravel roads and parking areas contributing to high soil erosion potential. Additionally, the site's proximity to agricultural lands and rural roads may have influenced sediment sources. Lastly, the area is well-drained, featuring inlets and storm sewer pipes that manage stormwater effectively.

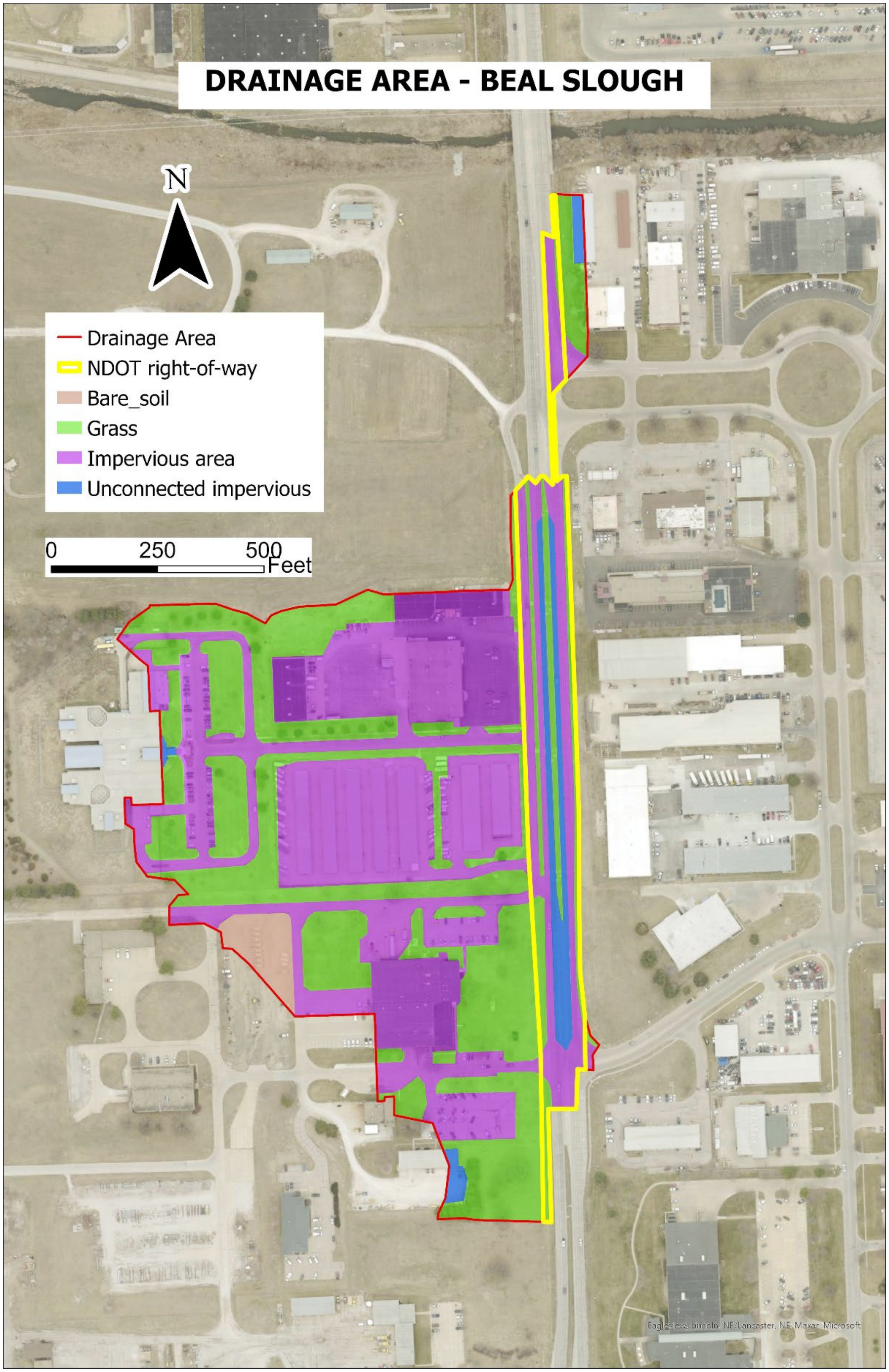

Figure 3.2 Drainage area and land use map of Beal Slough site

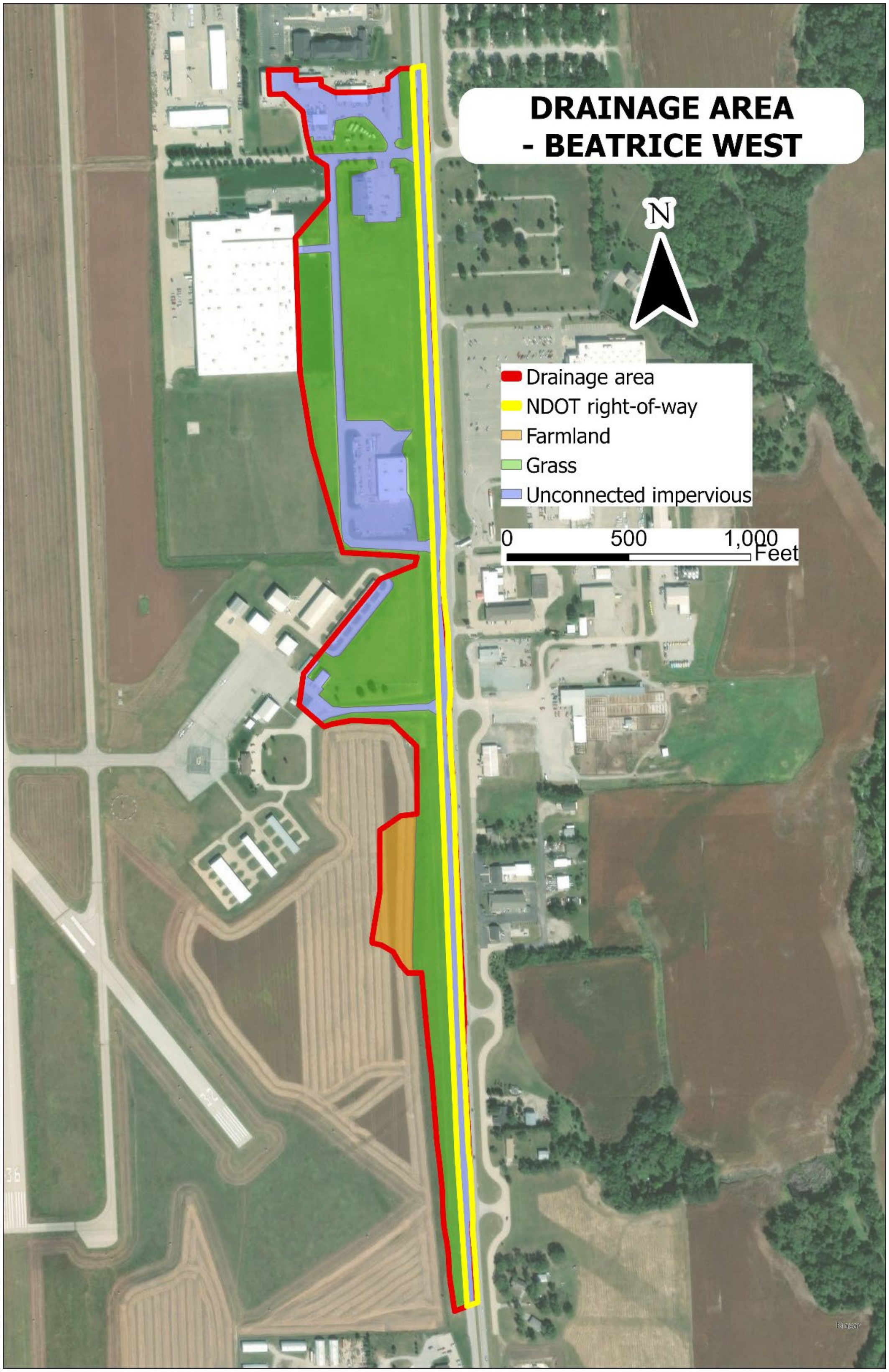

Figure 3.3 Drainage area and land use map of Beatrice West site

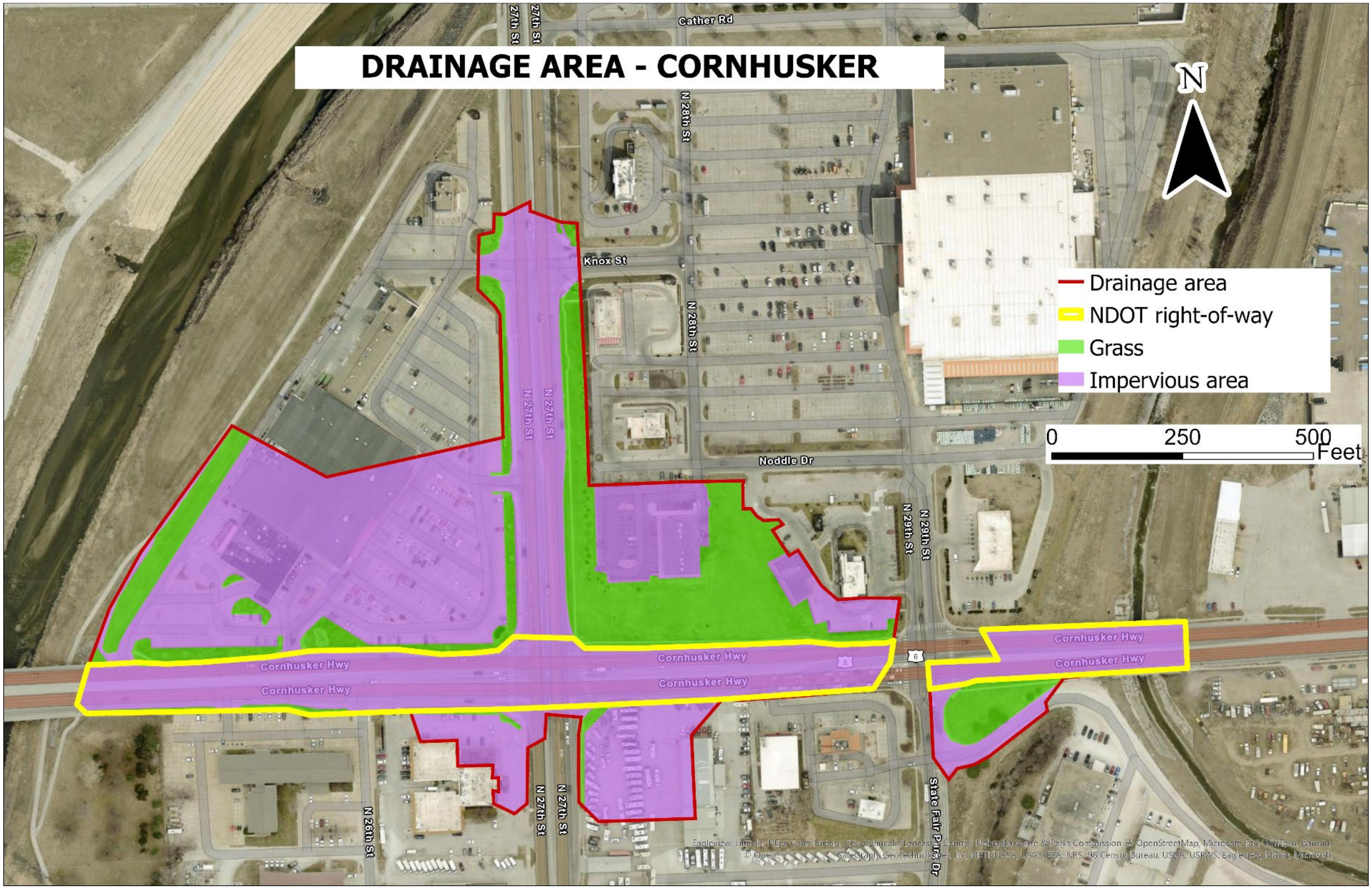

Figure 3.4 Drainage area and land use map of Cornhusker site

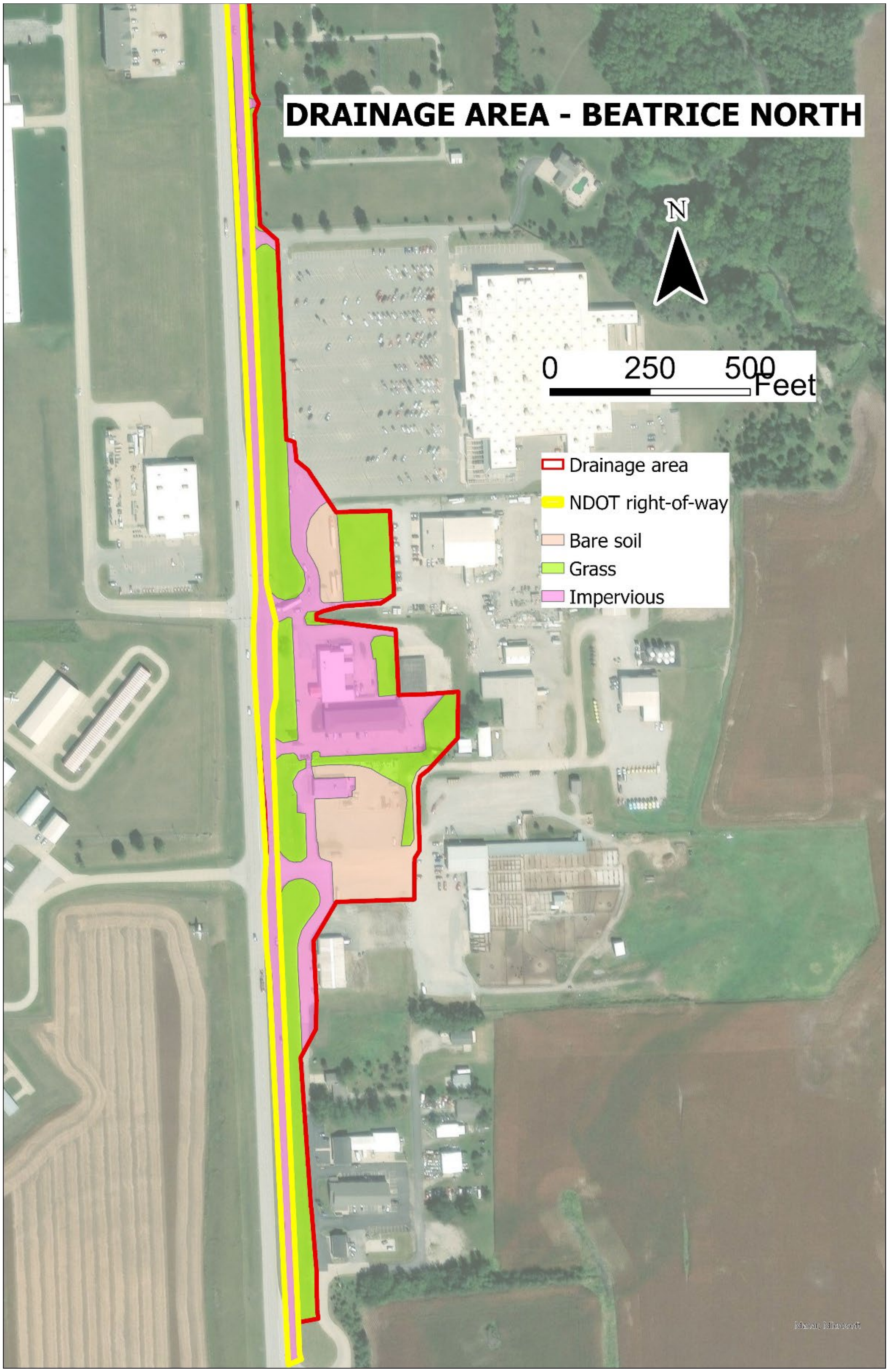

Figure 3.5 Drainage area and land use map of Beatrice North site

## 3.4 Historical Climate Data

Lincoln and Beatrice are in the central United States and experience a humid continental climate. Summers are hot and humid, with temperatures often exceeding 90°F, while winters are cold, with temperatures frequently dropping below freezing. The region receives a moderate annual rainfall of approximately 30 inches, based on 30 years of daily and monthly climate data provided by the National Weather Service, as listed in Table 3.2 and Table 3.3 (NWS 2025). Precipitation is distributed from early spring to late fall. This allows for sampling throughout most of the year, from March to early December.

Table 3.2 Monthly climate averages (1991 - 2020) - Lincoln, NE

| **Month** | **Total Precipitation Normal (inches)** | **Mean Max Temperature Normal (°F)** | **Mean Min Temperature Normal (°F)** | **Mean Avg Temperature Normal (°F)** |
|---|---|---|---|---|
| January | 0.7 | 35.6 | 14.4 | 25.0 |
| February | 0.9 | 40.6 | 18.4 | 29.5 |
| March | 1.6 | 53.6 | 28.7 | 41.2 |
| April | 2.7 | 64.8 | 39.2 | 52.0 |
| May | 4.9 | 75.0 | 51.2 | 63.1 |
| June | 4.5 | 85.2 | 62.1 | 73.7 |
| July | 3.3 | 89.4 | 66.7 | 78.1 |
| August | 3.3 | 87.2 | 64.1 | 75.6 |
| September | 2.9 | 80.1 | 54.3 | 67.2 |
| October | 2.1 | 66.6 | 41.0 | 53.8 |
| November | 1.3 | 51.7 | 28.0 | 39.8 |
| December | 1.2 | 39.4 | 18.2 | 28.8 |
| **Annual** | **29.3** | **64.1** | **40.5** | **52.3** |

*Data obtained from NWS: Daily/monthly normals (averages)

Table 3.3 Monthly climate averages (1991 - 2020) - Beatrice, NE

| **Month** | **Total Precipitation Normal (inches)** | **Mean Max Temperature Normal (°F)** | **Mean Min Temperature Normal (°F)** | **Mean Avg Temperature Normal (°F)** |
|---|---|---|---|---|
| January | 0.7 | 34.9 | 13.5 | 24.2 |
| February | 0.9 | 40.0 | 16.9 | 28.5 |
| March | 1.7 | 52.3 | 27.4 | 39.8 |
| April | 2.9 | 63.3 | 37.7 | 50.5 |
| May | 5.1 | 73.5 | 50.2 | 61.9 |
| June | 4.6 | 83.7 | 61.3 | 72.5 |
| July | 4.1 | 88.4 | 65.5 | 77.0 |
| August | 3.8 | 86.3 | 63.0 | 74.6 |
| September | 3.0 | 79.4 | 53.3 | 66.3 |
| October | 2.3 | 66.6 | 40.4 | 53.5 |
| November | 1.3 | 51.2 | 27.4 | 39.3 |
| December | 1.0 | 39.0 | 17.8 | 28.4 |
| **Annual** | **31.3** | **63.2** | **39.5** | **51.4** |

*Data obtained from NWS: Daily/monthly normals (averages)

## 3.5 Permit requirements

In this section, the key regulatory requirements and design assumptions from NDOT's *Drainage Design and Erosion Control Manual* are outlined (NDOT 2023). First, it covers the legal background, TSS removal requirements, permitted design practices, and areas where the permit lacks clear explanation. Then, it explains how this context is important for designing stormwater treatment facilities (STFs), such as the SAFL Baffle.

### *3.5.1 Regulatory background and context*

Federal and state regulations provide the basis for stormwater management in Nebraska. The National Pollutant Discharge Elimination System (NPDES), authorized under the Clean Water Act (CWA) (EPA 1972), regulates discharges into U.S. waters, including stormwater from Municipal Separate Storm Sewer Systems (MS4s). As a regulated MS4, the NDOT is required to meet permit conditions set by the Nebraska Department of Environment and Energy (NDEE) (NDOT 2023).

To meet these permit conditions, NDOT applies a combination of structural and non-structural strategies. These STFs are used to reduce pollutants in runoff from post-construction roadway surfaces. Structural STFs include detention ponds, grass swales, infiltration basins, and bioretention systems. In contrast, non-structural practices focus on land use planning, reducing impervious surfaces, and protecting environmentally sensitive areas (NDOT 2023).

Additional treatment may be required for sites that discharge into impaired water bodies. Under Section 303(d) of the CWA (U.S. EPA 1972), states must identify impaired water bodies and establish Total Maximum Daily Loads (TMDLs) for pollutants. If a project discharges into one of these waters and NDOT is assigned a waste load allocation, enhanced treatment measures may be needed. These situations are usually identified early in the project planning phase so that appropriate stormwater controls can be included in the design.

### *3.5.2 TSS removal requirement*

NDOT requires stormwater treatment practices to reduce TSS by at least 80% of the average annual load to meet water quality goals (NDOT 2023). This standard applies to priority stormwater outfalls, which are defined as concentrated discharges from areas with 5,000 square feet or more of new or renovated pavement within NDOT right-of-way (ROW) that drain directly to state waters within an MS4 boundary. To design appropriate stormwater treatment facilities (STFs), the Water Quality Volume (WQV) and WQV discharge rate must be calculated. WQV is based on the first 0.5 inches of rainfall from the treatment drainage area, which typically includes new impervious surfaces added within the NDOT ROW and may increase due to additional run-on from the off-site areas. The discharge rate is estimated using the NRCS Curve Number (CN) method, assuming a 0.75-inch, 24-hour design storm, CN of 98 for pavement, and a time of concentration (Tc) of 5 minutes.

### *3.5.3 Permitted design assumptions and areas of interpretation*

The NDOT permit (NDOT 2023) includes several design assumptions used during the treatment design process, though some are subject to interpretation. For example, while the permit states that only a "new impervious area" within the NDOT right-of-way (ROW) must be treated, in practice, the entire work zone is often treated as a new impervious area when any construction is done. This interpretation expands the treatment requirement to include all impervious surfaces within the project limits, including the existing pavement. However, the permit also allows treatment credit for existing pavement to offset the required 80% TSS removal. Interpreting the entire work zone as a new impervious area creates confusion about how such credit should be applied.

In some cases, run-on from off-site areas can be diverted away from the project area to reduce the size and cost of treatment facilities.

However, there are some areas open to interpretation in the permit. For example, the permit does not clearly explain how to assign treatment credit for off-site areas, especially if those flows eventually discharge into the same water body downstream. It is also unclear why only new pavement must be treated, even though managing runoff from existing roads could help meet TMDL waste load allocations more effectively. Another gap is the lack of guidance on the PSD in the stormwater runoff. PSD is important in stormwater treatment because the number of other pollutants attached to suspended sediments varies with particle size, and treatment efficiency of STFs often depends on the size distribution of particles in the stormwater runoff.

### *3.5.4 Relevance to this study*

The NDOT permit directly influenced the selection and evaluation of STFs in this study. The SAFL Baffle was selected as the recommended structural STF because it is more cost-effective and space-efficient than many other hydrodynamic separators or large-scale systems. The permit's 80% TSS removal requirement served as the basis for evaluating STF performance, and treatment credit was considered for off-site runoff that received treatment within the project area. The application of these permit requirements in evaluating SAFL performance is discussed in more detail in Chapter 5.

# Chapter 4 Methodology

## 4.1 Introduction

This chapter describes the methods used to collect and analyze stormwater data from the study sites. It explains how rainfall data were gathered from nearby weather stations and how stormwater samples were collected using automated samplers paired with flow meters. The chapter also covers the measurement of TSS and PSD in both the university laboratory and an external laboratory. Finally, it outlines the statistical methods used to analyze the data.

## 4.2 Precipitation data

Precipitation data were sourced from the National Weather Service (NWS) (NOAA: NWS 2025) and Weather Underground (Weather Underground 2025), with stations selected based on proximity to the sites. For Beal Slough and Cornhusker sites, data were obtained from Weather Underground stations, while Beatrice sites relied on the NWS station. Detailed maps showing the locations of weather stations are provided in Appendix B: Location of weather stations. To ensure data reliability, multiple nearby stations were considered for each site. Since their readings were consistent, the closest station was selected.

For Beal Slough, the primary rainfall data source was the KNELINCO140 station. Data from additional stations (KNELINCO680, KNELINCO461, and KNELINCO386) were also reviewed for validation. Similarly, for the Cornhusker site, data KNELINCO396 and KNELINCO93 were evaluated, with KNELINCO396 typically chosen due to its proximity to the catchment. For the Beatrice sites, rainfall data were primarily obtained from the Beatrice Municipal Airport station. These data were cross-checked with readings from Weather Underground stations to confirm accuracy.

The available data had time steps ranging from 5 to 20 minutes for Weather Underground stations and 20 minutes for NWS stations. Rainfall depth was directly measured at each station, while rainfall intensity was calculated using interpolated data at one-minute intervals. The maximum 20-minute and 60-minute intensities were then calculated for each storm event.

### 4.3 Stormwater monitoring and sampling

To evaluate stormwater quality and flow patterns, each site was equipped with automated monitoring systems designed for flow-paced composite sampling and runoff measurement. Each sampling station consisted of an autosampler paired with an Area-Velocity (AV) flow module. These were deployed near culvert access points to continuously monitor flow rates and collect stormwater samples during storms, as illustrated in Figure 4.1. Two distinct configurations were used for flow-paced composite sampling at each station. The first configuration consisted of an ISCO 6712 full-size portable sampler paired with a 750 AV flow module (Teledyne ISCO), deployed at Cornhusker and Beatrice West sites. The second configuration utilized an ISCO 3700 portable sampler with a 2150 AV flow module (Teledyne ISCO), implemented at the Beal Slough and Beatrice North sites. Detailed plan and section views of the monitoring site setup are shown in Appendix C: Plans and profiles of sampling locations.

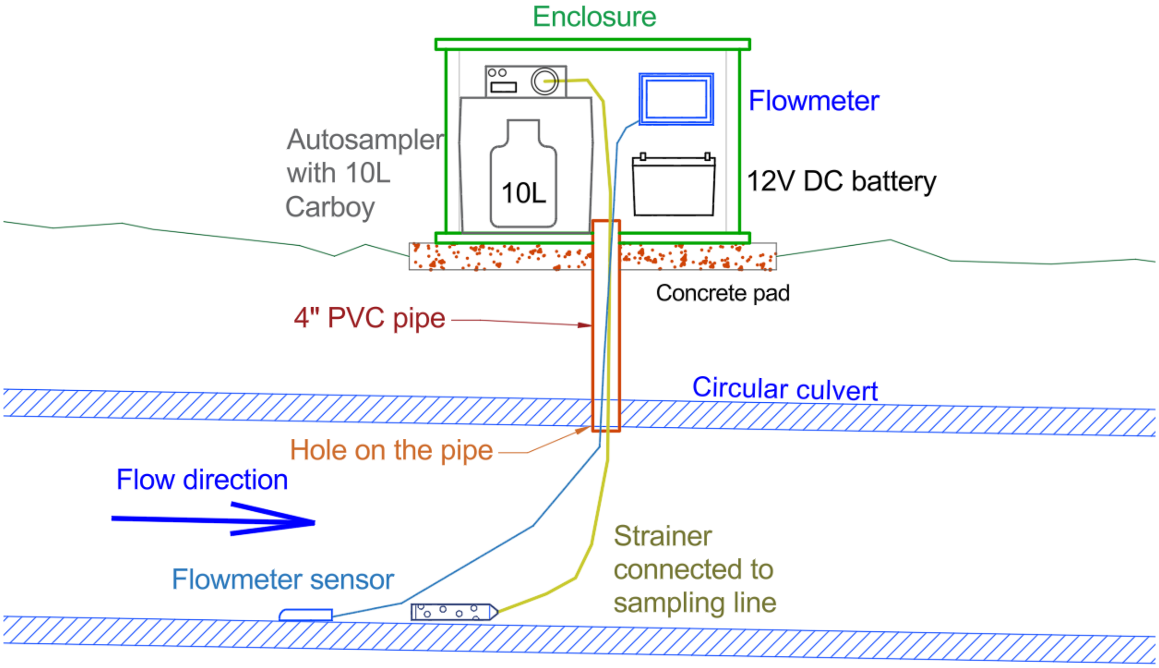

Figure 4.1 A section of typical stormwater monitoring station

The flowmeter measured runoff volume in the culvert and triggered the autosampler at predefined intervals (Table 4.1). At each interval, a 500-ml aliquot was pumped through a 3/8-inch vinyl suction line and deposited into a 10-L plastic carboy. A strainer at the sampling line inlet was used to avoid gross solids getting into the sample. During each storm event, a maximum of 20 aliquots (500 ml) were collected to produce a composite sample whose TSS would represent event mean concentration (EMC). Depending on rainfall characteristics, a sampling event could last anywhere from a few minutes to an entire day. However, since the flow-pacing interval was fixed for all storm events regardless of rainfall depth or intensity, the sampling method did not always capture the full hydrograph, as shown in Figure 4.2. The interval was generally set to collect samples for rainfall events producing just over 0.5 inches of depth as shown in Figure 4.3. Additional hydrograph response plots showing sampling times for all four sites are provided in Appendix G: Hydrograph response and sampling times. Therefore, for larger storms or high-intensity events with greater runoff volume, only a portion of the hydrograph was sampled—most often the rising limb.

Table 4.1 Sampler configuration at each site

| **Description** | **Beal Slough** | **Beatrice West** | **Cornhusker** | **Beatrice North** |
|---|---|---|---|---|
| Auto sampler model | 3700 | 6712 | 6712 | 3700 |
| Area-velocity model | 2150 | 750 | 750 | 2150 |
| Culvert size, ft. | 30 | 48 | 42 | 24 |
| Suction line length, ft. | 18 | 34 | 28 | 25 |
| Trigger interval, cu.ft. (pulses) | 200.5 (15) | 500 | 800 | 401 (30) |

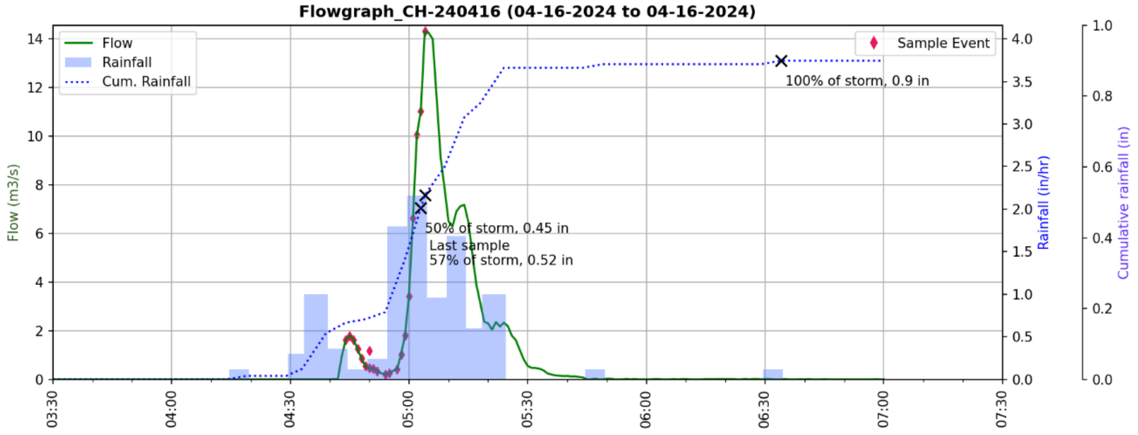

Figure 4.2 Example hydrograph showing partial sampling coverage

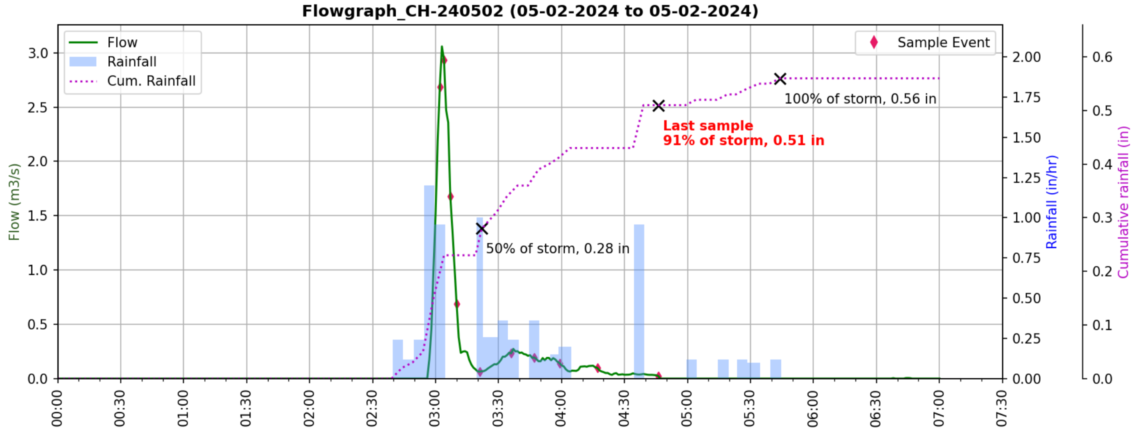

Figure 4.3 Example hydrograph showing full sampling coverage

Samples were retrieved within 24 hours of the storm's conclusion and taken for laboratory analysis. The dates of the processed samples are provided in Appendix G: Hydrograph response and sampling times**.** A total of 29, 22, 31, and 30 storm events were sampled and processed from Beal Slough, Beatrice West, Cornhusker, and Beatrice North, respectively.

## 4.4 Laboratory analysis for water quality

The objective of the laboratory analysis was to determine the TSS and PSD in each sample. Most samples were tested within 2 to 3 days after collection, although a few were analyzed after a week. Each sample passed through a 32 µm sieve to separate coarse and fine suspended solids for separate analysis. Although a 63 µm cutoff is more commonly used, a finer 32 µm threshold was chosen to provide greater detail in particle size distribution (Selbig and Bannerman 2011; Charters et al. 2015). The 63 µm sieve was also included in the analysis to allow comparability with previous studies.

The coarse TSS fraction (particles > 32 µm) was measured using sieve analysis followed by the evaporation method. The fine TSS fraction (particles < 32µm) was analyzed using the filtration method, where three 50 mL aliquots were processed and averaged. Both methods followed the procedures outlined in ASTM D3977-97 (ASTM 2013).

For PSD analysis, the coarse fraction was measured in the lab using a wet sieve analysis method with the following mesh sizes: 1000, 500, 250, 125, 63 and 32 µm. In contrast, the fine fraction was analyzed by an external laboratory using a laser diffraction method (Wilcock 1973). The analysis followed ASTM D4464, utilizing a Beckman Coulter LS13320 MW. It was equipped with the Universal Liquid Module (ULM) and a refractive index of 1.60 + 0.0001i was used. A detailed standard lab procedure is provided in Appendix H: Standard operating procedure to determine sediment concentration and particle size distribution in the laboratory.

The fine-fraction testing was conducted by Independent Particles Lab, Ohio. For each composite sample, a representative 200 ml aliquot of the fine portion was collected and refrigerated. Samples intended for external analysis were stored for less than six months before shipment. Once a batch of samples (typically 6 to 12) was ready, they were shipped overnight in a cooler with ice packs. Samples were processed by the lab on the same day they were received to minimize degradation or changes in particle characteristics.

### 4.5 Data Analysis

The data collected were analyzed using basic statistical methods to identify trends and variations in sediment concentration and particle sizes. Graphs and charts were created to visualize patterns in TSS and PSD across monitored sites.

The Kruskal-Wallis test (Kruskal and Wallis 1952) was used to test significant differences between rainfall parameters and water quality parameters between sites and seasons. This test is used when data are not normally distributed. When significant differences were detected, pairwise comparisons were conducted using Dunn’s test with a Bonferroni adjustment (Dunn, 1961).

Multiple linear regression analysis (Helsel and Hirsch 2020) was performed in SAS 9.4 using PROC REG procedure to test models with different combinations of explanatory variables. Residual vs. predicted plots were checked for constant variance; log transformation was applied if needed. The overall model significance was tested using $P(F) < 0.05$, and individual predictors were assessed using $P(|t|) < 0.05$. Variance Inflation Factor (VIF) values were reviewed to detect multicollinearity, with VIF > 10 considered problematic. Stepwise selection was used to identify the best-fit model. Response variables included TSS, coarse suspended solids (CSS), and fine suspended solids (FSS), while explanatory variables were rainfall depth, 20-min and 1-hr intensity, ADP, 7-day average temperature, and week number.

To understand the qualitative relationship between TSS and PSD, site characteristics were examined through multiple site visits and grab sampling. Factors such as land use, drainage conditions, flow patterns and anthropogenic activities were considered to explore how they might influence sediment transport and distribution.

# Chapter 5 Results and Discussion

## 5.1 Introduction

This chapter summarizes results from the stormwater monitoring carried out at the four study sites: Beal Slough, Beatrice West, Cornhusker, and Beatrice North. The discussion begins with a brief overview of how samples were collected, followed by a summary of rainfall patterns during the monitoring period. The primary focus is on sediment-related characteristics, specifically total suspended solids (TSS) and particle size distribution (PSD), which are important for understanding how runoff transports the sediment and the expected effectiveness of installed stormwater treatment systems.

The next sections explore trends observed at the sites and seasons and discuss how temporal and geographic characteristics at the sites, such as season, slope, impervious area, and land use affected sediment characteristics. The chapter also looks at how this data can be used to test whether the SAFL Baffle, a type of stormwater treatment device, meets NDOT's permit requirements. This evaluation was done using the SHSAM modeling tool. In the final part of the chapter, various design scenarios are tested using field data to assess the SAFL Baffle's performance, along with a discussion of its potential shortcomings and potential areas for improvement.

## 5.2 Stormwater sample collection

A total of 111 samples were collected and analyzed for total suspended solids (TSS) and particle size distribution (PSD) for the coarse fraction (>32 μm) across the four monitoring sites. The temporal distribution of samples is illustrated in Figure 5.1. The number of samples collected at each site is listed in red on the right side of Figure 5.1 and was as follows: Beal Slough had 29, Beatrice West had 22, Cornhusker had 30, and Beatrice North had 30. and the range of precipitation is shown in Figure 5.2. Of the samples collected, 83 were sent to an external laboratory for detailed PSD analysis of the finer fraction (<32 µm). These are referred to as “extended PSD samples” throughout this report, and their counts are shown in parentheses next to the total number of samples for each site by season and for the entire sampling period. Seasonally, 60 samples were collected during spring, 31 during summer, and 20 during fall across all sites.

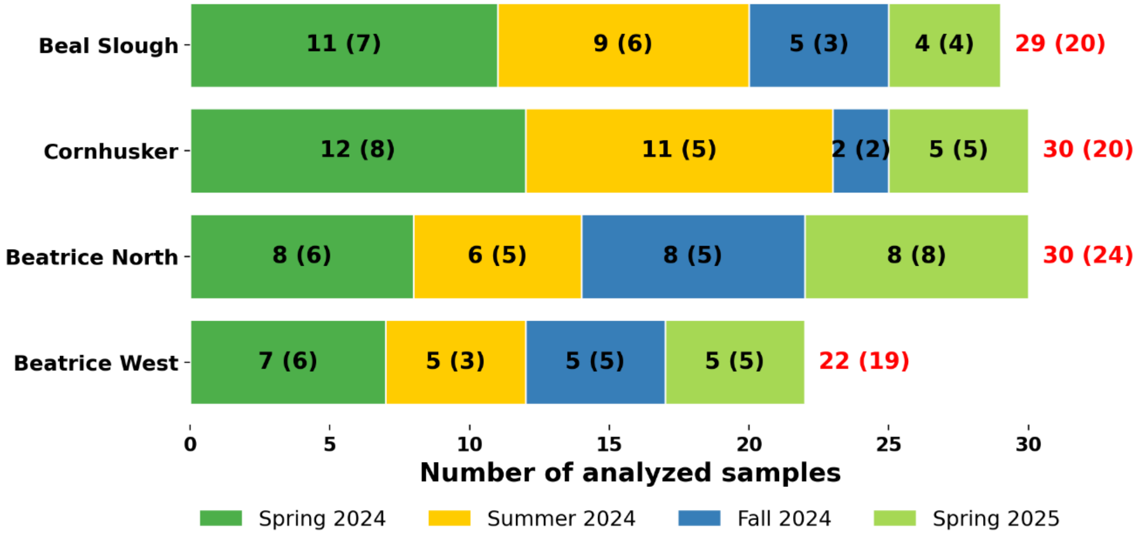

Figure 5.1 Summary of collected samples. Values in parentheses (e.g., 11 (7)) indicate the “extended PSD samples” analyzed for fine fraction PSD out of the total number of samples collected.

The number of samples collected was not consistent across all sites due to variations in rainfall patterns, challenges in capturing enough samples during small storms at certain locations, and occasional equipment malfunctions. Although Beatrice West and Beatrice North are adjacent, fewer samples were collected at Beatrice West because its mostly pervious surfaces allowed early storm infiltration and reduced runoff, especially during dry periods.

Samples were collected from a range of precipitation events. Figure 5.2 summarizes the number of events by storm size range, illustrating the frequency of storms with varying magnitudes during the monitoring period. The green line indicates the cumulative number of events exceeding each corresponding rainfall depth.

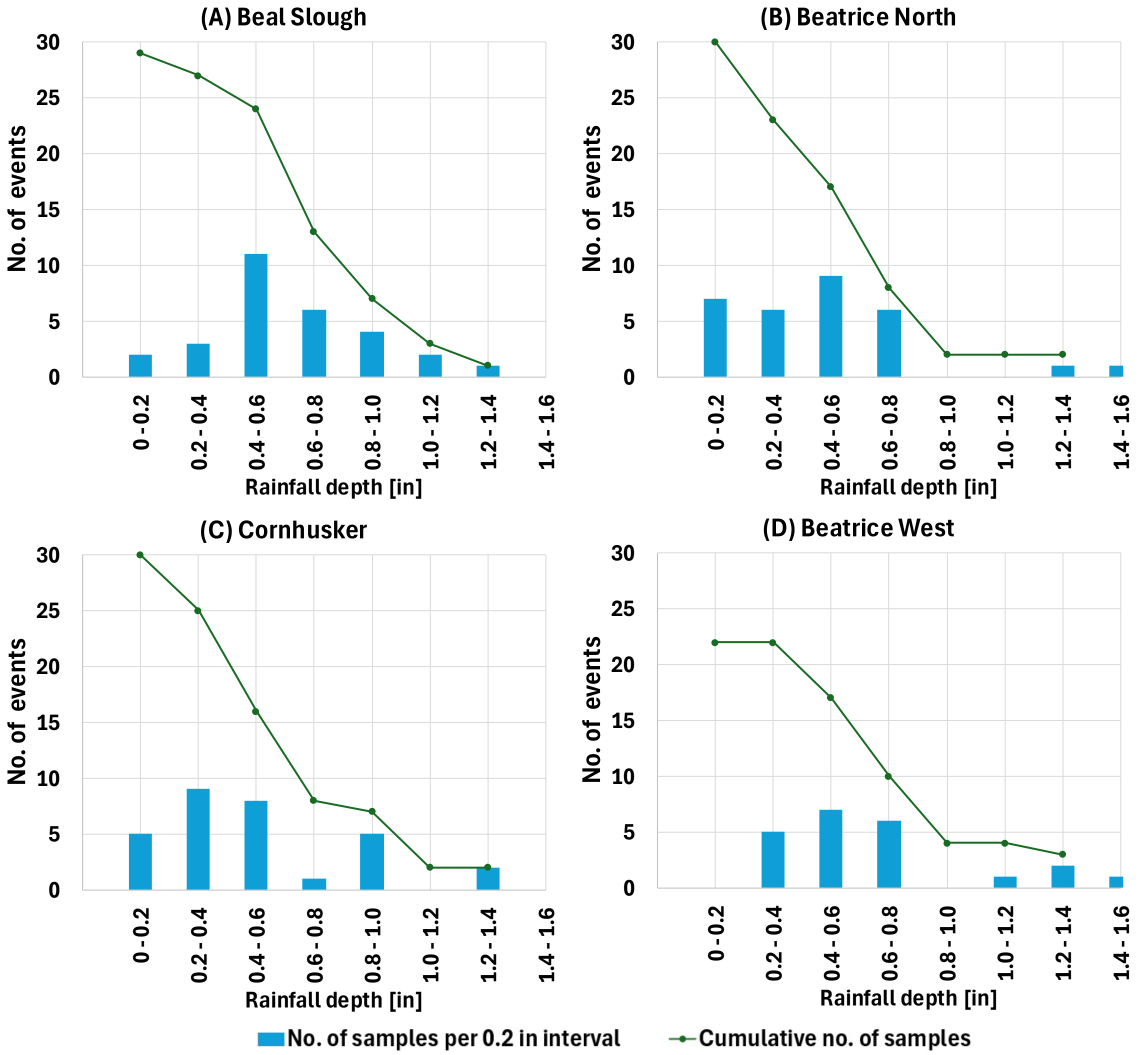
(A) Beal Slough

(B) Beatrice North

(C) Cornhusker

(D) Beatrice West

Figure 5.2 Number of analyzed samples categorized by storm size range at (A) Beal Slough (B) Beatrice North (C) Cornhusker and (D) Beatrice West

## 5.3 Descriptive summary of sampling data

This section presents descriptive statistics of sampling data collected during the monitoring period, including precipitation, total suspended solids (TSS), and particle size distribution (PSD). Rainfall patterns are described first, followed by an analysis of TSS concentrations and variability across sites and seasons. Finally, PSD results are discussed to highlight sediment composition differences among sites. Statistical tests were applied throughout to identify significant spatial and temporal trends in the dataset.

### *5.3.1 Precipitation*

In 2024, the average rainfall depth at monitoring sites ranged from 0.50 to 0.69 inches. In contrast, in 2025 the average rainfall depths ranged from 0.35 to 0.68 inches. In 2024, rainfall depths across all sites ranged from 0.04 to 1.50 in. In 2025, the range was 0.09 to 1.15 in. (Table 5.1). Additional rainfall characteristics, including peak 20-minute and 60-minute intensities as well as antecedent dry period in days, are also summarized in Table 5.1. However, it is important to note that the descriptive statistics for Beatrice West and Beatrice North are not identical, despite using data from the same rainfall station, due to differences in the number of sampling events and their collection dates.

Rainfall characteristics were found to be statistically similar across all monitoring sites and seasons. The Kruskal–Wallis test (Kruskal and Wallis 1952) showed no significant differences in rainfall parameters either between the four sites or across spring, summer, and fall. Differences were considered statistically significant when the Pr > Chi-Sq value was less than 0.05. However, no significant differences were observed in any rainfall parameter across sites or seasons, as all p-values exceeded the 0.05 threshold (Table 5.2).

Table 5.1 Precipitation summary of observed samples

| Site | 2024 | | | | | 2025 | | | | |
|---|---|---|---|---|---|---|---|---|---|---|
| | Metric | Rainfall depth [in] | Peak 20-min intensity [in/hr] | Peak 60-min intensity [in/hr] | Antecedent dry days | Stats | Rainfall depth [in] | Peak 20-min intensity [in/hr] | Peak 60-min intensity [in/hr] | Antecedent dry days |
| Beal Slough | Observations | 25 | | | | Observations | 4 | | | |
| | Minimum | 0.11 | 0.30 | 0.11 | 0 | Minimum | 0.18 | 0.20 | 0.14 | 2 |
| | Maximum | 1.22 | 1.62 | 0.77 | 21 | Maximum | 1.15 | 0.93 | 0.61 | 15 |
| | Median | 0.57 | 0.84 | 0.39 | 5 | Median | 0.69 | 0.58 | 0.39 | 3 |
| | Mean | 0.62 | 0.89 | 0.43 | 5 | Mean | 0.68 | 0.57 | 0.38 | 6 |
| | Std. dev | 0.25 | 0.43 | 0.20 | 4 | Std. dev | 0.44 | 0.32 | 0.25 | 6 |
| Beatrice West | Observations | 17 | | | | Observations | 5 | | | |
| | Minimum | 0.27 | 0.24 | 0.17 | 0 | Minimum | 0.26 | 0.12 | 0.11 | 1 |
| | Maximum | 1.41 | 2.67 | 1.04 | 8 | Maximum | 0.78 | 1.23 | 0.53 | 15 |
| | Median | 0.54 | 0.69 | 0.31 | 2 | Median | 0.45 | 0.31 | 0.22 | 2 |
| | Mean | 0.69 | 0.90 | 0.47 | 3 | Mean | 0.52 | 0.55 | 0.27 | 5 |
| | Std. dev | 0.37 | 0.63 | 0.29 | 2 | Std. dev | 0.24 | 0.46 | 0.16 | 6 |
| Cornhusker | Observations | 25 | | | | Observations | 4 | | | |
| | Minimum | 0.04 | 0.06 | 0.03 | 0 | Minimum | 0.09 | 0.07 | 0.18 | 1 |
| | Maximum | 1.39 | 2.22 | 1.06 | 21 | Maximum | 0.84 | 0.51 | 0.90 | 15 |
| | Median | 0.44 | 0.61 | 0.26 | 3 | Median | 0.24 | 0.10 | 0.28 | 3 |
| | Mean | 0.50 | 0.71 | 0.35 | 5 | Mean | 0.35 | 0.19 | 0.38 | 6 |
| | Std. dev | 0.36 | 0.57 | 0.28 | 5 | Std. dev | 0.31 | 0.18 | 0.29 | 6 |
| Beatrice North | Observations | 22 | | | | Observations | 8 | | | |
| | Minimum | 0.15 | 0.12 | 0.07 | 0 | Minimum | 0.10 | 0.06 | 0.04 | 0 |
| | Maximum | 1.50 | 1.65 | 1.04 | 25 | Maximum | 0.78 | 1.23 | 0.53 | 17 |
| | Median | 0.45 | 0.41 | 0.26 | 5 | Median | 0.23 | 0.20 | 0.13 | 3 |
| | Mean | 0.51 | 0.59 | 0.33 | 6 | Mean | 0.35 | 0.37 | 0.18 | 7 |
| | Std. dev | 0.35 | 0.47 | 0.26 | 5 | Std. dev | 0.29 | 0.43 | 0.17 | 7 |

Table 5.2 P-value of Kruskal-Wallis test of rainfall characteristics (all results are >0.05 meaning not statistically different)

| Rainfall parameters | Pr > Chi sq. | |
|---|---|---|
| | *Between sites* | *Between seasons* |
| Rainfall depth | 0.069 | 0.933 |
| Maximum 20 min intensity | 0.065 | 0.556 |
| Maximum 60 min intensity | 0.079 | 0.597 |
| Antecedent dry period in days | 0.153 | 0.184 |

### *5.3.2 Total suspended solids*

The overall median concentrations for 111 samples was 393 mg/L, with a standard deviation of 611 mg/L. TSS concentrations (mg/L) observed at the four monitoring sites are summarized in Table 5.3 and illustrated in Figure 5.3. In these illustrations, summaries of the coarse fraction (>32 µm) and fine fraction (<32 µm) of TSS are also provided, which were separated in the laboratory using the wet sieving method with a 32 µm sieve. Among the monitored sites, median total suspended solids (TSS) concentrations ranged from 158 to 580 mg/L. Beal Slough appeared to have a higher proportion of the coarse fraction, possibly related to the steeper gradient of the roadway. In contrast, Cornhusker and Beatrice North had higher fine fractions, which may be attributed to visible erosion from off-site areas. Previous studies on roadway runoff, as presented in Section 2.6, have reported TSS concentrations ranging from 35 to 400 mg/L, with many values below 200 mg/L. These results suggest that TSS levels at the Nebraska NDOT sites are generally at the upper end of, or exceed, the ranges reported in existing literature.

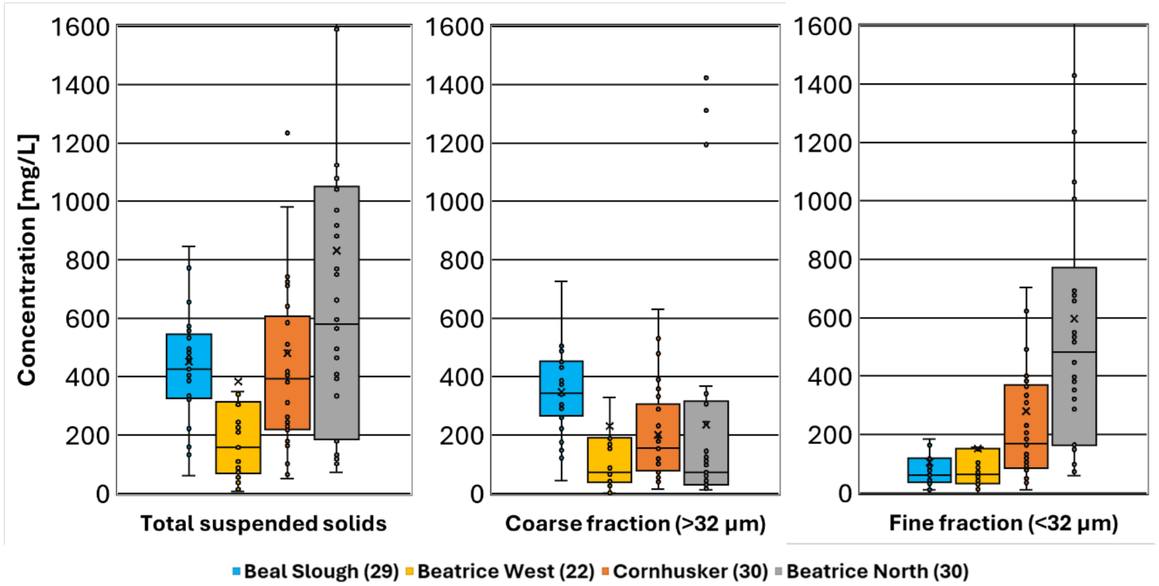

Figure 5.3 Distribution of Total Suspended Solids across monitoring sites

Table 5.3 Descriptive statistics of Total suspended solids (TSS)

| Site | Metric | TSS [mg/L] | | | | | Coarse fraction (>32μm) [mg/L] | | | | | Fine fraction (<32μm) [mg/L] | | | | |
|---|---|---|---|---|---|---|---|---|---|---|---|---|---|---|---|---|
| | | Spring | | Summer | Fall | All | Spring | | Summer | Fall | All | Spring | | Summer | Fall | All |
| | | 2024 | 2025 | 2024 | 2024 | | 2024 | 2025 | 2024 | 2024 | | 2024 | 2025 | 2024 | 2024 | |
| Beal Slough | Obs. | 11 | 4 | 9 | 5 | 29 | 11 | 4 | 9 | 5 | 29 | 11 | 4 | 9 | 5 | 29 |
| | Min | 324 | 459 | 61 | 132 | 61 | 222 | 342 | 43 | 122 | 43 | 49 | 117 | 18 | 11 | 11 |
| | Max | 877 | 1111 | 533 | 466 | 1111 | 727 | 505 | 456 | 451 | 727 | 445 | 622 | 77 | 45 | 622 |
| | Med | 482 | 714 | 334 | 169 | 426 | 390 | 491 | 300 | 148 | 342 | 84 | 215 | 40 | 15 | 61 |
| | Mean | 529 | 749 | 335 | 254 | 452 | 404 | 457 | 294 | 229 | 347 | 125 | 292 | 41 | 25 | 105 |
| | Std. | 180 | 274 | 137 | 145 | 233 | 137 | 77 | 128 | 144 | 146 | 113 | 229 | 19 | 18 | 134 |
| Beatrice West | Obs. | 7 | 5 | 5 | 5 | 22 | 7 | 5 | 5 | 5 | 22 | 7 | 5 | 5 | 5 | 22 |
| | Min | 157 | 7 | 55 | 15 | 7 | 70 | 7 | 26 | 1 | 1 | 71 | 0 | 29 | 13 | 0 |
| | Max | 2860 | 685 | 304 | 209 | 2860 | 1974 | 330 | 200 | 168 | 1974 | 886 | 355 | 103 | 45 | 886 |
| | Med | 340 | 231 | 99 | 37 | 158 | 188 | 154 | 49 | 6 | 73 | 153 | 77 | 43 | 31 | 63 |
| | Mean | 879 | 248 | 132 | 74 | 383 | 541 | 140 | 77 | 44 | 231 | 339 | 109 | 54 | 30 | 152 |
| | Std. | 1108 | 265 | 99 | 81 | 701 | 750 | 127 | 70 | 71 | 462 | 370 | 142 | 29 | 14 | 247 |
| Cornhusker | Obs. | 12 | 5 | 11 | 2 | 30 | 12 | 5 | 11 | 2 | 30 | 12 | 5 | 11 | 2 | 30 |
| | Min | 178 | 65 | 51 | 423 | 51 | 46 | 54 | 15 | 202 | 15 | 87 | 11 | 35 | 135 | 11 |
| | Max | 1235 | 2356 | 711 | 585 | 2356 | 531 | 631 | 479 | 288 | 631 | 703 | 1725 | 231 | 383 | 1725 |
| | Med | 433 | 595 | 224 | 504 | 393 | 137 | 178 | 107 | 245 | 155 | 257 | 334 | 79 | 259 | 169 |
| | Mean | 516 | 847 | 272 | 504 | 481 | 190 | 271 | 174 | 245 | 201 | 326 | 576 | 98 | 259 | 280 |
| | Std. | 330 | 879 | 185 | 115 | 448 | 144 | 238 | 152 | 61 | 159 | 218 | 666 | 60 | 175 | 332 |
| Beatrice North | Obs. | 8 | 8 | 6 | 8 | 30 | 8 | 8 | 6 | 8 | 30 | 8 | 8 | 6 | 8 | 30 |
| | Min | 180 | 72 | 101 | 103 | 72 | 16 | 13 | 28 | 16 | 13 | 164 | 59 | 73 | 83 | 59 |
| | Max | 2625 | 3530 | 881 | 1041 | 3530 | 1311 | 1423 | 342 | 349 | 1423 | 1430 | 2107 | 539 | 692 | 2107 |
| | Med | 999 | 870 | 294 | 364 | 580 | 296 | 61 | 80 | 37 | 73 | 842 | 660 | 218 | 309 | 482 |
| | Mean | 1273 | 1149 | 361 | 427 | 832 | 457 | 255 | 114 | 87 | 236 | 817 | 895 | 247 | 340 | 596 |
| | Std. | 910 | 1072 | 299 | 319 | 831 | 509 | 481 | 120 | 114 | 383 | 475 | 673 | 182 | 226 | 513 |

The Kruskal–Wallis test was used to evaluate significant differences in TSS concentrations between monitoring sites and across seasons, which are presented in Table 5.4 and Table 5.5. When significant differences were detected, pairwise comparisons were conducted using Dunn's test with a Bonferroni adjustment (Dunn 1961). Results from the Kruskal–Wallis tests indicated that TSS concentrations were not uniform across all sites or seasons. Pairwise comparisons revealed that Beal Slough and Beatrice West exhibited significantly different TSS concentrations. Seasonal analysis further showed that spring TSS concentrations differed significantly from those observed in both summer and fall, while no significant difference was found between summer and fall.

Table 5.4 P-value of Kruskal-Wallis test of Total Suspended Solids between sites (all results are >0.05**,** meaning not statistically different)

| | **p-value in K-W test: 0.005 (<0.05)** | | | | |
|---|---|---|---|---|---|
| | **Sites compared** | | **Pr > \|Z\|** | **Adjusted p** | **Results** |
| **TSS** | BS | CH | 0.5986 | 3.592 | Similar |
| | BS | BTN | 0.0882 | 0.529 | Similar |
| | BS | BTW | 0.0081 | 0.049 | Different |
| | CH | BTN | 0.098 | 0.588 | Similar |
| | CH | BTW | 0.0215 | 0.129 | Similar |
| | BTN | BTW | 0.0086 | 0.052 | Similar |
| | **p-value in K-W test: 0.0008 (<0.05)** | | | | |
| | **Sites compared** | | **Pr > \|Z\|** | **Adjusted p** | **Results** |
| **CSS (>32 µm)** | BS | CH | 0.0025 | 0.015 | Different |
| | BS | BTN | 0.0069 | 0.041 | Different |
| | BS | BTW | 0.0022 | 0.013 | Different |
| | CH | BTN | 0.4348 | 2.609 | Similar |
| | CH | BTW | 0.1322 | 0.793 | Similar |
| | BTN | BTW | 0.6699 | 4.019 | Similar |
| | **p-value in K-W test: 0.0001 (<0.05)** | | | | |
| | **Sites compared** | | **Pr > \|Z\|** | **Adjusted p** | **Results** |
| **FSS (<32 µm)** | BS | CH | 0.0003 | 0.002 | Different |
| | BS | BTN | 0.0001 | 0.001 | Different |
| | BS | BTW | 0.3823 | 2.294 | Similar |
| | CH | BTN | 0.0072 | 0.043 | Different |
| | CH | BTW | 0.0285 | 0.171 | Similar |
| | BTN | BTW | 0.0012 | 0.007 | Different |

Table 5.5 P-value of Kruskal-Wallis test of Total Suspended Solids between seasons for all combined data (all results are >0.05 meaning not statistically different)

| | | | | | |
|---|---|---|---|---|---|
| **TSS** | **p-value in K-W test: 0.0001 (<0.05)** | | | | |
| | **Seasons** | | **Pr > \|Z\|** | **Adjusted p** | **Results** |
| | Spring | Summer | 0.0001 | 0.0003 | Different |
| | Spring | Fall | 0.0095 | 0.0285 | Different |
| | Summer | Fall | 0.7888 | 2.3664 | Similar |
| **CSS (>32 µm)** | **p-value in K-W test: 0.0038 (<0.05)** | | | | |
| | **Seasons** | | **Pr > \|Z\|** | **Adjusted p** | **Results** |
| | Spring | Summer | 0.0161 | 0.0483 | Different |
| | Spring | Fall | 0.0035 | 0.0105 | Different |
| | Summer | Fall | 0.2535 | 0.7605 | Similar |
| **FSS (<32 µm)** | **p-value in K-W test: 0.0001 (<0.05)** | | | | |
| | **Seasons** | | **Pr > \|Z\|** | **Adjusted p** | **Results** |
| | Spring | Summer | 0.0001 | 0.0003 | Different |
| | Spring | Fall | 0.0242 | 0.0726 | Similar |
| | Summer | Fall | 0.6798 | 2.0394 | Similar |

### *5.3.3 Relation between Total suspended solids and Rainfall depth*

The TSS and rainfall depth did not show strong correlation across the sites. Among the four sites, only Beatrice North displayed a clear positive trend. In Figure 5.4, trend lines are drawn between TSS and rainfall depth for all storms (orange) and for storms with rainfall depths less than 0.5 inches (blue). The data points for the storms above 0.5 inches of precipitation are orange and those below 0.5 are blue. For both Lincoln sites, Beal Slough and Cornhusker, there was no observable trend in either group. At Beatrice North, both trend lines showed a positive relationship. In contrast, Beatrice West showed a slight upward trend in the full dataset due to two storms with very high TSS levels, but this trend disappeared in the subset of storms smaller than 0.5 inches. Additionally, the median TSS values at Beatrice North were 486 mg/L for all storms and 415 mg/L for storms under 0.5 inches, while at Beatrice West they were 157 mg/L and 106 mg/L, respectively. This suggests that there is little correlation between TSS and rainfall depth once a few extreme TSS events are excluded, although TSS was slightly lower at both Beatrice sites when only storms smaller than 0.5 in. of precipitation were considered.

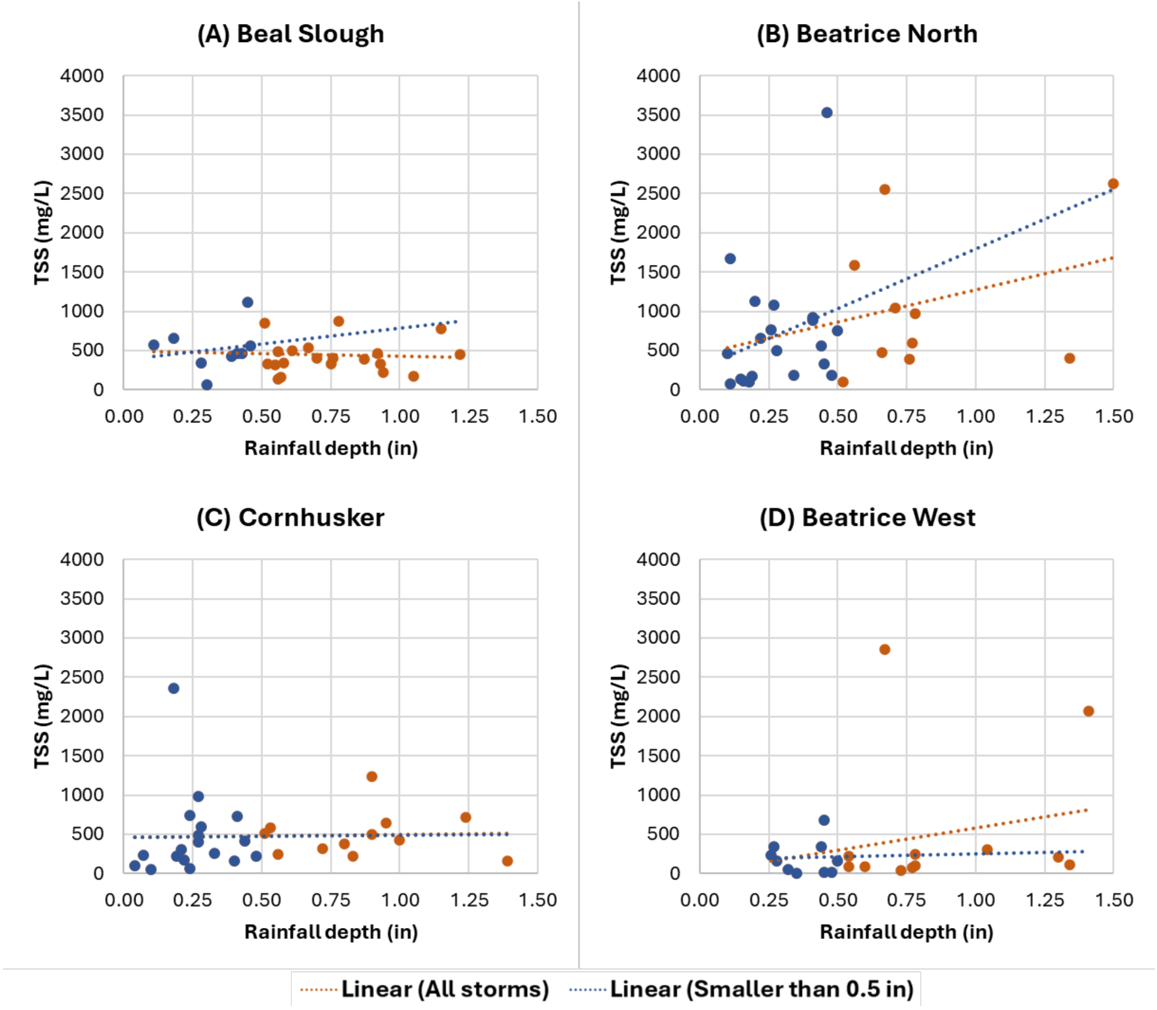

Figure 5.4 Relation between Total suspended solids and Rainfall depth

### *5.3.4 TSS loading from sampled runoff*

TSS loads for all monitored sites were calculated for each sampled storm using measured TSS concentrations and flow volumes recorded by the flow meter. The results, summarized in Table 5.6 and Figure 5.5, cover four seasons from spring 2024 to spring 2025. The total sediment load ranged from 1,401-kg TSS to a maximum of 10,838-kg TSS at Beatrice North. The lower

TSS load at Beal Slough was likely due to smaller flow volumes and minimal off-site erosion compared to the other sites. Seasonal differences were also observed, with spring showing the highest TSS loads across all sites. At the Beatrice sites, two large storms on 5/4/2024 and 5/31/2024 contributed the most sediment, producing 5,122 kg-TSS at Beatrice North and 6,861 kg-TSS at Beatrice West. This indicates that erosion was greater in spring, leading to higher sediment loads at all sites.

Table 5.6 Summary of Sediment Load (kg-TSS) from sampled storms

| **Season** | **Beal Slough** | **Cornhusker** | **Beatrice North** | **Beatrice West** |
|---|---|---|---|---|
| 2024 Spring | 758 | 3231 | 6298 | 7056 |
| 2024 Summer | 474 | 2222 | 726 | 543 |
| 2024 Fall | 46 | 0 | 945 | 180 |
| 2025 Spring | 123 | 1437 | 2869 | 201 |
| Total | 1401 | 6890 | 10838 | 7980 |
| Remarks | | Flowmeter failed during Fall | Very high sediment load from two big storms in Spring of 2024 | |

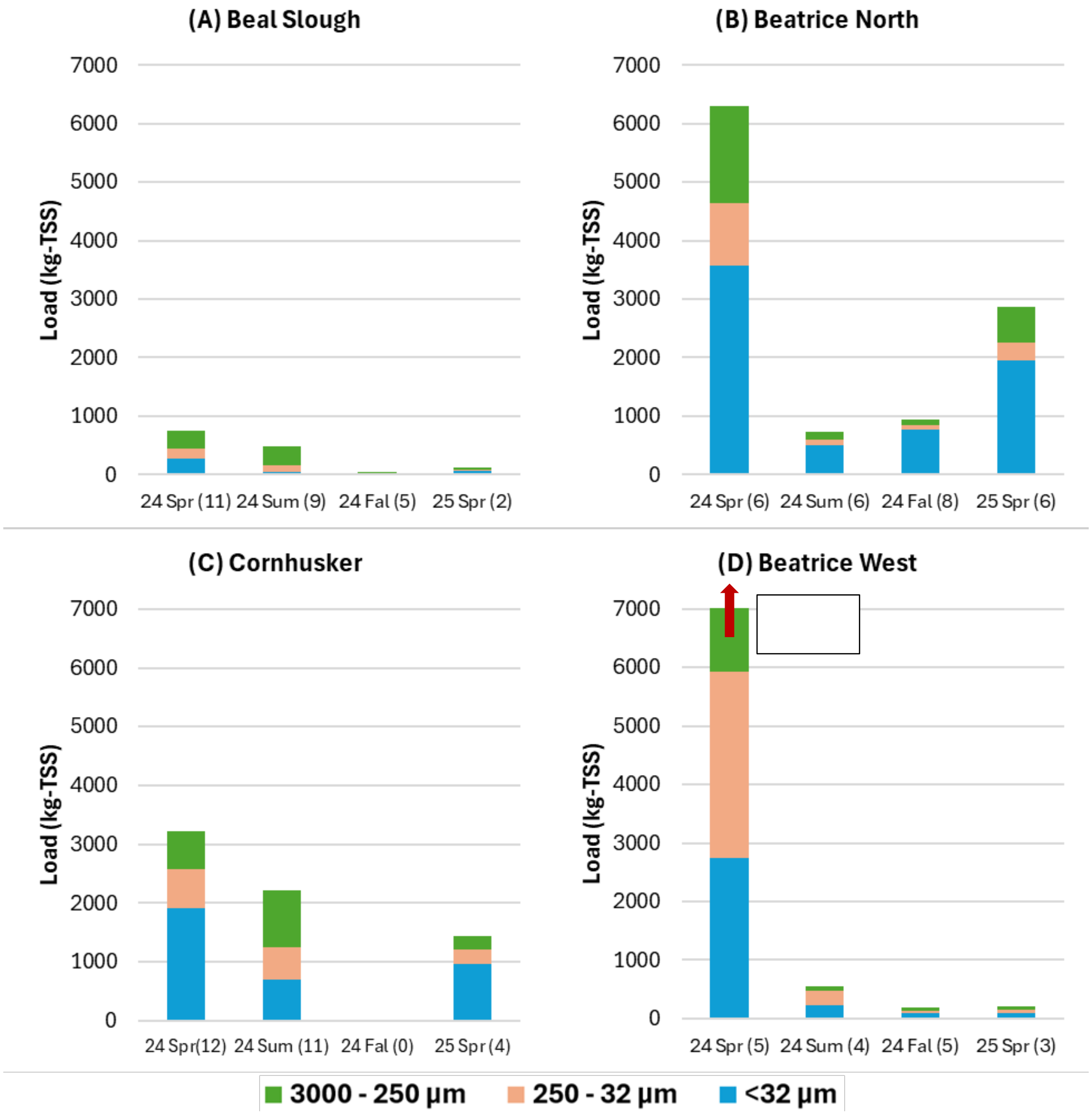

Figure 5.5 Sediment load (kg-TSS) at monitored sites and seasons

### *5.3.5 Particle size distribution*

Particle size distribution was determined using two different methods, as explained in detail in Section 4.4. First, the coarse fraction of sediment (>32 µm) retained on the 32 µm sieve was further analyzed in the lab using multiple sieve sizes. Second, a small volume of the finer sediment (<32 µm) collected from the sieve analysis was sent to an external lab for analysis using the laser diffraction method. A total of 111 samples were analyzed for the complete PSD across the four sites in 2024 and 2025 using the first method, with each site contributing between 22 and 30 samples. Due to cost limitations, only about 68 "extended PSD samples" of the 111 samples were sent to the external lab to determine the particle size distribution for particles smaller than 32 µm.

#### 5.3.5.1 Particle size distribution of coarse fraction (>32 µm)

Median PSD values for particles larger than 32 µm from all collected samples are shown as solid lines in Figure 5.6, with the number of samples for each site noted in the legend. Dotted lines in the figure represent PSDs available in SHSAM, as described in Table 2.3. The NURP (Nationwide Urban Runoff Program) PSD was developed using data from 28 catch basins across the U.S. (U.S. EPA 1983). The NJCAT (New Jersey Corporation for Advanced Technology) PSD was created for testing hydrodynamic separators (NJCAT 2023). The Janna-Omid PSD was developed by Barr Engineering using expert judgment and findings from multiple roadway runoff studies (Mohseni, pers. comm. 2024). The OK 110 PSD is a commercially available distribution used for BMP testing (Minnesota PCA), and the MnDOT PSD is based on particles collected during roadway cleaning (Mohseni, pers. comm. 2024). Additionally, a PSD from a study focused solely on roadway sites is also included (Winston et al. 2023). The vertical purple line in the figure marks the 32 µm threshold.

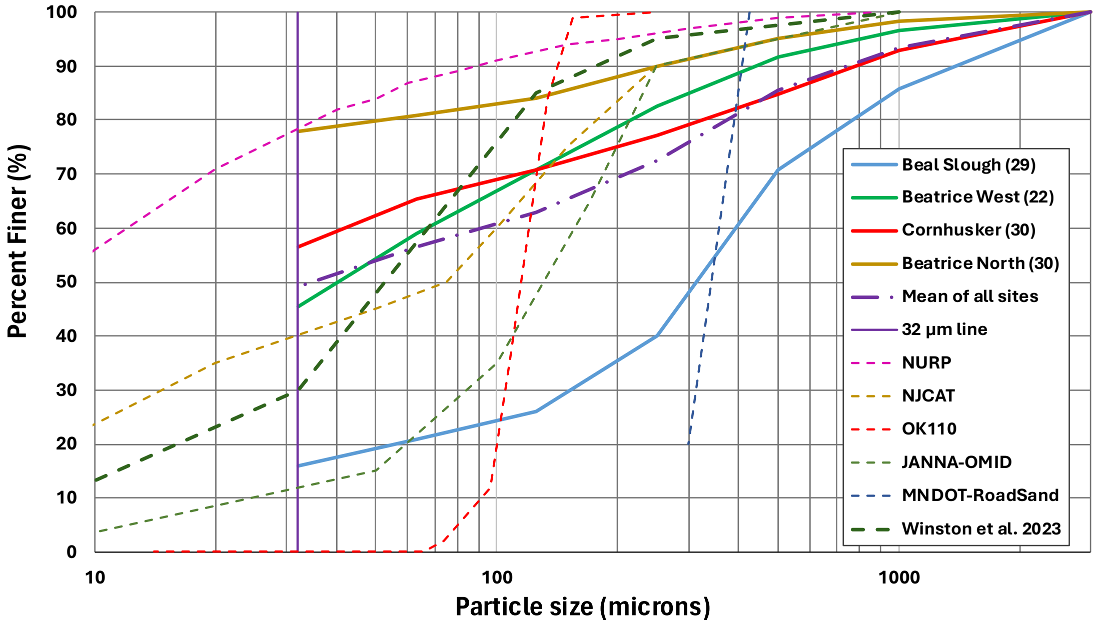

Figure 5.6 Median particle size distribution above 32 µm

The figure shows that PSDs from the study sites varied widely. Beatrice North had a much higher percentage of fine particles, while Beal Slough showed a much coarser distribution, possibly due to steeper gradient of the roadway. PSDs at Beatrice West and Cornhusker were similar to each other and fell between the other two sites, though both still had a higher proportion of fine particles compared to most other roadway studies.

### 5.3.5.2 Particle size distribution of fine fraction (<32 µm)

To better assess the fine fraction, due to cost constraints "extended PSD samples" from a subset of the sampled storms were sent to an external laboratory for detailed analysis of particles smaller than 32 µm (Figure 5.6). Figure 5.6 is based on median PSD values of 83 samples—19 to 24 per site of the 111 samples, where data from both methods of PSD determination were combined to create a continuous PSD curve.

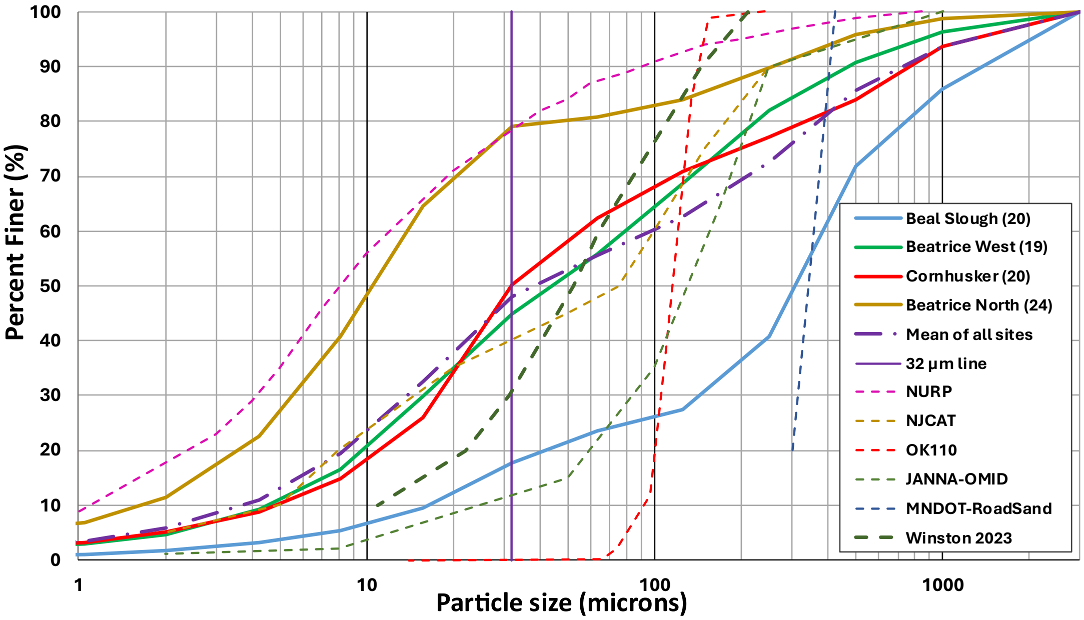

Figure 5.7 Median particle size distribution across monitoring sites

The particle size distribution (PSD) data from our study sites show a wide range of sediment sizes. Compared to PSDs from other roadway-focused studies, three sites—Beatrice North, Cornhusker, and Beatrice West—have a higher proportion of fine particles, except for NURP, which includes runoff from mixed land uses. This suggests that areas beyond the roadway, such as nearby land uses or exposed soil surfaces, may be contributing additional fine sediment to the stormwater runoff.

Compared to the PSD reported by Winston et al. (2023), our sites had similar median particle sizes but exhibited a broader and more graded distribution of sediment sizes. Winston's PSD likely reflects roadway-only conditions, as the study avoided sites with off-site runoff. However, the possibility remains that some sediment contributions may have come from nearby medians or exposed soils within the contributing area, even if not clearly identified as erosion sources. In contrast, the MnDOT PSD data differs noticeably from all other datasets, as they were based on sand particles collected directly from the roadway surface, likely originating from winter maintenance activities rather than from active runoff processes.

#### 5.3.5.3 Variability in PSD for each site

This section presents the PSDs of individual sampling events to highlight their variability. Figure 5.8 shows the particle size distributions (PSDs) for all storm events, while Figure 5.9 presents the extended PSDs, each including a median PSD line in red. The PSDs in Figure 5.8 are based on sieve analysis only and exclude particles smaller than 32 µm. This approach is useful for designing hydrodynamic separators because devices such as the SAFL Baffle are generally ineffective at removing such fine particles. In contrast, the PSDs in Figure 5.9 combine sieve and laser diffraction data for selected samples, extending the range to include finer particles. While the overall trends resemble Figure 5.8, they provide a more complete view of sediment composition that is useful for other applications as well.

The PSD plots show the cumulative percentage of particles finer than a given size. As a result, the PSD lines in Figure 5.8 do not drop to 0% at the 32 µm mark since the entire sample mass from each storm event was used in the analysis. For example, in Figure 5.8 (B), approximately 80% of the sample is smaller than 32 µm on average. Similarly, in the plots of extended PSD samples, the PSD line does not drop to 0% on the 1 µm mark, because the size distribution includes particles finer than this threshold. For example, in Figure 5.9 (B), an average of 9% of particles are smaller than 1 µm. In addition, the curves do not align smoothly around the 32 µm mark due to differences in the laboratory methods used for measuring coarse and fine fractions. These PSD plots illustrate the wide variability in particle size distributions observed across different storm events.

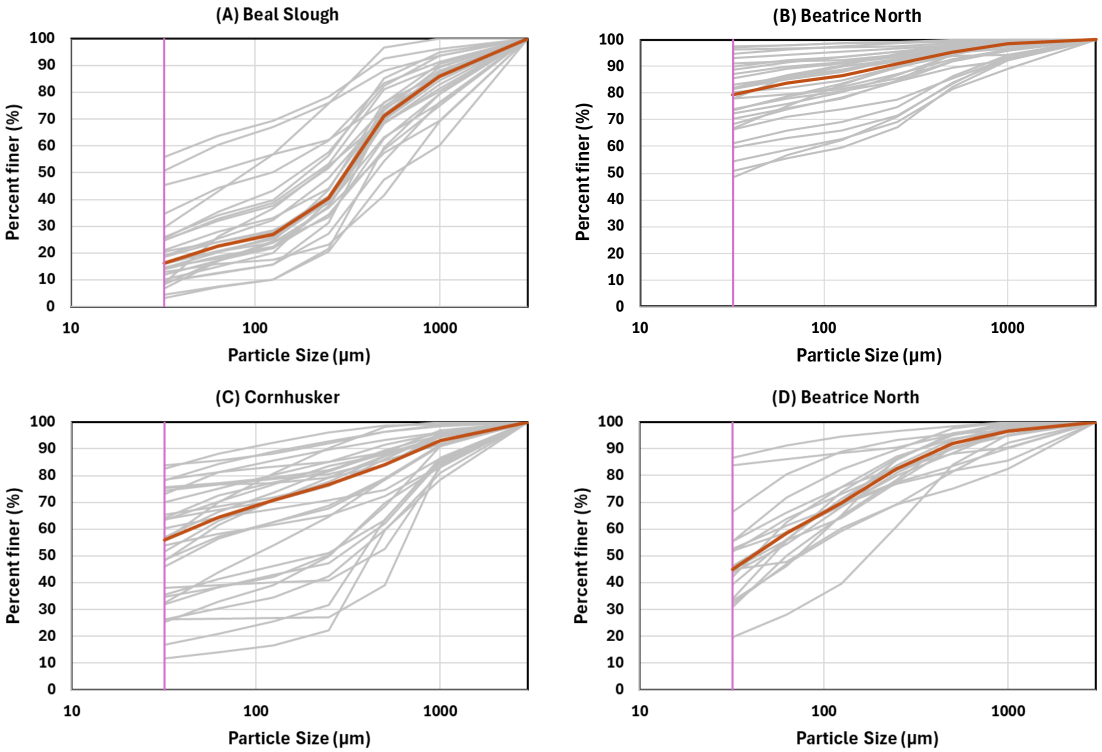

Figure 5.8 PSD distribution for all storm events with median PSD

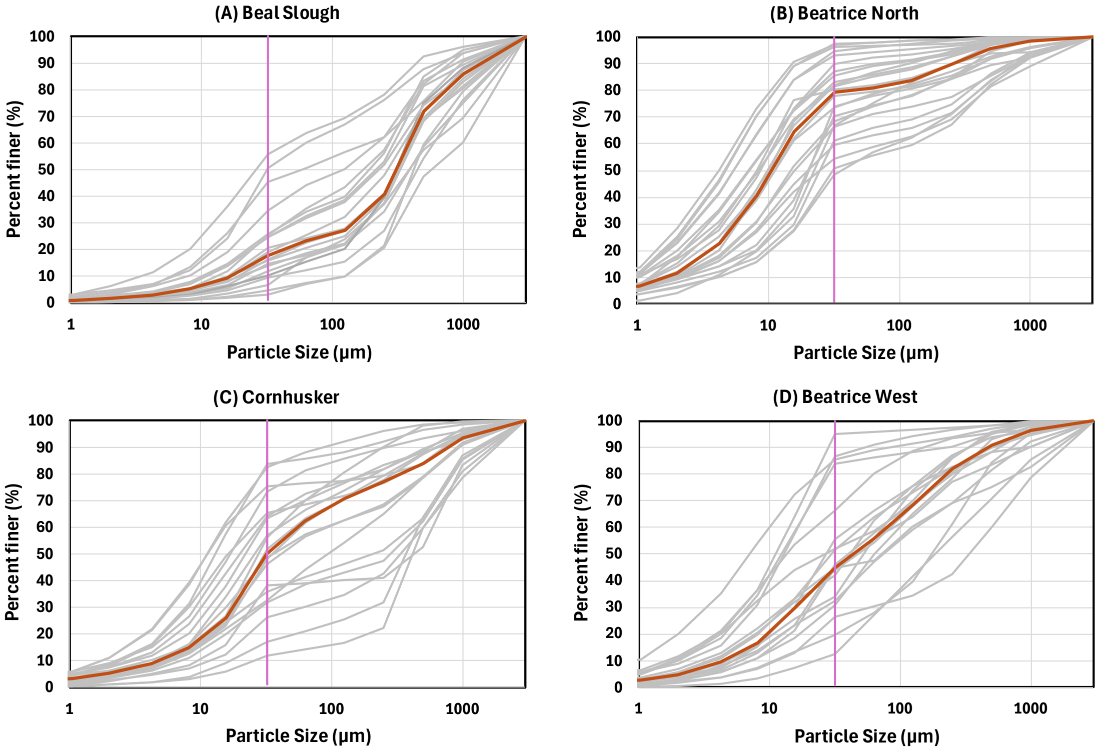

Figure 5.9 PSD distribution for extended PSD samples with median PSD

### 5.3.5.4 Particle size distribution parameters

To further illustrate differences in sediment size among the sites, median particle size (d50) along with d10 and d90 values were compared across locations. The d50 represents the median particle size, meaning 50% of the particles are smaller than this size; d10 and d90 indicate the particle sizes below which 10% and 90% of the particles fall, respectively. The median particle size (d50) was 322 µm at Beal Slough, 43 µm at Beatrice West, 31 µm at Cornhusker, and 16 µm at Beatrice North. These findings suggest that sediment at Beal Slough is primarily sand-sized, whereas the other sites are dominated by finer, silt-sized particles (Figure 5.9). Similarly, the distribution of d10 and d90 particle sizes for each site is also shown in this figure.

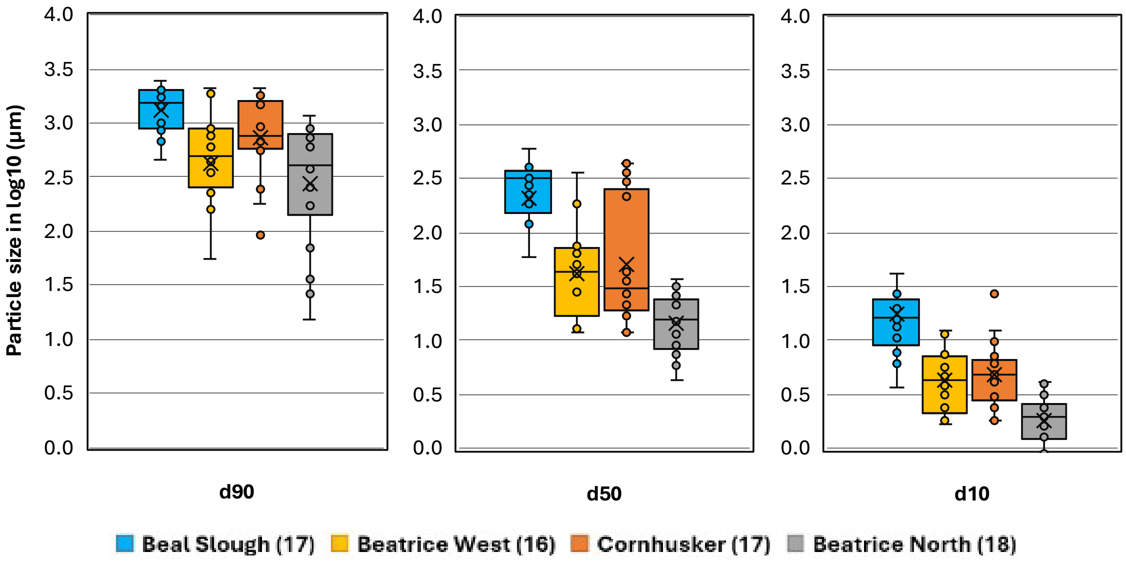

Figure 5.10 Distribution of particle size parameters across monitoring sites

To evaluate differences in particle size distribution across sites and seasons, the Kruskal–Wallis test was performed for PSD parameters, including d90, d50, and d10, as presented in Table 5.7, Table 5.8, and Table 5.9. Results indicated that these parameters varied significantly across monitoring sites but showed no significant differences across seasons. Follow-up pairwise comparisons using Dunn’s test with Bonferroni adjustment revealed that the PSD parameters at CH and BTW were not significantly different from each other, while all other site pairs showed statistically significant differences. These results suggest that PSD characteristics are site-specific and cannot be reliably used to represent other monitored sites. In the case of seasonal comparisons, Table 5.7 shows no significant variation in PSD parameters across seasons. Similarly, Table 5.8, which presents site-specific seasonal comparisons, indicates that PSD parameters within each site did not differ significantly among seasons. Overall, these findings confirm that seasonal effects on PSD are not sufficiently large to be statistically significant for the number of sampled storm events across all monitored locations.

Table 5.7 P-value in Kruskal-Wallis test of PSD parameters between sites (all results are >0.05 meaning not statistically different)

| | | | | | |
|---|---|---|---|---|---|
| **d90** | **p-value in K-W test: 0.0001 (<0.05)** | | | | |
| | **Sites compared** | | **Pr > \|Z\|** | **Adjusted p** | **Results** |
| | BS | CH | 0.0254 | 0.152 | Similar |
| | BS | BTN | 0.0003 | 0.002 | Different |
| | BS | BTW | 0.0038 | 0.023 | Different |
| | CH | BTN | 0.0297 | 0.178 | Similar |
| | CH | BTW | 0.1213 | 0.728 | Similar |
| | BTN | BTW | 0.585 | 3.510 | Similar |
| **d50** | **p-value in K-W test: 0.0001 (<0.05)** | | | | |
| | **Sites compared** | | **Pr > \|Z\|** | **Adjusted p** | **Results** |
| | BS | CH | 0.0149 | 0.089 | Similar |
| | BS | BTN | 0.0001 | 0.001 | Different |
| | BS | BTW | 0.0005 | 0.003 | Different |
| | CH | BTN | 0.0026 | 0.016 | Different |
| | CH | BTW | 0.6447 | 3.868 | Similar |
| | BTN | BTW | 0.0053 | 0.032 | Different |
| **d10** | **p-value in K-W test: 0.0001 (<0.05)** | | | | |
| | **Sites compared** | | **Pr > \|Z\|** | **Adjusted p** | **Results** |
| | BS | CH | 0.0012 | 0.007 | Different |
| | BS | BTN | 0.0001 | 0.001 | Different |
| | BS | BTW | 0.0008 | 0.005 | Different |
| | CH | BTN | 0.0011 | 0.007 | Different |
| | CH | BTW | 0.4879 | 2.927 | Similar |
| | BTN | BTW | 0.0102 | 0.061 | Similar |

Table 5.8 P-value in Kruskal-Wallis test of PSD parameters between seasons (all results are >0.05 meaning not statistically different)

<table>
<tr><td><b>d90</b></td><td colspan="5"><b>p-value in K-W test: 0.1507 (>0.05)</b></td></tr>
<tr><td rowspan="6"><b>d50</b></td><td colspan="5"><b>p-value in K-W test:0.0318 (<0.05)</b></td></tr>
<tr><td colspan="2">Seasons</td><td>Pr > |Z|</td><td>Adjusted p</td><td>Results</td></tr>
<tr><td>Spring</td><td>Summer</td><td>0.0669</td><td>0.2007</td><td>Similar</td></tr>
<tr><td>Spring</td><td>Fall</td><td>0.2222</td><td>0.6666</td><td>Similar</td></tr>
<tr><td>Summer</td><td>Fall</td><td>0.0221</td><td>0.0663</td><td>Similar</td></tr>
<tr><td colspan="5">Remarks: Bonferroni correction may be too conservative.</td></tr>
<tr><td><b>d10</b></td><td colspan="5"><b>p-value in K-W test: 0.0519 (>0.05)</b></td></tr>
</table>

Table 5.9 P-value in Kruskal-Wallis test of PSD parameters between seasons for each site (all results are >0.05 meaning not statistically different)

| PSD-parameter | Beal Slough | Cornhusker | Beatrice North | Beatrice West |
|---|---|---|---|---|
| **d90** | 0.412 | 0.067 | 0.858 | 0.133 |
| **d50** | 0.229 | 0.053 | 0.334 | 0.133 |
| **d10** | 0.091 | 0.050 | 0.276 | 0.257 |

## 5.4 Site-specific trends

This section discusses trends in site characteristics and their influence on hydrologic and hydraulic patterns. It then looks at possible reasons why sediment characteristics vary, including the effects of catchment features, land use, and sources of sediment. Finally, it examines seasonal patterns by comparing sediment data across the three seasons of 2024 and the spring season of 2025.

### *5.4.1 Hydrologic and Hydraulic response patterns across sites*

The monitored sites showed distinct hydrograph responses to rainfall events, driven largely by differences in catchment slope, size, land use, and flow patterns. For instance, Beal Slough (Figure 5.10), which has the steepest slope among all sites, produced a flashy hydrograph with a sharp rising limb and a quick peak. However, the recession limb often lacked recorded flow data, likely due to limitations in the flow meter’s sensitivity during low flows. In contrast, Beatrice West (Figure 5.11) showed a delayed response, typically lagging 0.5 to 5 hours after rainfall. This attenuation is attributed to its large, flat catchment and long flow path across vegetated swales. Cornhusker (Figure 5.12) responded more quickly due to its compact and highly impervious drainage area. This setting not only generated a prompt peak but also allowed sufficient flow detection in the recession limb. Lastly, Beatrice North (Figure 5.13), being the smallest and most impervious site, responded the fastest to rainfall with minimal lag, producing sharp and brief hydrograph peaks. These variations in timing and shape of the hydrographs highlight how catchment characteristics influence flow dynamics during storm events.

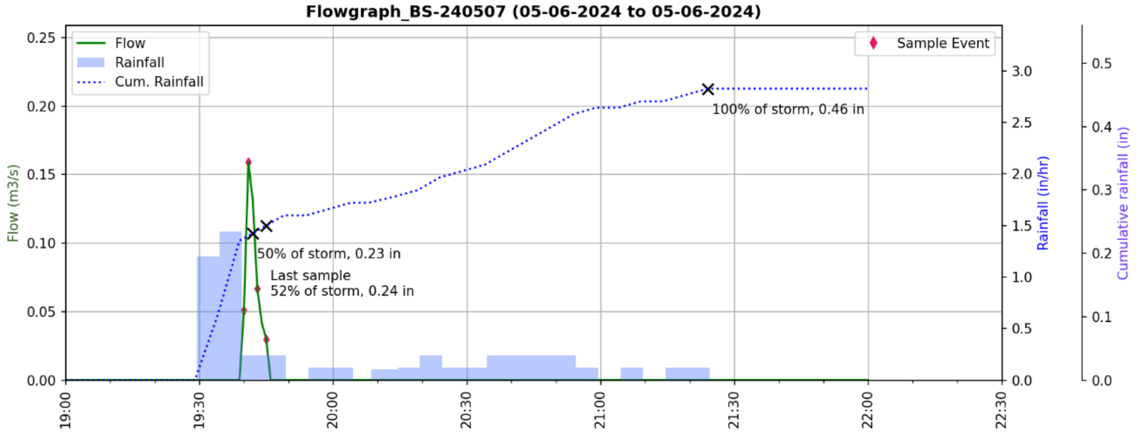

Figure 5.11 Typical flow hydrograph (Beal Slough)

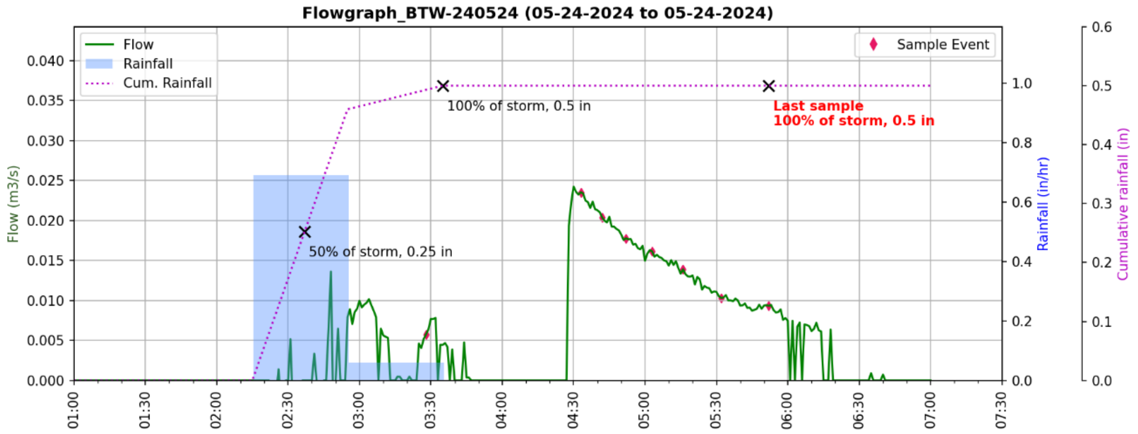

Figure 5.12 Typical flow hydrograph (Beatrice West)

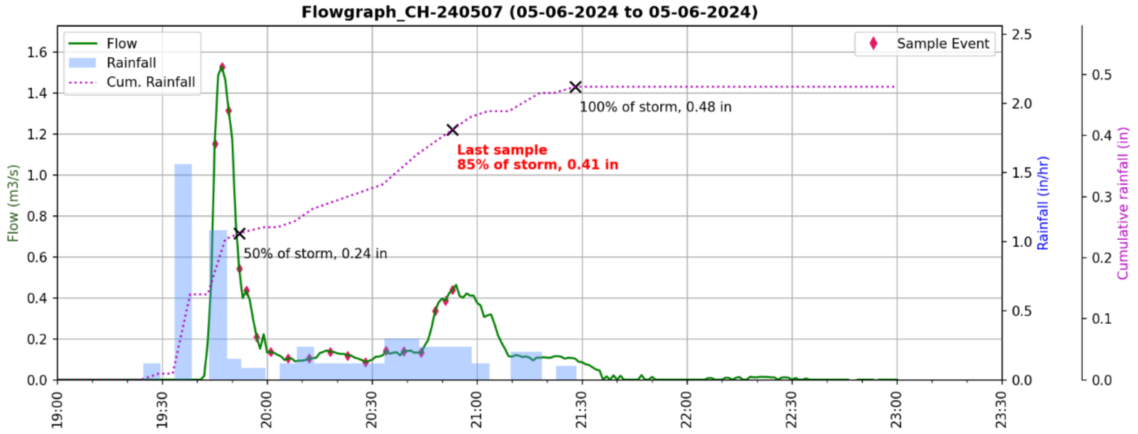

Figure 5.13 Typical flow hydrograph (Cornhusker)

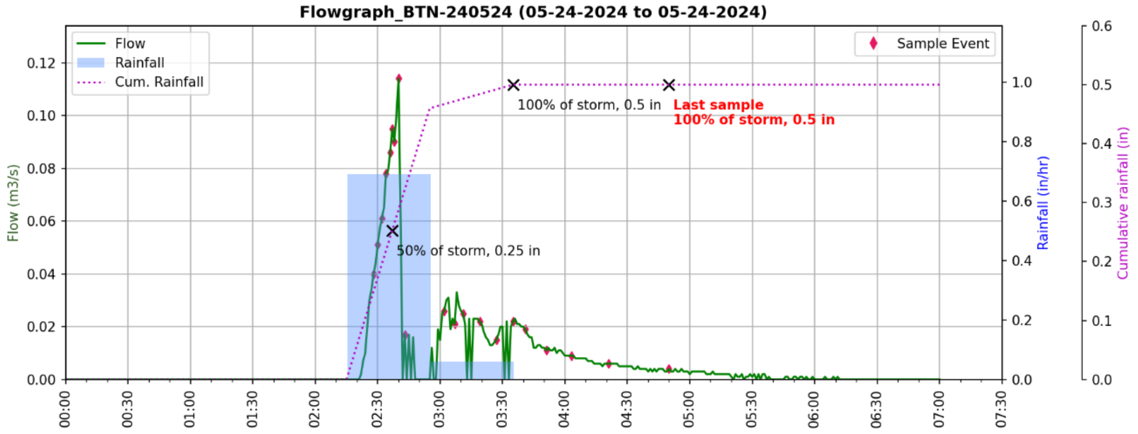

Figure 5.14 Typical flow hydrograph (Beatrice North)

Average cumulative flow volume per storm ranged from 105.8 to 511.1 m³ across sites, while peak flow rates varied from 0.10 to 0.28 m³/s (Table 5.8).

Table 5.10 Summary of flow at each site

| Site | Beal Slough | | Beatrice West | | Cornhusker | | Beatrice North | |
|---|---|---|---|---|---|---|---|---|
| Metric | Max. flow ($m^3/s$) | Flow volume ($m^3$) | Max. flow ($m^3/s$) | Flow volume ($m^3$) | Max. flow ($m^3/s$) | Flow volume ($m^3$) | Max. flow ($m^3/s$) | Flow volume ($m^3$) |
| Obs. | 29 | | 22 | | 30 | | 30 | |
| Minimum | 0.01 | 0.50 | 0.01 | 0.1 | 0.01 | 49.6 | 0.01 | 55.8 |
| Maximum | 2.87 | 433.5 | 0.43 | 2186 | 1.17 | 2074 | 0.41 | 1202 |
| Median | 0.14 | 67.4 | 0.04 | 262.9 | 0.21 | 350.2 | 0.05 | 210.8 |
| Mean | 0.25 | 105.8 | 0.10 | 505.8 | 0.28 | 511.8 | 0.11 | 322.4 |
| Std. dev. | 0.54 | 101.3 | 0.11 | 573.3 | 0.27 | 502.5 | 0.12 | 287.4 |

### *5.4.2 Sediment characteristics*

The four monitoring sites exhibited distinct land use characteristics, which were reflected in both their total suspended solids (TSS) concentrations and particle size distribution (PSD). Beal Slough was dominated by coarser particles, while Beatrice North had the finest median particle size among all sites. Based on median TSS concentrations, the sites ranked from highest to lowest as follows: Beatrice North, Beal Slough, Cornhusker, and Beatrice West. Although Cornhusker and Beatrice West displayed similar PSD curves, Cornhusker consistently showed higher TSS concentrations and a greater proportion of fine particles. Except for two events in the spring of 2024, Beatrice West consistently exhibited lower TSS concentrations than the other three sites, likely due to the presence of a swale that facilitated sediment settling.

Site-specific factors help explain the observed sediment patterns. At Beatrice North, a gravel parking lot near the sampling point was the likely source of high soil erosion and contributed to the finer sediment distribution. Cornhusker received frequent soil runoff from nearby lawns, especially during spring, which coincided with the observed increase in fine sediment content. In contrast, Beal Slough, which drains a relatively steep roadway, exhibited a coarser PSD, possibly due to increased mobilization of larger particles (Macdonald et al. 2000; Bilby et al. 1989). In addition, no distinct external erosion sources were identified in this site, due to which the proportion of fine particles was lower compared to other sites. Finally, the presence of a well-vegetated swale at Beatrice West likely filtered runoff before it entered the storm drain, resulting in lower TSS concentrations and reduced fine particle contributions across most sampling events.

Note that with a sample size of four sites, trends related to the land use mix at each site with the PSD and sediment loading were unable to be identified.

### *5.4.3 Temporal trends*

All four sites exhibited a general decline in median sediment concentration over the course of the year, with the highest concentrations occurring in spring and lower values in summer and fall (Figure 5.14 and Figure 5.15). These figures present the seasonal variation in TSS concentrations categorized by particle size, highlighting patterns observed throughout 2024 and comparing spring data between 2024 and 2025. This trend was especially pronounced at Beatrice North and Cornhusker, where finer particles (<32 μm) showed a distinct seasonal pattern: elevated concentrations during spring, followed by a drop in summer and a slight rise in fall. A similar pattern was observed at Beal Slough and Beatrice West, although the differences were less prominent. When comparing spring TSS data between 2024 and 2025, Beal Slough exhibited an increase in fine particle fractions, while other sites showed little year-to-year variation. These seasonal trends may be explained by reduced vegetation cover in spring, which makes soil more prone to erosion as noted in previous studies, along with the effects of winter roadway maintenance that can lead to sediment buildup and greater wash-off during early spring storms.

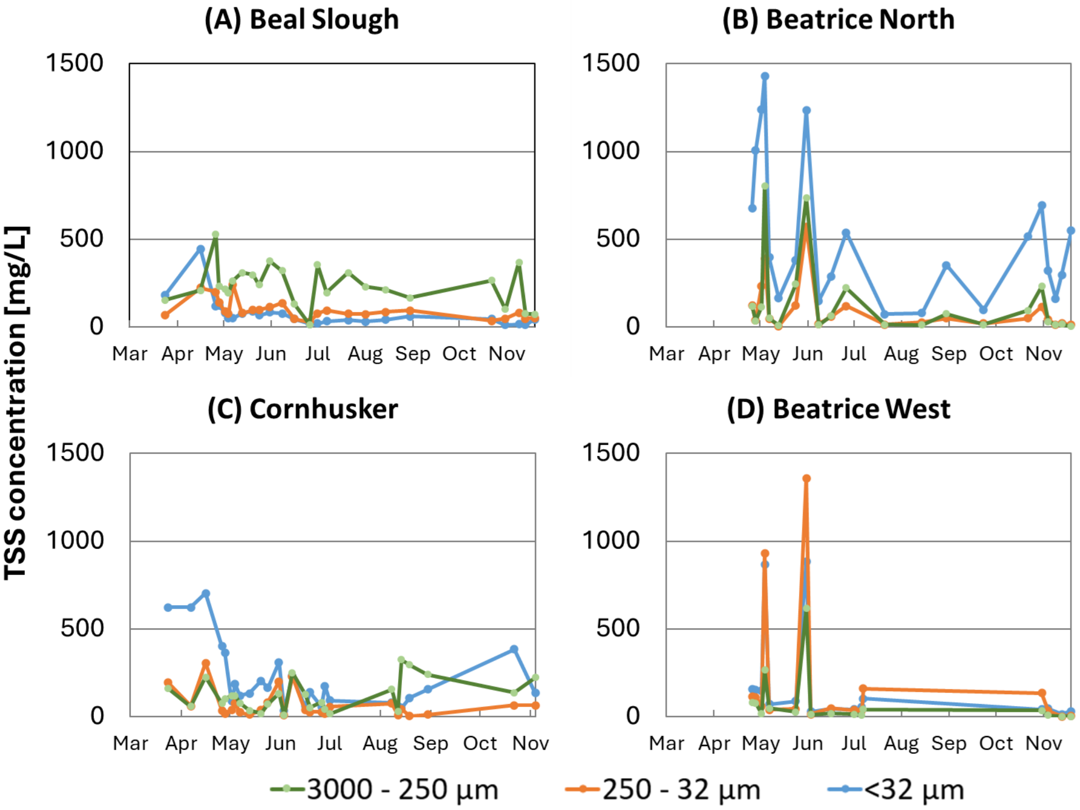

Figure 5.15 Temporal trends in TSS concentration by particle size class (2024)

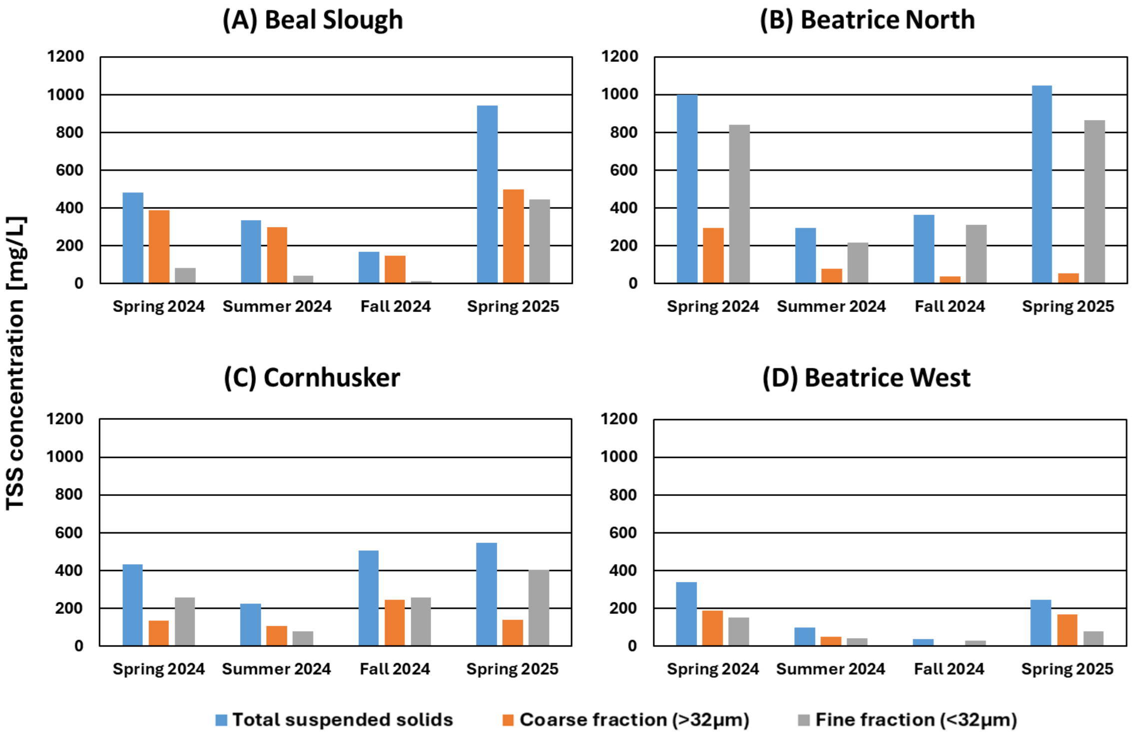

Figure 5.16 Median TSS concentrations by season for each site

Seasonal variation in particle size distribution (PSD) also varied among sites, shown in Figure 5.17 based on the dataset that includes all samples collected across seasons and monitoring sites. In some locations, such as Beal Slough and Cornhusker in Lincoln, the PSD was noticeably finer in spring compared to the rest of the year. This pattern suggests that winter sediment buildup and limited vegetation cover in spring increased erosion and the transport of fine particles. In contrast, little seasonal difference was observed at Beatrice North and Beatrice West. The gravel parking area at Beatrice North and the vegetated buffer and swale at Beatrice West likely influenced the particle characteristics, reducing the typical seasonal variation.

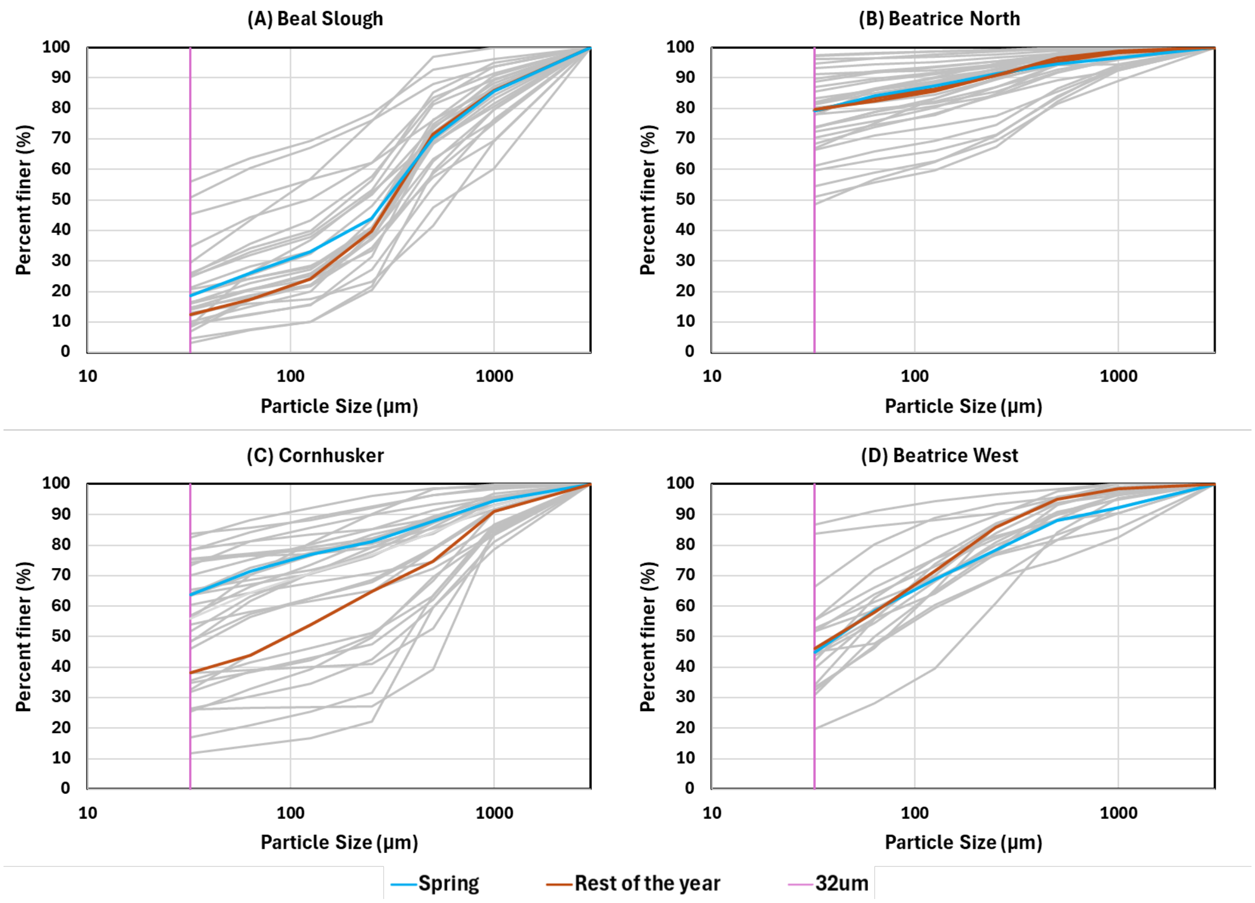

Figure 5.17 PSD distributions showing average PSD for spring and the rest of the year

The seasonality of the TSS, especially fines, as well as the observation for the degree of off-site contribution to the fines, suggests that additional emphasis on erosion control at the source for off-site contributions may be valuable for reducing sediment in the runoff. And by reducing the load of fines in the runoff, systems like a hydrodynamic separator may be more effective.

## 5.5 Role of Vegetated buffer and Grass swale in Beatrice West

At the Beatrice West (BTW) site, the highway runoff flows over a vegetative filter strip approximately 20 feet wide before entering a grass swale that runs along the length of the catchment and eventually drains to the outlet. This promotes both infiltration and filtering of the runoff before it exits the site. During smaller storms, especially following dry periods, no flow was recorded at the outlet, which suggests a high rate of infiltration within the vegetated buffer. As shown in Table 5.10, several small storms occurred in the fall, typically less than 0.5 inches in depth. During these events, Beatrice North (BTN) recorded flow and samples, while no flow was observed at Beatrice West (BTW). It is also important to note that the drainage area at BTW is nearly three times larger than that of BTN. However, the median total runoff volume was only about 1.25 times greater (Table 5.9), further supporting the presence of substantial infiltration. The two largest TSS events at Beatrice West are bolded in Table 5.10. These observations indicate that for storms under approximately 0.5 inches, the vegetative filter strip and grass swale at BTW allow high infiltration and provide effective pretreatment of roadway runoff.

Table 5.11 Event based comparison of rainfall depth and TSS between Beatrice sites

| Sample collection date | Rainfall depth (in) | TSS | |
|---|---|---|---|
| | | **Beatrice West** | **Beatrice North** |
| 4/26/2024 | 0.44 | 348 | 918 |
| 4/28/2024 | 0.27 | 340 | 1079 |
| 5/2/2024 | 0.56 | 226 | 1590 |
| **5/4/2024** | **1.5** | **2066** | **2625** |
| 5/7/2024 | 0.28 | 159 | 495 |
| 5/13/2024 | 0.34 | No flow | 180 |
| 5/24/2024 | 0.5 | 157 | 750 |
| **5/31/2024** | **0.67** | **2860** | **2548** |
| 6/3/2024 | 0.32 | 55 | Sampler failed |
| 6/8/2024 | 0.19 | No flow | 179 |
| 6/16/2024 | 1.34 | 109 | 408 |
| 6/26/2024 | 0.41 | No flow | 881 |
| 7/1/2024 | 0.54 | 91 | Sampler failed |
| 7/6/2024 | 0.78 | 99 | |
| 7/7/2024 | 1.04 | 304 | |
| 7/21/2024 | 0.52 | No flow | 101 |
| 8/14/2024 | 0.16 | | 118 |
| 8/30/2024 | 0.66 | | 476 |
| 9/23/2024 | 0.15 | | 132 |
| 10/22/2024 | 0.22 | | 662 |
| 10/31/2024 | 1.3 | 209 | 1041 |
| 11/4/2024 | 0.76 | 87 | 393 |
| 11/9/2024 | 0.48 | 20 | 185 |
| 11/13/2024 | 0.45 | 15 | 334 |
| 11/19/2024 | 0.73 | 37 | 564 |
| 12/14/2024 | 0.18 | No flow | 103 |
| 3/6/2025 | 0.11 | | 1669 |
| 3/20/2025 | 0.2 | | 1125 |
| 4/2/2025 | 0.46 | 685 | 3530 |
| 4/4/2025 | 0.1 | No flow | 465 |
| 5/20/2025 | 0.78 | 245 | 970 |
| 5/27/2025 | 0.35 | 7 | 72 |
| 6/2/2025 | 0.26 | 231 | 769 |
| 6/4/2025 | 0.77 | 73 | 595 |

TSS data also supports that the vegetated filter strip and grass swale at BTW help improve water quality. As shown in Figure 5.3, both the distribution and median TSS concentrations at BTW were lower than those at the other sites. Most storms resulted in relatively low sediment levels, except for two storms in 2024 where TSS went over 2,000 mg/L and one storm in spring 2025 where it was just over 500 mg/L. These higher values were associated with rainfall depths greater than 0.5 inches and higher intensities, as summarized in Appendix I: Laboratory measurements of samples analyzed. Literature also supports the idea that vegetated surfaces help reduce sediment in runoff. Grass swales and filter strips along roads have shown TSS removal rates up to 91% (Characklis & Wiesner, 1997; Barrett et al., 2004). Li et al. (2008) found that grass-covered roadsides removed most TSS and metals within about 13 feet of pavement. These studies suggest that the effectiveness of vegetated buffer and swale is consistent with the 80% TSS reduction goal in NDOT's permit. While high sediment runoff did occur during a few large storms, those events typically occur beyond the first 0.5 inches of rainfall. Overall, the data indicates that this vegetated buffer and swale configuration can be a practical and effective BMP for treating typical roadway runoff.

### 5.6 Street sweeping

The data was analyzed to examine if there was a relationship between street sweeping times and sediment in the runoff.  Street sweeping data were available only for the Lincoln sites, Beal Slough and Cornhusker, while no records were provided for Beatrice since street sweeping is not performed there. In Lincoln, streets are cleaned using mechanical sweepers that remove debris and sediment from roadway surfaces. The sweeping records obtained from the City of Lincoln showed 13 sweeping events for Beal Slough and 15 for Cornhusker during the monitoring period. Sweeping was carried out between March 2024 and May 2025—specifically from March 7, 2024, to May 14, 2025, for Beal Slough, and from March 12, 2024, to May 7, 2025, for Cornhusker (Appendix O: Street sweeping and regression analysis). Stormwater samples were collected within these same periods. Figure 5.18 presents the timing of street sweeping events and the sampled storms with corresponding rainfall depth.

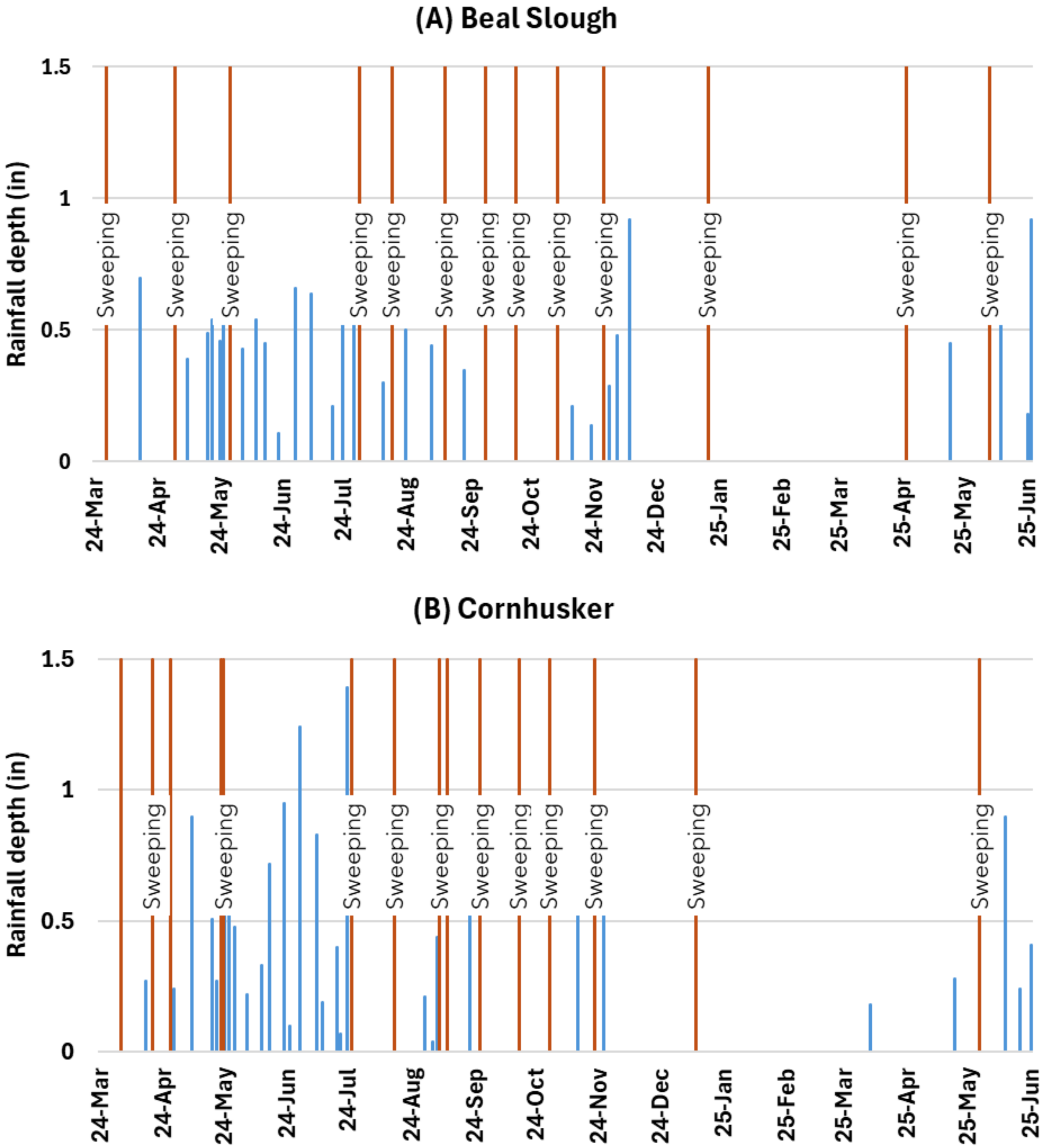

Figure 5.18 Street sweeping frequency at Lincoln sites

A regression analysis was conducted to evaluate whether street sweeping affected TSS levels or trends. Both street sweeping and rainfall can remove sediment from roadway surfaces.

So, the analysis used the shorter of the two intervals: days since the last sweeping or days since the last rainfall. The calculated values are presented in Table 5.11.

Table 5.12 Shorter of days since sweeping or rainfall at Lincoln sites

| Sample | Shorter of days since sweeping and rainfall | Sample | Shorter of days since sweeping and rainfall |
|---|---|---|---|
| BS-240324 | 9 | CH-240324 | 9 |
| BS-240416 | 6 | CH-240407 | 2 |
| BS-240426 | 8 | CH-240416 | 9 |
| BS-240428 | 0 | CH-240426 | 8 |
| BS-240502 | 1 | CH-240428 | 0 |
| BS-240504 | 1 | CH-240502 | 1 |
| BS-240507 | 1 | CH-240504 | 1 |
| BS-240513 | 5 | CH-240507 | 1 |
| BS-240520 | 6 | CH-240513 | 5 |
| BS-240524 | 2 | CH-240520 | 6 |
| BS-240531 | 5 | CH-240524 | 2 |
| BS-240608 | 3 | CH-240531 | 5 |
| BS-240616 | 6 | CH-240603 | 0 |
| BS-240626 | 7 | CH-240608 | 3 |
| BS-240701 | 3 | CH-240616 | 6 |
| BS-240707 | 1 | CH-240619 | 2 |
| BS-240721 | 8 | CH-240626 | 7 |
| BS-240801 | 7 | CH-240628 | 0 |
| BS-240814 | 5 | CH-240701 | 3 |
| BS-240830 | 9 | CH-240808 | 15 |
| BS-241022 | 8 | CH-240812 | 3 |
| BS-241031 | 8 | CH-240814 | 1 |
| BS-241109 | 2 | CH-240819 | 2 |
| BS-241113 | 3 | CH-241022 | 14 |
| BS-241119 | 4 | CH-241104 | 1 |
| BS-250425 | 4 | CH-250315 | 9 |
| BS-250520 | 6 | CH-250425 | 3 |
| BS-250602 | 3 | CH-250520 | 13 |
| BS-250604 | 2 | CH-250527 | 3 |
|  |  | CH-250602 | 3 |

The regression results are provided in Appendix O: Street sweeping and regression analysis. The model coefficients showed little statistical significance, like previous findings. The results indicated that including street sweeping in the model explained only a small portion of the variation in the data. The in-sample $R^2$ values were 0.36, 0.26, and 0.28 for TSS, CSS, and FSS, showing weak relationships. The cross-validation $R^2$ values were negative for all except log-FSS (0.02), which means the models did not perform well when applied to new data.

Overall, the analysis showed that street sweeping did not have a strong statistical influence on TSS or its trend. However, sweeping still plays an important role in removing debris and coarse sediment from roadways. The lack of correlation between sweeping frequency and measured TSS may be due to high off-site sediment contributions, frequent sweeping during the monitoring period, or the large variability in rainfall intensity and TSS loading between storms.

## 5.7 Permit context for stormwater treatment design

This section examines how stormwater monitoring data can be used to evaluate compliance if stormwater treatment facilities meet NDOT's permit requirements. It starts by explaining the key permit rules and the assumptions used when applying them to different sites. Then, it outlines how the SAFL Baffle, a stormwater treatment device, is evaluated using site-specific data and simulated through the SHSAM model. The final part of the section examines how well the SAFL Baffle performs under different conditions at each site and discusses situations where it may not be sufficient on its own to meet the required TSS removal targets.

### *5.7.1 Understanding NDOT's regulatory criteria for Stormwater Treatment*

Based on NDOT's permit requirements outlined in the *Drainage Design and Erosion Control Manual* (NDOT 2024), several key assumptions are used when interpreting stormwater treatment obligations for right-of-way (ROW) sites. The definition of the treatment area varies depending on how the ROW is interpreted. In a narrow interpretation, ROW includes only the roadway and easement areas directly maintained by NDOT. A broader view includes adjacent access or secondary roads maintained by other public agencies, such as the state or city. An even more inclusive interpretation considers the NDOT ROW area along with off-site areas that contribute to roadway runoff as part of the treatment area.

Accordingly, this report evaluates three possible **ROW definition cases:**

- **Case 1**: The entire drainage area of the catchment is included—this covers NDOT ROW, adjacent access roads, and all contributing off-site areas.
- **Case 2**: Only NDOT ROW and access roads maintained by other public agencies are considered.
- **Case 3**: Only the NDOT ROW easement is treated as the contributing area.

These cases are illustrated in Figure 5.19 where the respective areas for each case are highlighted with red boundaries.

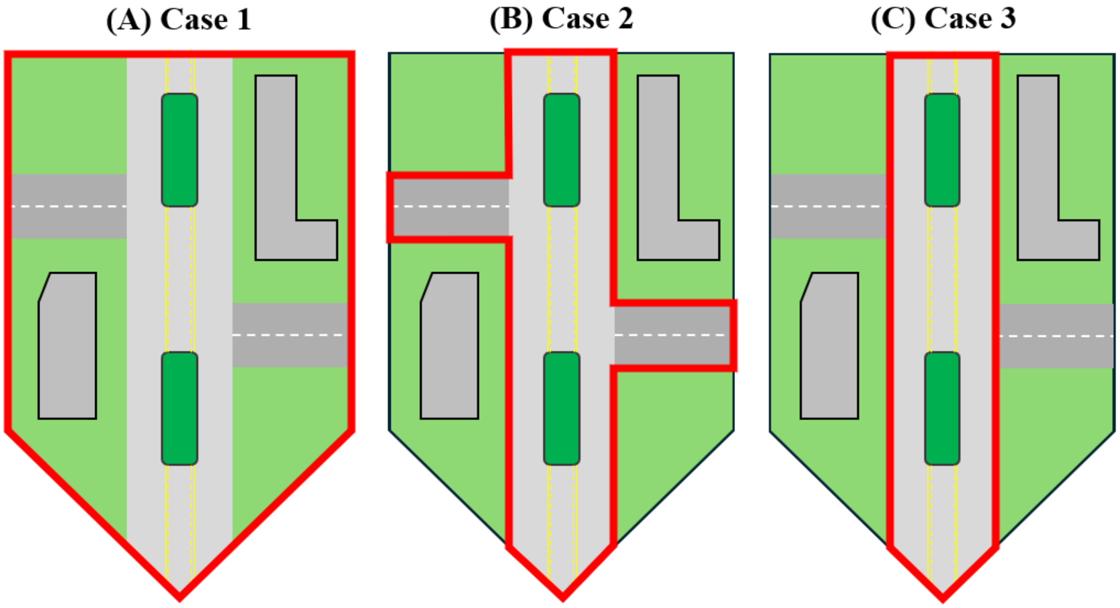

Figure 5.19 Possible ROW cases. (A) Entire catchment, (B) Roadway maintained by public agencies, and (C) Only the NDOT ROW

In practice, most Nebraska roadway sites receive runoff from nearby off-site areas that discharge into a common stormwater system. Therefore, for Cases 2 and 3, sediment removal achieved from treating these off-site areas may be credited toward fulfilling the 80% TSS removal requirement for the NDOT ROW portion.

Water Quality Volume (WQV) is calculated using 0.5 inches of rainfall over the treatment drainage area, where the area is defined solely as impervious cover within the NDOT ROW. This means the required treatment volume is based only on impervious surfaces under NDOT jurisdiction. These assumptions form the basis for evaluating the effectiveness of hydrodynamic separators, such as the SAFL Baffle, using an area-weighted TSS removal equation which is given as:

$$0.8 \cdot \frac{Area_{road}}{Area_{catchment}} \cdot \frac{TSS_{road}}{TSS_{catchment}} \leq Removal\,\% \qquad (5.1)$$

where:

$Area_{road}$ = impervious area within NDOT right-of-way (acres)

$Area_{catchment}$ = impervious area within contributing catchment of the outfall (acres)

$TSS_{road}$ = TSS concentration from roadway runoff (mg/L)

$TSS_{catchment}$ = TSS concentration from total contributing catchment (mg/L)

*Removal %* = removal efficiency of hydrodynamic separator (%)

The left-hand side of Equation 5.1 represents the required removal efficiency for a contributing catchment, calculated based on the proportion of the treatment area relative to the total contributing catchment area. The variables $\mathrm{Area_{road}}$ and $\mathrm{Area_{catchment}}$ denote the impervious areas within the NDOT right-of-way and the contributing off-site catchment, respectively. These areas can be estimated using a combination of GIS tools, digital elevation models (DEMs), and field verification. The TSS concentration specific to roadway runoff, $\mathrm{TSS_{road}}$, can be derived from published studies that focus on pollutant loading from road surfaces—for example, Winston et al. (2023) or data from Beal Slough site, which provides roadway-specific TSS concentration values. Meanwhile, the TSS concentration for the entire contributing catchment, $\mathrm{TSS_{catchment}}$, may be estimated based on field data collected from catchments with similar land use, drainage patterns, and climatic conditions. These sources provide the necessary inputs to estimate the required efficiency of a hydrodynamic separator.

### *5.7.2 Assessing potential for permit compliance using SAFL Baffle*

The SAFL Baffle, introduced in Section 2.3.3, is a structural best management practice (BMP) and is a hydrodynamic separator recommended by NDOT due to its cost-effectiveness and compact design. Compared to other structural BMPs, it requires less space, making it suitable for constrained urban roadway settings. The system operates by using a sump manhole to capture sediment through gravitational settling while reducing the potential for resuspension.

However, for optimal performance, periodic maintenance is essential to remove accumulated sediment. The SAFL Baffle is available in several size options, and Figure 5.20 illustrates the relative sump depths below the baffle within the manhole. The figure also presents the corresponding sediment removal efficiencies observed at the monitored sites.

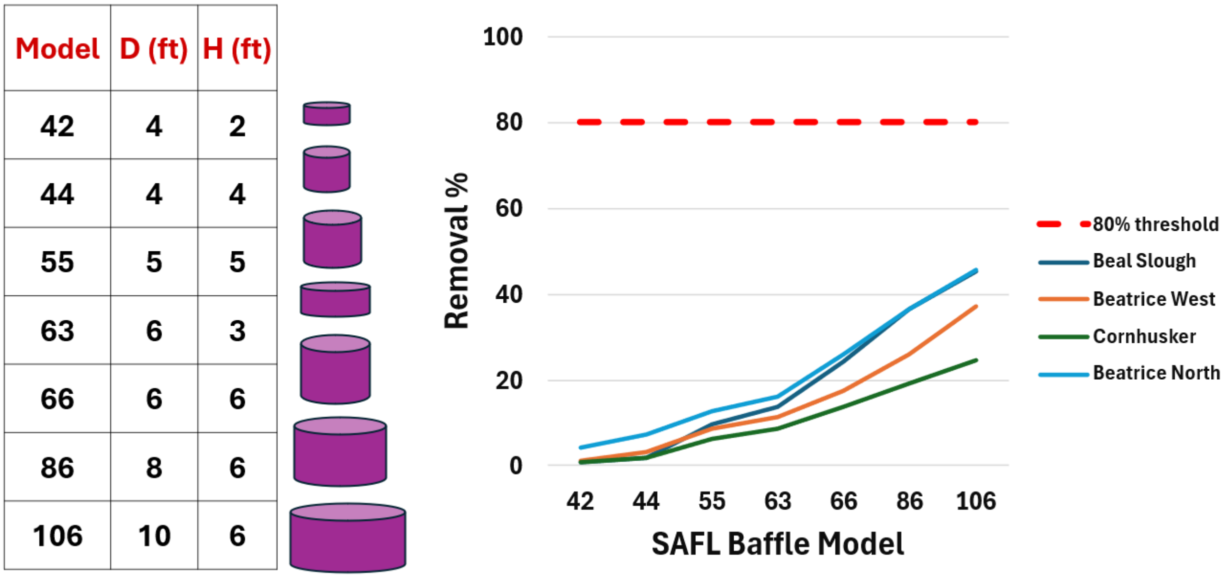

| Model | D (ft) | H (ft) |
|---|---|---|
| 42 | 4 | 2 |
| 44 | 4 | 4 |
| 55 | 5 | 5 |
| 63 | 6 | 3 |
| 66 | 6 | 6 |
| 86 | 8 | 6 |
| 106 | 10 | 6 |

Figure 5.20 Sump sizes used in the SHSAM model (A) and corresponding sediment removal percentages at the monitoring sites (B)

To estimate the TSS removal efficiency of the SAFL Baffle under site-specific conditions, NDOT utilizes the SHSAM (Sizing Hydrodynamic Separators and Manholes) software. SHSAM is a modeling tool developed to evaluate the performance of hydrodynamic separators based on design inputs and site characteristics (Omid, 2010). The software requires several key inputs, including sump geometry and inflow pipe diameter, both of which can be selected from default configurations provided within SHSAM. Additionally, high-resolution rainfall data (typically 15-minute intervals) spanning multiple years, or a defined study period is needed to simulate runoff events.

Accurate estimation of TSS removal also depends on sediment and catchment characteristics. Sediment input includes TSS concentration and PSD, which are ideally obtained through field monitoring or adapted from comparable studies. As shown in Figure 5.21, most of the effective removal occurs within the coarser particle size range, while finer particles are removed to a much lesser extent. This highlights the importance of accurately representing PSD, since overall TSS removal efficiency largely depends on the proportion of coarse sediment present in the inflow.

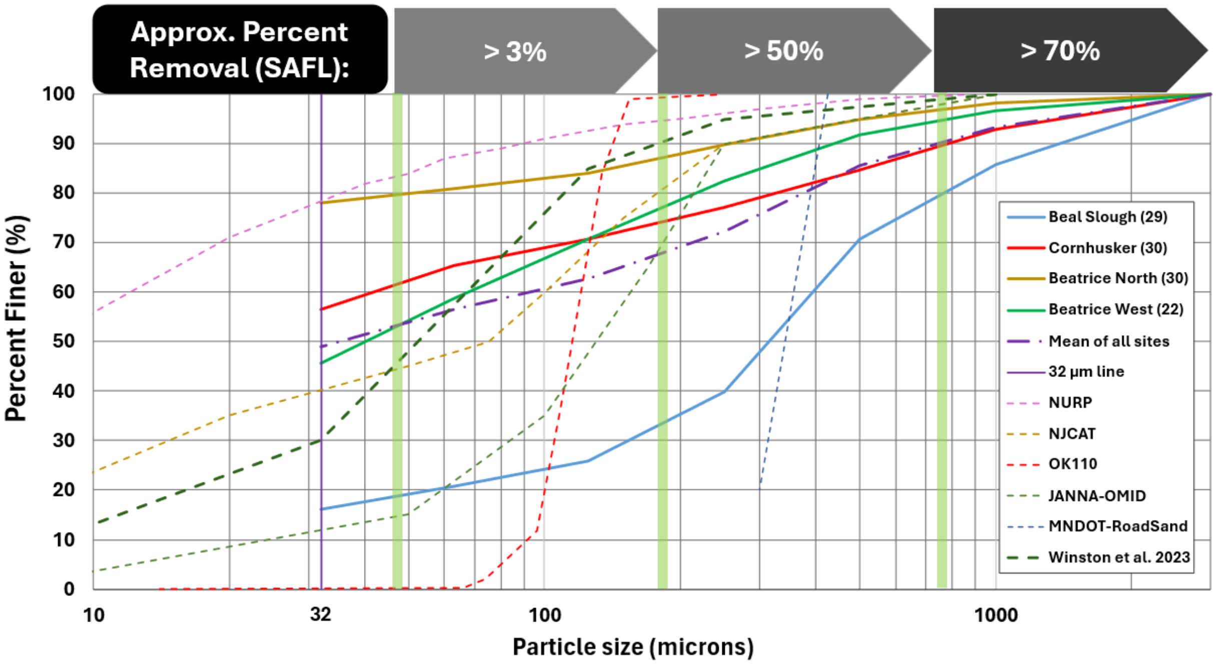

Figure 5.21 Approximate removal percentages for different particle size ranges. *Vertical shaded regions indicate the estimated sediment removal efficiencies by the SAFL Baffle based on SHSAM simulations at one representative site.*

Catchment parameters such as total drainage area (in acres), impervious surface percentage, hydraulic length, average slope, and curve number (for pervious areas) are typically derived using GIS tools, digital elevation data (USDA NRCS 2024) and field validation. These inputs collectively allow SHSAM to simulate treatment performance under realistic Nebraska roadway conditions and assess whether the SAFL Baffle meets regulatory requirements.

### *5.7.3 Assessing removal efficiency of SAFL Baffle for monitored sites*

Based on the three ROW definition cases outlined in Section 5.5.1, the performance of the SAFL Baffle can be evaluated under varying treatment area scenarios. The SAFL Baffle is typically evaluated based on its annual TSS removal performance. Accordingly, sediment data from the 2024 monitoring period were used for all four sites to assess its effectiveness using the SHSAM software. The year 2024 was selected because data were available for all seasons. Equation 5.1 was applied to calculate the required removal efficiency based on contributing catchment conditions and treatment area coverage. The input parameters required for this evaluation, including TSS concentrations, particle size distribution, and catchment characteristics reflecting different treatment areas for each case, are summarized in Table 5.12, Table 5.13, and Table 5.14. The methods used to determine catchment characteristics are described in Section 6.3. Impervious areas within the NDOT right-of-way, which are used to define the treatment area, are delineated in Figures 5.19 through 5.22.

Table 5.13 Catchment characteristics and median TSS at monitored sites (2024)

| **SITE** | ***Units*** | **Beal Slough** | **Beatrice West** | **Cornhusker** | **Beatrice North** |
|---|---|---|---|---|---|
| Area | *acres* | 27.6 | 39.81 | 19.45 | 13.22 |
| Impervious Area | *%* | 60 | 34 | 77 | 45 |
| Hydraulic length | *ft* | 2620 | 4388 | 2111 | 3395 |
| Average Slope | *%* | 2.9 | 0.75 | 0.74 | 0.48 |
| CN (pervious) | | 81 | 75 | 74 | 84 |
| NDOT ROW area (Impervious area) | *acres* | 4.45 (3.13) | 4.40 (4.31) | 4.67 (4.67) | 2.63 (2.58) |
| Access road area (Impervious area) | *acres* | 0.44 (0.44) | 2.67 (2.38) | 3.20 (3.04) | 0.36 (0.21) |
| Impervious area of the whole catchment | *acres* | 17.16 | 13.63 | 15.03 | 7.97 |
| Median TSS value | mg/L | 405 | 157 | 317 | 486 |

Table 5.14 Impervious areas under different ROW definition cases used as treatment area

| **ROW definition cases** | **Beal Slough** | **Beatrice West** | **Cornhusker** | **Beatrice North** |
|---|---|---|---|---|
| | *Areas in acres* | | | |
| Case 1 | 17.16 | 13.63 | 15.03 | 7.97 |
| Case 2 | 3.57 | 6.69 | 7.71 | 2.79 |
| Case 3 | 3.13 | 4.31 | 4.67 | 2.58 |

Table 5.15 Median particle size distribution by site (2024)

| **Particle size (µm)** | **Percent finer (%)** | | | |
|---|---|---|---|---|
| | **Beal Slough** | **Beatrice West** | **Cornhusker** | **Beatrice North** |
| 3000 | 100 | 100 | 100 | 100 |
| 1000 | 86 | 96 | 92 | 98 |
| 500 | 70 | 94 | 84 | 95 |
| 250 | 40 | 84 | 76 | 90 |
| 125 | 25 | 73 | 71 | 83 |
| 63 | 21 | 61 | 64 | 79 |
| 32 | 15 | 46 | 55 | 76 |
| 0 | 0 | 0 | 0 | 0 |

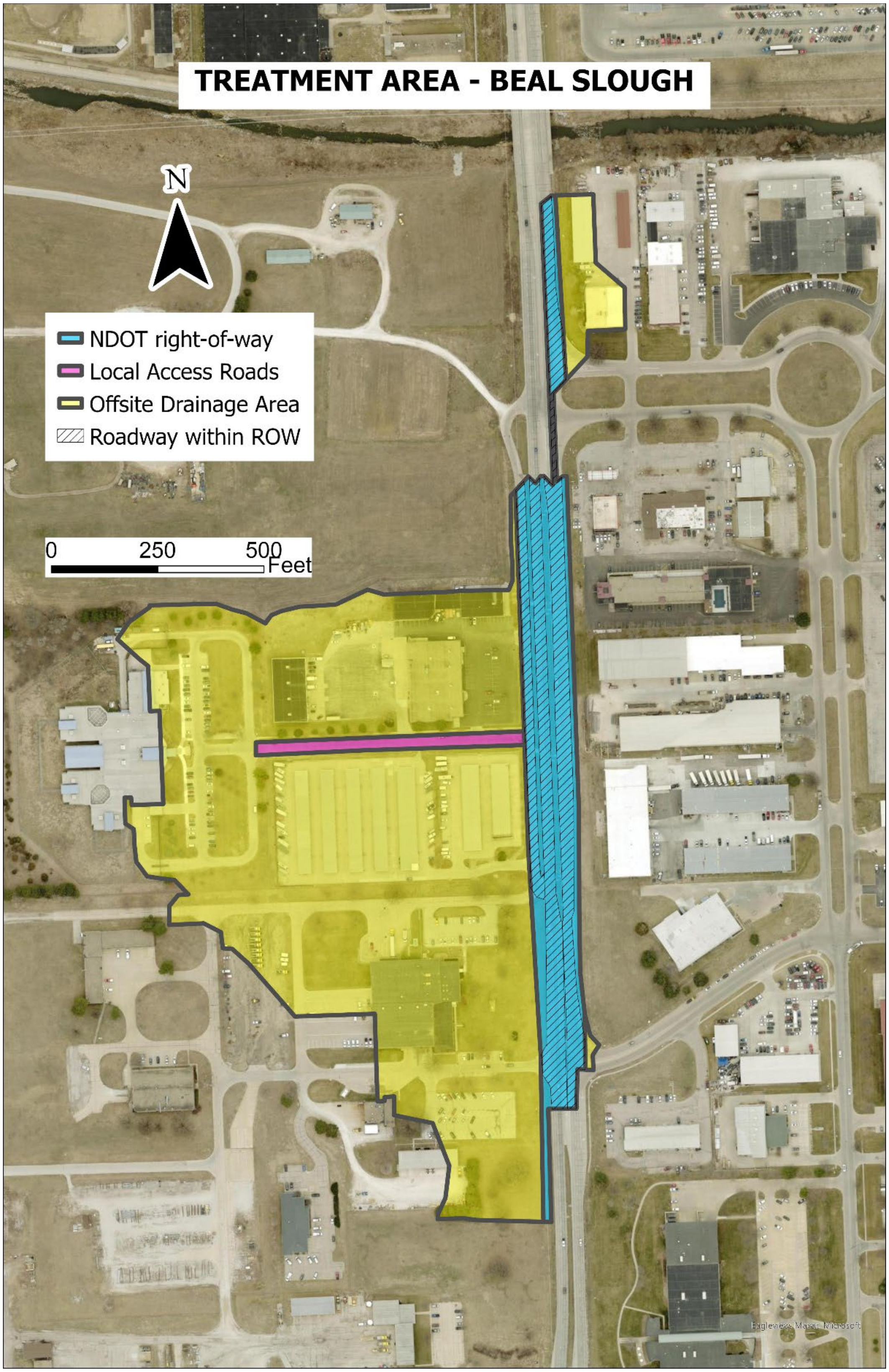

Figure 5.22 Treatment area within in NDOT right of way – Beal Slough

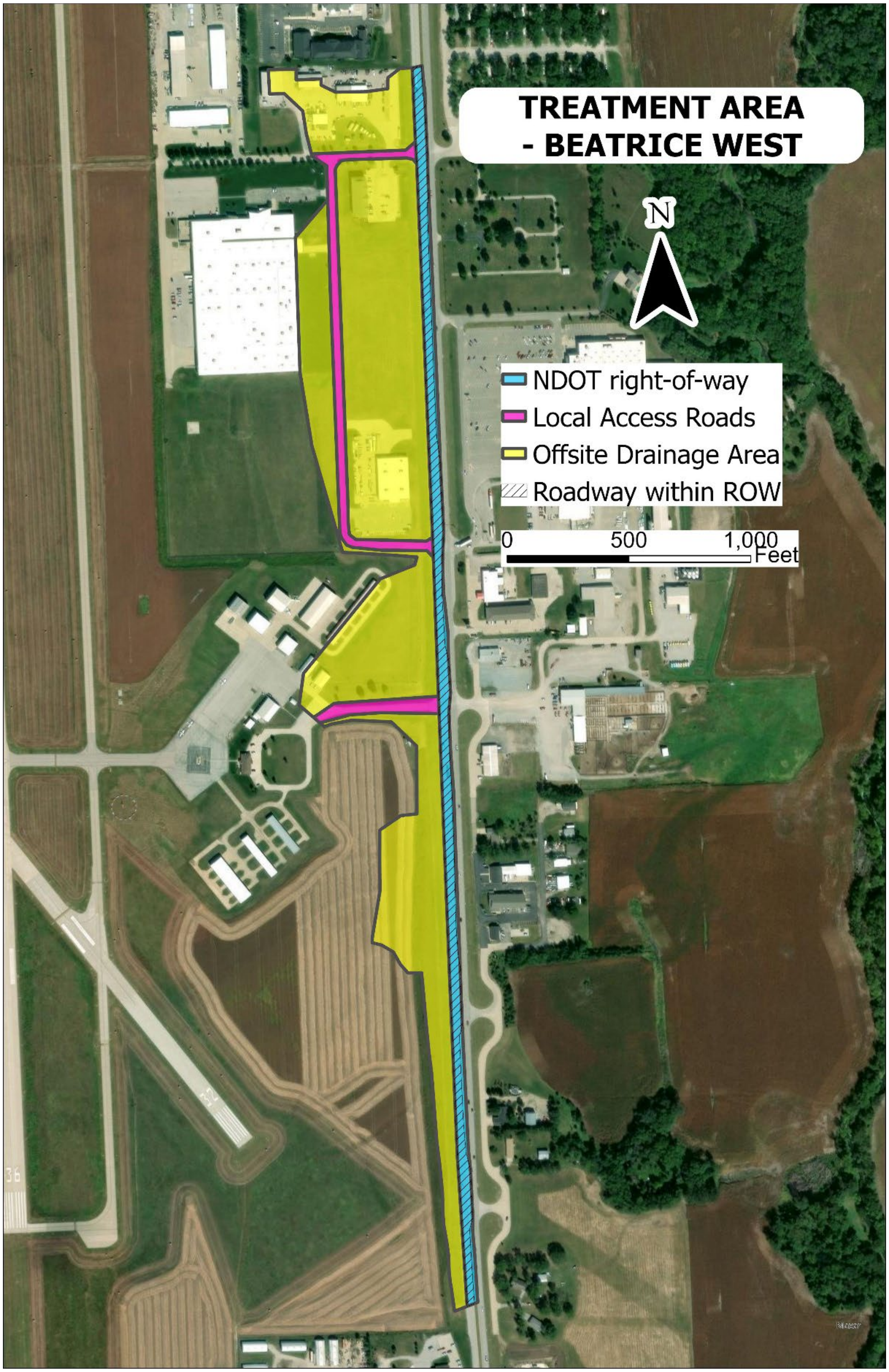

Figure 5.23 Treatment area within in NDOT right of way – Beatrice West

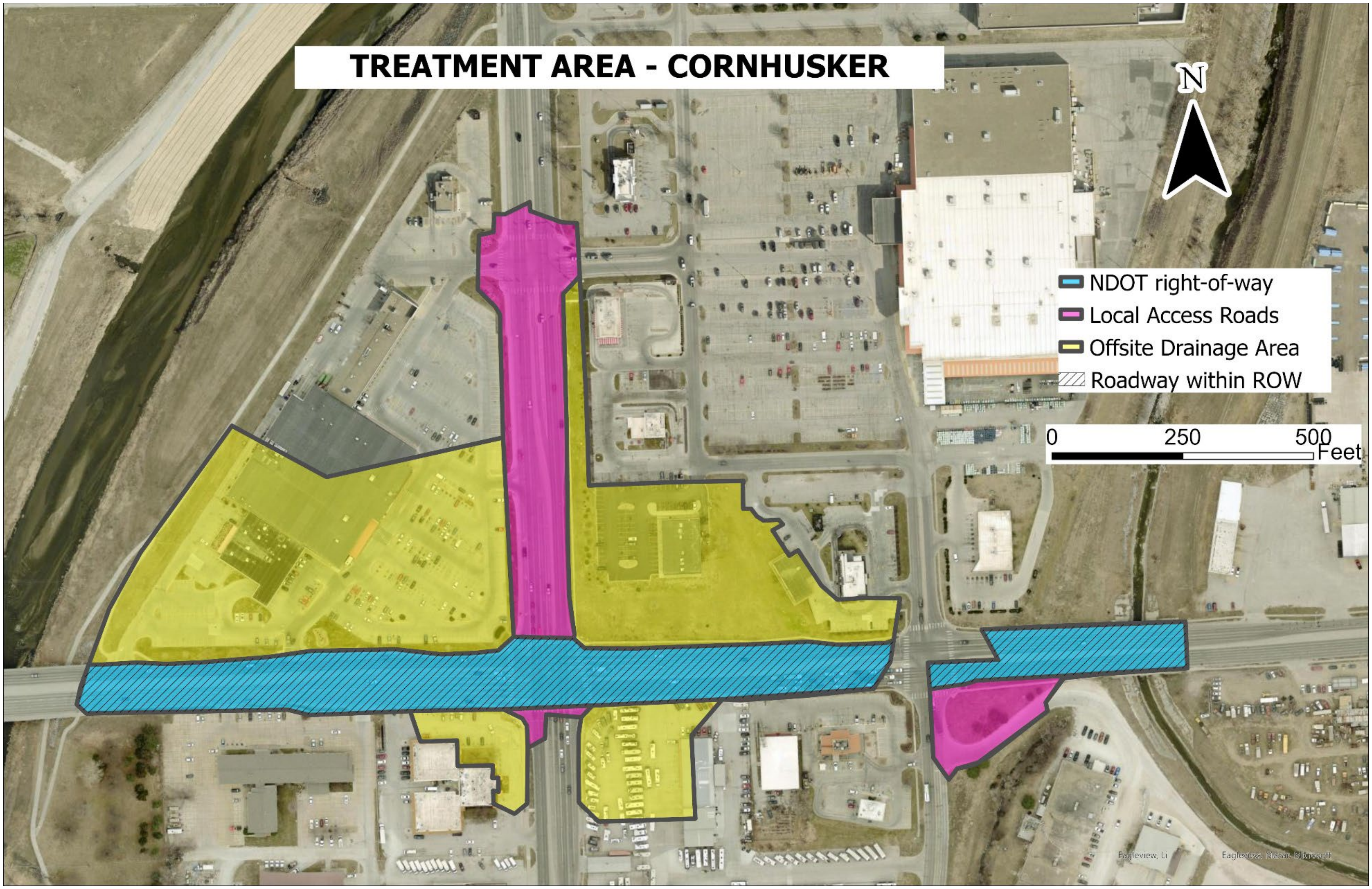

Figure 5.24 Treatment area within in NDOT right of way – Cornhusker

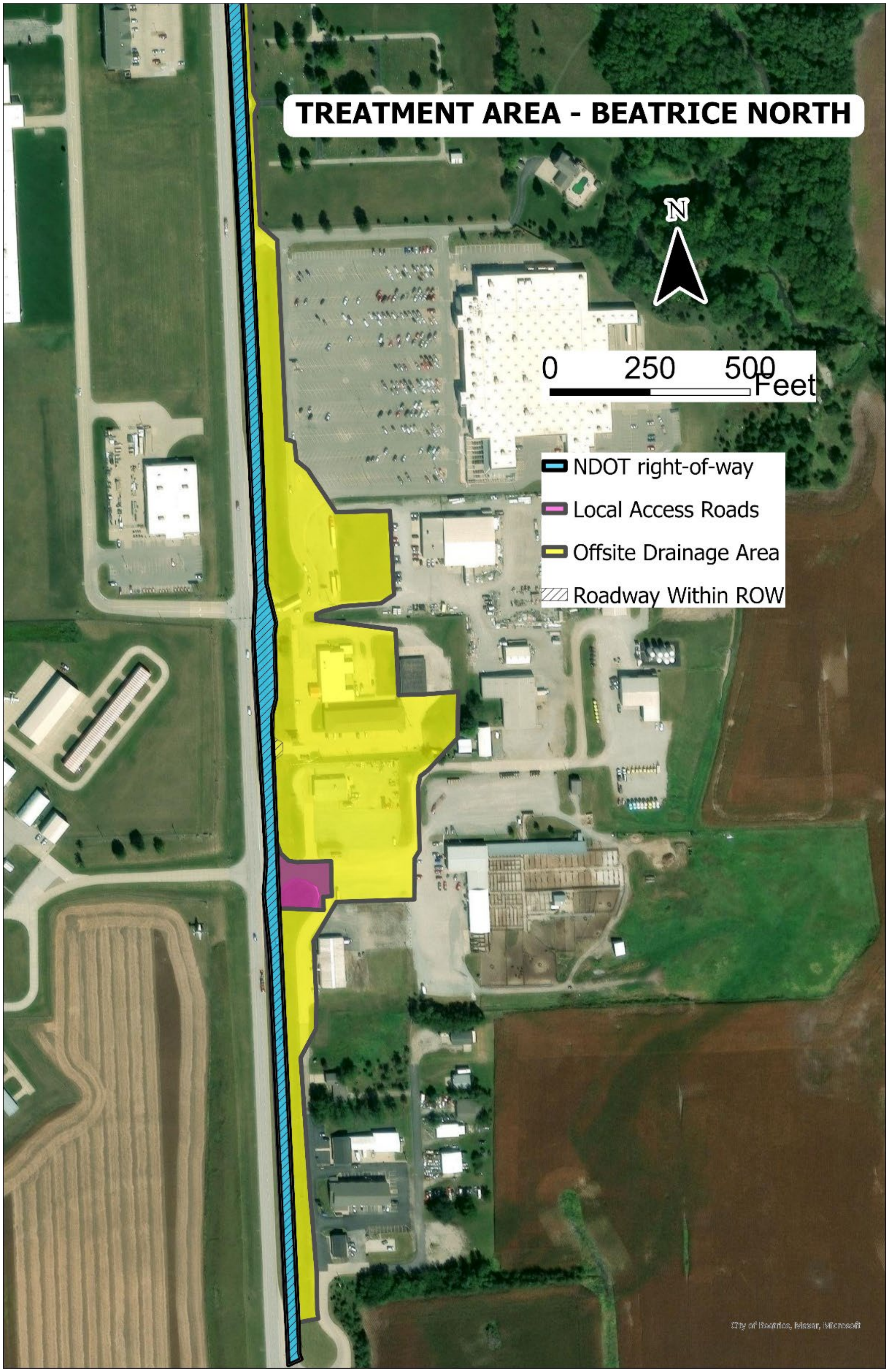

Figure 5.25 Treatment area within in NDOT right of way – Beatrice North

5.7.3.1 Evaluating SAFL Baffle based on data for all storms

SAFL Baffle models are evaluated under different ROW definition cases to assess their removal efficiency based on all sediment data from the year 2024.

For **Case 1**, which includes all areas within the catchment that contribute to total runoff, the SHSAM simulation results are summarized in Table 5.15. These results show that, when treating runoff from the entire catchment, the SAFL Baffle alone does not achieve the 80% sediment removal requirement at any of the sites. This finding suggests that full-catchment treatment using SAFL may be insufficient on its own.

Table 5.16 Removal efficiency of SAFL Baffle by site using SHSAM

| **Model** | | | **Load Removal Efficiency (%)** | | | |
|---|---|---|---|---|---|---|
| **Name** | **Sump diameter (ft)** | **Sump height (ft)** | **Beal Slough** | **Beatrice West** | **Cornhusker** | **Beatrice North** |
| 42 | 4 | 2 | 0.7 | 1.2 | 0.7 | 4.2 |
| 44 | 4 | 4 | 1.8 | 3.1 | 1.9 | 7.3 |
| 55 | 5 | 5 | 9.7 | 8.7 | 6.2 | 12.7 |
| 63 | 6 | 3 | 13.7 | 11.5 | 8.7 | 16 |
| 66 | 6 | 6 | 24.1 | 17.4 | 13.7 | 25.8 |
| 86 | 8 | 6 | 36.5 | 25.8 | 19.3 | 36.4 |
| 106 | 10 | 6 | 45.4 | 37.1 | 24.6 | 45.7 |

For **Case 2** and **Case 3,** the treatment areas are defined as the NDOT ROW easement along with access roads, and the NDOT ROW easement alone, respectively. In both cases, a substantial portion of runoff originates from off-site areas. According to the NDOT permit, treatment of sediment from these off-site sources can be credited toward meeting the permit requirements. Therefore, a follow-up analysis using Equation 5.1 was conducted to assess whether treating a combination of NDOT and off-site runoff could offset the required removal and satisfy permit requirements for both cases.

The selection of an appropriate SAFL Baffle model depends on both the assumed $TSS_{road}$ and the specific sediment and catchment characteristics of each site. Table 5.16 presents a series of checks for **Case 2** using Equation 5.1 to evaluate whether the SAFL Baffle can meet the permit requirement of removing 80% of sediment from the defined NDOT right-of-way (ROW). This analysis assumed the SAFL Baffle treats runoff from the entire catchment, and sediment removed from non-ROW areas was considered excess removal that may offset the required treatment.

Column B (Source of TSS) lists different assumed $TSS_{road}$ values used to calculate the target removal load—defined as 80% of the total roadway sediment load. Values of 13, 35, and 70 mg/L were adopted from Winston et al. (2023) to represent the minimum, median, and maximum $TSS_{road}$ concentrations observed in roadway runoff. Additionally, a value of 405 mg/L, based on measured TSS at Beal Slough, was included to represent locally observed roadway conditions. In Column C, the target load removal was calculated as 80% of the sediment load, using the product of the water quality volume (WQV) and the $TSS_{road}$ from the treatment area.

In Column D, the best-fitting SAFL Baffle models were identified for each case, with their removal efficiency in Column E. Models were selected based on their ability to remove the sediment load equivalent to the target removal load from the entire catchment. As baffle size number increases, a larger, deeper and more expensive baffle and associated manhole is required. A hypothetical $TSS_{road}$ value, referred to as “Max Treatable TSS,” is also presented. This value represents the highest roadway TSS concentration that the largest available SAFL Baffle model could theoretically handle under the given conditions. Similarly, an evaluation of **Case 3** is also presented in Table 5.17.

Table 5.17 Removal efficiency of SAFL Baffle for Case 2 using SHSAM

| **Site** | A | B | C | D | E | F | G |
|---|---|---|---|---|---|---|---|
| | **Assumed Roadway TSS (mg/L)** | **Source of TSS** | **Target load - 80% of roadway (kg)** | **Best SAFL Baffle model** | **% Removal of selected SAFL Baffle** | **Load removed by SAFL Baffle (kg)** | **Does it meet the target? (F>C?)** |
| Beal Slough | 13 | Winston et al. 2023 | 1.9 | 42 | 0.7 | 2.5 | Yes |
| | 35 | Winston et al. 2023 | 5.1 | 44 | 1.8 | 6.4 | Yes |
| | 70 | Winston et al. 2023 | 10.3 | 55 | 9.7 | 34.6 | Yes |
| | 405 | Beal Slough | 59.4 | 66 | 24.1 | 86.1 | Yes |
| | **1105** | **Max Treatable TSS** | **162.1** | **106** | **45.4** | **162.2** | **Yes** |
| Beatrice West | 13 | Winston et al. 2023 | 3.6 | 55 | 8.7 | 9.6 | Yes |
| | 35 | Winston et al. 2023 | 9.6 | 66 | 17.4 | 19.1 | Yes |
| | 70 | Winston et al. 2023 | 19.3 | 86 | 25.8 | 28.4 | Yes |
| | **148** | **Max Treatable TSS** | **40.7** | **106** | **37.1** | **40.8** | **Yes** |
| | 157 | Beatrice West | 43.2 | 106 | 37.1 | 40.8 | No |
| | 405 | Beal Slough | 111.4 | 106 | 37.1 | 40.8 | No |
| Cornhusker | 13 | Winston et al. 2023 | 4.1 | 44 | 1.9 | 4.7 | Yes |
| | 35 | Winston et al. 2023 | 11.1 | 55 | 6.2 | 15.2 | Yes |
| | 70 | Winston et al. 2023 | 22.2 | 66 | 13.7 | 33.5 | Yes |
| | **190** | **Max Treatable TSS** | **60.2** | **106** | **24.6** | **60.2** | **Yes** |
| | 317 | Cornhusker | 100.5 | 106 | 24.6 | 60.2 | No |
| | 405 | Beal Slough | 128.4 | 106 | 24.6 | 60.2 | No |
| Beatrice North | 13 | Winston et al. 2023 | 1.5 | 42 | 4.2 | 8.4 | Yes |
| | 35 | Winston et al. 2023 | 4.0 | 42 | 4.2 | 8.4 | Yes |
| | 70 | Winston et al. 2023 | 8.0 | 42 | 4.2 | 8.4 | Yes |
| | 405 | Beal Slough | 46.5 | 66 | 25.8 | 51.4 | Yes |
| | 486 | Beatrice North | 55.8 | 86 | 36.4 | 72.5 | Yes |
| | **793** | **Max Treatable TSS** | **91.0** | **106** | **45.7** | **91.0** | **Yes** |

Table 5.18 Site specific design of SAFL Baffle for Case 3 using Equation 5.1

| **Site** | A | B | C | D | E | F | G |
|---|---|---|---|---|---|---|---|
| | **Assumed Roadway TSS (mg/L)** | **Source of TSS** | **Target load - 80% of roadway (kg)** | **Best SAFL Baffle model** | **% Removal of selected SAFL Baffle** | **Load removed by SAFL Baffle (kg)** | **Does it meet the target? (F>C?)** |
| Beal Slough | 13 | Winston et al. 2023 | 1.7 | 42 | 0.7 | 2.5 | Yes |
| | 35 | Winston et al. 2023 | 4.5 | 44 | 1.8 | 6.4 | Yes |
| | 70 | Winston et al. 2023 | 9.0 | 55 | 9.7 | 34.6 | Yes |
| | 405 | Beal Slough | 52.1 | 66 | 24.1 | 86.1 | Yes |
| | **1260** | **Max Treatable TSS** | **162.2** | **106** | **45.4** | **162.2** | **Yes** |
| Beatrice West | 13 | Winston et al. 2023 | 2.3 | 44 | 3.1 | 3.4 | Yes |
| | 35 | Winston et al. 2023 | 6.2 | 55 | 8.7 | 9.6 | Yes |
| | 70 | Winston et al. 2023 | 12.4 | 63 | 11.5 | 12.6 | Yes |
| | 157 | Beatrice West | 27.8 | 86 | 25.8 | 28.4 | Yes |
| | **230** | **Max Treatable TSS** | **40.8** | **106** | **37.1** | **40.8** | **Yes** |
| | 405 | Beal Slough | 71.8 | 106 | 37.1 | 40.8 | No |
| Cornhusker | 13 | Winston et al. 2023 | 2.5 | 44 | 1.9 | 4.7 | Yes |
| | 35 | Winston et al. 2023 | 6.7 | 55 | 6.2 | 15.2 | Yes |
| | 70 | Winston et al. 2023 | 13.4 | 55 | 6.2 | 15.2 | Yes |
| | **314** | **Max Treatable TSS** | **60.2** | **106** | **24.6** | **60.2** | **Yes** |
| | 317 | Cornhusker | 60.9 | 106 | 24.6 | 60.2 | No |
| | 405 | Beal Slough | 77.8 | 106 | 24.6 | 60.2 | No |
| Beatrice North | 13 | Winston et al. 2023 | 1.4 | 42 | 4.2 | 8.4 | Yes |
| | 35 | Winston et al. 2023 | 3.7 | 42 | 4.2 | 8.4 | Yes |
| | 70 | Winston et al. 2023 | 7.4 | 42 | 4.2 | 8.4 | Yes |
| | 405 | Beal Slough | 43.0 | 66 | 25.8 | 51.4 | Yes |
| | 486 | Beatrice North | 51.6 | 86 | 36.4 | 72.5 | Yes |
| | **858** | **Max Treatable TSS** | **91.0** | **106** | **45.7** | **91.0** | **Yes** |

In Case 2 (Table 5.16), the size of the baffle needed depended on the $TSS_{road}$ value used. When the TSS value measured at Beal Slough was used to estimate concentrations coming from the impervious surfaces, the required baffle size was much larger than when using the lower values from Winston et al. (2023). At Beal Slough and Beatrice North, the SAFL Baffle could meet the 80% sediment removal goal if $TSS_{road}$ was the same as the average TSS for the whole catchment. Also, the "maximum treatable TSS" values were much higher than typical TSS values seen on roadways, showing that the baffle had extra capacity in these cases. For Beatrice West and Cornhusker, though, no baffle size met the requirement if the same TSS was assumed for the roadway as for the whole catchment. These sites also needed much larger baffle models than Beal Slough and Beatrice North, which suggests that treating these areas is more difficult.

In Case 3 (Table 5.17), results were found to be similar to those in Case 2, except that the SAFL Baffle performed better due to the smaller treatment area. At Beal Slough and Beatrice North, improved performance was achieved using the same baffle models, mainly because less area was required to be treated. For Beatrice West and Cornhusker, lower sediment loads from the roadway were calculated due to the reduced treatment area, but only Beatrice West had an identified baffle that met the 80% removal requirement.

#### 5.7.3.2 Evaluating SAFL Baffle based on data for storms smaller than 0.5 in

The NDOT permit requires treatment of the first 0.5 inches of rainfall depth; therefore, TSS data from storms with less than 0.5 inches of rainfall were evaluated separately to see if there were potential differences in the results of this type of analysis. Table 5.18 provides a comparison between TSS values from all storms and those with rainfall depths under 0.5 inches. This shows that the median TSS values for storms with rainfall depths less than 0.5 inches were lower compared to the median TSS values from all storm events except for Beal Slough where an opposite trend was observed.

Table 5.19 Median TSS values in 2024 for all storms and storms smaller than 0.5 in

| Site | All storms | | Storms smaller than 0.5 in | |
|---|---|---|---|---|
| | Events | Median TSS [mg/L] | Events | Median TSS [mg/L] |
| Beal Slough | 25 | 405 | 7 | 466 |
| Beatrice West | 17 | 157 | 7 | 106 |
| Cornhusker | 25 | 317 | 14 | 246 |
| Beatrice North | 22 | 486 | 14 | 415 |

The same calculation using all storms in Section 5.6.3.1 was repeated using TSS values from storms with rainfall depths less than 0.5 inches. **For Case 1**, SHSAM simulation results are summarized in Table 5.19. These results show that, similar to when treating runoff from the entire catchment, the SAFL Baffle alone did not achieve the 80% sediment removal requirement at any of the sites.

Table 5.20 Removal efficiency of SAFL Baffle by site using SHSAM (<0.5 in)

| **Model** | | | **Removal Efficiency (%)** | | | |
|---|---|---|---|---|---|---|
| **Name** | **Sump diameter (ft)** | **Sump height (ft)** | **Beal Slough** | **Beatrice West** | **Cornhusker** | **Beatrice North** |
| 42 | 4 | 2 | 0.8 | 1.0 | 0.6 | 4.3 |
| 44 | 4 | 4 | 3.2 | 2.4 | 1.7 | 7.5 |
| 55 | 5 | 5 | 9.5 | 7.8 | 5.9 | 13.5 |
| 63 | 6 | 3 | 14.2 | 10.9 | 8.6 | 16.5 |
| 66 | 6 | 6 | 24.2 | 16.5 | 13.3 | 26.2 |
| 86 | 8 | 6 | 36.5 | 24.4 | 18.9 | 36.7 |
| 106 | 10 | 6 | 45.6 | 35.3 | 24.2 | 45.7 |

Similar to the evaluation using all storm TSS data, Case 2 and Case 3 were also evaluated to assess SAFL Baffle performance. For both cases, the SAFL Baffle generally showed slightly worse performance, as seen in Table 5.20 and Table 5.21, except at the Beal Slough site where smaller baffle sizes were sufficient in some scenarios. Other than that, the results for Case 2 were similar. However, in Case 3, the SAFL Baffle did not meet the 80% removal requirement at the Beatrice West site when the same TSS concentration was assumed for both the roadway and the entire catchment. This slightly reduced performance for smaller storms could be due to the loss of treatment credit from offsite areas as we used a smaller TSS value for the catchment.

Table 5.21 Site specific design of SAFL Baffle for Case 2 (<0.5 in)

| **Site** | A | B | C | D | E | F | G |
|---|---|---|---|---|---|---|---|
| | **Assumed Roadway TSS (mg/L)** | **Source of TSS** | **Target load - 80% of roadway (kg)** | **Best SAFL Baffle model** | **% Removal of selected SAFL Baffle** | **Load removed by SAFL Baffle (kg)** | **Does it meet the target? (F>C?)** |
| Beal Slough | 13 | Winston et al. 2023 | 1.9 | 42 | 0.8 | 3.3 | Yes |
| | 35 | Winston et al. 2023 | 5.1 | 44 | 3.2 | 13.2 | Yes |
| | 70 | Winston et al. 2023 | 10.3 | 44 | 3.2 | 13.2 | Yes |
| | 466 | Beal Slough | 68.4 | 66 | 24.2 | 99.5 | Yes |
| | **1276** | **Max Treatable TSS** | **187.3** | **106** | **45.6** | **187.4** | **Yes** |
| Beatrice West | 13 | Winston et al. 2023 | 3.6 | 55 | 7.8 | 5.8 | Yes |
| | 35 | Winston et al. 2023 | 9.6 | 66 | 16.5 | 12.3 | Yes |
| | 70 | Winston et al. 2023 | 19.3 | 106 | 35.3 | 26.2 | Yes |
| | **95** | **Max Treatable TSS** | **26.1** | **106** | **35.3** | **26.2** | **Yes** |
| | 106 | Beatrice West | 29.2 | 106 | 35.3 | 26.2 | No |
| | 466 | Beal Slough | 128.2 | 106 | 35.3 | 26.2 | No |
| Cornhusker | 13 | Winston et al. 2023 | 4.1 | 55 | 5.9 | 11.2 | Yes |
| | 35 | Winston et al. 2023 | 11.1 | 55 | 5.9 | 11.2 | Yes |
| | 70 | Winston et al. 2023 | 22.2 | 66 | 13.3 | 25.3 | Yes |
| | **144** | **Max Treatable TSS** | **45.6** | **106** | **24.2** | **46.0** | **Yes** |
| | 246 | Cornhusker | 78.0 | 106 | 24.2 | 46.0 | No |
| | 466 | Beal Slough | 147.7 | 106 | 24.2 | 46.0 | No |
| Beatrice North | 13 | Winston et al. 2023 | 1.5 | 42 | 4.3 | 7.3 | Yes |
| | 35 | Winston et al. 2023 | 4.0 | 42 | 4.3 | 7.3 | Yes |
| | 70 | Winston et al. 2023 | 8.0 | 44 | 7.5 | 12.7 | Yes |
| | 415 | Beatrice North | 47.6 | 86 | 36.7 | 62.4 | Yes |
| | 466 | Beal Slough | 53.5 | 86 | 36.7 | 62.4 | Yes |
| | **676** | **Max Treatable TSS** | **77.5** | **106** | **45.7** | **77.7** | **Yes** |

Table 5.22 Site specific design of SAFL Baffle for Case 3 (<0.5 in)

| **Site** | A | B | C | D | E | F | G |
|---|---|---|---|---|---|---|---|
| | **Assumed Roadway TSS (mg/L)** | **Source of TSS** | **Target load - 80% of roadway (kg)** | **Best SAFL Baffle model** | **% Removal of selected SAFL Baffle** | **Load removed by SAFL Baffle (kg)** | **Does it meet the target? (F>C?)** |
| Beal Slough | 13 | Winston et al. 2023 | 1.7 | 42 | 0.8 | 3.3 | Yes |
| | 35 | Winston et al. 2023 | 4.5 | 44 | 3.2 | 13.2 | Yes |
| | 70 | Winston et al. 2023 | 9.0 | 44 | 3.2 | 13.2 | Yes |
| | 466 | Beal Slough | 60.0 | 66 | 24.2 | 99.5 | Yes |
| | **1456** | **Max Treatable TSS** | **187.4** | **106** | **45.6** | **187.4** | **Yes** |
| Beatrice West | 13 | Winston et al. 2023 | 2.3 | 55 | 7.8 | 5.8 | Yes |
| | 35 | Winston et al. 2023 | 6.2 | 63 | 10.9 | 8.1 | Yes |
| | 70 | Winston et al. 2023 | 12.4 | 86 | 24.4 | 18.1 | Yes |
| | 106 | Beatrice West | 18.8 | 106 | 35.3 | 26.2 | Yes |
| | **147** | **Max Treatable TSS** | **26.0** | **106** | **35.3** | **26.2** | **Yes** |
| | 466 | Beal Slough | 82.6 | 106 | 35.3 | 26.2 | No |
| Cornhusker | 13 | Winston et al. 2023 | 2.5 | 44 | 1.7 | 3.2 | Yes |
| | 35 | Winston et al. 2023 | 6.7 | 55 | 5.9 | 11.2 | Yes |
| | 70 | Winston et al. 2023 | 13.4 | 63 | 8.6 | 16.3 | Yes |
| | **239** | **Max Treatable TSS** | **45.9** | **106** | **24.2** | **46.0** | **Yes** |
| | 246 | Cornhusker | 47.2 | 106 | 24.2 | 46.0 | No |
| | 466 | Beal Slough | 89.5 | 106 | 24.2 | 46.0 | No |
| Beatrice North | 13 | Winston et al. 2023 | 1.4 | 42 | 4.3 | 7.3 | Yes |
| | 35 | Winston et al. 2023 | 3.7 | 42 | 4.3 | 7.3 | Yes |
| | 70 | Winston et al. 2023 | 7.4 | 44 | 7.5 | 12.7 | Yes |
| | 415 | Beatrice North | 44.0 | 66 | 26.2 | 44.5 | Yes |
| | 466 | Beal Slough | 49.4 | 86 | 36.7 | 62.4 | Yes |
| | **731** | **Max Treatable TSS** | **77.5** | **106** | **45.7** | **77.7** | **Yes** |

As shown above, the selection of a suitable SAFL Baffle configuration is highly sensitive to both site-specific conditions and to the assumed $TSS_{road}$, highlighting the importance of accurate input data in design decisions.

## 5.8 Limitations of SAFL Baffle under permit requirements

For typical Nebraska roadway sites, the effectiveness of the SAFL Baffle in meeting NDOT's TSS removal requirements depends on multiple factors, including the assumed $TSS_{road}$ and the ratio of impervious ROW area to the total impervious area of the contributing catchment. When $TSS_{road}$ is relatively high—as in the case of Beal Slough, where a value of 405 mg/L was observed—it becomes increasingly difficult to achieve the required removal efficiency using the SAFL Baffle alone, especially if the ROW represents a large portion of the total impervious area. Additionally, the ratio of $TSS_{road}$ to overall catchment TSS also influences the treatment demand. For instance, at Beatrice West and Cornhusker sites, if the $TSS_{road}$ is assumed to match the 405 mg/L value from Beal Slough, even the largest available SAFL Baffle model fails to meet the removal efficiency required by Equation 5.1. Additionally, catchments with erosion-prone surfaces like gravel roads or exposed soils will have higher sediment loads, which fill up the sump manhole faster and ultimately increase the maintenance costs of similar BMPs. In such cases, a combination of the SAFL Baffle with other best management practices (BMPs) would be necessary to meet NDOT's TSS treatment criteria.

# Chapter 6 Models and Recommendations

## 6.1 Introduction

The following sections provide guidance on selecting relevant sediment characteristics and particle size distributions for a specific catchment for choosing an appropriate SAFL Baffle. They also compare SAFL Baffle removal efficiencies of selected models against permit requirements. These recommendations are based on limited datasets, the technical literature, and the authors' judgment. The user is encouraged to apply their own judgment related to the specific site in question. First, the chapter shows how to roughly estimate average total suspended sediment (TSS) concentration and particle size distribution (PSD) based on catchment characteristics, using data from monitored sites supported by literature. Then, it describes methods for estimating the removal efficiency of SAFL Baffle models and comparing them to the required efficiency to support proper sizing.

## 6.2 Estimating TSS and PSD values based on catchment characteristics

This section provides a preliminary approximation of TSS and PSD for given catchment characteristics based on available monitored data and previous literature studies. Different recommendations are provided for estimating sediment characteristics based on the right-of-way (ROW) definition for cases outlined in Section 5.5.1. These recommendations are based on limited data and multiple assumptions. While these data reflect typical mixed catchments found in Nebraska, they include both ROW and non-ROW contributions, making it difficult to study the effect of specific land features. Also, this study does not include roadway-only sites in Nebraska, which would improve TSS estimates for ROW areas. Thus, the recommendations in this section should be viewed as a first step toward developing a more refined tool and are expected to improve as more site-specific sediment data become available.

### *6.2.1 Estimating TSS using catchment characteristics*

This section outlines a method for estimating TSS based on catchment characteristics. The approach for Case 1, where the entire drainage area is considered, is described using data from four monitored sites: Beal Slough, Beatrice West, Cornhusker, and Beatrice North. Specific features of the catchment affect how much sediment is removed by runoff. Table 6.1 and Figure 6.1 show a basic starting point and how different factors can increase or decrease TSS values.

Table 6.1 Summary of observations from this study concerning variations in sediment concentration from baseline

| **Site factor** | **Effect on sediment concentration (Coarse/ Fine TSS)** | **Based on observation from:** |
|---|---|---|
| Roadway slope | Coarse fraction increases linearly by up to 250 mg/L (1-3% slope) | Beal Slough |
| Unvegetated surface | Greater than 10% bare soil or gravel area increases coarse by 30 mg/L and fine by 280 mg/L | Beatrice North |
| Lawn erosion | Visible lawn erosion increases coarse by 150 mg/L and fine by 110 mg/L | Cornhusker |
| Vegetated buffer | Majority of Runoff through vegetated buffer reduces coarse by 30 mg/L and fine by 60 mg/L | Beatrice West |

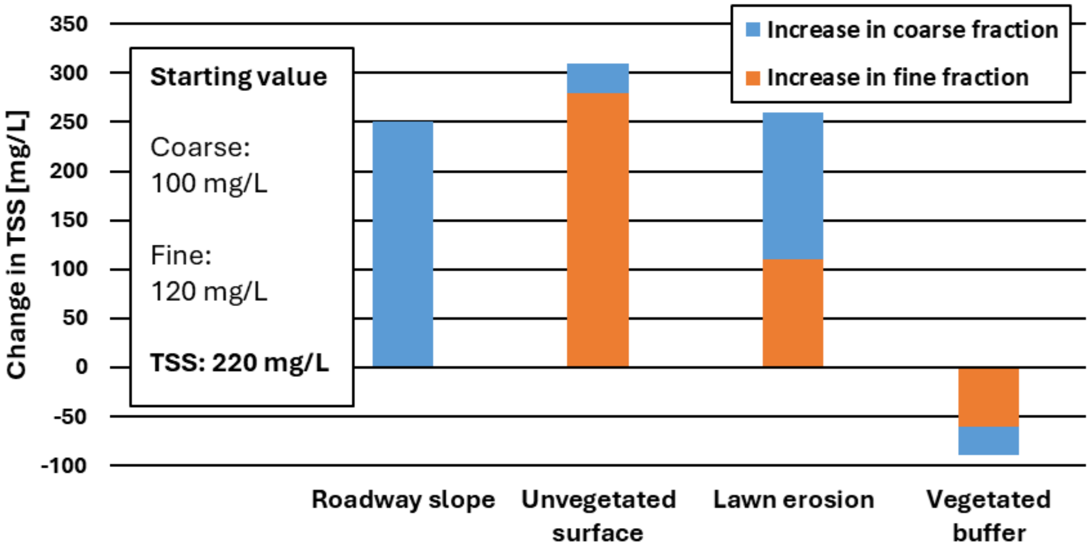

Figure 6.1 TSS estimation for using catchment characteristics

The base TSS value used was approximately 220 mg/L, with 100 mg/L for coarse particles and 120 mg/L for fine particles. The base values of 100 mg/L for coarse and 120 mg/L for fine suspended sediment were chosen to represent typical sediment concentrations when no clear sediment source or dominant sediment contributing catchment feature was observed. The fine sediment baseline was based on monitored values from Beal Slough, a site with no obvious fine sediment sources. However, none of the sites had purely roadway runoff or were free from features that influence coarse sediment transport. Therefore, the coarse baseline was set as a midpoint between values observed at Beatrice West (70 mg/L) and Beatrice North (125 mg/L). Beatrice West includes a vegetated swale that likely filters coarse sediment, while Beatrice North has gravel parking that contributes both coarse and fine sediment. Neither site had strong, isolated features affecting coarse concentration, so an average between them was considered a reasonable starting point.

Depending on site conditions, the base TSS values were adjusted upward or downward. An increase of up to 250 mg/L in the coarse fraction was applied when the roadway slope was between 1% and 3%; this was based on observation of the Beal Slough site, where the sloped pavement likely allowed transport of larger particles. If more than 10% of the drainage area consisted of exposed soil or gravel parking, an increase of about 30 mg/L in coarse and 280 mg/L in fine sediment was applied; this adjustment was based on Beatrice North, where gravel parking and bare soil patches clearly contributed sediment to runoff. An additional 150 mg/L of coarse and 110 mg/L of fine sediment was assumed when adjacent lawn erosion was present; this estimate was based on visual signs of turf erosion adjacent to roadway at the Cornhusker site. In contrast, a reduction of about 30 mg/L in coarse and 60 mg/L in fine particles was applied where vegetated buffers or swales were present. This was based on observation from the Beatrice West site, where a grassed swale along the highway filtered roadway runoff. While these values are approximate, they offered a practical starting point for estimating sediment loads during BMP design.

Similarly, for Case 2 and Case 3 of the ROW definition, which include mostly roadway and local access roads, TSS values from the Winston et al. (2023) study can be used. In that study, TSS concentrations ranged from 13 to 70 mg/L, with an average of 35 mg/L.

### *6.2.2 PSD recommendations*

PSD can also be estimated using catchment characteristics, similar to TSS. This recommendation is based on data collected from the four monitored sites in this study. However, since none of the monitored sites had flows exclusively from the roadway, additional reference was taken from Winston et al. (2023) to represent PSD. Table 6.2 and Figure 6.2 provide guidance for selecting a PSD profile that best matches the characteristics of a new catchment where stormwater treatment is being planned. For Case 1 of the ROW definition, PSD estimates can be based on observations from the four monitored sites. For Cases 2 and 3, where runoff is primarily from roadway or access roads, PSD values from Winston et al. (2023) are recommended until additional data from Nebraska sites that drain primarily roadways are available.

Table 6.2 Estimating particle size distribution based on catchment characteristics

| Site description | Highways; roadway only | Steep slope; less erosion | Presence of vegetative swale | Erosion from lawn | Erosion from gravel surfaces |
|---|---|---|---|---|---|
| **Particle size (µm)** | **Percent finer** | | | | |
| 1000 | 100 | 100 | 100 | 100 | 100 |
| 250 | 95 | 46 | 86 | 83 | 92 |
| 125 | 85 | 30 | 75 | 77 | 85 |
| 32 | 30 | 17 | 47 | 60 | 78 |
| 8 | 10 | 6 | 17 | 17 | 29 |
| 0 | 0 | 0 | 0 | 0 | 0 |
| **Sources** | **Winston et al. 2023** | **Beal Slough** | **Beatrice West** | **Cornhusker** | **Beatrice North** |

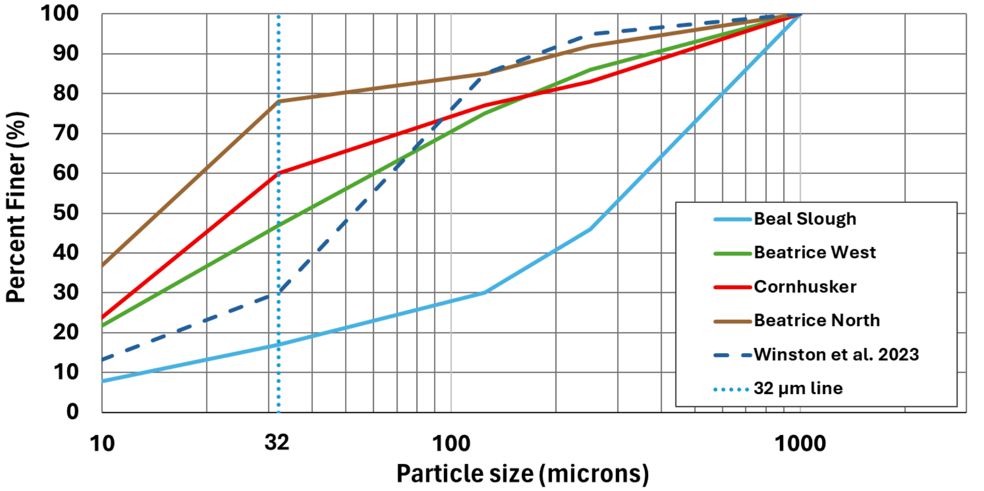

Figure 6.2 Estimating particle size distribution based on catchment characteristics

## 6.3 Methodology for selecting and validating SAFL Baffle Models

To properly design and size a SAFL Baffle model for a priority outfall, the following steps are recommended.

1. Identify paved areas within the NDOT right-of-way and the total paved area in the contributing drainage area. Paved areas can be estimated by using satellite imagery in GIS software such as ArcGIS with Geometry Calculator tools. These areas are used to calculate water quality volume (WQV), defined as runoff from the first 0.5 inches of rainfall from the impervious area. This follows guidelines in Section 6.A of the NDOT Drainage Design and Erosion Control Manual (NDOT 2023).
2. Collect catchment parameters required for SHSAM analysis.
    - **Total drainage area (acre):** The approximate drainage area contributing to the outfall can be delineated using a combination of resources, including a 1-meter Digital Elevation Model (DEM) (NRCS Geospatial Data Gateway n.d.), storm sewer as-built drawings provided by the City or Department of Transportation, and field observations. GIS software such as QGIS, ArcGIS, or HEC-RAS Mapper is used to process these data sources. Typically, contours are first extracted from the DEM, and information from maps and site visits is used to refine the drainage boundary.
    - **Impervious percentage (%):** The ratio of total impervious surfaces within the delineated catchment area draining to the outfall. Impervious areas include pavements, roofs, gravel parking lot and gravel roads.
    - **Hydraulic length (ft):** It is the longest flow path from the farthest point in the catchment to the outfall.

- **Average slope (%):** It is the average slope of multiple profile lines drawn perpendicular to contour lines across the drainage area at evenly spaced intervals.
- **CN number of pervious area:** The Curve Number (CN) for pervious areas within the catchment can be determined following the methodology provided in TR-55 (USDA NRCS 1986). Hydrologic Soil Group (HSG) information can be obtained from the NRCS Web Soil Survey (USDA NRCS 2019).

3. Estimate sediment load from the paved area within NDOT right-of-way (roadway and frontage road) and the full drainage area. TSS values can also be obtained from monitored sites collected from roadway only runoff, such as Beal Slough site, which had a measured median TSS of 405 mg/L. Literature values can also be used; for example, Winston et al. (2023) reported a range of 13 to 70 mg/L.

   *Sediment load = Water quality volume (WQV) x Assumed TSS*

4. Select an appropriate SAFL Baffle model based on estimated sediment removal efficiency using SHSAM. Select the smallest model which achieves at least 80% removal of the target sediment load from the impervious area within the NDOT right-of-way.

   *80% of mass from impervious within ROW <= Mass removed from whole catchment*

Alternatively, Equation 5.1 can be used to evaluate compliance with the permit requirements.

$$0.8 \, . \frac{Area_{road}}{Area_{catchment}} . \frac{TSS_{road}}{TSS_{catchment}} \leq Removal\, \% \qquad (5.1)$$

where:

$Area_{road}$ = impervious area within NDOT right-of-way (acres)

$Area_{catchment}$ = impervious area within contributing catchment of the outfall (acres)

$TSS_{road}$ = TSS concentration from roadway runoff (mg/L)

$TSS_{catchment}$ = TSS concentration from total contributing catchment (mg/L)

*Removal %* = removal efficiency of hydrodynamic separator (%)

Two example calculations demonstrating the prediction of TSS and PSD, along with the selection of an appropriate SAFL Baffle design, are provided in Appendix K: TSS and PSD estimation and SAFL Baffle selection, for two sets of catchment characteristics.

### 6.4 Supplementary charts to evaluate sufficiency of SAFL Baffle models

The performance of SAFL Baffle models can be roughly evaluated to see if they meet compliance requirements using some pre-created charts. These charts are based on the two sides of Equation 5.1; one shows the removal efficiency of the SAFL Baffle and another shows the removal required by the permit. The difference between these two gives excess removal. A positive value indicates that the SAFL Baffle meets the permit requirements.

$$\text{Excess removal (\%)} = \text{Removal}_{\text{SAFL}}\text{ (\%)} - \text{Removal}_{\text{Reqd}}\text{ (\%)}$$

$\mathbf{Removal_{SAFL}}$ is the predicted performance of a particular SAFL Baffle model or size based on given site characteristics and rainfall data. This value can only be calculated using SHSAM software.

$\mathbf{Removal_{Reqd}}$ is the required removal percentage based on the size of the impervious area within both the NDOT right-of-way and the entire drainage basin, as well as the predicted TSS concentrations from those areas.

These two values can be manually determined using arithmetic calculation in combination with SHSAM modeling. However, they can also be approximately estimated using the charts provided below.

Figure 6.3 can be used to estimate the required removal efficiency based on drainage areas and TSS concentrations. To use the figure, first estimate the values of $Area_{catchment}$ and $Area_{road}$. Then, determine the ratio of $TSS_{road}$ to $TSS_{catchment}$ to select the appropriate chart from the four available. Within each chart, multiple lines are provided, one of which can be selected based on the value of $Area_{road}$. The required removal efficiency can then be read from the x-axis value corresponding to the $Area_{catchment}$.

To estimate the removal efficiency of different SAFL Baffle models, Figure 6.4, Figure 6.5, and Figure 6.6 were created using multiple SHSAM simulations. To use these charts, a PSD type applicable to the site is first selected. Then, the appropriate plot is identified by estimating the impervious percentage of the catchment and calculating √S/L, where *S* is the catchment slope (in %) and *L* is the hydraulic length (in miles). In each plot, the removal efficiency is estimated for different available SAFL models based on the area of the catchment. These figures provide approximate removal efficiencies for SAFL Baffle models in catchments with particle size distributions (PSD) similar to Beal Slough, Beatrice West, and Beatrice North, respectively. An example illustrating how to use these charts based on catchment characteristics is provided in Appendix L: Use of Charts to Estimate Required Removal and SAFL Baffle Efficiency.

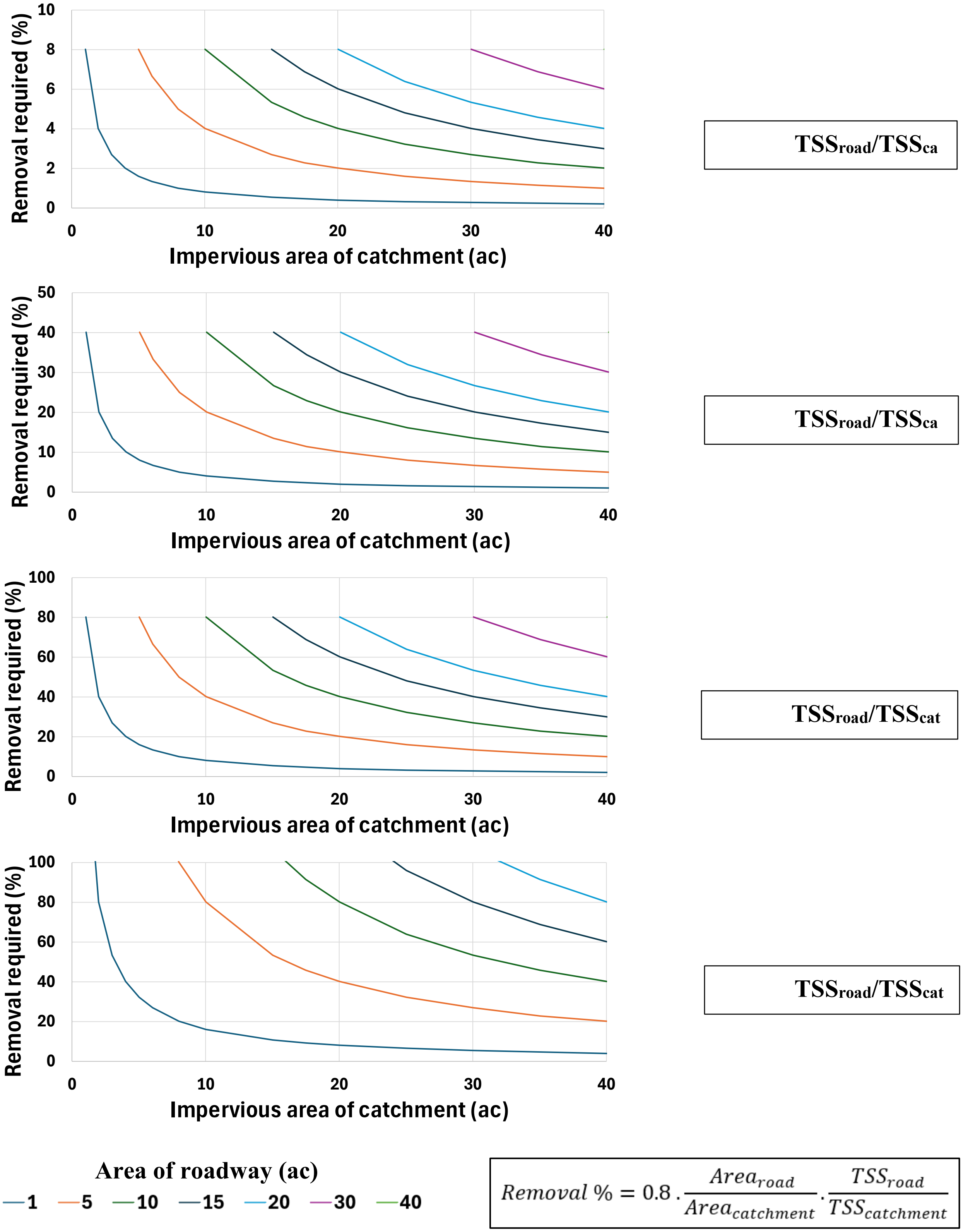

$$Removal\ \% = 0.8 \cdot \frac{Area_{road}}{Area_{catchment}} \cdot \frac{TSS_{road}}{TSS_{catchment}}$$

Figure 6.3 Required removal efficiency based on impervious areas and TSS values

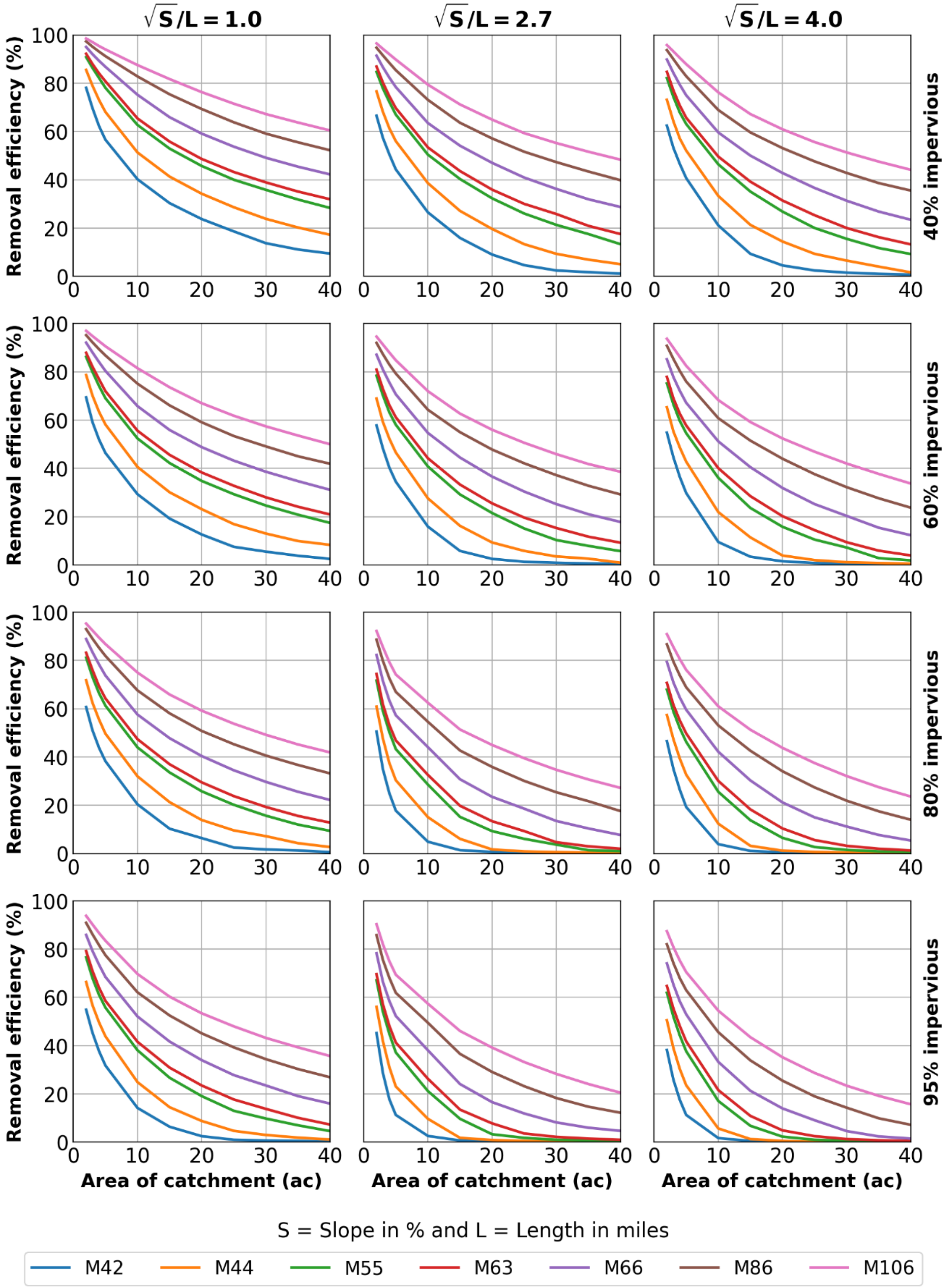

Figure 6.4 Estimated removal efficiency of SAFL Baffle for Beal Slough PSD

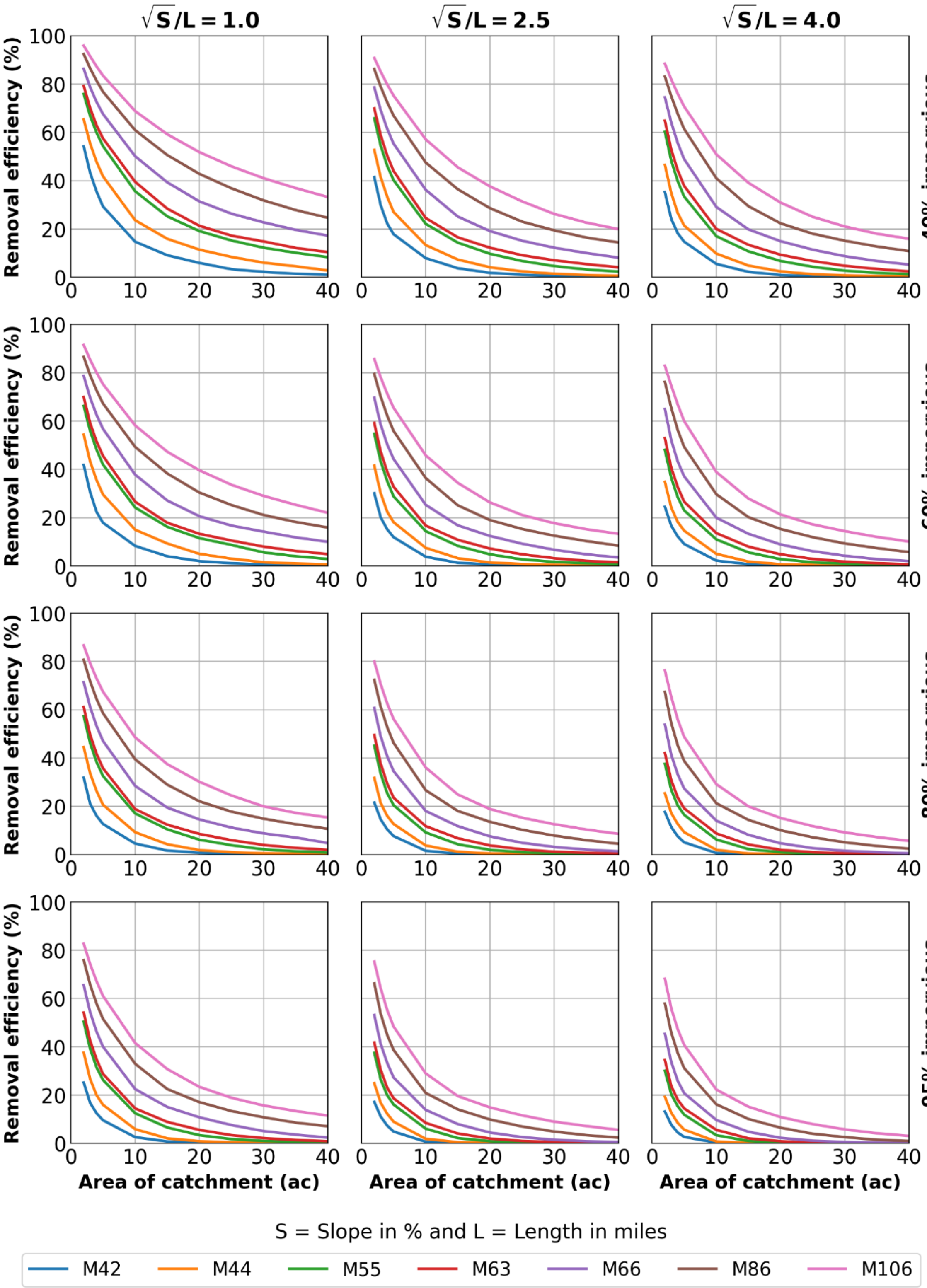

Figure 6.5 Estimated removal efficiency of SAFL Baffle for Beatrice West PSD

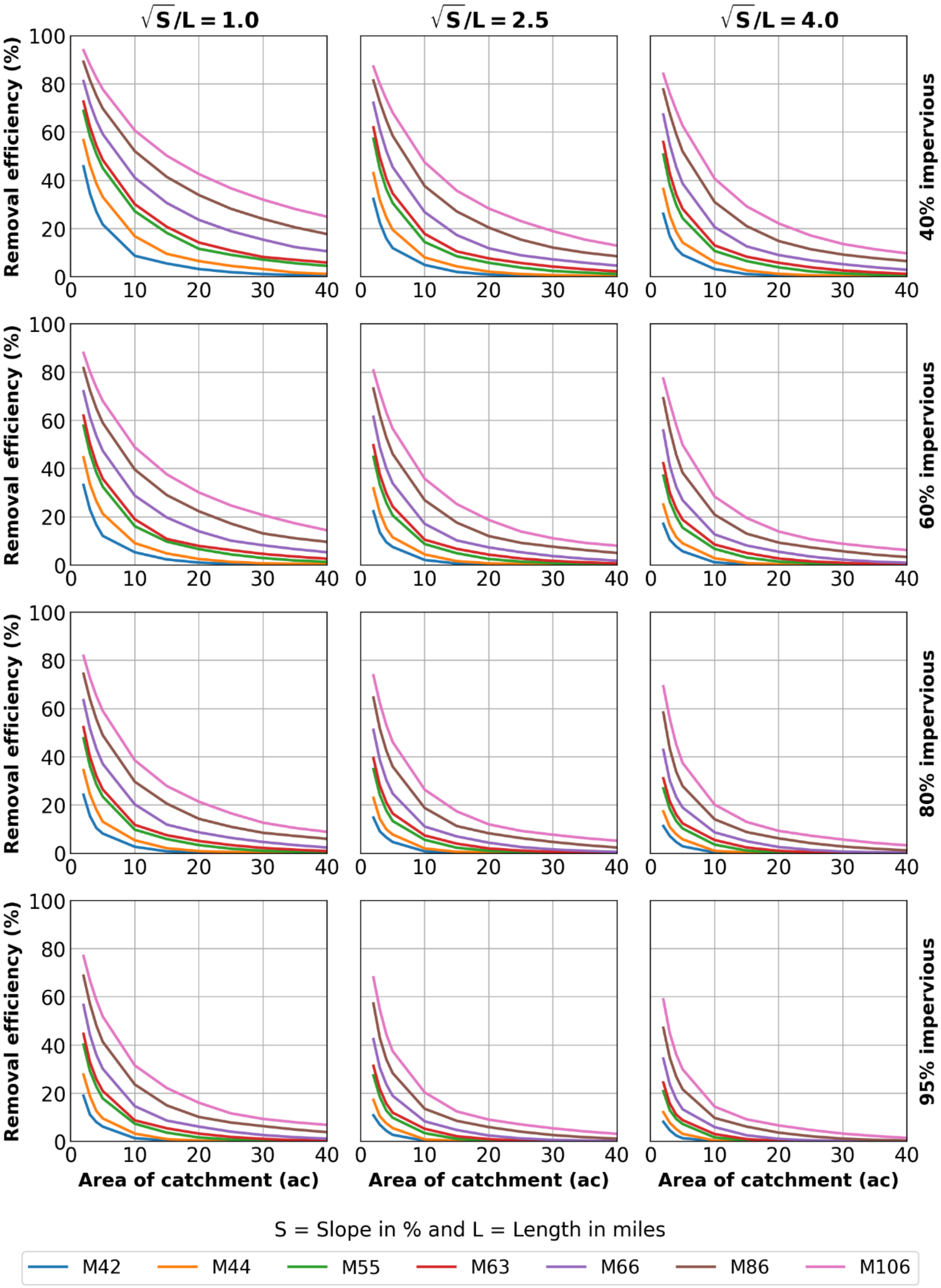

Figure 6.6 Estimated removal efficiency of SAFL Baffle for Beatrice North PSD

# Chapter 7 Conclusions

## 7.1 Report summary

This study focused on characterizing sediment in Nebraska roadway runoff by measuring total suspended solids (TSS) and particle size distribution (PSD). The main objective was to collect sediment data from representative NDOT-maintained roadway catchments to support the design and application of a specific type of hydrodynamic separator known as the SAFL Baffle. A total of 111 stormwater samples were collected over a 1.5-year monitoring period, from spring 2024 through spring 2025, at two sites in Lincoln and two in Beatrice, using flow-paced automatic sampling. Laboratory analyses were performed to determine TSS concentrations and PSD of the coarse fraction (>32 µm). Of these, 68 selected "extended PSD samples" were sent for additional analysis to quantify the fine fraction (<32 µm) and provide a complete PSD curve. The collected sediment data were used to evaluate SAFL Baffle sizing through SHSAM (Sizing Hydrodynamic Separators and Manholes) modeling for the monitored sites and to develop a recommendation framework to support BMP design at similar roadway locations.

## 7.2 Key findings

The following key conclusions can be drawn from this study:

1. During site selection, most sites in MS4 communities with multiple storm inlets were found to receive a significant portion of runoff from areas outside the NDOT right-of-way.
2. Three of the four monitored sites were found to receive substantial runoff and sediment input from areas outside the NDOT right-of-way, indicating that off-site sources significantly influence catchment sediment loads. With a sample size of four sites, no observations were able to be drawn related to sediment concentration and PSD and site land use.
3. Site-specific observations to locate the primary source of sediment during storm events showed distinct behaviors:

    - At the Beatrice North (BTN) site, runoff from an off-site gravel parking lot was observed to contribute a high volume of fine sediment.
    - At the Cornhusker (CH) site, visible lawn erosion during spring was found to be a notable source of soil runoff.
    - At the Beal Slough (BS) site, no distinct external erosion sources were identified, and the sediment was predominantly coarse, suggesting it may have originated primarily from impervious roadway surfaces.
    - At the Beatrice West (BTW) site, a long, gently sloped grassed swale appeared to provide filtering and infiltration for most events, except for two storms in the spring of 2024.

4. At the BTW site, delayed and reduced runoff response during small storm events was attributed to the swale's infiltration capacity, which often prevented sample collection under low rainfall conditions.
5. Median total suspended solids (TSS) concentrations at three of the four sites—CH (393 mg/L), BS (426 mg/L), and BTN (832 mg/L)—were found to be substantially higher than those reported in other literature with roadway runoff studies.
6. The particle size distributions (PSD) at three sites (BTN, BTW, and CH) showed higher proportions of fine particles compared to values typically observed in some roadway-only studies, suggesting a significant contribution from non-roadway areas.
7. The PSDs observed at these sites contained a higher proportion of fine particles than most PSDs available in the SHSAM and some in the literature. The results were most comparable to those presented by Winston et al. (2023) and the NJCAT (New Jersey Corporation for Advanced Technology, 2023) verification report.

8. Seasonal variation was evident across all sites, with median TSS concentrations generally highest in spring and decreasing during summer and fall, likely reflecting poor vegetation cover and residual sediment from winter application during spring. But the differences were not statistically significant, noting that the number of storm events limits the statistical power of the analysis.
9. Slightly higher fine particle content in spring at BS and CH suggested seasonal influences such as winter deposition and reduced vegetation growth, whereas little variation at BTN and BTW likely reflects the dominant influence of gravel surfaces and vegetated buffers throughout the year.
10. At the Beatrice West site, the combination of a vegetated filter strip and grass swale effectively reduced runoff and sediment loads during small to moderate storms, demonstrating that this treatment approach can serve as a practical BMP for meeting stormwater permit requirements.
11. The seasonality of the TSS, especially fines, as well as the observation for the degree of off-site contribution to the fines, suggests that additional emphasis on erosion control at the source for off-site contributions may be valuable for reducing sediment in the runoff. And by reducing the load of fines in the runoff, systems like a hydrodynamic separator may become more effective in providing a high removal.
12. Street sweeping schedules at the Lincoln sites explained little variation in TSS and PSD characteristics.
13. Based on SHSAM modeling with measured PSDs, none of the sites are anticipated to meet the NDOT permit's 80% TSS removal requirement to address all the runoff using the SAFL

Baffle alone, due to its reduced efficiency in capturing fine particles and relatively large catchment areas.

14. However, field observations and site data showed that a substantial portion of sediment originates from off-site areas outside the NDOT ROW. Under the NDOT permit, the treatment of such off-site sediment may help meet permit requirements using treatment credits.
15. When literature-based roadway TSS values are applied to the roadway portion of the catchment, and site-specific sediment data are used for the full drainage area, with treatment credit applied for off-site sediment, it is projected that the SAFL Baffle could meet permit requirements under many storm and site conditions.

# References

American Public Health Association (APHA), American Water Works Association, and Water Environment Federation. (2022). *Standard Methods for the Examination of Water and Wastewater: Section 2540 D — Total Suspended Solids Dried at 103–105 °C*. 23rd ed., Washington, DC. Retrieved July 5, 2025, from http://standardmethods.org

Andral, M. C., Roger, S., Montréjaud-Vignoles, M., and Herremans, L. (1999). "Particle size distribution and hydrodynamic characteristics of solid matter carried by runoff from motorways." *Water Environment Research*, **71**(4), 398–407. https://doi.org/10.2175/106143097X122130

ASTM International. (2013). *Standard test methods for determining sediment concentration in water samples* (ASTM D3977–97, reapproved 2013). ASTM International, West Conshohocken, PA. Retrieved August 26, 2023, from https://www.astm.org/d3977-97r13.html

ASTM International. (2020). *Standard test method for particle size distribution of catalytic materials by laser-light scattering* (ASTM D4464-15, reapproved 2020). ASTM International, West Conshohocken, PA. Retrieved July 5, 2025, from https://www.astm.org/d4464-15r20.html

Barrett, M. E., and U. of T. at A. C. for R. in W. Resources. 1995. A Review and Evaluation of Literature Pertaining to the Quantity and Control of Pollution from Highway Runoff and Construction. DIANE Publishing.

Barrett, M., A. Lantin, and S. Austrheim-Smith. 2004. "Storm Water Pollutant Removal in Roadside Vegetated Buffer Strips." *Transportation Research Record*, 1890 (1): 129–140. SAGE Publications Inc. https://doi.org/10.3141/1890-16.

Beck, H. J., and G. F. Birch. 2012. "Metals, nutrients and total suspended solids discharged during different flow conditions in highly urbanized catchments." *Environ Monit Assess*, 184 (2): 637–653. https://doi.org/10.1007/s10661-011-1992-z

Bilby, R. E., K. Sullivan, and S. H. Duncan. 1989. "The Generation and Fate of Road-Surface Sediment in Forested Watersheds in Southwestern Washington." *Forest Science*, 35 (2): 453–468. https://doi.org/10.1093/forestscience/35.2.453.

Brodie, I., and F. Young. 2007. "Case Studies of Applying Urban Surface Data in Evaluating Stormwater Management Issues."

Characklis, G. W., and M. R. Wiesner. 1997. "Particles, Metals, and Water Quality in Runoff from Large Urban Watershed." *Journal of Environmental Engineering*, 123 (8): 753–759. American Society of Civil Engineers. https://doi.org/10.1061/(ASCE)0733-9372(1997)123:8(753).

Charters, F. J., T. A. Cochrane, and A. D. O'Sullivan. 2015. "Particle size distribution variance in untreated urban runoff and its implication on treatment selection." *Water Research*, 85: 337–345. https://doi.org/10.1016/j.watres.2015.08.029.

Dunn, O. J. (1961). "Multiple comparisons among means." *Journal of the American Statistical Association*, **56**(293), 52–64. https://doi.org/10.1080/01621459.1961.10482090

Farmer, D. 2017. "Hydrological Patterns and the Effects of Land Use on TSS Concentrations and Yields in the McCarthy Creek Watershed, Portland, Oregon." *Environmental Science and Management Professional Master's Project Reports*. https://doi.org/10.15760/mem.10.

Górska, K., J. Górski, Ł. Bąk, A. Sałata, J. Muszyńska, and J. Gawdzik. 2020. "Relationship between selected pollution indicators of stormwater from urban catchments." *Desalination and Water Treatment*, 199: 473–485. https://doi.org/10.5004/dwt.2020.26328.

Graczyk, D. J., D. M. Robertson, P. D. Baumgart, and K. Fermanich. 2011. Hydrology, phosphorus, and suspended solids in five agricultural streams in the Lower Fox River and Green Bay Watersheds, Wisconsin, Water Years 2004-06. Scientific Investigations Report. U.S. Geological Survey.

Gupta, K., and A. J. Saul. 1996. "Specific relationships for the first flush load in combined sewer flows." *Water Research*, 30 (5): 1244–1252. https://doi.org/10.1016/0043-1354(95)00282-0.

Hathaway, J. M., and W. F. Hunt. 2011. "Evaluation of First Flush for Indicator Bacteria and Total Suspended Solids in Urban Stormwater Runoff." *Water Air Soil Pollut*, 217 (1): 135–147. https://doi.org/10.1007/s11270-010-0574-y.

Helsel, D. R., and Hirsch, R. M. (2020). *Statistical methods in water resources* (USGS Techniques and Methods 4-A3). U.S. Geological Survey, Reston, VA. https://doi.org/10.3133/tm4A3

Hilliges, R., M. Endres, A. Tiffert, E. Brenner, and T. Marks. 2016. "Characterization of road runoff with regard to seasonal variations, particle size distribution and the correlation of fine particles and pollutants." *Water Science and Technology*, 75 (5): 1169–1176. https://doi.org/10.2166/wst.2016.576.

Huang, J., P. Du, C. Ao, M. Ho, M. Lei, D. Zhao, and Z. Wang. 2007. "Multivariate Analysis for Stormwater Quality Characteristics Identification from Different Urban Surface Types in Macau." *Bull Environ Contam Toxicol*, 79 (6): 650–654. https://doi.org/10.1007/s00128-007-9297-1.

Jillavenkatesa, A., Dapkunas, S. J., and Lum, L.-S. (2001). *NIST recommended practice guide: Particle size characterization* (NIST SP 960-1). National Institute of Standards and Technology, Gaithersburg, MD. https://doi.org/10.6028/NBS.SP.960-1

Karamalegos, A. M., M. E. Barret, D. F. Lawler, and J. F. Malina. 2005. "Particle Size Distribution of Highway Runoff and Modification Through Stormwater Treatment." *Center* *for Research in Water Resources, The University of Texas at Austin*, Particle Size Distribution of Highway Runoff and Modification Through Stormwater Treatment.

Kayhanian, M., C. Suverkropp, A. Ruby, and K. Tsay. 2007. “Characterization and prediction of highway runoff constituent event mean concentration.” *Journal of Environmental Management*, 85 (2): 279–295. https://doi.org/10.1016/j.jenvman.2006.09.024.

Kim, J.-Y., and J. J. Sansalone. 2008. “Event-based size distributions of particulate matter transported during urban rainfall-runoff events.” *Water Research*, 42 (10): 2756–2768. https://doi.org/10.1016/j.watres.2008.02.005.

Kim, S., M. Yaqub, J. Lee, and W. Lee. 2021. “Comparison of pollutants in stormwater runoff from asphalt and concrete roads.” *1*, 12 (5): 253–259.

Kruskal, W. H., and Wallis, W. A. (1952). “Use of ranks in one-criterion variance analysis.” *Journal of the American Statistical Association*, **47**(260), 583–621. https://doi.org/10.1080/01621459.1952.10483441

Li, D., J. Wan, Y. Ma, Y. Wang, M. Huang, and Y. Chen. 2015. “Stormwater Runoff Pollutant Loading Distributions and Their Correlation with Rainfall and Catchment Characteristics in a Rapidly Industrialized City.” *PLOS ONE*, 10 (3): e0118776. Public Library of Science. https://doi.org/10.1371/journal.pone.0118776.

Li, M.-H., M. E. Barrett, P. Rammohan, F. Olivera, and H. C. Landphair. 2008. “Documenting Stormwater Quality on Texas Highways and Adjacent Vegetated Roadsides.” *Journal of Environmental Engineering*, 134 (1): 48–59. American Society of Civil Engineers. https://doi.org/10.1061/(ASCE)0733-9372(2008)134:1(48).

Lin, H., G. Ying, and J. Sansalone. 2009. “Granulometry of Non-colloidal Particulate Matter Transported by Urban Runoff.” *Water Air Soil Pollut*, 198 (1): 269–284. https://doi.org/10.1007/s11270-008-9844-3.

MacDonald, L. H., R. W. Sampson, and D. M. Anderson. 2001. “Runoff and road erosion at the plot and road segment scales, St John, US Virgin Islands.” *Earth Surface Processes and Landforms*, 26 (3): 251–272. https://doi.org/10.1002/1096-9837(200103)26:3<251::AID-ESP173>3.0.CO;2-X.

Minnesota Department of Natural Resources (Minnesota DNR). (2023). *Sump manhole with SAFL Baffle BMP*. Minnesota DNR, St. Paul, MN. Retrieved July 5, 2025, from https://www.dnr.state.mn.us/water_access/bmp/sump_manhole_with_safl_baffle_bmp.html

Minnesota Pollution Control Agency (MPCA). (2023). *Minnesota stormwater manual*. Minnesota Pollution Control Agency, St. Paul, MN. Retrieved April 1, 2025, from https://stormwater.pca.state.mn.us

Mrowiec, M. 2020. “Analysis of particle size distribution and concentration of suspended solids in stormwater runoffs.” *Desalination and Water Treatment*, 199: 159–168. https://doi.org/10.5004/dwt.2020.25651.

Murphy, L. U., T. A. Cochrane, and A. O'Sullivan. 2015. "Build-up and wash-off dynamics of atmospherically derived Cu, Pb, Zn and TSS in stormwater runoff as a function of meteorological characteristics." *Science of The Total Environment*, 508: 206–213. https://doi.org/10.1016/j.scitotenv.2014.11.094.

National Weather Service (NWS). (2025). *Daily or monthly climate normals*. National Oceanic and Atmospheric Administration (NOAA), Washington, DC. Retrieved July 5, 2025, from https://www.weather.gov/wrh/Climate?wfo=oax

Nayeb Yazdi, M., D. J. Sample, D. Scott, X. Wang, and M. Ketabchy. 2021. "The effects of land use characteristics on urban stormwater quality and watershed pollutant loads." *Science of The Total Environment*, 773: 145358. https://doi.org/10.1016/j.scitotenv.2021.145358.

Nebraska Department of Transportation (NDOT). (2025). *Nebraska Interactive GIS Map Viewer*. Nebraska Department of Transportation, Lincoln, NE. https://gis.ne.gov/portal/apps/webappviewer/index.html?id=8ed4b009b0d546f19f0284e5bba0f972

NDOT. (2023). *Drainage design and erosion control manual*. Nebraska Department of Transportation, Lincoln, NE. https://dot.nebraska.gov/media/ro0ivtgy/a-drainage-design-and-erosion-control-manual.pdf

Neary, V. S., T. C. Neel, and J. B. Dewey. 2012. "Pollutant Washoff and Loading from Parking Lots in Cookeville, Tennessee." 1–14. American Society of Civil Engineers. https://doi.org/10.1061/40644(2002)220.

New Jersey Corporation for Advanced Technology (NJCAT). (2023). *UT SAFL Baffle Stormwater Treatment Unit* (Verification Report). NJCAT. http://www.njcat.org/uploads/newDocs/NJCATUTSAFLBaffleVerificationReportFinal.pdf

Niu, S., Y. Chen, J. Yu, Z. Rao, and N. Zhan. 2019. "Characteristics of particle size distribution and related contaminants of highway-deposited sediment, Maanshan City, China." *Environ Geochem Health*, 41 (6): 2697–2708. https://doi.org/10.1007/s10653-019-00327-1.

O. M. Mohseni (personal communication, August 14, 2024)

Pitt, R. E., Clark, S., Eppakayala, V. K., and Sileshi, R. (2017). "Don't throw the baby out with the bathwater—Sample collection and processing issues associated with particulate solids in stormwater." *Journal of Water Management Modeling*, **C416**, 1–14. https://doi.org/10.14796/JWMM.C416

Poudel, D. D., C. Y. Jeong, and A. DeRamus. 2010. "Surface Run-Off Water Quality from Agricultural Lands and Residential Areas." *Outlook Agric*, 39 (2): 95–105. SAGE Publications Ltd. https://doi.org/10.5367/000000010791745394.

Sandoval, S., and J.-L. Bertrand-Krajewski. 2016. "Influence of sampling intake position on suspended solid measurements in sewers: two probability/time-series-based approaches." *Environ Monit Assess*, 188 (6): 347. https://doi.org/10.1007/s10661-016-5335-y.

Sansalone, J. J., J. M. Koran, J. A. Smithson, and S. G. Buchberger. 1998. “Physical Characteristics of Urban Roadway Solids Transported during Rain Events.” *Journal of Environmental Engineering*, 124 (5): 427–440. American Society of Civil Engineers. https://doi.org/10.1061/(ASCE)0733-9372(1998)124:5(427).

Schiff, K., L. Tiefenthaler, S. Bay, and D. Greenstein. 2016. “Effects of Rainfall Intensity and Duration on the First Flush from Parking Lots.” *Water*, 8 (8): 320. https://doi.org/10.3390/w8080320.

Selbig, W. R., and R. T. Bannerman. 2011. Characterizing the size distribution of particles in urban stormwater by use of fixed-point sample-collection methods. Open-File Report. U.S. Geological Survey.

Selbig, W. R., M. N. Fienen, J. A. Horwatich, and R. T. Bannerman. 2016. “The Effect of Particle Size Distribution on the Design of Urban Stormwater Control Measures.” *Water*, 8 (1): 17. Multidisciplinary Digital Publishing Institute. https://doi.org/10.3390/w8010017.

Simpson, I. M., R. J. Winston, and M. R. Brooker. 2022. “Effects of land use, climate, and imperviousness on urban stormwater quality: A meta-analysis.” *Science of The Total Environment*, 809: 152206. https://doi.org/10.1016/j.scitotenv.2021.152206.

Smith, J. S., R. J. Winston, R. A. Tirpak, D. M. Wituszynski, K. M. Boening, and J. F. Martin. 2020. “The seasonality of nutrients and sediment in residential stormwater runoff: Implications for nutrient-sensitive waters.” *Journal of Environmental Management*, 276: 111248. https://doi.org/10.1016/j.jenvman.2020.111248.

Soil Survey Staff, Natural Resources Conservation Service, United States Department of Agriculture (USDA NRCS). (2025). *Web Soil Survey*. Retrieved July 5, 2025, from https://websoilsurvey.nrcs.usda.gov/

Teledyne ISCO. (2013). *750 area velocity module: User manual*. Teledyne ISCO, Lincoln, NE. Retrieved July 5, 2025, from https://www.teledyneisco.com/en-us/Water_/Sampler%20Documents/Manuals/750%20Area%20Velocity%20Module%20User%20Manual.pdf

U.S. Department of Agriculture Natural Resources Conservation Service (USDA NRCS). (2025). *Geospatial data gateway*. U.S. Department of Agriculture, Washington, DC. Retrieved July 5, 2025, from https://datagateway.nrcs.usda.gov/

U.S. Department of Agriculture, Soil Conservation Service (USDA SCS). (1986). *Urban hydrology for small watersheds* (Technical Release 55, TR-55). U.S. Department of Agriculture, Washington, DC.

U.S. Environmental Protection Agency. (1983). *Results of the Nationwide Urban Runoff Program: Volume 1, Final Report*. Water Planning Division, EPA, Washington, DC. Retrieved January 11, 2024, from https://www3.epa.gov/npdes/pubs/sw_nurp_vol_1_finalreport.pdf

U.S. Environmental Protection Agency. (1999). *Preliminary data summary of urban storm-water best management practices* (EPA 821-R-99-012). Office of Water, Washington, DC. Retrieved July 5, 2025, from https://www.epa.gov/sites/default/files/2015-11/documents/urban-stormwater-bmps_preliminary-study_1999.pdf

U.S. EPA (1972). Federal Water Pollution Control Act Amendments of 1972 (Clean Water Act), Public Law 92–500, 33 U.S.C. §§1251–1387.

United States Environmental Protection Agency. (2004). Stormwater Best Management Practice Design Guide: Volume 1 General Considerations. Rep. No. EPA/600/R-04/121, Office of Research and Development, Washington D.C.

Upstream Technologies. (2016). *SAFL Baffle: Stormwater pretreatment device*. Upstream Technologies, LLC, Blaine, MN. Retrieved June 20, 2025, from https://www.upstreamtechnologies.us/products/safl.shtml

USDA NRCS. (1986). *Urban hydrology for small watersheds* (Technical Release 55, 2nd ed.). Natural Resources Conservation Service, U.S. Department of Agriculture, Washington, DC. Retrieved July 5, 2025, from https://www.nrc.gov/docs/ML1421/ML14219A437.pdf

Weather Underground. (2025). *Historical weather data for Lincoln, NE*. The Weather Company, LLC. Retrieved July 5, 2025, from https://www.wunderground.com/history/daily/us/ne/lincoln/KLNK

Wilcock, W. L. (1973). Method for determining specific characteristics of fluid-suspended particles. U.S. Patent 3,873,206, filed Oct. 3, 1973.

Winston, R. J., and W. F. Hunt. 2017. “Characterizing Runoff from Roads: Particle Size Distributions, Nutrients, and Gross Solids.” *Journal of Environmental Engineering*, 143 (1): 04016074. American Society of Civil Engineers. https://doi.org/10.1061/(ASCE)EE.1943-7870.0001148.

Winston, R. J., J. D. Witter, and A. Ohio State University. Dept. of Dept of Food &. Biological Engineering. 2019. *Evaluating the Particle Size Distribution and Gross Solids Contribution of Stormwater Runoff From Ohio’s Roads*.

Winston, R. J., J. D. Witter, and R. A. Tirpak. 2023. “Measuring sediment loads and particle size distribution in road runoff: Implications for sediment removal by stormwater control measures.” *Science of The Total Environment*, 902: 166071. https://doi.org/10.1016/j.scitotenv.2023.166071.

Yan, H., D. Z. Zhu, M. R. Loewen, W. Zhang, S. Zhao, B. van Duin, L. Chen, and K. Mahmood. 2024. “Effects of mixed land use on urban stormwater quality under different rainfall event types.” *Science of The Total Environment*, 950: 175124. https://doi.org/10.1016/j.scitotenv.2024.175124.

Yan, H., D. Z. Zhu, M. R. Loewen, W. Zhang, Y. Yang, S. Zhao, B. van Duin, L. Chen, and K. Mahmood. 2024. “Particle size distribution of total suspended sediments in urban stormwater runoff: Effect of land uses, precipitation conditions, and seasonal variations." *Journal of Environmental Management*, 365: 121467. https://doi.org/10.1016/j.jenvman.2024.121467.

Zhang, T. C., Stansbury, J., Moussavi, M., Jones, D., and Richter-Egger, D. L. (2013). *Development and evaluation of best management practices (BMPs) for highway runoff pollution control*. Final Report No. SPR-P1(12) M314, Nebraska Department of Roads, Lincoln, NE.

Zhang, W., T. Li, and M. Dai. 2015. "Influence of rainfall characteristics on pollutant wash-off for road catchments in urban Shanghai." *Ecological Engineering*, 81: 102–106. https://doi.org/10.1016/j.ecoleng.2015.04.016.

Zhao, H., Y. Ma, J. Fang, L. Hu, and X. Li. 2022. "Particle size distribution and total suspended solid concentrations in urban surface runoff." *Science of The Total Environment*, 815: 152533. https://doi.org/10.1016/j.scitotenv.2021.152533.

# List of Appendices

Appendix A: HEC-HMS analysis of all four sites

Appendix B: Location of weather stations

Appendix C: Plans and profiles of sampling locations

Appendix D: Standard operating procedure for sample collection

Appendix E: Collection dates of processed samples

Appendix F: Rainfall and flow characteristics for sampling events

Appendix G: Hydrograph response and sampling times

Appendix H: Standard operating procedure to determine sediment concentration and particle size distribution in the laboratory

Appendix I: Laboratory measurements of samples analyzed

Appendix J: Data of extended Particle size distribution samples

Appendix K: TSS and PSD estimation and SAFL Baffle selection

Appendix L: Use of Charts to Estimate Required Removal and SAFL Baffle

Appendix M: List of equipment and supplies for sample collection and analysis

Appendix N: Information for submitting samples to External lab for Particle size distribution analysis

Appendix O: Street sweeping and regression analysis

# Appendix A HEC-HMS analysis of all four sites

HEC-HMS analysis of the sites was performed using the SCS runoff curve number method as outlined in the TR-55 manual (USDA SCS 1986), simulating a hypothetical rainfall event of 0.5 inches. Input parameters are shown in Table A.1 and Figure A.1, while resulting hydrographs and flow outputs are presented in Table A.2 and Figures A.2, A.3, A.4 and A.5.

Table A.1 Input data for HEC-HMS simulation

| **Parameters** | **Unit** | **Beal Slough** | **Beatrice North** | **Beatrice West** | **Cornhusker** |
|---|---|---|---|---|---|
| Area | *miles$^2$* | 0.0431 | 0.0207 | 0.0622 | 0.0304 |
| Initial Abstraction | *in* | 0.47 | 0.38 | 0.67 | 0.7 |
| CN (pervious) | | 81 | 84 | 75 | 74 |
| Impervious | *%* | 60 | 45 | 34 | 77 |
| Lag time | *min* | 10 | 36 | 12 | 15 |

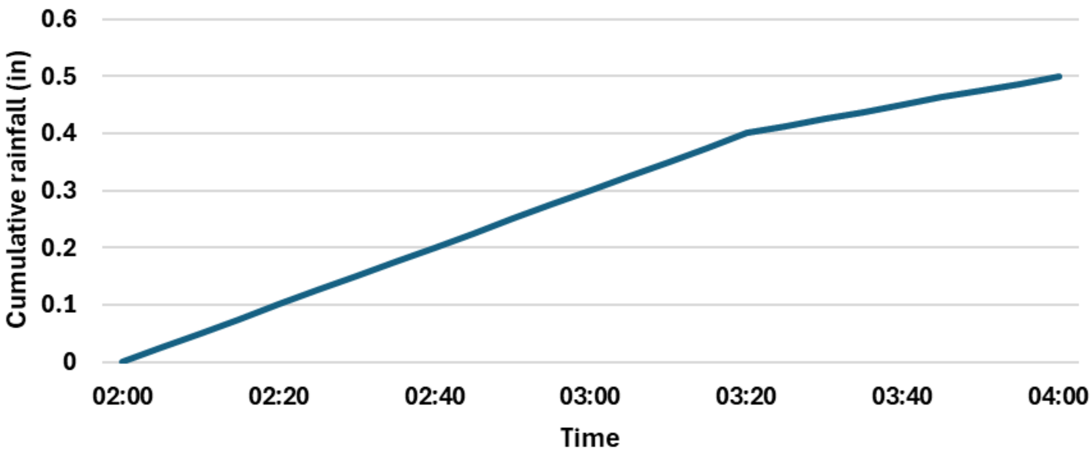

Figure A.1 Hypothetical rainfall used for HEC-HMS simulation

Table A.2 Summary of HEC-HMS simulation results

| Site | Area (sq.miles) | Peak discharge (cfs) | Time of Peak | Volume (in) |
|---|---|---|---|---|
| Beal Slough | 0.043 | 5.01 | 1 July 2024, 03:20 | 0.30 |
| Beatrice North | 0.021 | 1.67 | 1 July 2024, 03:30 | 0.23 |
| Beatrice West | 0.062 | 4.09 | 1 July 2024, 03:20 | 0.17 |
| Cornhusker | 0.030 | 4.53 | 1 July 2024, 03:20 | 0.38 |

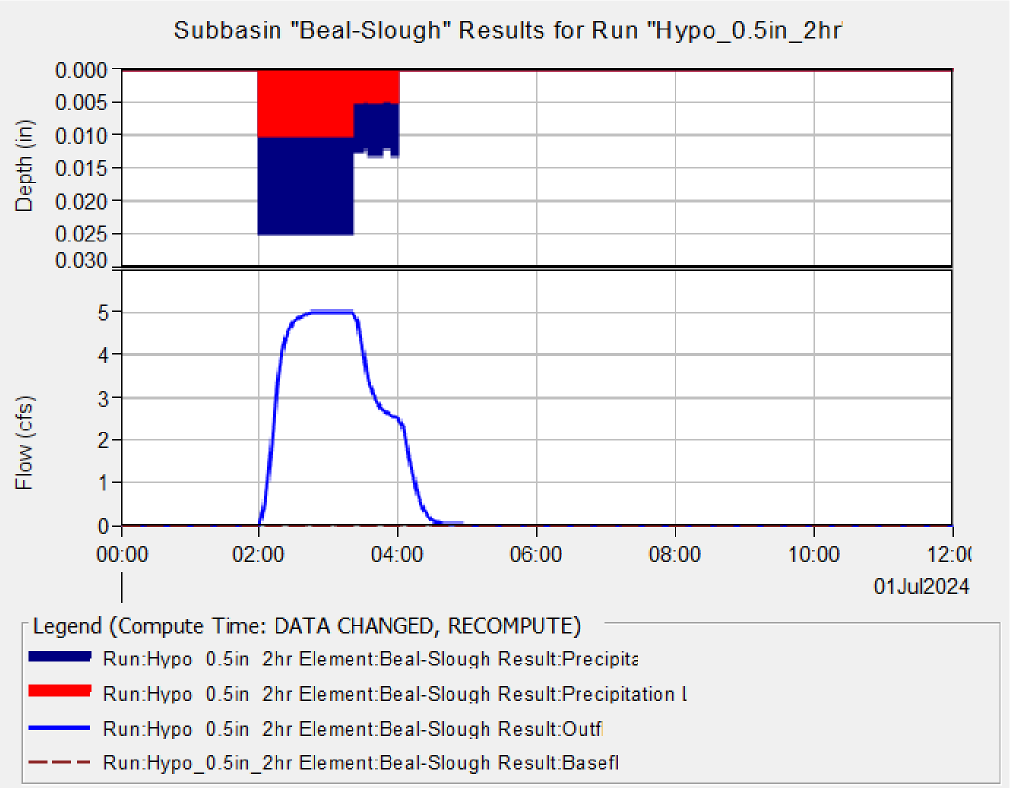

Figure A.2 Rainfall-runoff response at Beal Slough

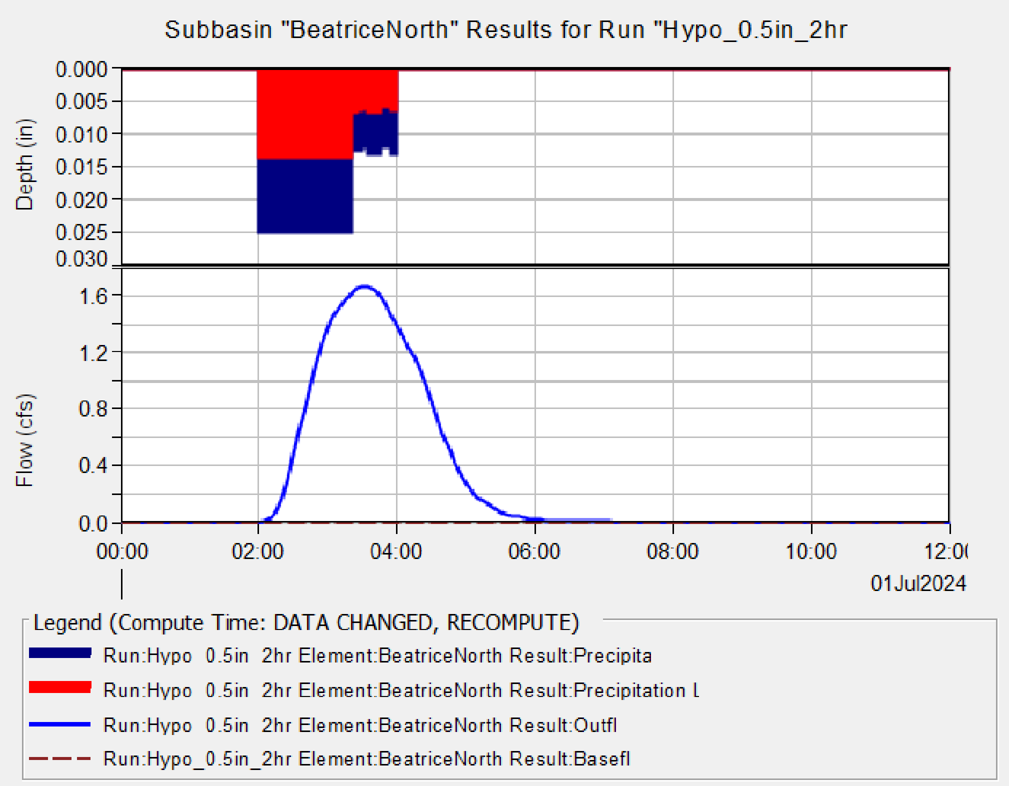

Figure A.3 Rainfall-runoff response at Beatrice North

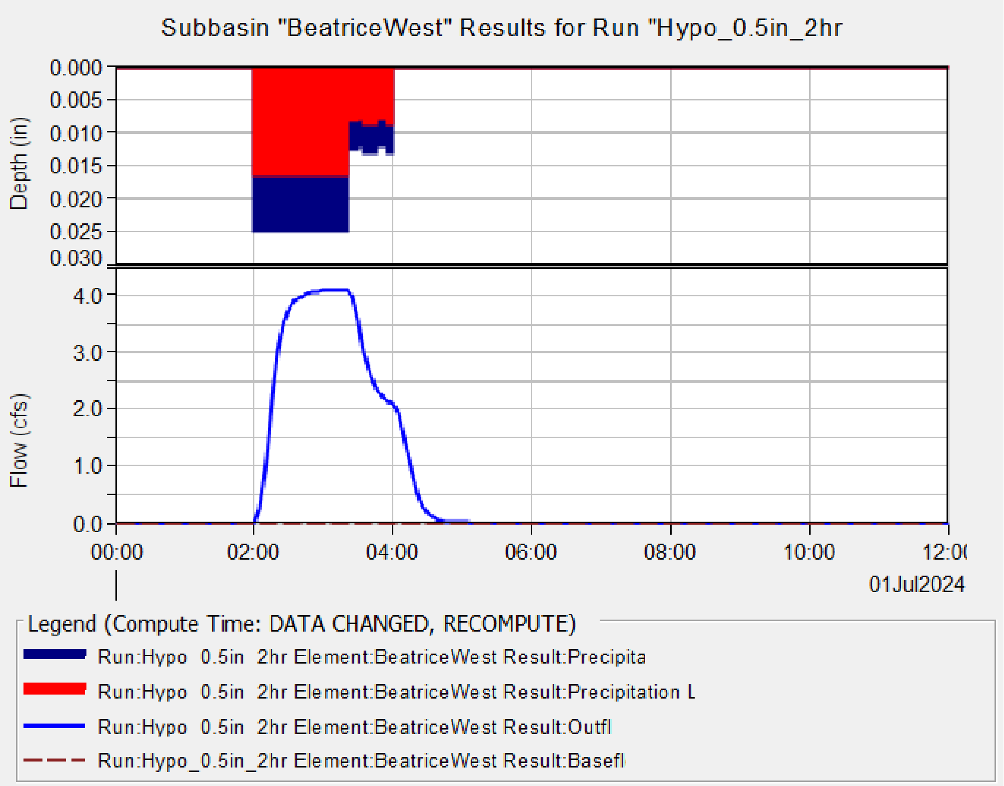

Figure A.4 Rainfall-runoff response at Beatrice West

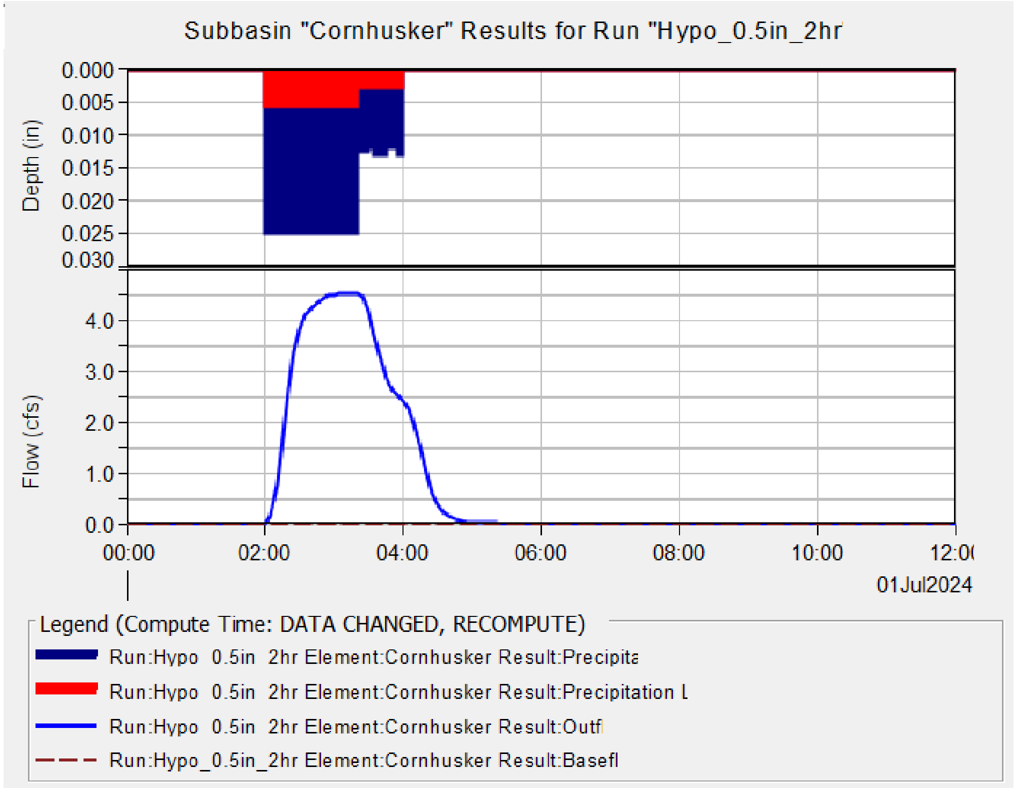

Figure A.5 Rainfall-runoff response at Cornhusker

# Appendix B Location of weather stations

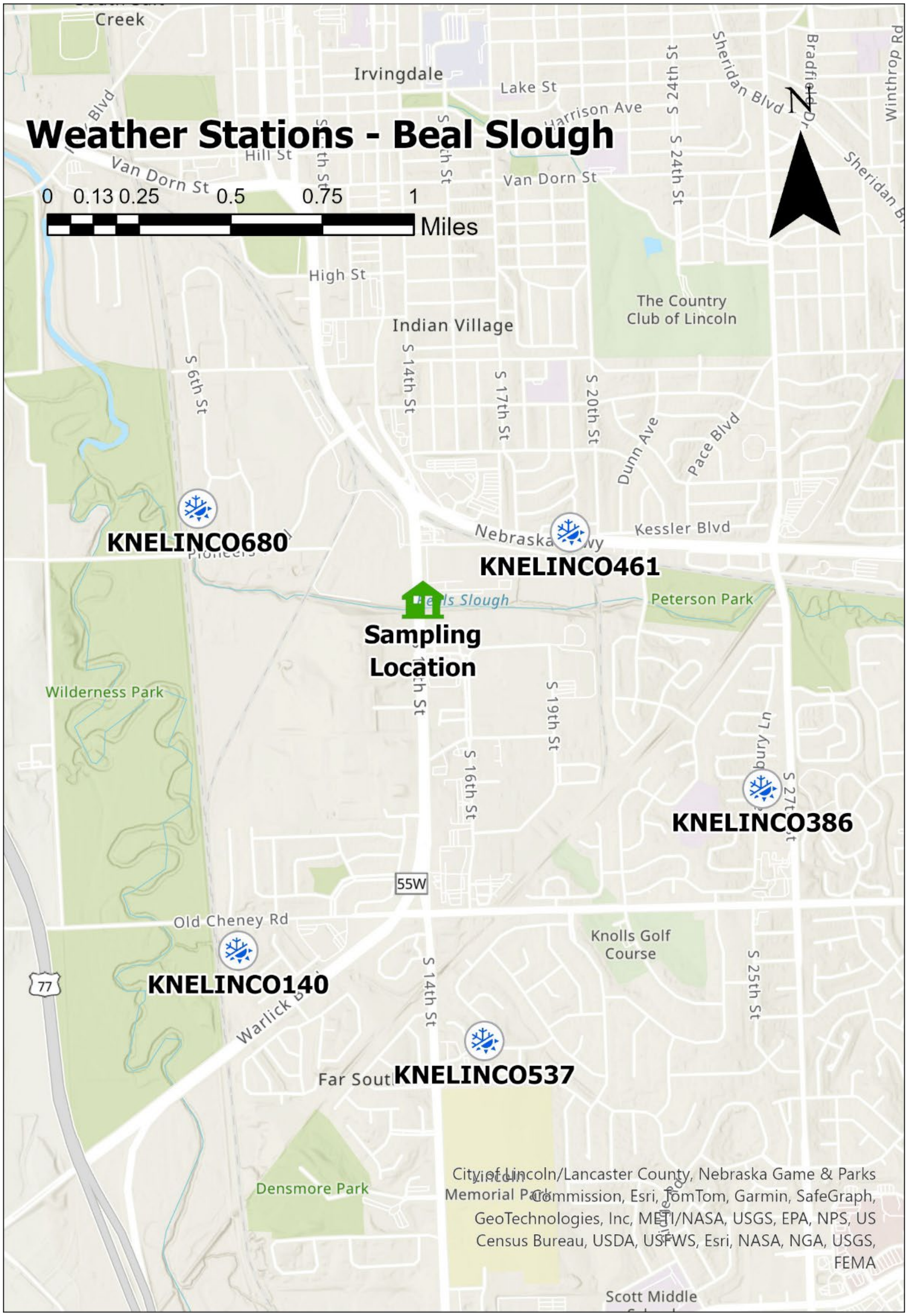

Figure B.1 Location of weather stations around Beal Slough site

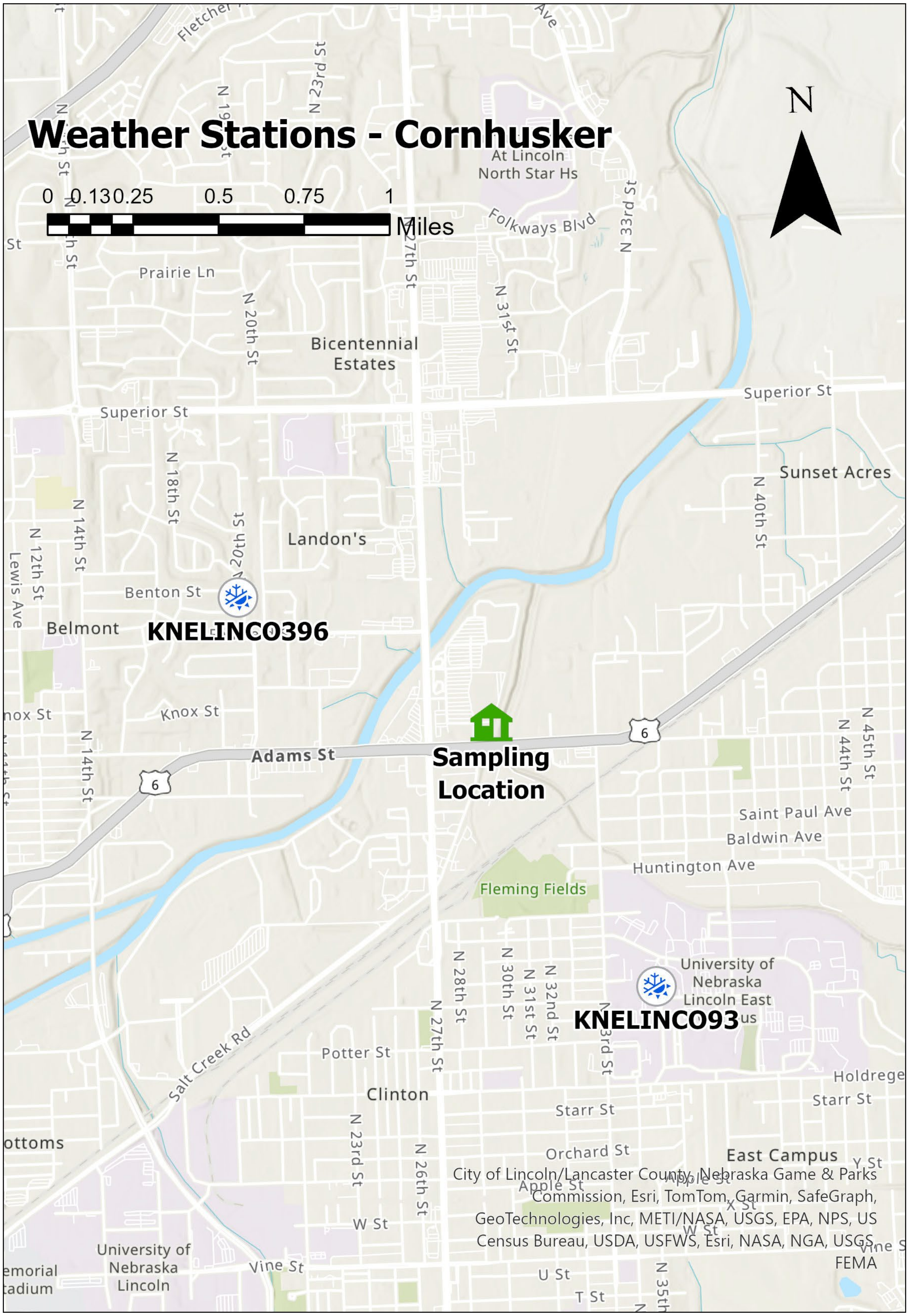

Figure B.2 Location of weather stations around Cornhusker site

Figure B.3 Location of weather stations around Beatrice sites

# Appendix C Plans and profiles of sampling locations

The following figures present plan and profile views of each site, illustrating the general layout and equipment installation. While the drawings are not to scale, they help illustrate the overall setup.

Each site included an equipment enclosure, installed on a four-inch-thick concrete pad. A four-inch PVC conduit was buried to connect the enclosure to the nearby culvert, allowing the sampling line and flow meter cable to pass through. Inside each enclosure, an automatic water sampler, flow meter, batteries, and other necessary accessories were housed.

At the Beatrice sites, the two enclosures were installed side by side and shared the same manhole and PVC access pipe. However, they collected samples from two separate pipes, one from the west (Beatrice West site) and one from the northwest (Beatrice North site), that discharged into the manhole.

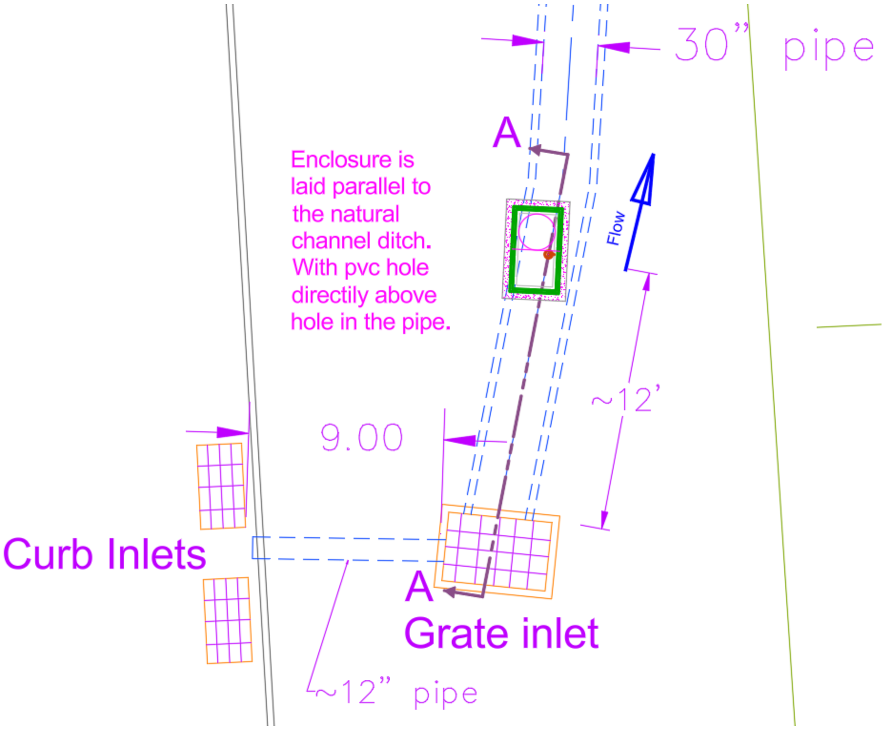

Figure C.1 Plan view of monitoring site at Beal Slough

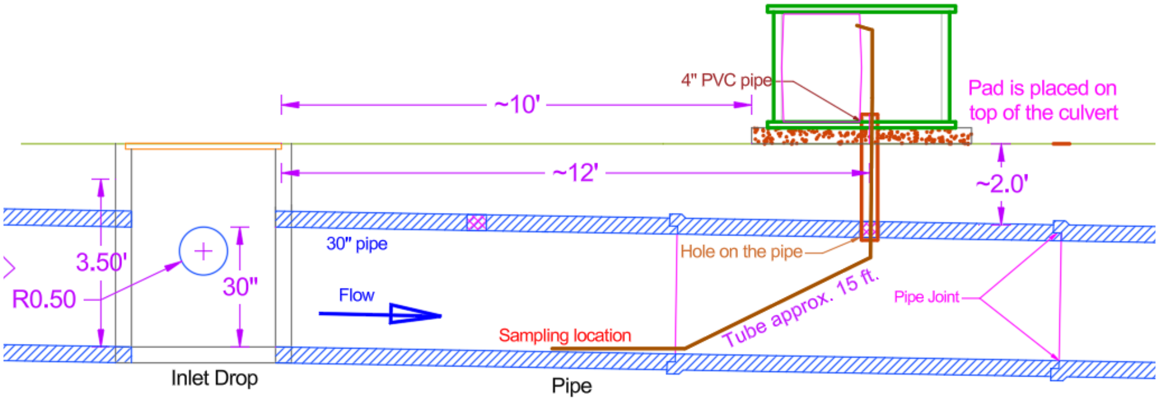

Figure C.2 Profile view of monitoring site at Beal Slough

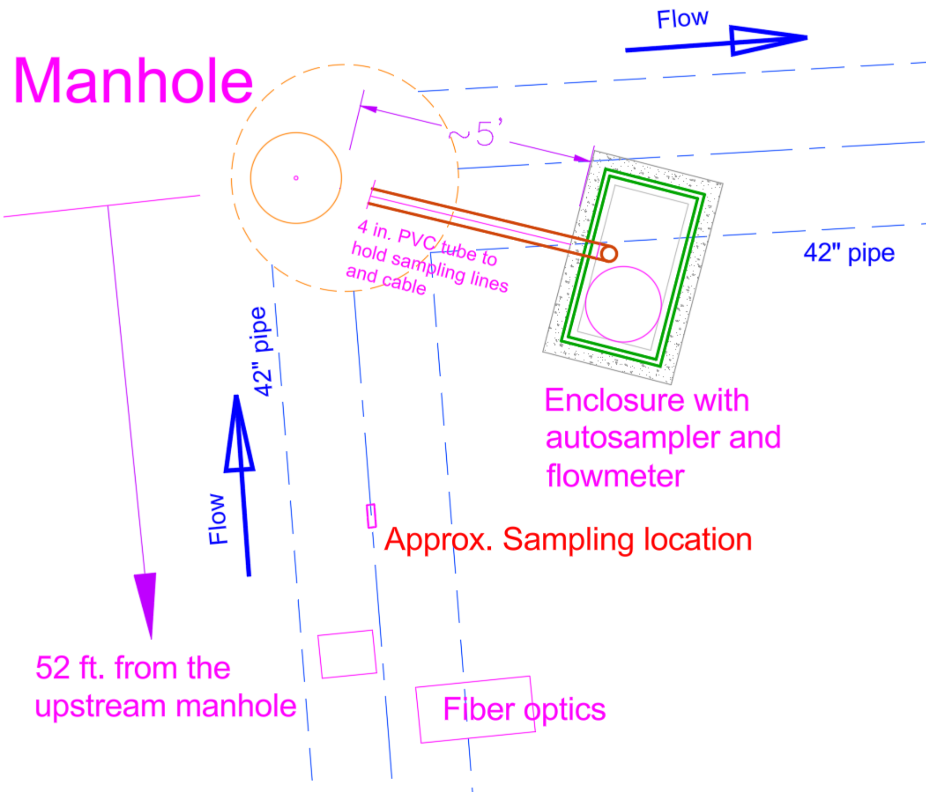

Figure C.3 Plan view of monitoring site at Cornhusker

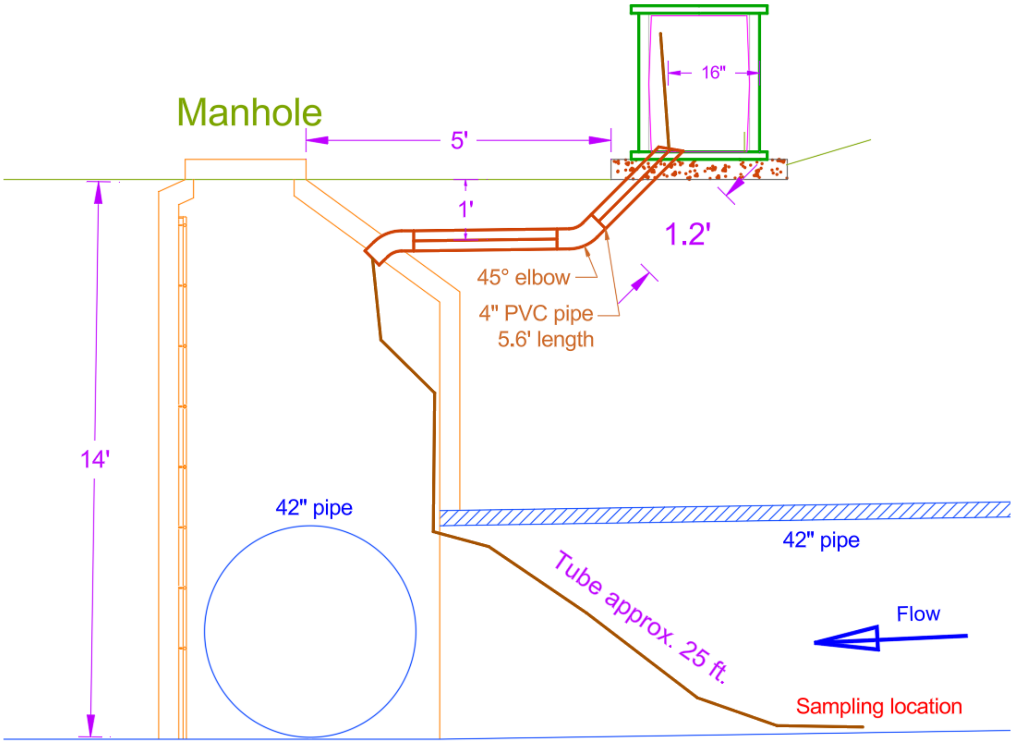

Figure C.4 Profile view of monitoring site at Cornhusker

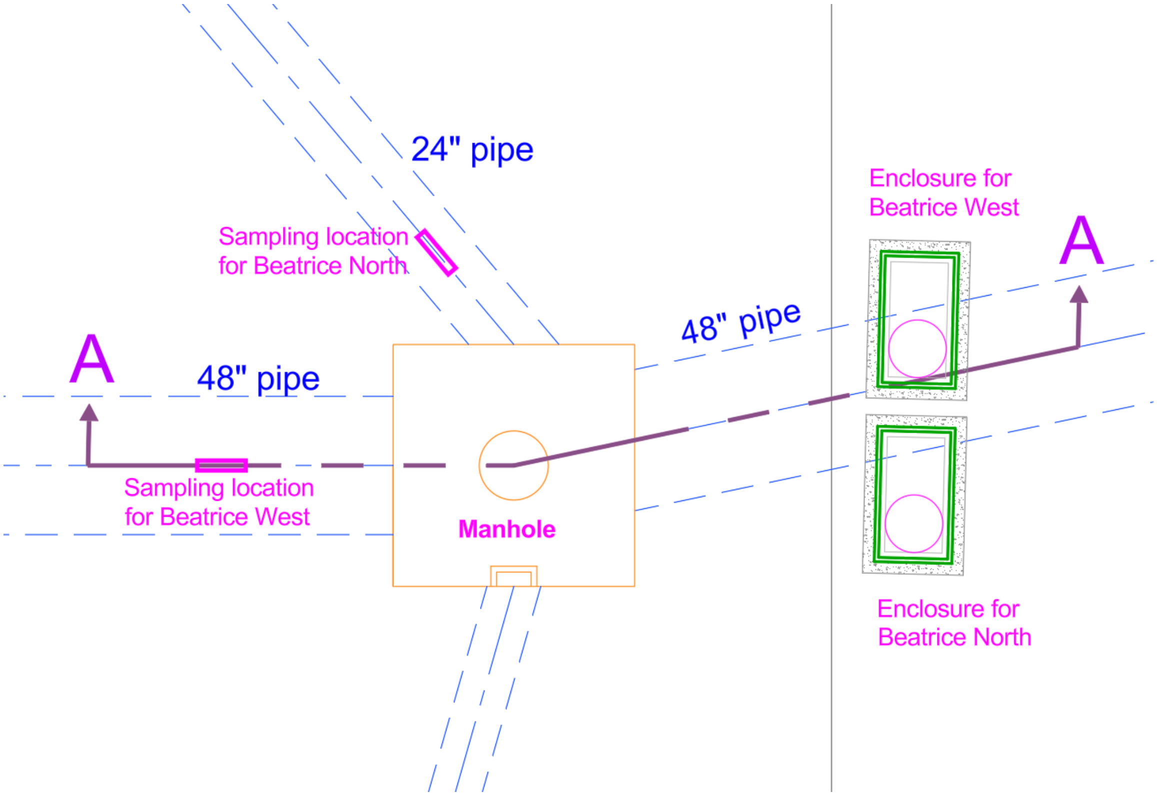

Figure C.5 Plan view of monitoring site at Beatrice

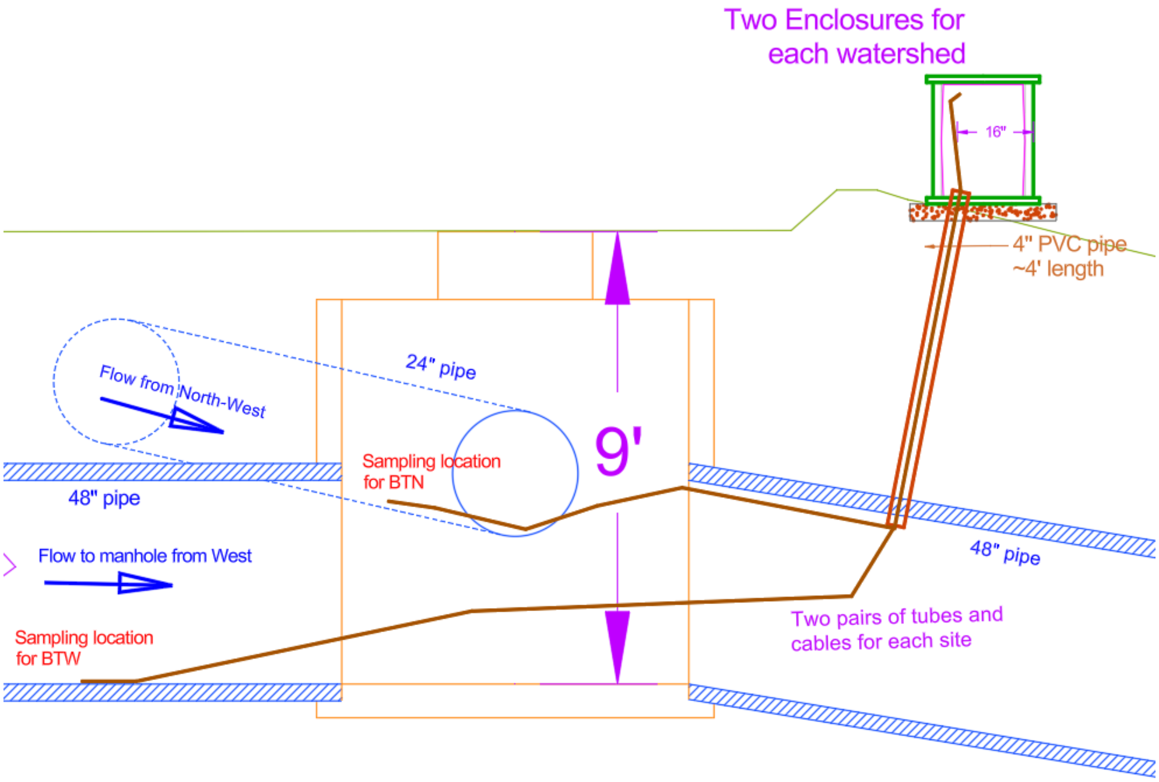

Figure C.6 Profile view of monitoring site at Beatrice

## Appendix D Standard operating procedure for sample collection

Samples are collected after a storm, with one composite sample taken per site. After collecting, the sites should be prepared for the next storm. The following procedure ensures effective sample collection and storage.

Preparation

1. Prior to the storm event, look for the weather forecast to plan the collection date.
2. Reserve a car from UNL Fleet management service.
3. Collect required items listed in Table D.1 before sample collection day.

Table D.1 List of items required for sample collection

| **Item Name** | **Quantity** | **Purpose** | **Location** |
|---|---|---|---|
| Site Keys | 1 per site | To open enclosure | Office |
| 10-L carboys | 1 per site | Sampling for next storm | Lab |
| Laptop with Flowlink | 1 | Download data | Office |
| Communication cable for 6712 sampler | 1 | Download data | Lab |
| Communication cable for 2150 AV module | 1 | Download data | Lab |
| 12 V deep cycle battery | 2 | Replace used batteries | Lab |
| Voltmeter | 1 | Check the voltage of battery | Office |
| Labeling tape | 1 | Mark samples | Lab |
| Sharpie | 1 | Mark samples | Lab |

Day of sample collection

4. Bring all the items in the car and head out to each site.
5. Collect the carboy with the collected sample and label it by site and date of collection. Put empty carboy back into the auto sampler.
6. Connect Laptop to the auto sampler or flowmeter with the help of communication cable. Download all data.

7. For the 3700 sampler, manually note the time and date of each sample. For the 6712 sampler it is not necessary.
8. Replace batteries for two sites in alternating cycles. For example, batteries for Lincoln sites are replaced in one storm event and Beatrice sites are replaced in another storm event.
9. Measure and note down voltage readings of batteries.
10. Restart the programming to get it ready for the next storm.
11. Data loggers are to be placed in each enclosure to monitor temperature. Data can be downloaded periodically.

<u>Sample storage</u>

12. Bring back samples to the lab and store them in the refrigerator at 40°F before they are processed.
13. Return all the items to their respective locations.
14. Recharge the used batteries.

# Appendix E Collection dates of processed samples

The tables below provide the list of dates when samples were collected from each site, along with the dates of the storms during which the autosampler was triggered. Depending on the timing, samples were collected either on the day of the storm, the day after, or sometimes two days later. If the storm event spanned multiple days, all relevant dates are included.

All samples included in the table were tested in the lab for total suspended solids (TSS) and particle size distribution (PSD). A select number of these samples were also sent to an external lab for extended particle size analysis, specifically for particles smaller than 32 µm. These samples are shown in bold fonts.

Table E.1 Collection dates with Storm dates – Beal Slough

| **Collection dates** | **Storm dates** |
|---|---|
| **3/24/2024** | 3/24/2024 |
| **4/16/2024** | 4/16/2024 |
| **4/26/2024** | 4/25/2024 - 4/26/2024 |
| **4/28/2024** | 4/27/2024 |
| 5/2/2024 | 5/2/2024 |
| **5/4/2024** | 5/4/2024 |
| 5/7/2024 | 5/6/2024 |
| 5/13/2024 | 5/12/2024 |
| 5/20/2024 | 5/19/2024 |
| **5/24/2024** | 5/24/2024 |
| **5/31/2024** | 5/30/2024 |
| 6/8/2024 | 6/7/2024 |
| **6/16/2024** | 6/15/2024 |
| 6/26/2024 | 6/26/2024 |
| **7/1/2024** | 7/1/2024 |
| 7/7/2024 | 7/6/2024 |
| 7/21/2024 | 7/19/2024 - 7/20/2024 |
| 8/1/2024 | 7/31/2024 |
| **8/14/2024** | 8/14/2024 |
| **8/30/2024** | 8/29/2024 |
| 10/22/2024 | 10/21/2024 |
| **10/31/2024** | 10/30/2024 |
| **11/9/2024** | 11/8/2024 |
| 11/13/2024 | 11/13/2024 |
| **11/19/2024** | 11/18/2024 |
| **4/25/2025** | 4/24/2025 |
| **5/20/2025** | 5/18/2025 |
| 6/2/2025 | 5/31/2025 |
| **6/4/2025** | 6/3/2025 |

Table E.2 Collection dates with Storm dates – Cornhusker

| **Collection dates** | **Storm dates** |
|---|---|
| **3/24/2024** | 3/24/2024 |
| **4/7/2024** | 4/6/2024 - 4/7/2024 |
| 4/16/2024 | 4/16/2024 |
| 4/26/2024 | 4/25/2024 - 4/262024 |
| **4/28/2024** | 4/26/2024 - 4/28/2024 |
| **5/2/2024** | 5/2/2024 |
| **5/4/2024** | 5/4/2024 |
| 5/7/2024 | 5/6/2024 |
| 5/13/2024 | 5/12/2024 - 5/13/2024 |
| 5/20/2024 | 5/19/2024 |
| 5/24/2024 | 5/24/2024 |
| **5/31/2024** | 5/30/2024 |
| 6/3/2024 | 6/3/2024 |
| 6/8/2024 | 6/7/2024 |
| **6/16/2024** | 6/15/2024 |
| 6/19/2024 | 6/18/2024 |
| 6/26/2024 | 6/26/2024 |
| 6/28/2024 | 6/27/2024 |
| **7/1/2024** | 7/1/2024 |
| 8/8/2024 | 8/8/2024 |
| 8/12/2024 | 8/12/2024 |
| **8/14/2024** | 8/14/2024 |
| 8/19/2024 | 8/17/2024 - 8/18/2024 |
| **10/22/2024** | 10/21/2024 - 10/22/2024 |
| **11/4/2024** | 11/3/2024 |
| 3/15/2025 | 3/14/2025 |
| **4/25/2025** | 4/24/2025 - 4/25/2025 |
| **5/20/2025** | 5/18/2025 - 5/19/2025 |
| 5/27/2025 | 5/25/2025 - 5/26/2025 |
| **6/2/2025** | 5/31/2025 |

Table E.3 Collection dates with Storm dates – Beatrice North

| Collection dates | Storm dates |
|---|---|
| **4/26/2024** | 4/25/2024 - 4/26/2024 |
| **4/28/2024** | 4/27/2024 - 4/28/2024 |
| 5/2/2024 | 5/1/2024 - 5/2/2024 |
| **5/4/2024** | 5/3/2024 - 5/4/2024 |
| **5/7/2024** | 5/6/2024 - 5/7/2024 |
| 5/13/2024 | 5/12/2024 - 5/13/2024 |
| **5/24/2024** | 5/24/2024 |
| **5/31/2024** | 5/30/2024 |
| 6/8/2024 | 6/7/2024 - 6/8/2024 |
| **6/16/2024** | 6/15/2024 - 6/15/2024 |
| **6/26/2024** | 6/26/2024 |
| 7/21/2024 | 7/20/2024 |
| **8/14/2024** | 8/14/2024 |
| **8/30/2024** | 8/29/2024 - 8/30/2024 |
| 9/23/2024 | 9/21/2024 - 9/22/2024 |
| **10/22/2024** | 10/21/2024 |
| **10/31/2024** | 10/29/2024 - 10/30/2024 |
| 11/4/2024 | 11/2/2024 - 11/3/2024 |
| **11/9/2024** | 11/8/2024 - 11/9/2024 |
| 11/13/2024 | 11/13/2024 - 11/13/2024 |
| **11/19/2024** | 11/18/2024 |
| **12/14/2024** | 12/14/2024 |
| 3/6/2025 | 3/4/2025 |
| 3/20/2025 | 3/19/2025 |
| **4/2/2025** | 4/1/2025 - 4/2/2025 |
| 4/4/2025 | 4/4/2025 |
| **5/20/2025** | 5/18/2025 - 5/19/2025 |
| 5/27/2025 | 5/26/2025 |
| 6/2/2025 | 5/31/2025 |
| **6/4/2025** | 6/3/2025 |

Table E.4 Collection dates with Storm dates – Beatrice West

| **Collection dates** | **Storm dates** |
|---|---|
| 4/26/2024 | 4/25/2024 - 4/26/2024 |
| **4/28/2024** | 4/28/2024 |
| **5/2/2024** | 5/2/2024 |
| **5/4/2024** | 5/4/2024 |
| **5/7/2024** | 5/6/2024 - 5/7/2024 |
| **5/24/2024** | 5/24/2024 |
| **5/31/2024** | 5/30/2024 |
| 6/3/2024 | 6/3/2024 |
| **6/16/2024** | 6/15/2024 |
| **7/1/2024** | 6/28/2024 |
| 7/6/2024 | 7/4/2024 |
| 7/7/2024 | 7/6/2024 |
| **10/31/2024** | 10/29/2024 - 10/30/2024 |
| **11/4/2024** | 11/2/2024 - 11/3/2024 |
| **11/9/2024** | 11/8/2024 - 11/9/2024 |
| **11/13/2024** | 11/13/2024 - 11/13/2024 |
| **11/19/2024** | 11/18/2024 |
| **4/2/2025** | 4/1/2025 - 4/2/2025 |
| **5/20/2025** | 5/18/2025 - 5/19/2025 |
| 5/27/2025 | 5/26/2025 |
| 6/2/2025 | 5/31/2025 |
| **6/4/2025** | 6/3/2025 |

## Appendix F Rainfall and flow characteristics for sampling events

Table F.1 Rainfall and flow characteristics of Beal Slough

| Date | Peak 20 min intensity [in/hr] | Peak 1 hr intensity [in/hr] | Rainfall depth [in] | Peak discharge [$m^3/s$] | Total flow volume [$m^3$] |
|---|---|---|---|---|---|
| 3/24/2024 | 0.78 | 0.43 | 0.70 | 0.06 | 55.39 |
| 4/16/2024 | 1.50 | 0.74 | 0.78 | 0.61 | 433.50 |
| 4/26/2024 | 0.54 | 0.18 | 0.51 | 0.07 | 34.68 |
| 4/28/2024 | 1.02 | 0.42 | 0.61 | 0.28 | 129.48 |
| 5/2/2024 | 1.35 | 0.61 | 0.87 | 0.24 | 104.04 |
| 5/4/2024 | 0.61 | 0.39 | 0.75 | 0.07 | 40.80 |
| 5/7/2024 | 0.78 | 0.33 | 0.46 | 0.16 | 28.80 |
| 5/13/2024 | 0.51 | 0.36 | 0.43 | 0.14 | 89.40 |
| 5/20/2024 | 0.84 | 0.44 | 0.56 | 0.16 | 81.60 |
| 5/24/2024 | 1.38 | 0.71 | 0.76 | 0.21 | 252.84 |
| 5/31/2024 | 0.33 | 0.11 | 0.11 | 0.04 | 16.02 |
| 6/8/2024 | 1.53 | 0.66 | 0.67 | 0.39 | 245.28 |
| 6/16/2024 | 1.44 | 0.64 | 0.94 | 0.15 | 93.60 |
| 6/26/2024 | 0.63 | 0.24 | 0.30 | 0.08 | 14.46 |
| 7/1/2024 | 1.26 | 0.77 | 1.22 | 0.26 | 297.84 |
| 7/7/2024 | 1.62 | 0.74 | 0.93 | 0.32 | 178.56 |
| 7/21/2024 | 0.87 | 0.38 | 0.39 | 0.09 | 39.54 |
| 8/1/2024 | 1.23 | 0.50 | 0.52 | 0.15 | 115.38 |
| 8/14/2024 | 1.17 | 0.56 | 0.58 | 2.87 | 172.02 |
| 8/30/2024 | 0.96 | 0.37 | 0.55 | 0.14 | 45.90 |
| 10/22/2024 | 0.30 | 0.21 | 0.28 | 0.01 | 0.54 |
| 10/31/2024 | 0.39 | 0.13 | 0.57 | 0.05 | 62.88 |
| 11/9/2024 | 0.36 | 0.22 | 0.41 | 0.04 | 15.00 |
| 11/13/2024 | 0.42 | 0.32 | 0.56 | 0.04 | 48.90 |
| 11/19/2024 | 0.46 | 0.28 | 1.05 | 0.07 | 129.72 |
| 4/25/2025 | 0.45 | 0.19 | 0.45 | 0.06 | 64.32 |
| 5/20/2025 | 0.93 | 0.59 | 1.15 | 0.08 | 67.38 |
| 6/2/2025 | 0.20 | 0.14 | 0.18 | 0.06 | 16.00 |
| 6/4/2025 | 0.70 | 0.61 | 0.92 | 0.20 | 110.01 |

Table F.2 Rainfall and flow characteristics of Beatrice West

| Date | Peak 20 min intensity [in/hr] | Peak 1 hr intensity [in/hr] | Rainfall depth [in] | Peak discharge [$m^3/s$] | Total flow volume [$m^3$] |
|---|---|---|---|---|---|
| 4/26/2024 | 0.24 | 0.17 | 0.44 | 0.01 | 69.20 |
| 4/28/2024 | 0.42 | 0.18 | 0.27 | 0.02 | 119.17 |
| 5/2/2024 | 0.39 | 0.29 | 0.54 | 0.04 | 427.36 |
| 5/4/2024 | 1.65 | 1.04 | 1.41 | 0.43 | 2186.35 |
| 5/7/2024 | 0.36 | 0.20 | 0.28 | 0.01 | 115.74 |
| 5/24/2024 | 0.69 | 0.48 | 0.50 | 0.02 | 98.68 |
| 5/31/2024 | 1.26 | 0.66 | 0.67 | 0.28 | 819.56 |
| 6/3/2024 | 0.57 | 0.29 | 0.32 | 0.02 | 166.02 |
| 6/16/2024 | 1.26 | 0.68 | 1.34 | 0.25 | 1169.89 |
| 7/1/2024 | 0.75 | 0.31 | 0.54 | 0.08 | 556.92 |
| 7/6/2024 | 0.90 | 0.45 | 0.78 | 0.11 | 0.09 |
| 7/7/2024 | 2.67 | 1.03 | 1.04 | 0.21 | 903.03 |
| 10/31/2024 | 1.50 | 0.85 | 1.30 | 0.04 | 320.54 |
| 11/4/2024 | 1.14 | 0.57 | 0.60 | 0.14 | 577.17 |
| 11/9/2024 | 0.36 | 0.24 | 0.48 | 0.03 | 237.76 |
| 11/13/2024 | 0.63 | 0.29 | 0.45 | 0.02 | 276.61 |
| 11/19/2024 | 0.54 | 0.31 | 0.73 | 0.11 | 1579.56 |
| 4/2/2025 | 0.81 | 0.31 | 0.45 | 0.04 | 184.98 |
| 5/20/2025 | 1.23 | 0.53 | 0.78 | 0.08 | 249.27 |
| 5/27/2025 | 0.12 | 0.11 | 0.35 | 0.01 | 58.92 |
| 6/2/2025 | 0.31 | 0.22 | 0.26 | 0.04 | 150.23 |
| 6/4/2025 | 0.27 | 0.18 | 0.77 | 0.02 | 72.18 |

Table F.3 Rainfall and flow characteristics of Cornhusker

| Date | Peak 20 min intensity [in/hr] | Peak 1 hr intensity [in/hr] | Rainfall depth [in] | Peak discharge [$m^3/s$] | Total flow volume [$m^3$] |
|---|---|---|---|---|---|
| 3/24/2024 | 0.42 | 0.19 | 0.27 | 0.15 | 92.51 |
| 4/7/2024 | 0.27 | 0.16 | 0.24 | 0.09 | 295.68 |
| 4/16/2024 | 1.65 | 0.87 | 0.90 | 0.78 | 1078.64 |
| 4/26/2024 | 0.72 | 0.24 | 0.51 | 0.28 | 350.24 |
| 4/28/2024 | 0.25 | 0.17 | 0.27 | 0.14 | 467.48 |
| 5/2/2024 | 0.63 | 0.36 | 0.56 | 0.31 | 426.56 |
| 5/4/2024 | 0.61 | 0.38 | 0.80 | 0.28 | 699.23 |
| 5/7/2024 | 0.69 | 0.31 | 0.48 | 0.21 | 433.85 |
| 5/13/2024 | 0.36 | 0.18 | 0.22 | 0.11 | 314.01 |
| 5/20/2024 | 0.32 | 0.17 | 0.33 | 0.12 | 223.76 |
| 5/24/2024 | 1.32 | 0.65 | 0.72 | 0.41 | 752.18 |
| 5/31/2024 | 2.22 | 0.95 | 0.95 | 0.82 | 568.88 |
| 6/3/2024 | 0.15 | 0.07 | 0.10 | 0.03 | 104.07 |
| 6/8/2024 | 1.85 | 0.66 | 1.24 | 1.17 | 1752.80 |
| 6/16/2024 | 1.11 | 0.50 | 0.83 | 0.28 | 733.04 |
| 6/19/2024 | 0.34 | 0.14 | 0.19 | 0.08 | 109.66 |
| 6/26/2024 | 0.46 | 0.27 | 0.40 | 0.24 | 517.19 |
| 6/28/2024 | 0.17 | 0.07 | 0.07 | 0.07 | 49.62 |
| 7/1/2024 | 1.26 | 1.06 | 1.39 | 0.39 | 1079.52 |
| 8/8/2024 | 0.45 | 0.18 | 0.21 | 0.28 | 156.98 |
| 8/12/2024 | 0.06 | 0.03 | 0.04 | 0.05 | 88.37 |
| 8/14/2024 | 0.88 | 0.41 | 0.44 | 0.46 | 757.30 |
| 8/19/2024 | 0.18 | 0.13 | 0.27 | 0.07 | 337.74 |
| 3/15/2025 | 0.45 | 0.17 | 0.18 | 0.18 | 129.82 |
| 4/25/2025 | 0.24 | 0.10 | 0.28 | 0.10 | 169.53 |
| 5/20/2025 | 0.84 | 0.51 | 0.90 | 0.37 | 2074.13 |
| 5/27/2025 | 0.09 | 0.07 | 0.24 | 0.01 | 55.04 |
| 6/2/2025 | 0.14 | 0.09 | 0.29 | 0.05 | 420.58 |

Table F.4 Rainfall and flow characteristics of Beatrice North

| Date | Peak 20 min intensity [in/hr] | Peak 1 hr intensity [in/hr] | Rainfall depth [in] | Peak discharge [$m^3/s$] | Total flow volume [$m^3$] |
|---|---|---|---|---|---|
| 4/26/2024 | 0.24 | 0.17 | 0.41 | 0.03 | 194.70 |
| 4/28/2024 | 0.42 | 0.18 | 0.27 | 0.04 | 96.78 |
| 5/2/2024 | 0.39 | 0.29 | 0.56 | 0.08 | 398.40 |
| 5/4/2024 | 1.65 | 1.04 | 1.50 | 0.32 | 1202.76 |
| 5/7/2024 | 0.36 | 0.20 | 0.28 | 0.06 | 204.60 |
| 5/13/2024 | 0.15 | 0.07 | 0.34 | 0.02 | 217.02 |
| 5/24/2024 | 0.69 | 0.48 | 0.50 | 0.11 | 157.92 |
| 5/31/2024 | 1.26 | 0.66 | 0.67 | 0.41 | 771.24 |
| 6/8/2024 | 0.15 | 0.12 | 0.19 | 0.02 | 103.02 |
| 6/16/2024 | 1.26 | 0.68 | 1.34 | 0.27 | 947.10 |
| 6/26/2024 | 0.66 | 0.38 | 0.41 | 0.15 | 193.80 |
| 7/21/2024 | 0.62 | 0.38 | 0.52 | 0.04 | 167.64 |
| 8/14/2024 | 0.21 | 0.16 | 0.16 | 0.03 | 55.80 |
| 8/30/2024 | 0.60 | 0.27 | 0.66 | 0.09 | 267.00 |
| 9/23/2024 | 0.15 | 0.07 | 0.15 | 0.02 | 57.72 |
| 10/22/2024 | 0.24 | 0.09 | 0.22 | 0.04 | 72.96 |
| 10/31/2024 | 1.50 | 0.71 | 0.71 | 0.21 | 219.45 |
| 11/4/2024 | 1.14 | 0.57 | 0.76 | 0.21 | 583.05 |
| 11/9/2024 | 0.36 | 0.24 | 0.48 | 0.07 | 484.68 |
| 11/13/2024 | 0.63 | 0.29 | 0.45 | 0.21 | 583.05 |
| 11/19/2024 | 0.24 | 0.16 | 0.44 | 0.04 | 228.78 |
| 12/14/2024 | 0.12 | 0.07 | 0.18 | 0.03 | 166.50 |
| 3/6/2025 | 0.06 | 0.05 | 0.11 | 0.03 | 98.04 |
| 3/20/2025 | 0.12 | 0.07 | 0.20 | 0.02 | 261.30 |
| 4/2/2025 | 0.81 | 0.31 | 0.46 | 0.32 | 506.70 |
| 4/4/2025 | 0.06 | 0.04 | 0.10 | 0.02 | 162.78 |
| 5/20/2025 | 1.23 | 0.53 | 0.78 | 0.28 | 559.80 |
| 5/27/2025 | 0.06 | 0.06 | 0.11 | 0.01 | 63.36 |
| 6/2/2025 | 0.31 | 0.22 | 0.26 | 0.05 | 198.57 |
| 6/4/2025 | 0.27 | 0.18 | 0.77 | 0.03 | 550.85 |

# Appendix G Hydrograph response and sampling times

The following graphs show the hydrograph for each individual storm event during which samples were collected at each site. In these plots, the flow hydrograph is shown in green, rainfall intensity is displayed as blue bars, and cumulative rainfall is represented by a dotted blue line. Red markers indicate the times when samples were taken. Each plot also includes labels for the 50% and 100% storm points based on cumulative rainfall depth, as well as the total rainfall depth recorded at the time of the last sample. It should be noted that not all storm events are shown here; however, the ones presented are representative of the overall dataset.

# Hydrograph plots from Beal Slough

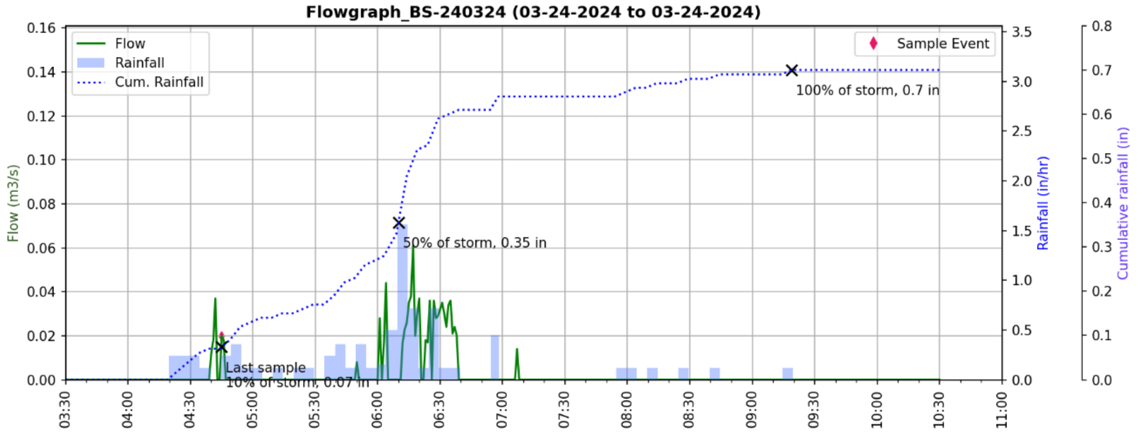

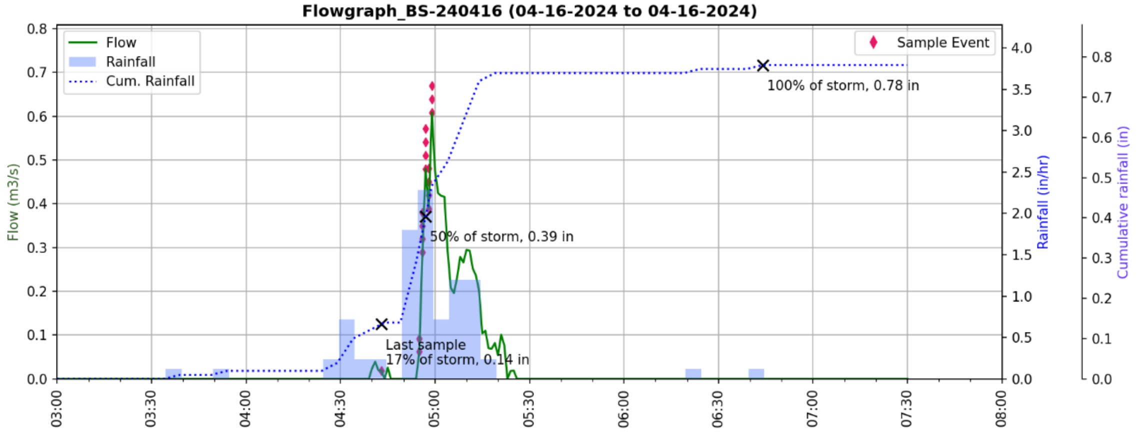

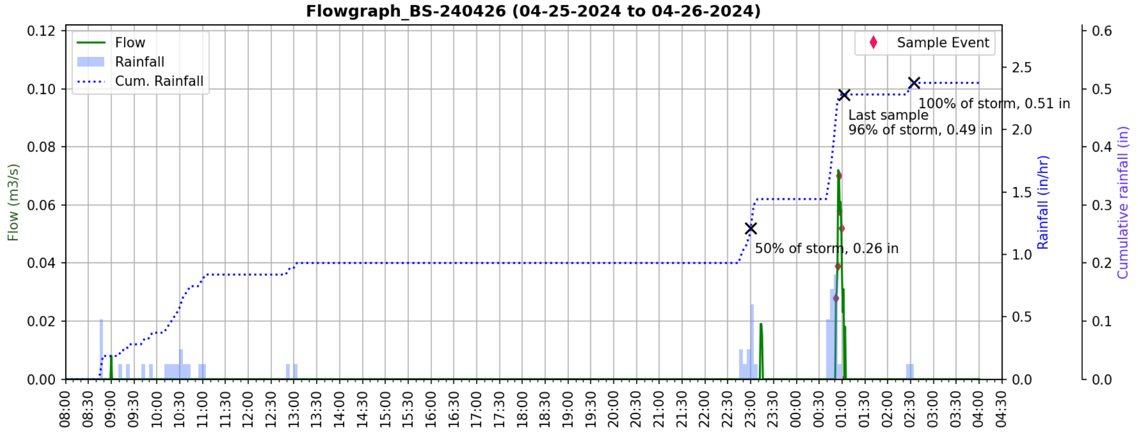

Time of day (HH:MM)

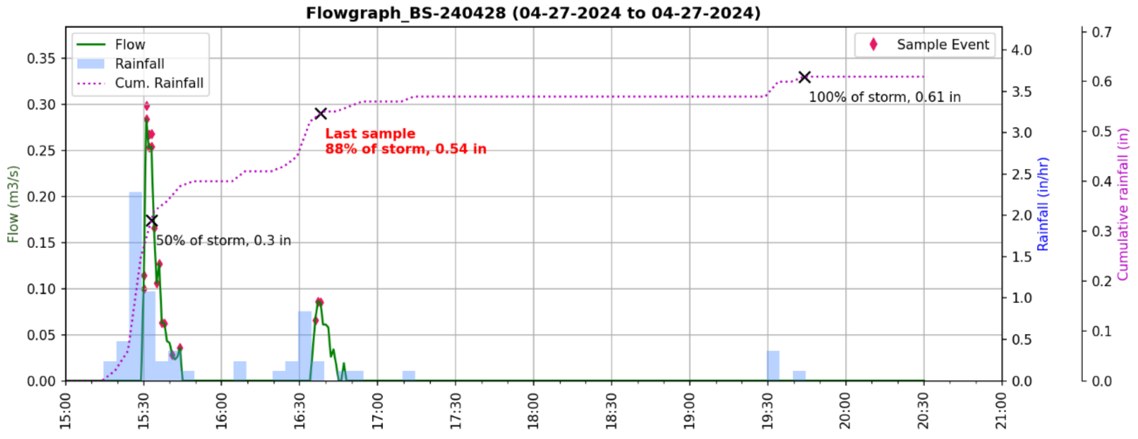
Flowgraph_BS-240428 (04-27-2024 to 04-27-2024)
Flow
Rainfall
Cum. Rainfall
Sample Event
Flow (m3/s)
Rainfall (in/hr)
Cumulative rainfall (in)
Last sample
88% of storm, 0.54 in
50% of storm, 0.3 in
100% of storm, 0.61 in
0.00
0.05
0.10
0.15
0.20
0.25
0.30
0.35
15:00
15:30
16:00
16:30
17:00
17:30
18:00
18:30
19:00
19:30
20:00
20:30
21:00

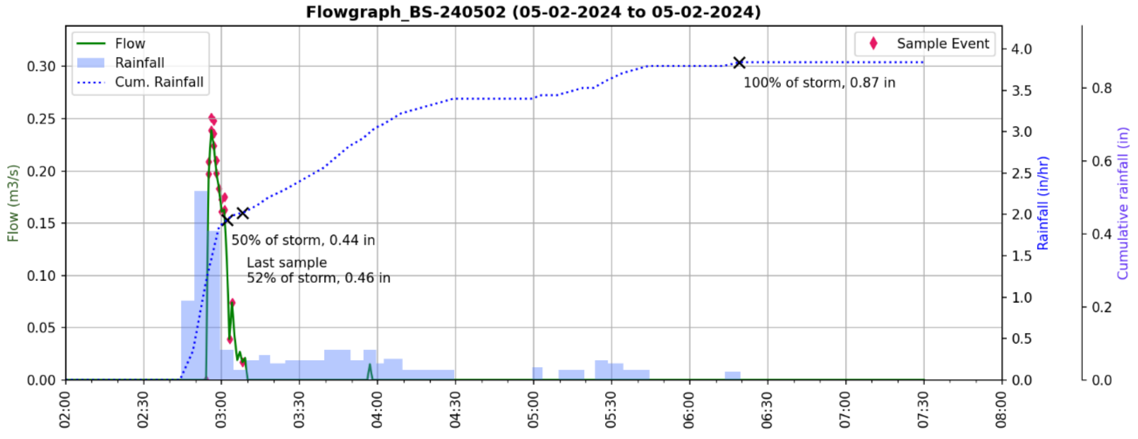
Flowgraph_BS-240502 (05-02-2024 to 05-02-2024)
Flow
Rainfall
Cum. Rainfall
Sample Event
Flow (m3/s)
Rainfall (in/hr)
Cumulative rainfall (in)
50% of storm, 0.44 in
Last sample
52% of storm, 0.46 in
100% of storm, 0.87 in
02:00
02:30
03:00
03:30
04:00
04:30
05:00
05:30
06:00
06:30
07:00
07:30
08:00

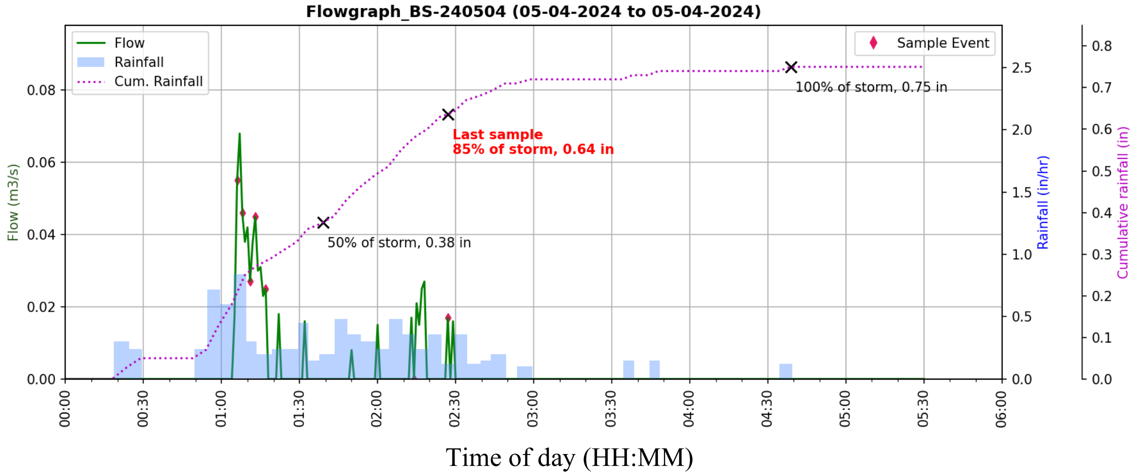
Flowgraph_BS-240504 (05-04-2024 to 05-04-2024)
Flow
Rainfall
Cum. Rainfall
Sample Event
Flow (m3/s)
Rainfall (in/hr)
Cumulative rainfall (in)
Last sample
85% of storm, 0.64 in
50% of storm, 0.38 in
100% of storm, 0.75 in
00:00
00:30
01:00
01:30
02:00
02:30
03:00
03:30
04:00
04:30
05:00
05:30
06:00
Time of day (HH:MM)

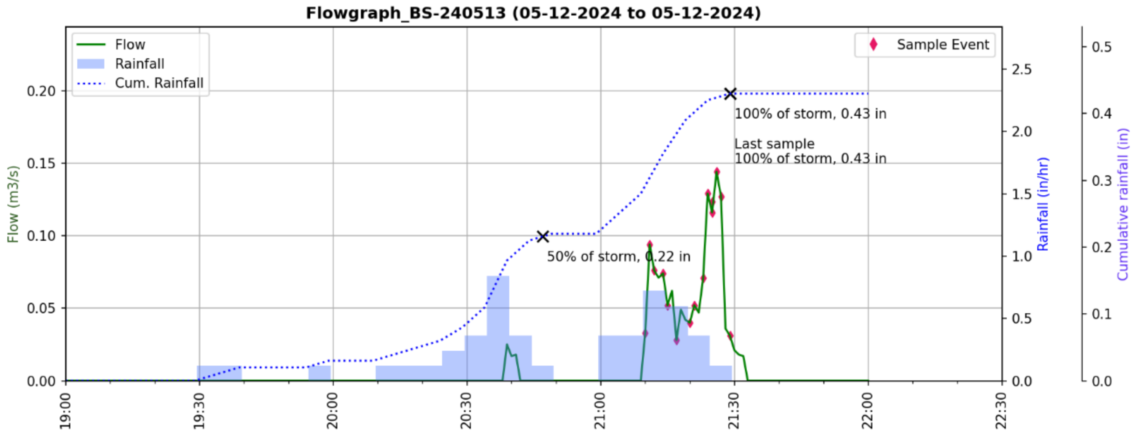

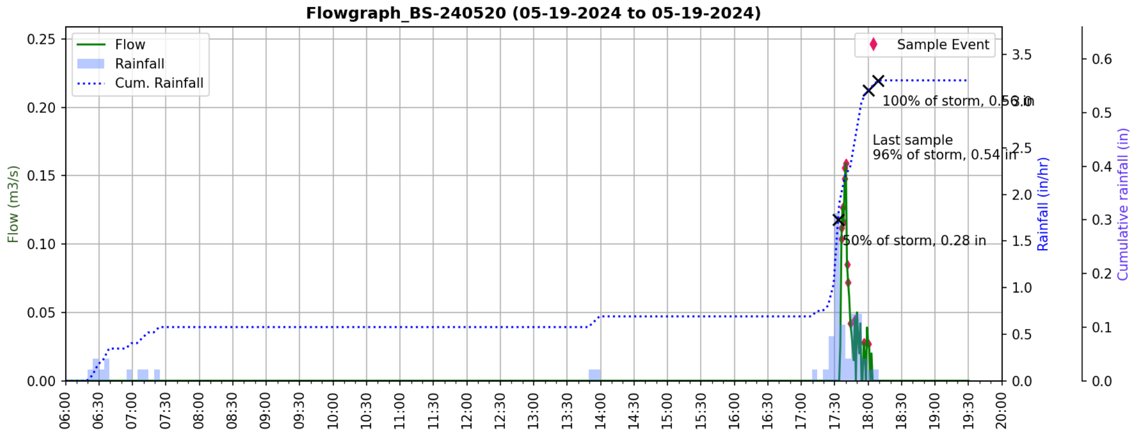

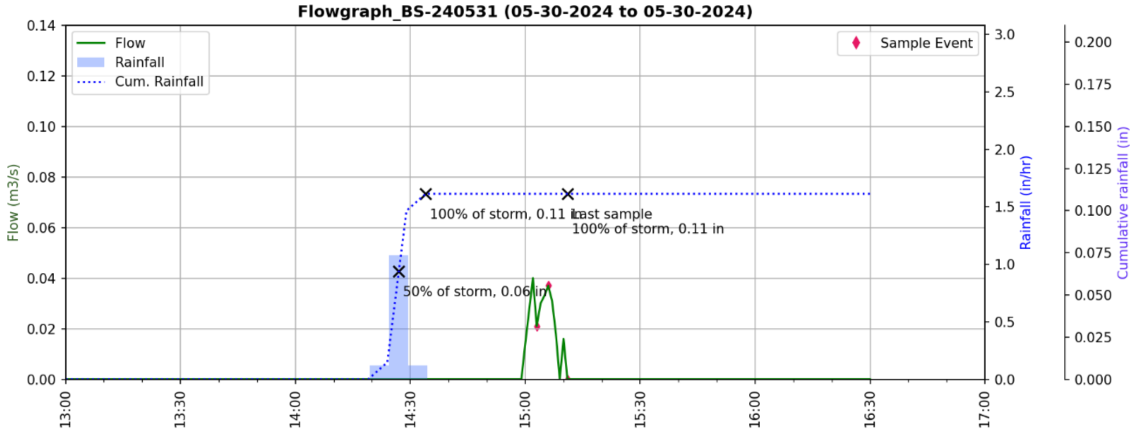

Time of day (HH:MM)

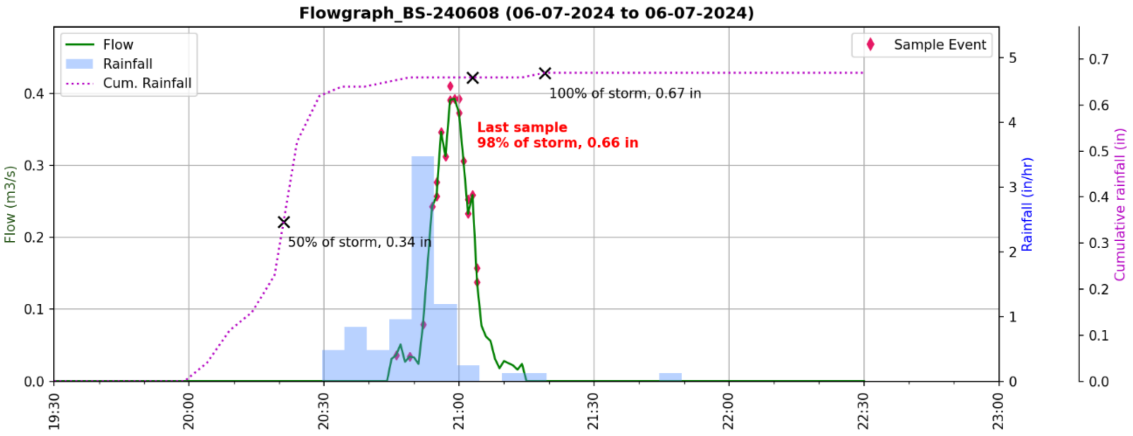

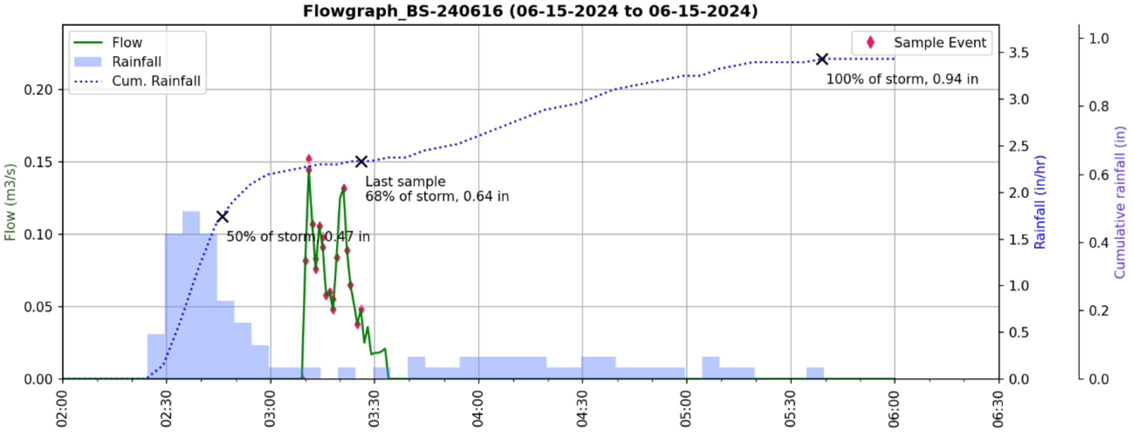

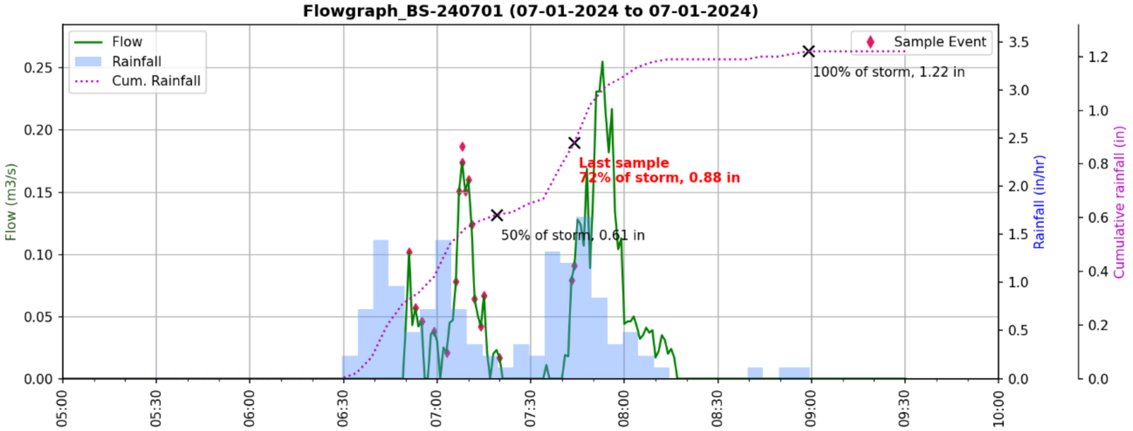

Time of day (HH:MM)

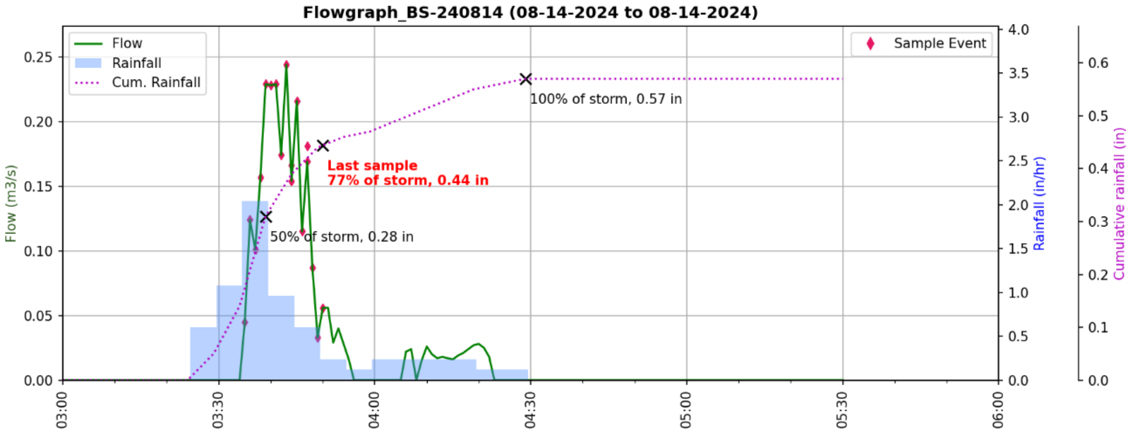

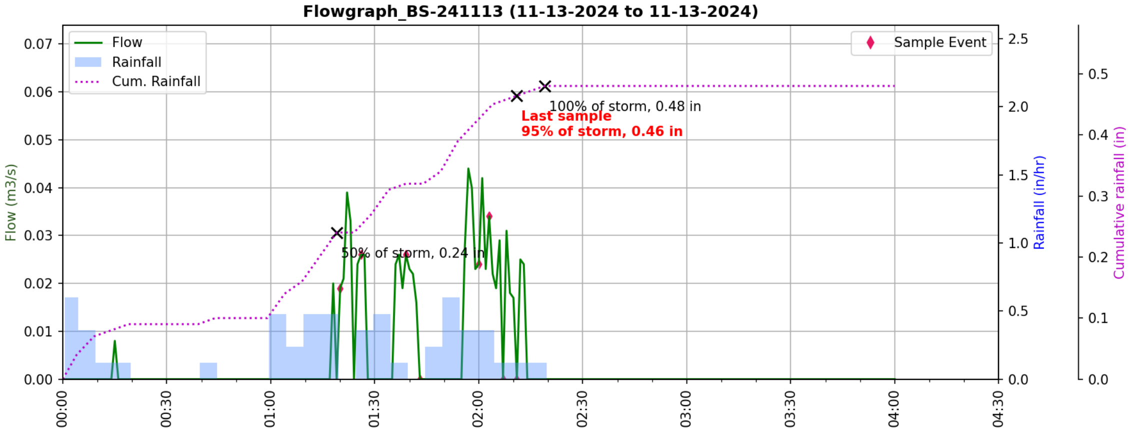

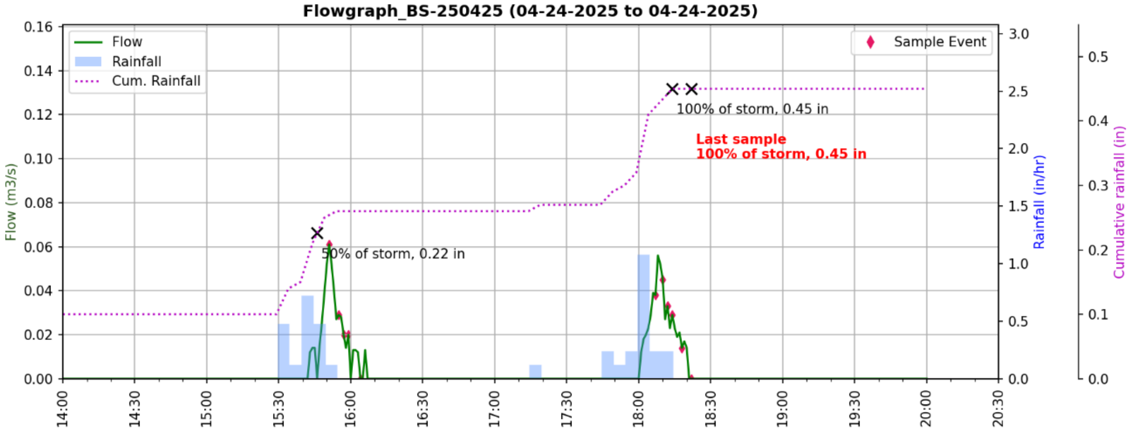

Time of day (HH:MM)

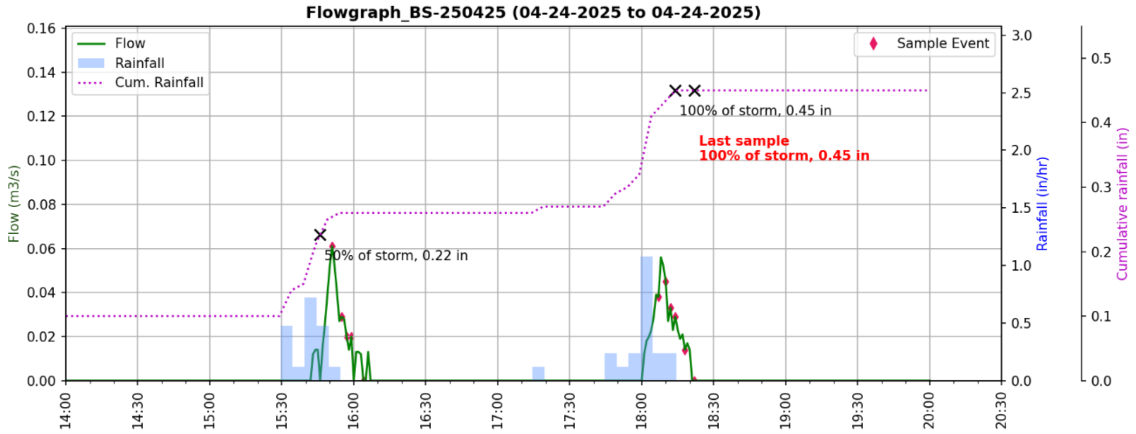

Time of day (HH:MM)

# Hydrograph plots from Cornhusker

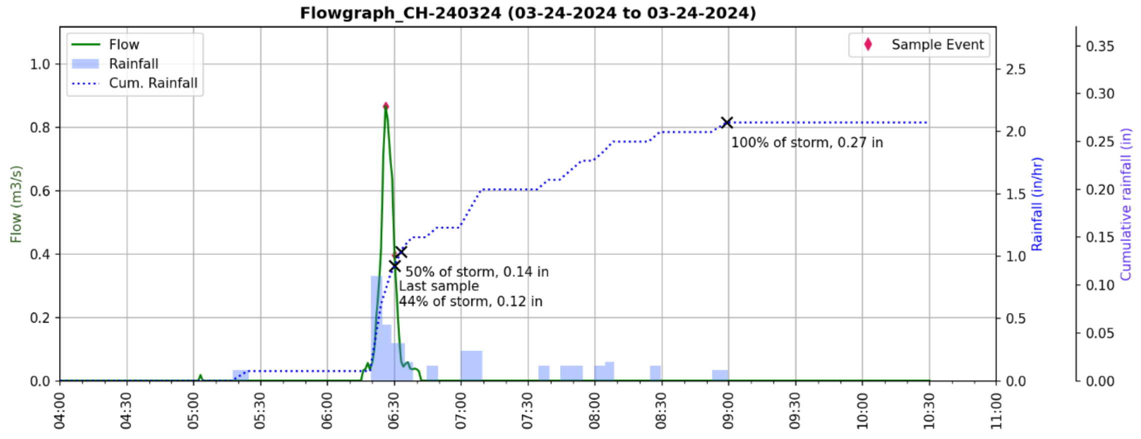

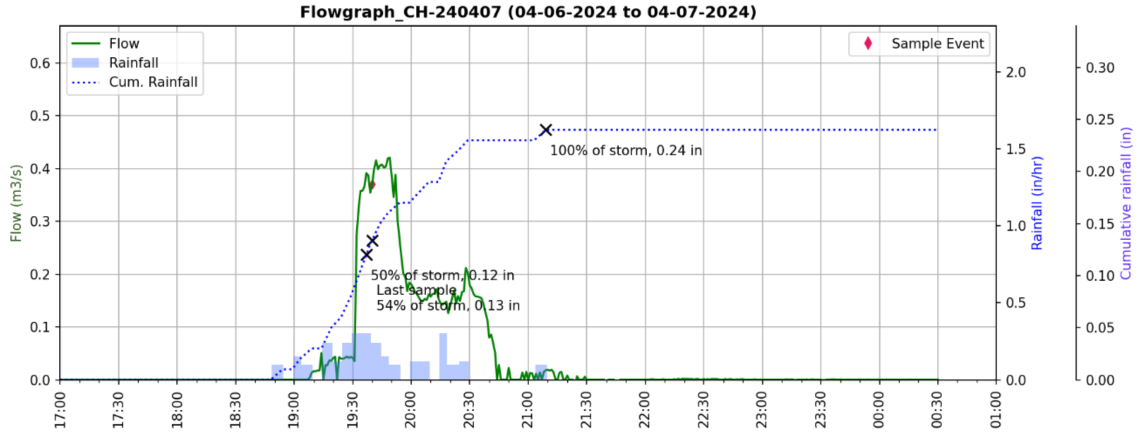

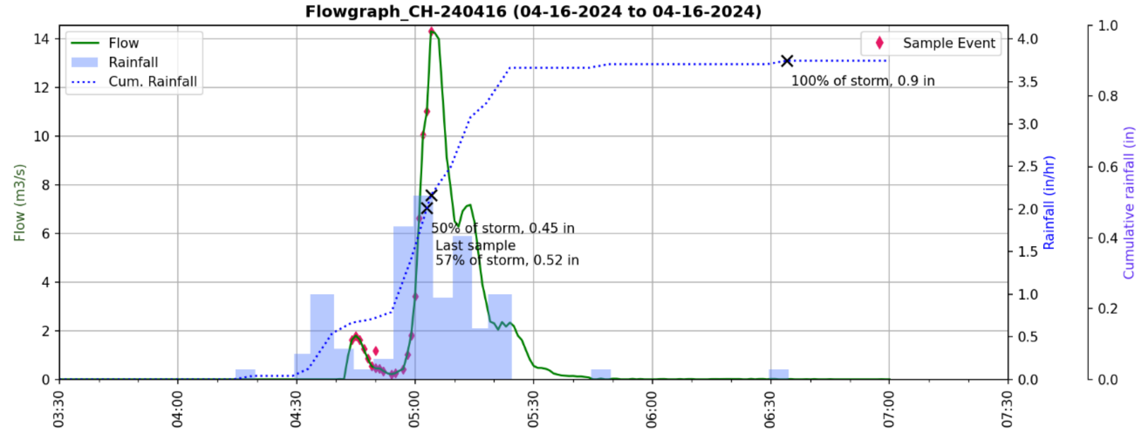

Time of day (HH:MM)

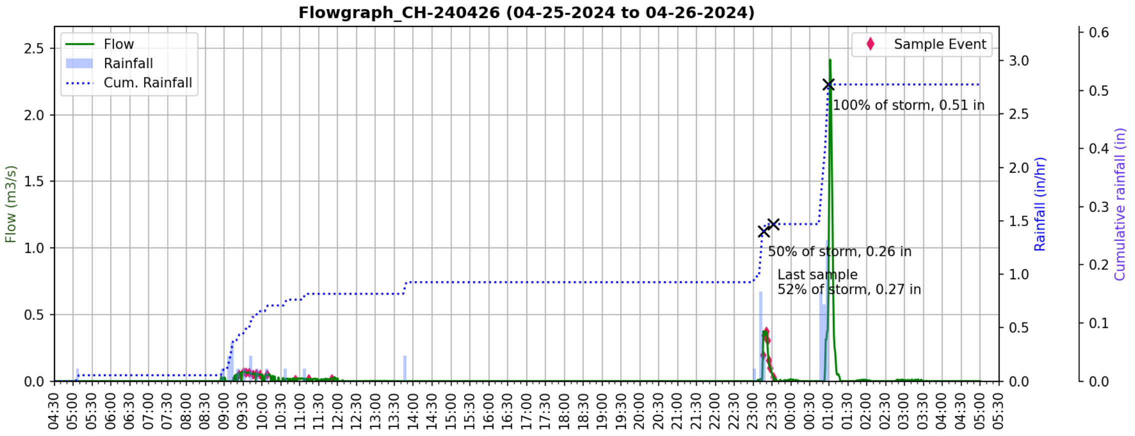
Flowgraph_CH-240426 (04-25-2024 to 04-26-2024)
Flow
Rainfall
Cum. Rainfall
Sample Event
100% of storm, 0.51 in
50% of storm, 0.26 in
Last sample
52% of storm, 0.27 in
Flow (m3/s)
Rainfall (in/hr)
Cumulative rainfall (in)

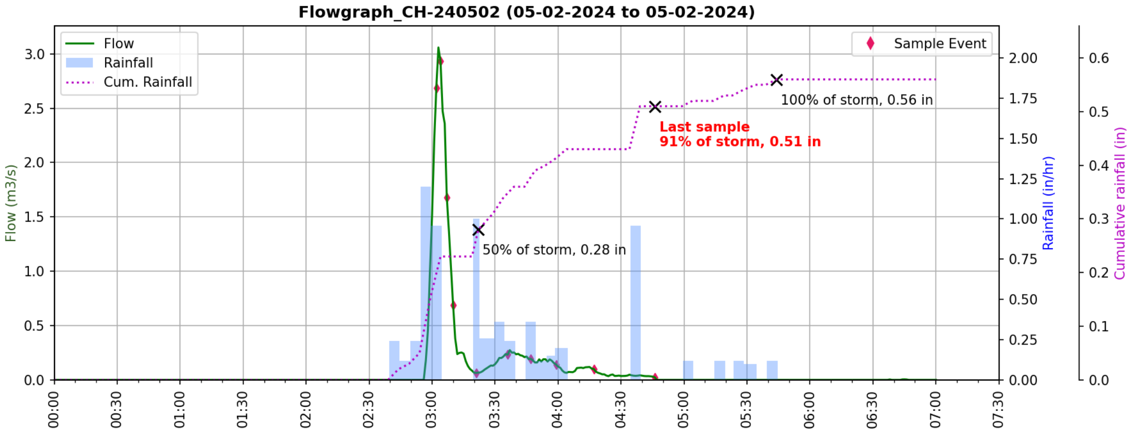
Flowgraph_CH-240502 (05-02-2024 to 05-02-2024)
Flow
Rainfall
Cum. Rainfall
Sample Event
100% of storm, 0.56 in
Last sample
91% of storm, 0.51 in
50% of storm, 0.28 in
Flow (m3/s)
Rainfall (in/hr)
Cumulative rainfall (in)

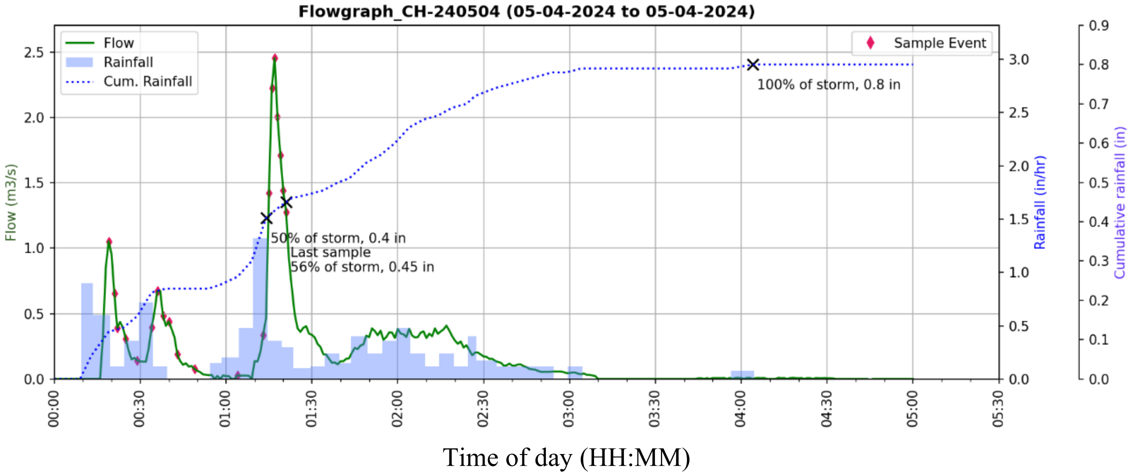
Flowgraph_CH-240504 (05-04-2024 to 05-04-2024)
Flow
Rainfall
Cum. Rainfall
Sample Event
100% of storm, 0.8 in
50% of storm, 0.4 in
Last sample
56% of storm, 0.45 in
Flow (m3/s)
Rainfall (in/hr)
Cumulative rainfall (in)
Time of day (HH:MM)

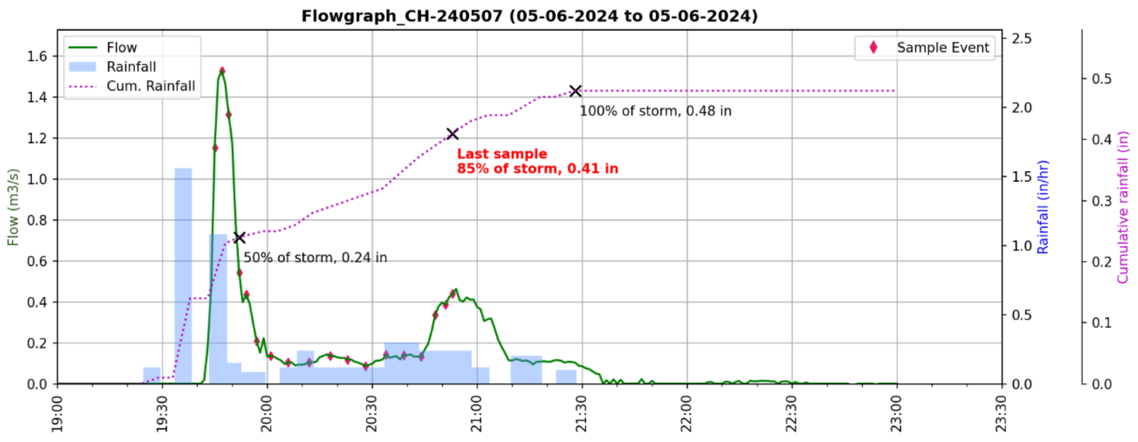

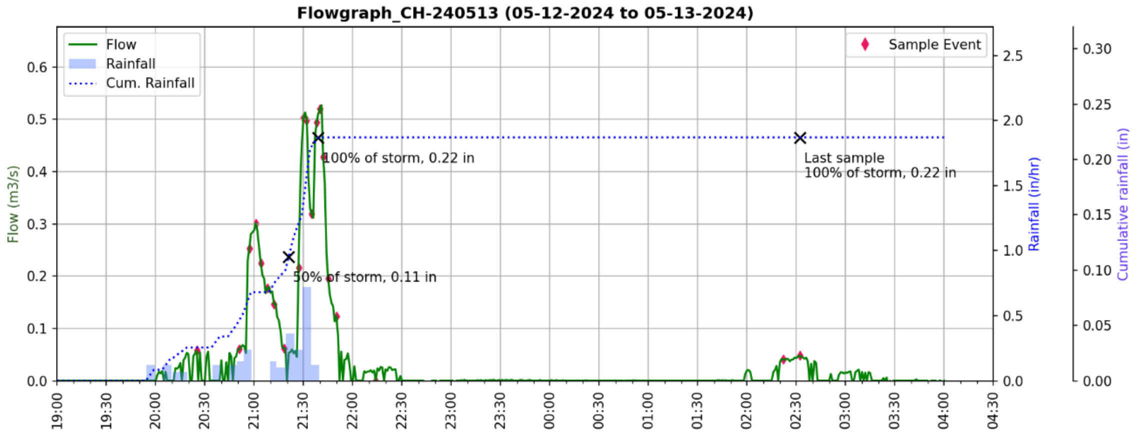

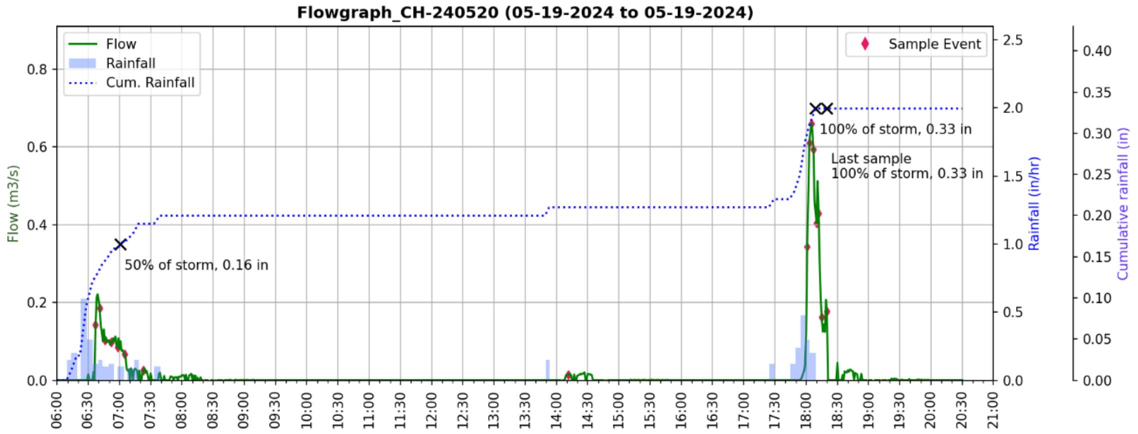

Time of day (HH:MM)

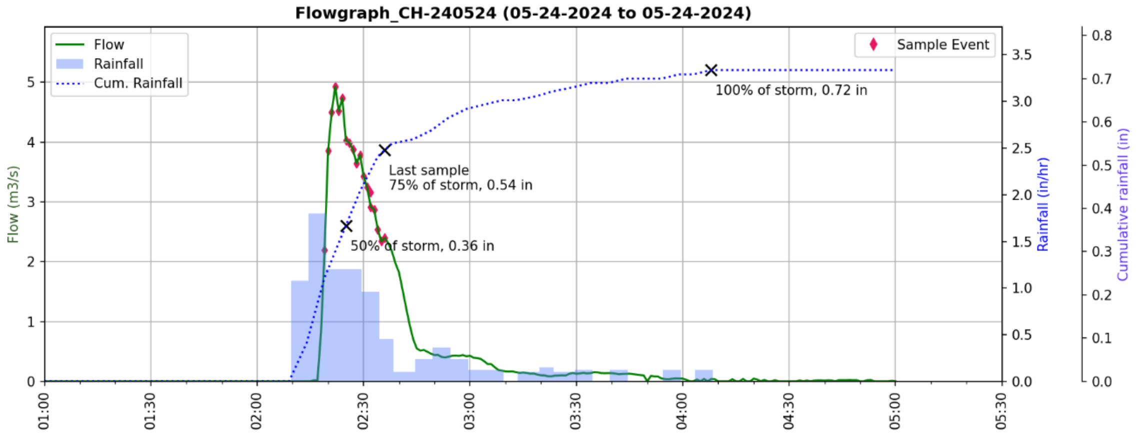

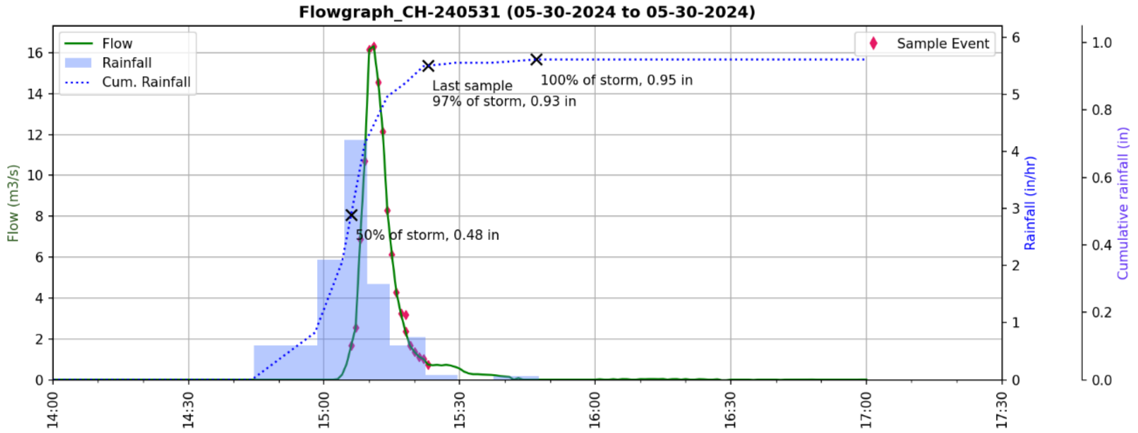

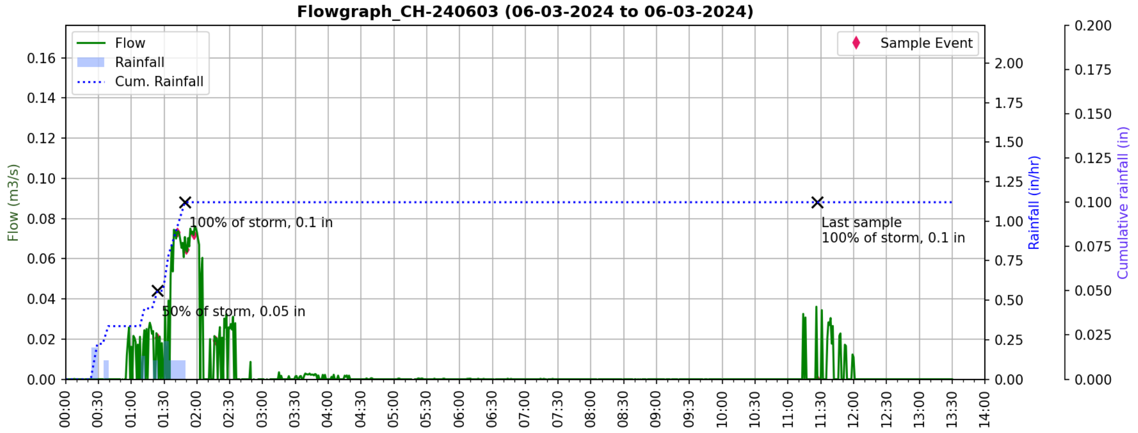

Time of day (HH:MM)

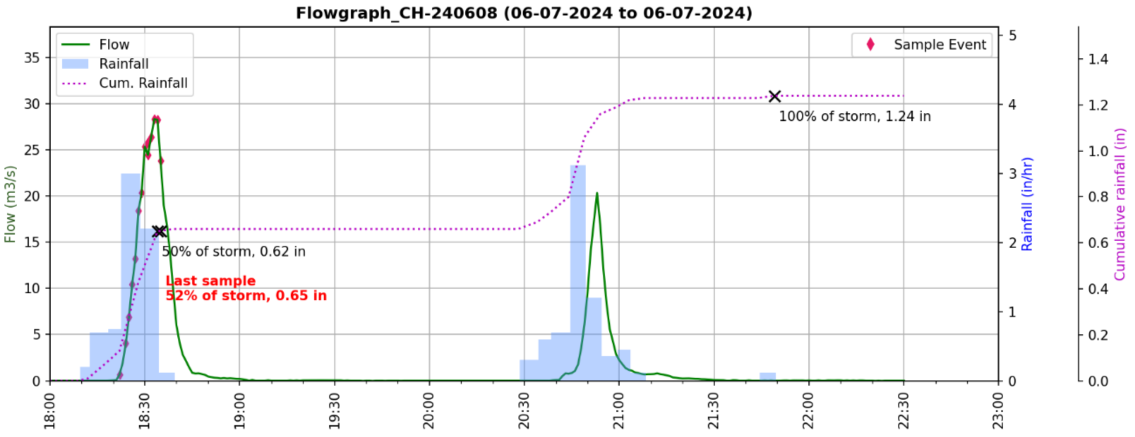
Flowgraph_CH-240608 (06-07-2024 to 06-07-2024)

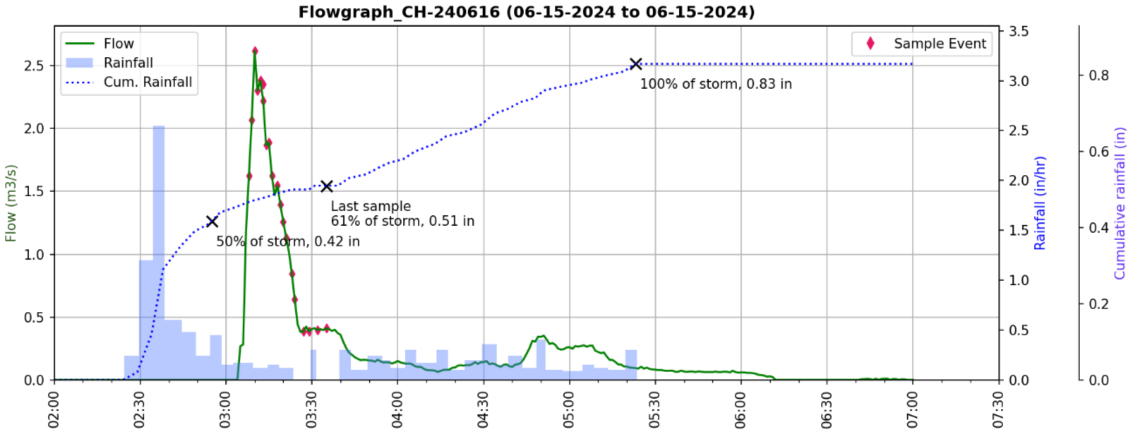
Flowgraph_CH-240616 (06-15-2024 to 06-15-2024)

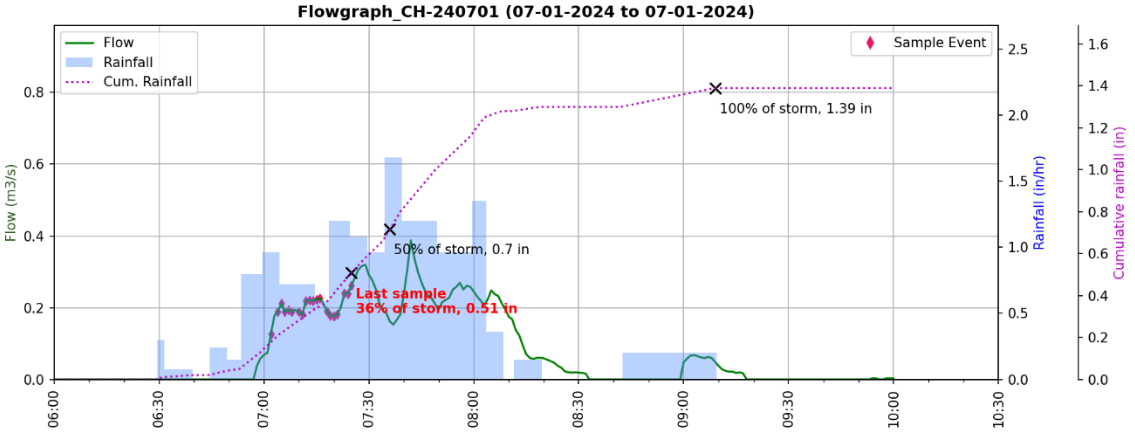
Flowgraph_CH-240701 (07-01-2024 to 07-01-2024)

Time of day (HH:MM)

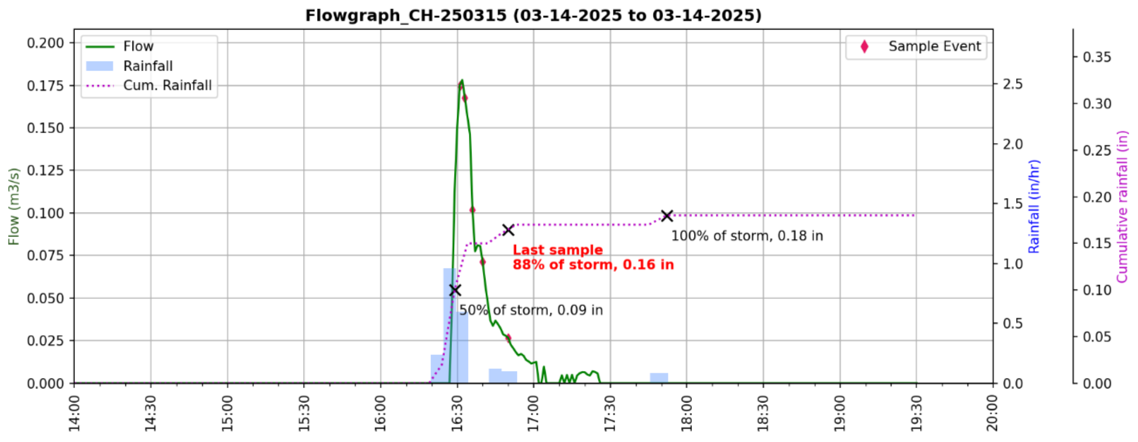

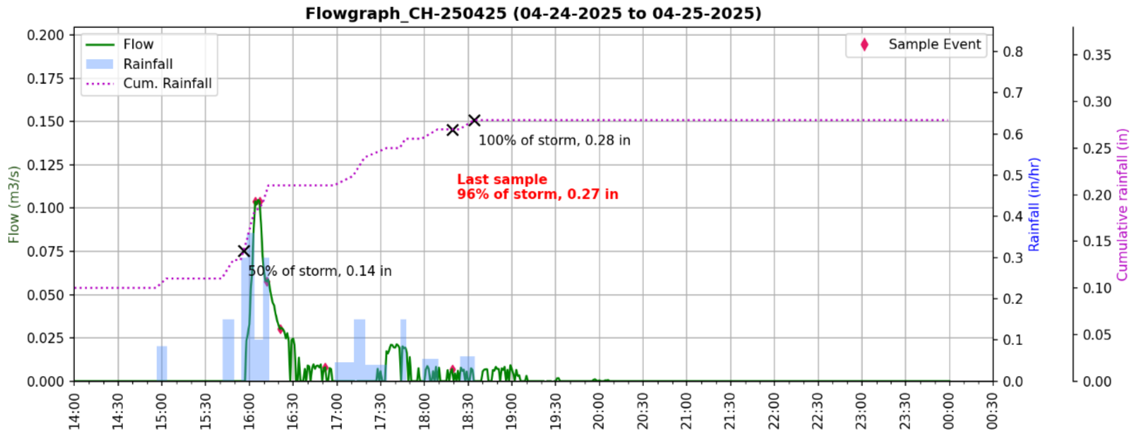

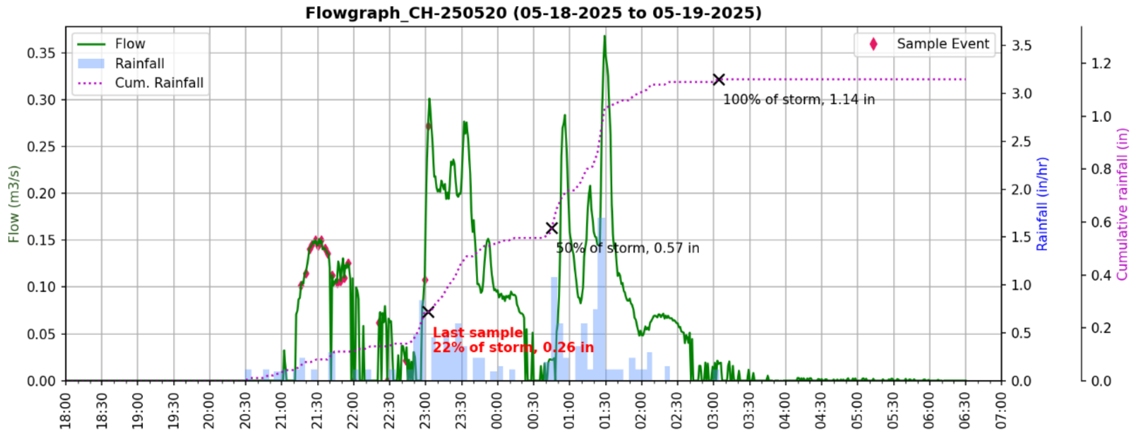

Time of day (HH:MM)

# Hydrograph plots from Beatrice North

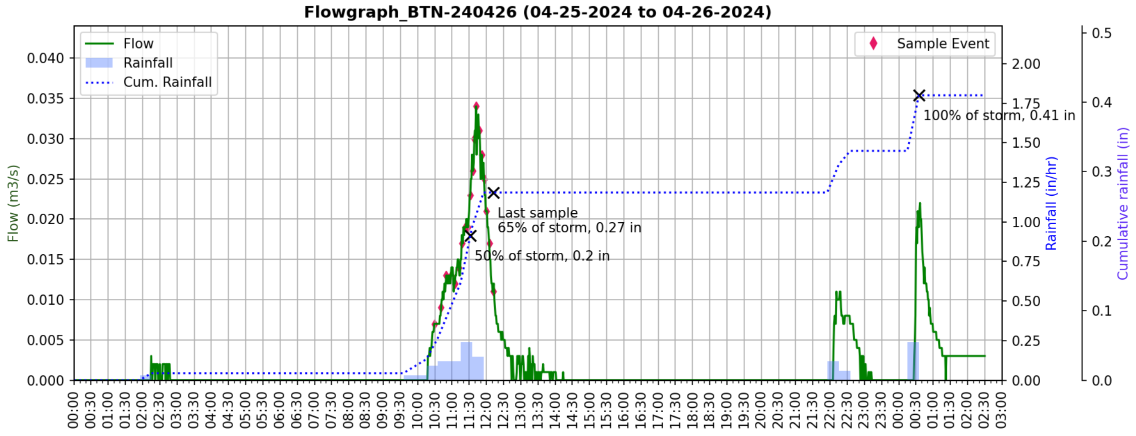

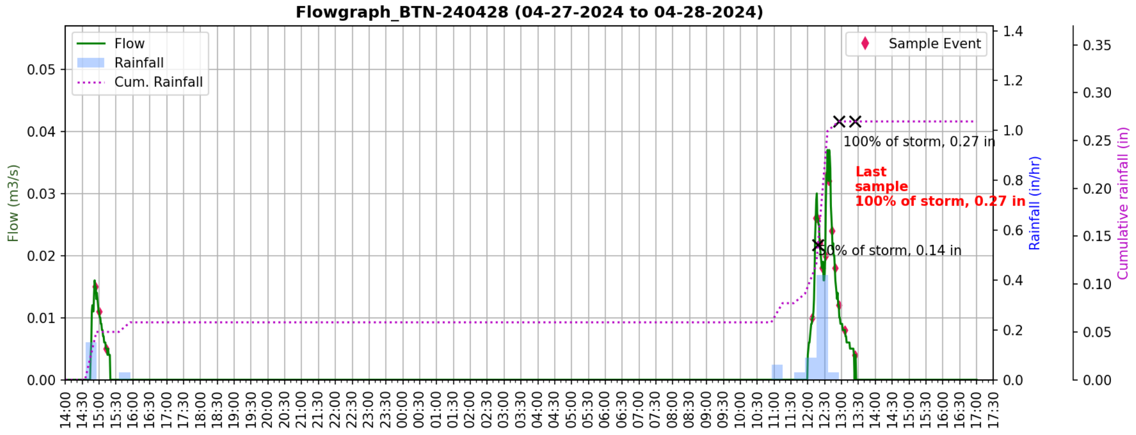

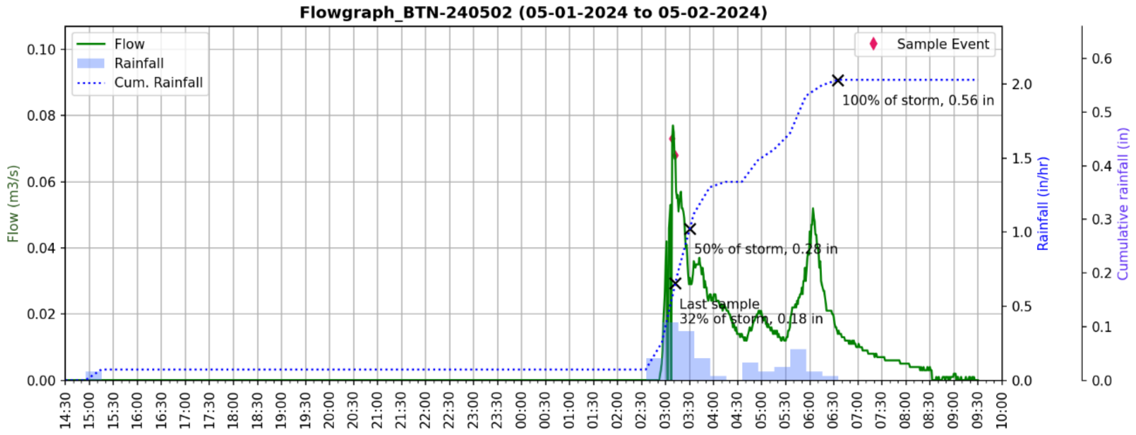

Time of day (HH:MM)

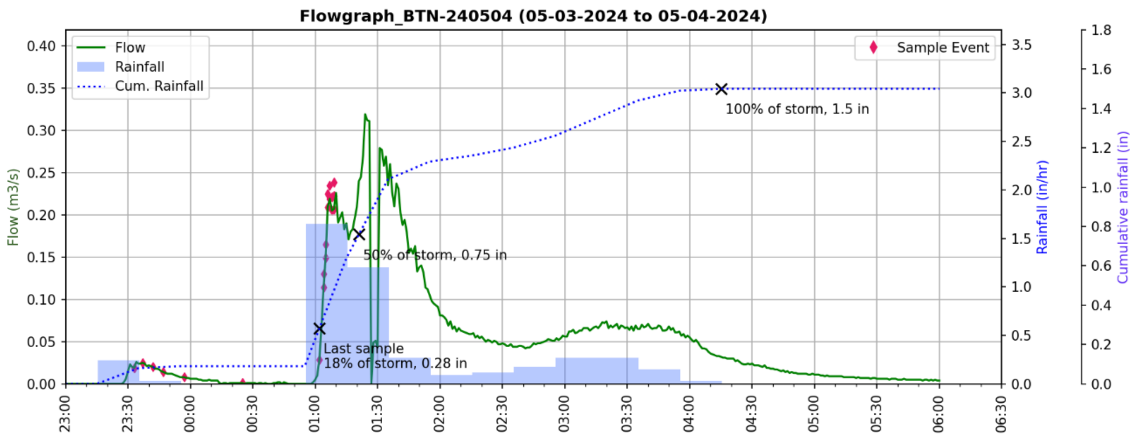

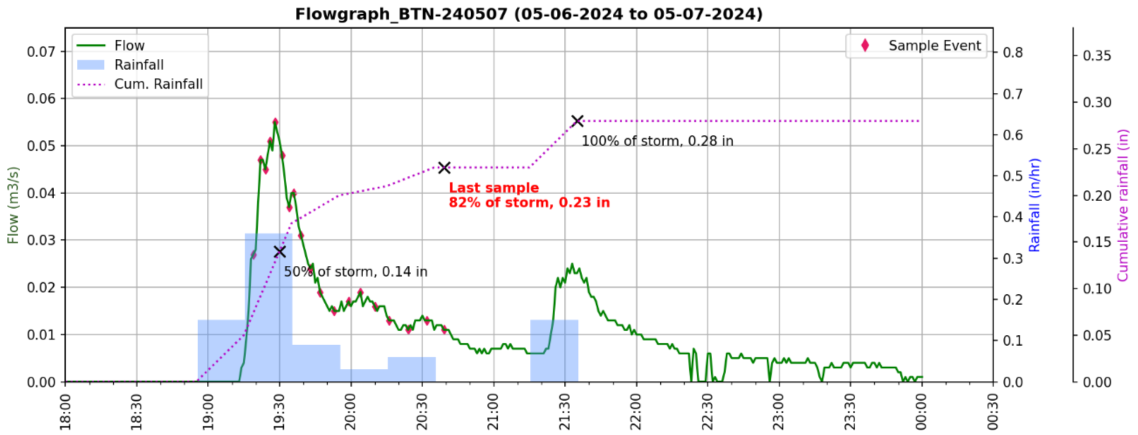

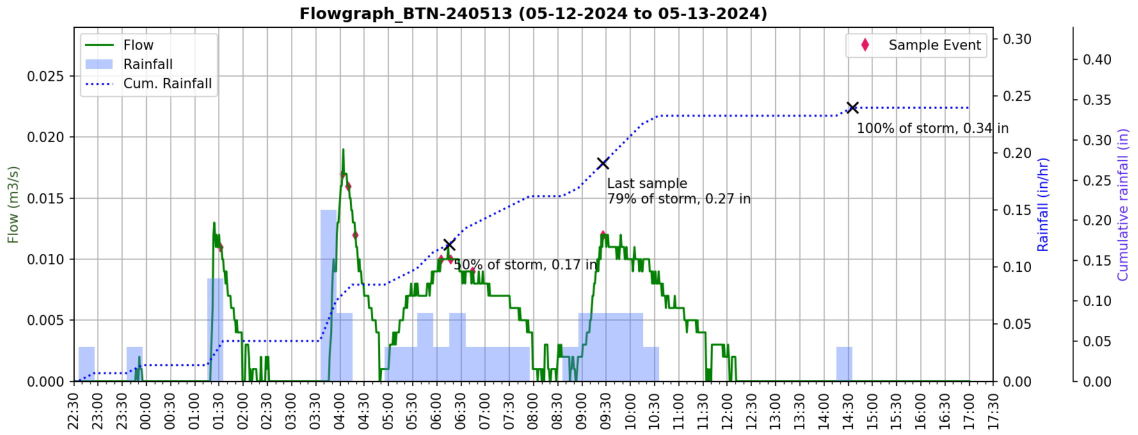

Time of day (HH:MM)

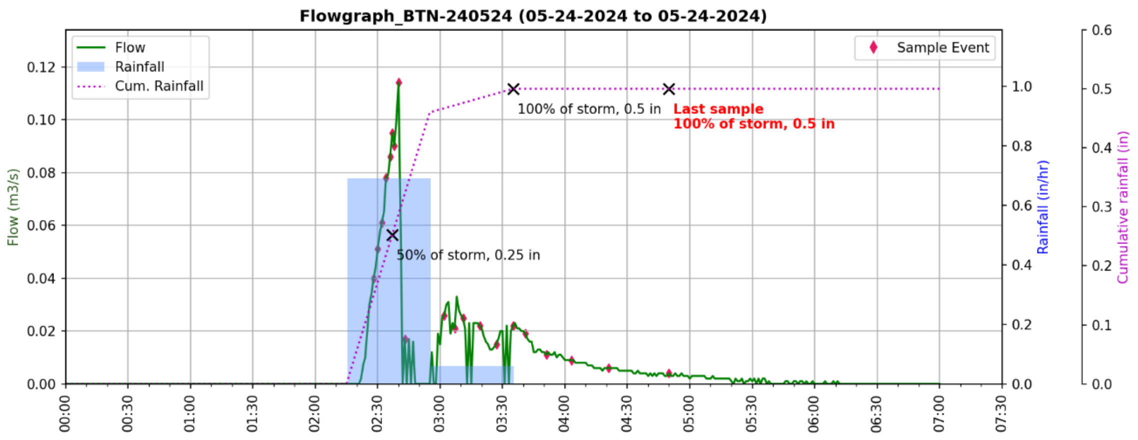
Flowgraph_BTN-240524 (05-24-2024 to 05-24-2024)
Flow
Rainfall
Cum. Rainfall
Sample Event
100% of storm, 0.5 in
Last sample
100% of storm, 0.5 in
50% of storm, 0.25 in
Flow (m3/s)
Rainfall (in/hr)
Cumulative rainfall (in)
0.00
0.02
0.04
0.06
0.08
0.10
0.12
0.0
0.2
0.4
0.6
0.8
1.0
0.0
0.1
0.2
0.3
0.4
0.5
0.6
00:00
00:30
01:00
01:30
02:00
02:30
03:00
03:30
04:00
04:30
05:00
05:30
06:00
06:30
07:00
07:30

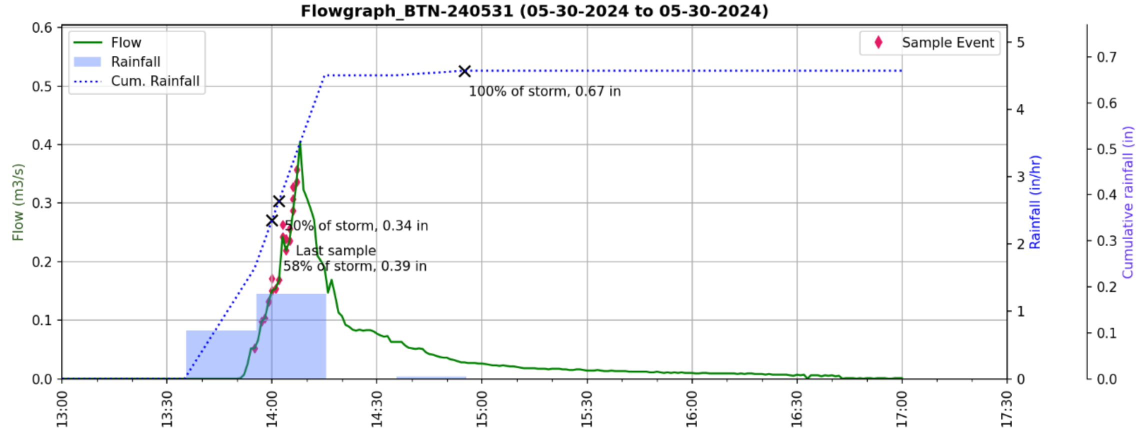
Flowgraph_BTN-240531 (05-30-2024 to 05-30-2024)
Flow
Rainfall
Cum. Rainfall
Sample Event
100% of storm, 0.67 in
50% of storm, 0.34 in
Last sample
58% of storm, 0.39 in
Flow (m3/s)
Rainfall (in/hr)
Cumulative rainfall (in)
0.0
0.1
0.2
0.3
0.4
0.5
0.6
0
1
2
3
4
5
0.0
0.1
0.2
0.3
0.4
0.5
0.6
0.7
13:00
13:30
14:00
14:30
15:00
15:30
16:00
16:30
17:00
17:30

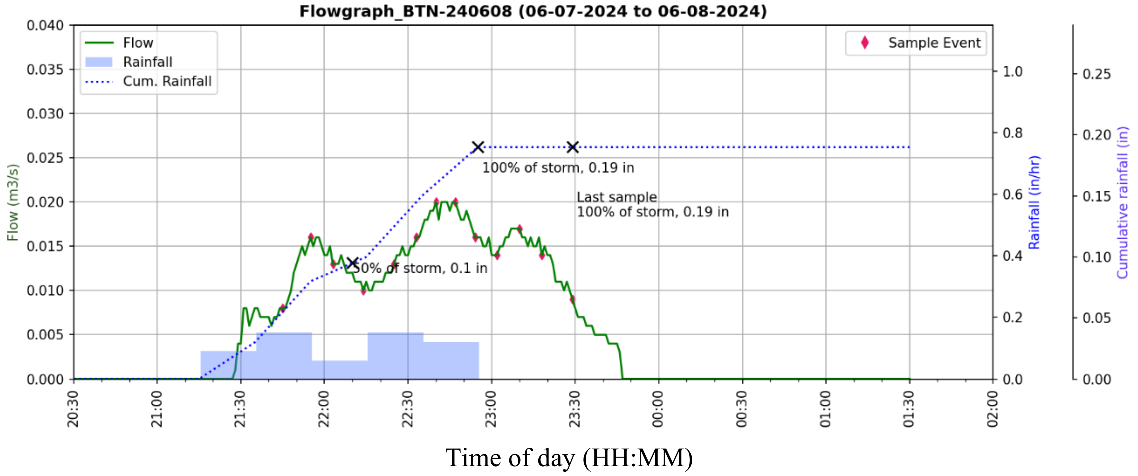
Flowgraph_BTN-240608 (06-07-2024 to 06-08-2024)
Flow
Rainfall
Cum. Rainfall
Sample Event
100% of storm, 0.19 in
Last sample
100% of storm, 0.19 in
50% of storm, 0.1 in
Flow (m3/s)
Rainfall (in/hr)
Cumulative rainfall (in)
0.000
0.005
0.010
0.015
0.020
0.025
0.030
0.035
0.040
0.0
0.2
0.4
0.6
0.8
1.0
0.00
0.05
0.10
0.15
0.20
0.25
20:30
21:00
21:30
22:00
22:30
23:00
23:30
00:00
00:30
01:00
01:30
02:00
Time of day (HH:MM)

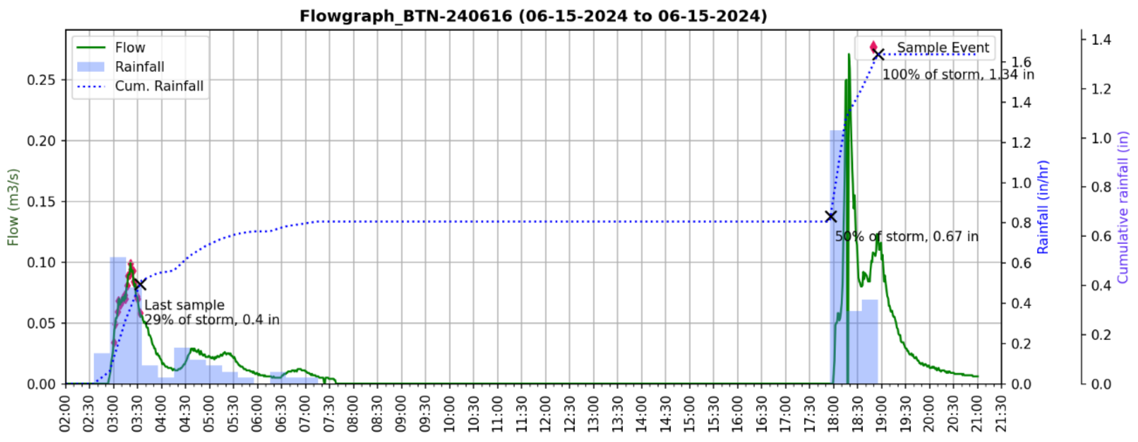

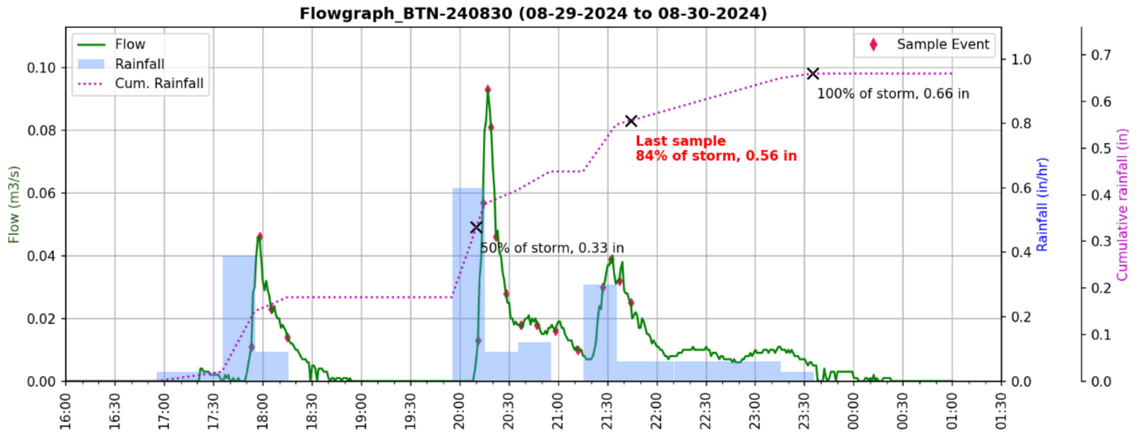

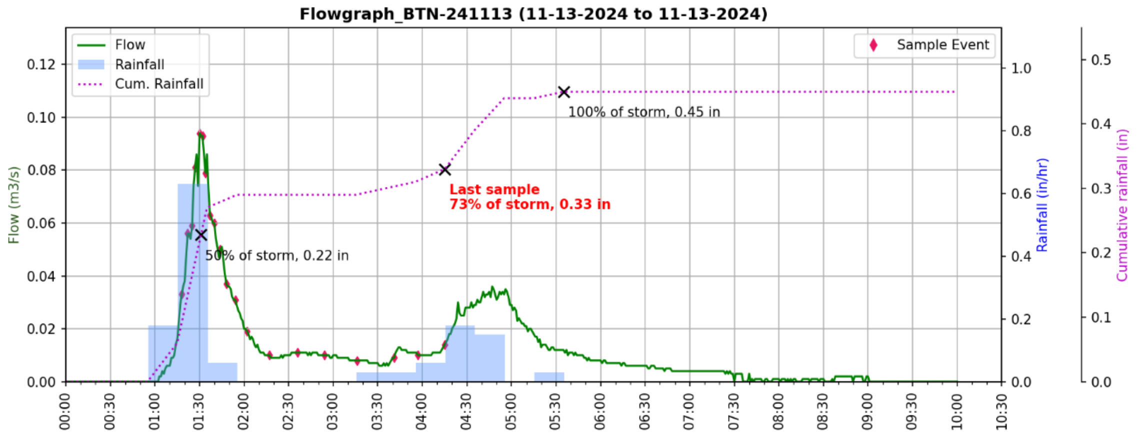

Time of day (HH:MM)

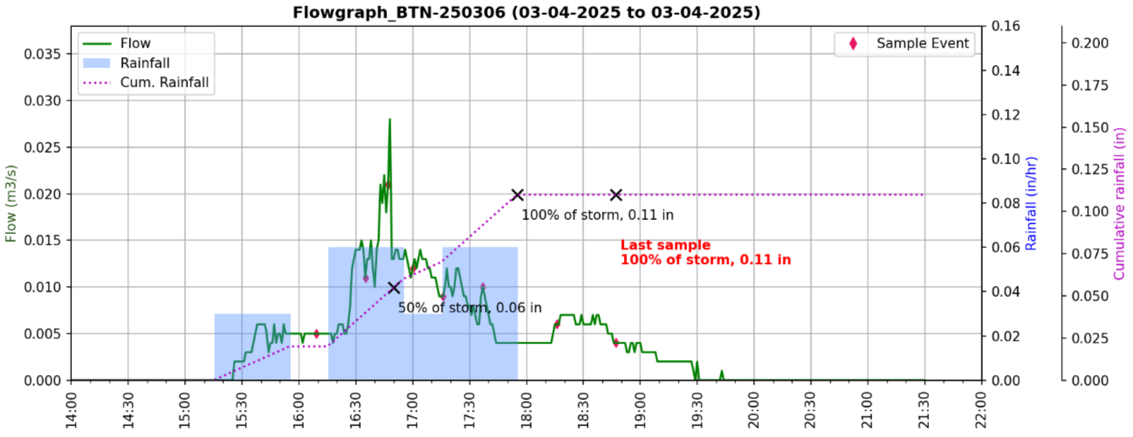

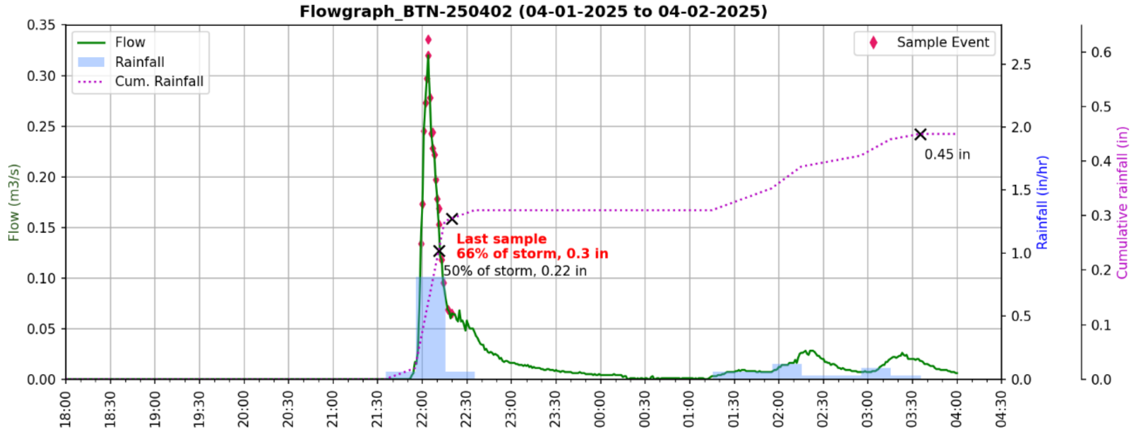

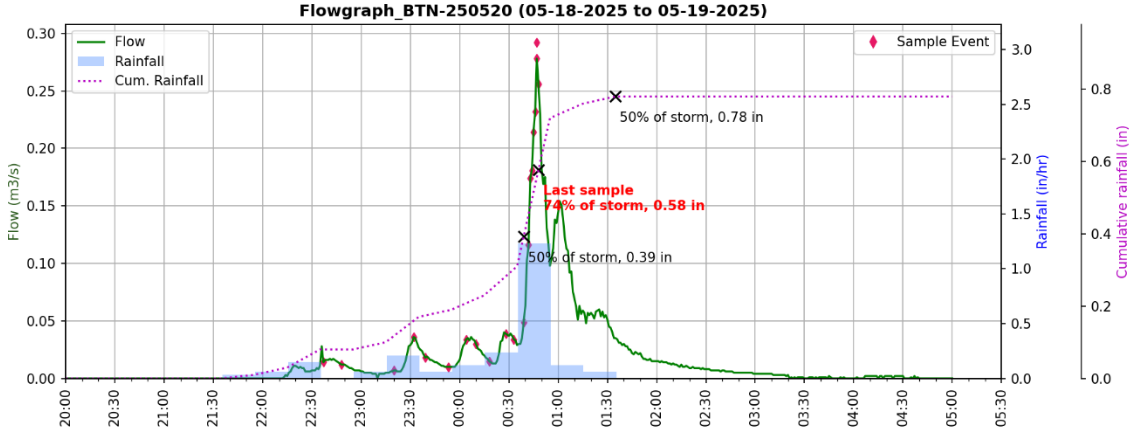

Time of day (HH:MM)

# Hydrograph plots from Beatrice West

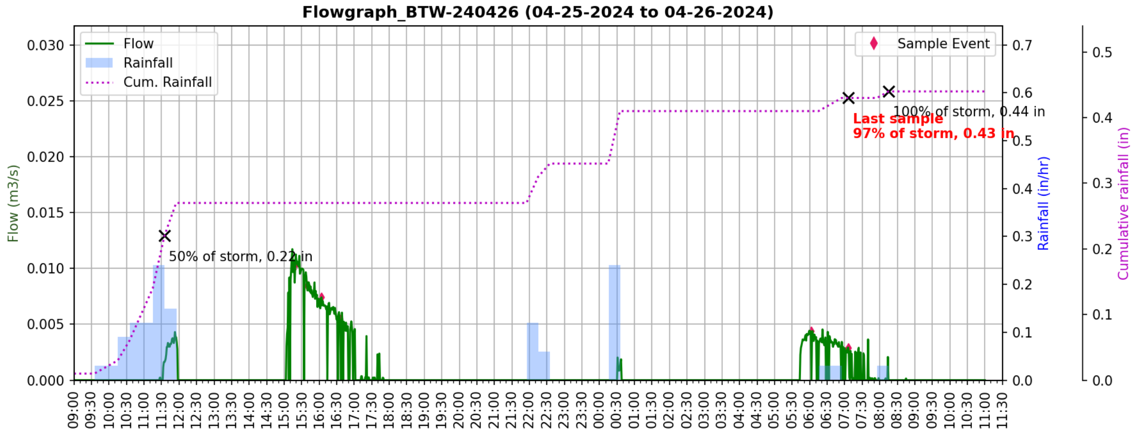

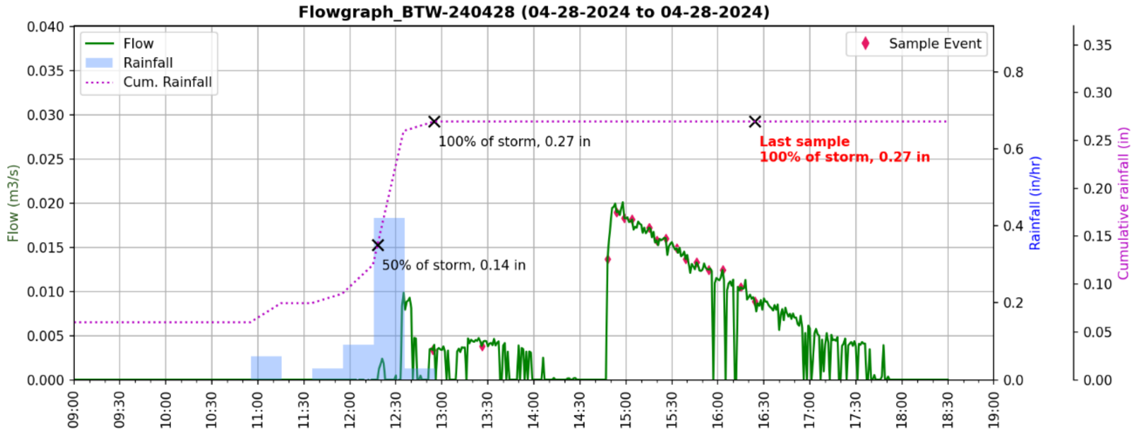

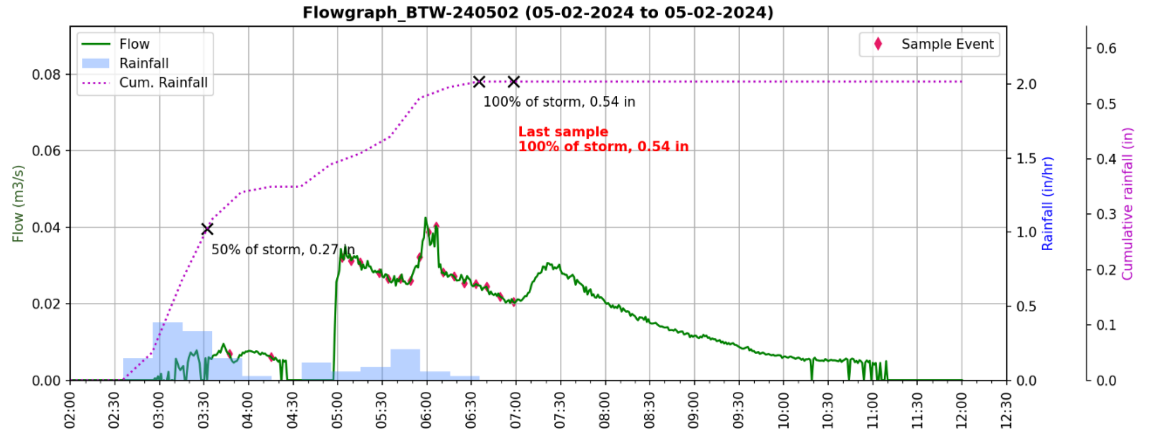

Time of day (HH:MM)

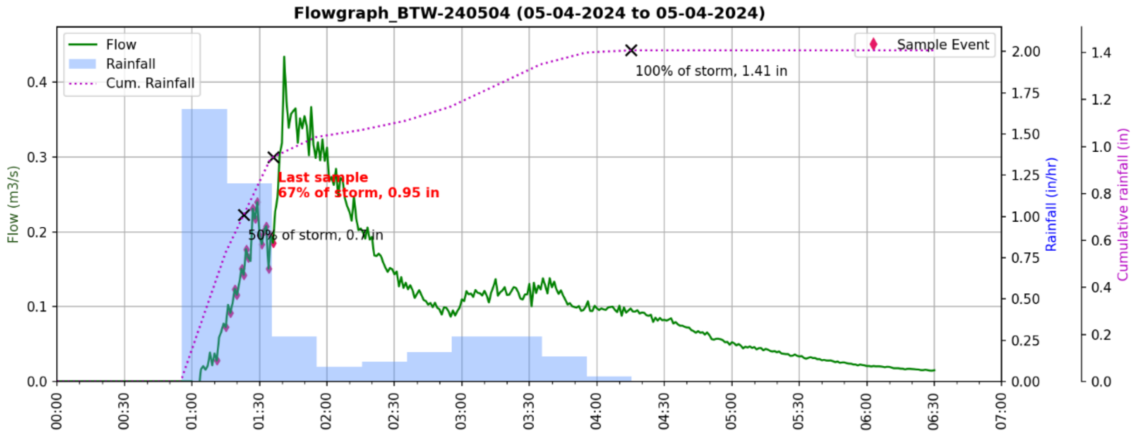

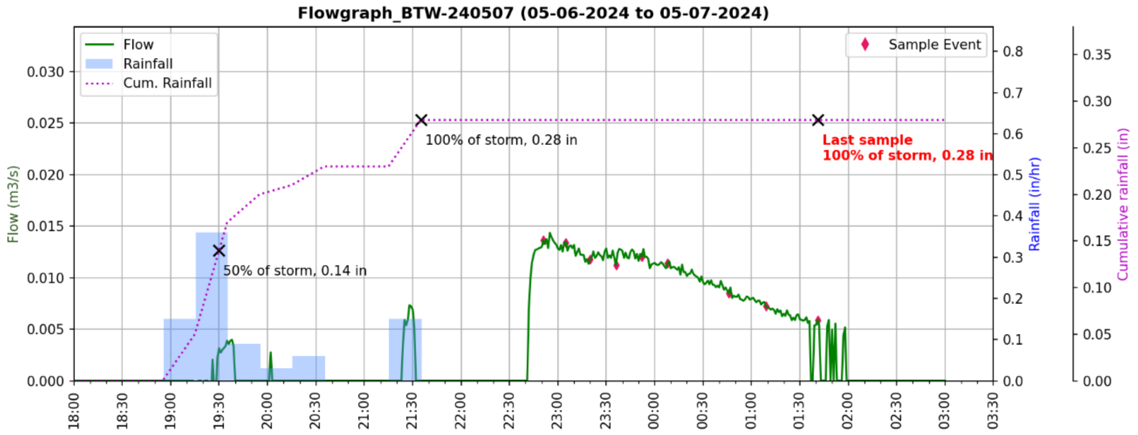

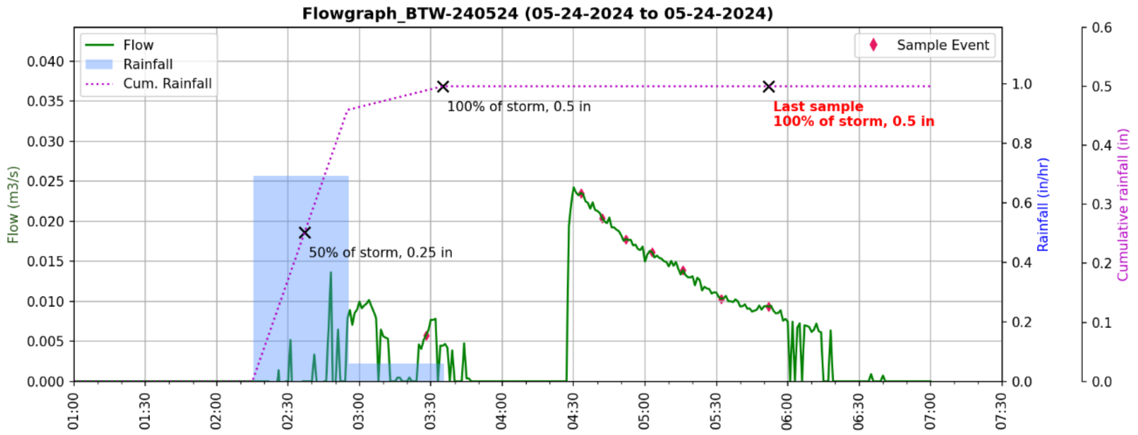

Time of day (HH:MM)

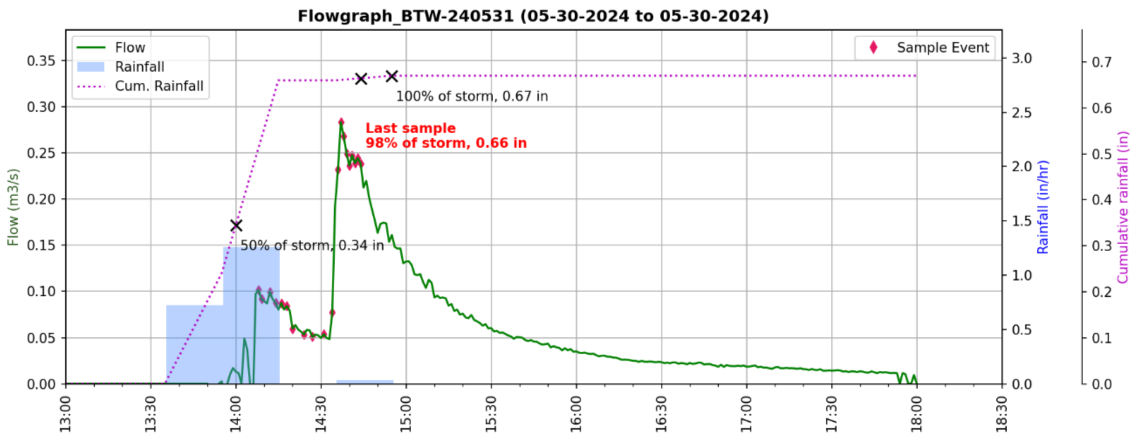

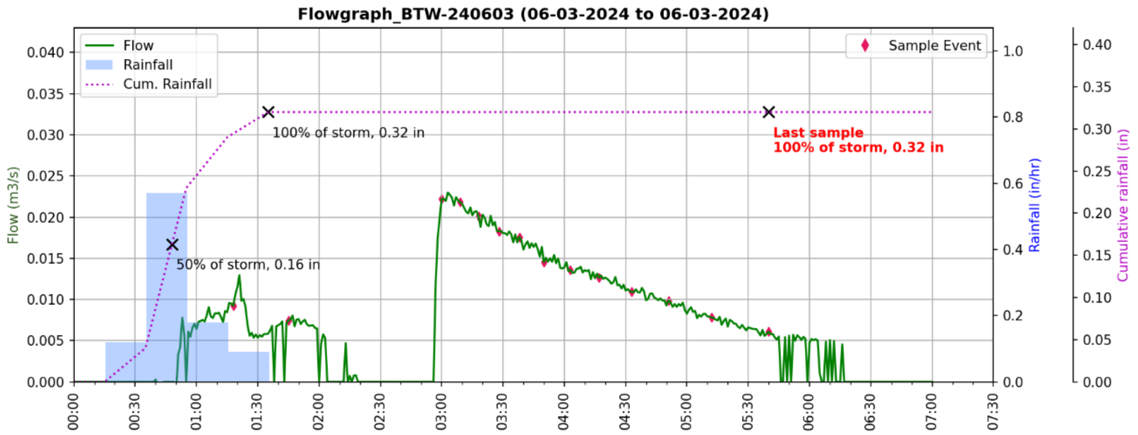

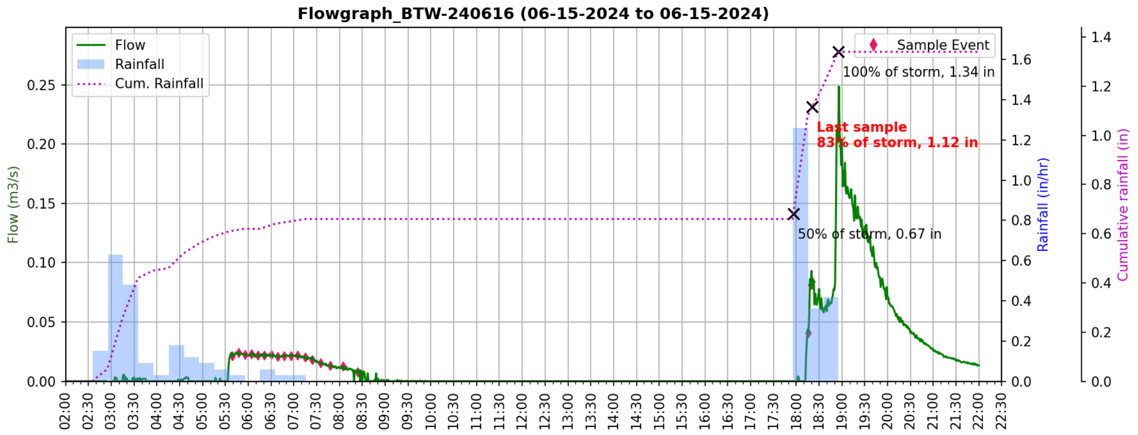

Time of day (HH:MM)

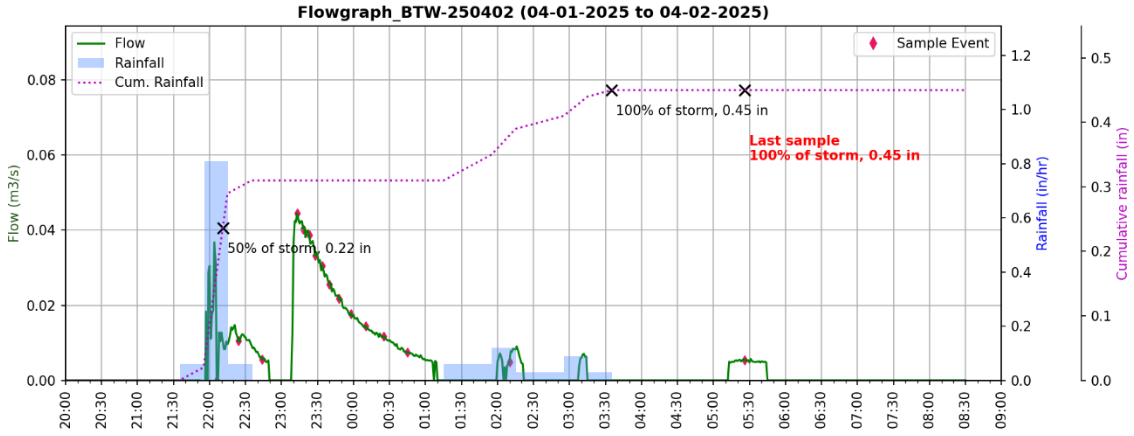
Flowgraph_BTW-250402 (04-01-2025 to 04-02-2025)
Flow
Rainfall
Cum. Rainfall
Sample Event
Flow (m3/s)
Rainfall (in/hr)
Cumulative rainfall (in)
50% of storm, 0.22 in
100% of storm, 0.45 in
Last sample
100% of storm, 0.45 in
0.00
0.02
0.04
0.06
0.08
0.0
0.2
0.4
0.6
0.8
1.0
1.2
0.0
0.1
0.2
0.3
0.4
0.5
20:00
20:30
21:00
21:30
22:00
22:30
23:00
23:30
00:00
00:30
01:00
01:30
02:00
02:30
03:00
03:30
04:00
04:30
05:00
05:30
06:00
06:30
07:00
07:30
08:00
08:30
09:00

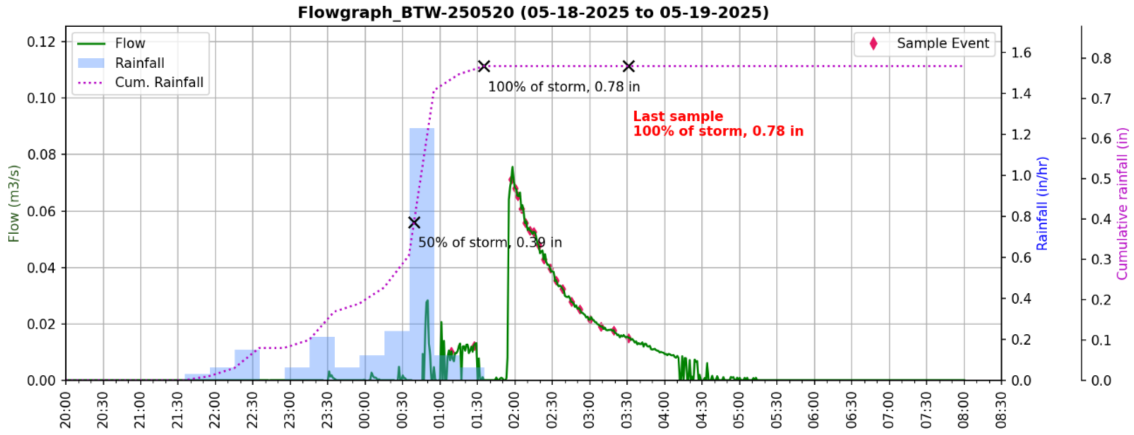
Flowgraph_BTW-250520 (05-18-2025 to 05-19-2025)
Flow
Rainfall
Cum. Rainfall
Sample Event
Flow (m3/s)
Rainfall (in/hr)
Cumulative rainfall (in)
50% of storm, 0.39 in
100% of storm, 0.78 in
Last sample
100% of storm, 0.78 in
0.00
0.02
0.04
0.06
0.08
0.10
0.12
0.0
0.2
0.4
0.6
0.8
1.0
1.2
1.4
1.6
0.0
0.1
0.2
0.3
0.4
0.5
0.6
0.7
0.8
20:00
20:30
21:00
21:30
22:00
22:30
23:00
23:30
00:00
00:30
01:00
01:30
02:00
02:30
03:00
03:30
04:00
04:30
05:00
05:30
06:00
06:30
07:00
07:30
08:00
08:30

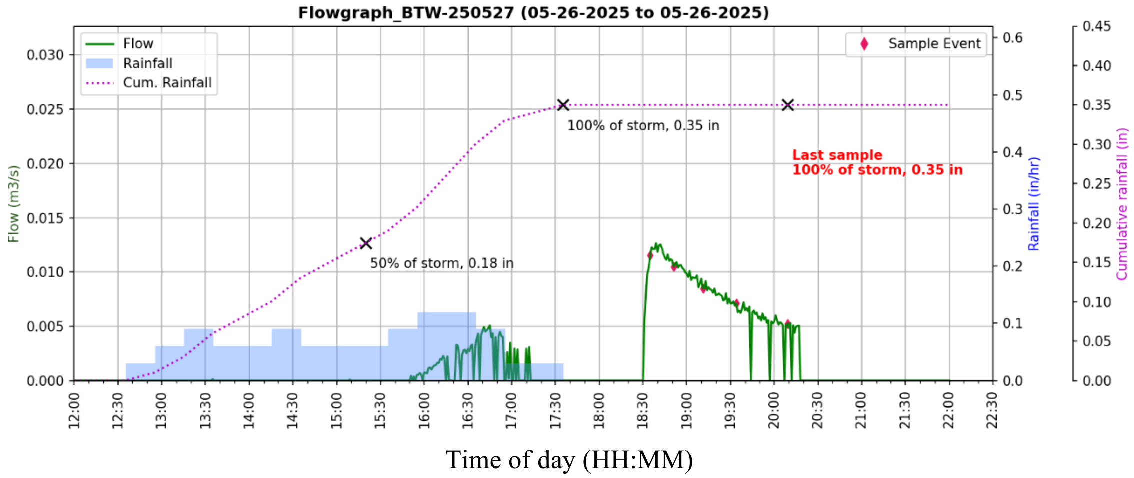
Flowgraph_BTW-250527 (05-26-2025 to 05-26-2025)
Flow
Rainfall
Cum. Rainfall
Sample Event
Flow (m3/s)
Rainfall (in/hr)
Cumulative rainfall (in)
50% of storm, 0.18 in
100% of storm, 0.35 in
Last sample
100% of storm, 0.35 in
0.000
0.005
0.010
0.015
0.020
0.025
0.030
0.0
0.1
0.2
0.3
0.4
0.5
0.6
0.00
0.05
0.10
0.15
0.20
0.25
0.30
0.35
0.40
0.45
12:00
12:30
13:00
13:30
14:00
14:30
15:00
15:30
16:00
16:30
17:00
17:30
18:00
18:30
19:00
19:30
20:00
20:30
21:00
21:30
22:00
22:30
Time of day (HH:MM)

# Appendix H Standard operating procedure to determine sediment concentration and particle size distribution in the laboratory

## 1 Background

The procedure listed here is used to characterize sediment obtained from stormwater runoff. It includes separating the sediment into coarse and fine fractions, determining the suspended sediment concentration of the sample, and finding the particle size distribution of the coarse particles greater than 32 µm.

Specifically, the methods used were evaporation, filtration, and wet sieving as described in ASTM D3977-97 (2013). The specific techniques used in this study follow the standard methods and include evaporation, filtration, wet sieving, and sieve analysis. Sieve analysis for particle size distribution of the coarse sediments was conducted using 1000-, 500-, 250-, 125-, 63- and 32-µm sieves, following the approach of Selbig and Bannerman (2011). The principle of dividing the sample into representative sub-samples using a splitter was inspired by the procedure described by Karamalegos et al. (2005), though the equipment used was different.

## 2 Sample Collection

2.1.1 Plan before the storm event.

2.1.2 Go to the site within 24 hours after the storm event.

2.1.3 Take out the sampling bottle and mark each bottle. Replace the empty bottles inside the sampler (four extra bottles required, one for each site). Follow the SOP for sampling.

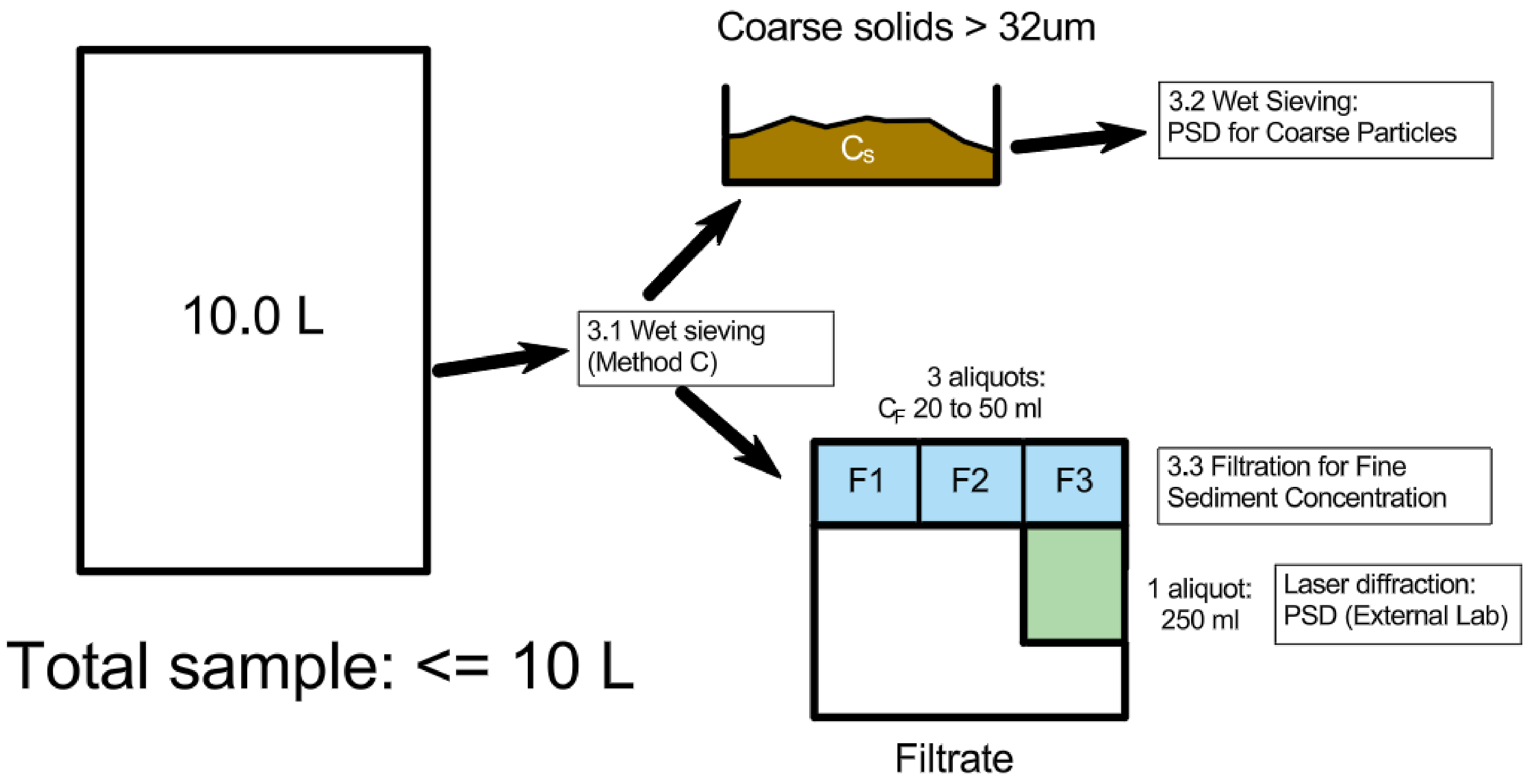

Figure H.1 Schematic of division of whole sample

## 3 Laboratory procedure

### 3.1 Sediment Concentration: Coarse Particles

To determine Suspended Sediment Concentration of coarse fraction, the collected sample will be separated into coarse and fine portion using a 32-µm sieve. It will be followed by the evaporation method to determine net dried weight of coarse sediment.

We will be determining Suspended Sediment Concentration of coarse particles. Therefore, we will require a whole sample for testing.

Table H.1 Laboratory items required for coarse particle separation

| Apparatus | Quantity | Purpose |
|---|---|---|
| 32-µm sieve of 8-inch diameter | 1 | Separate coarse and fine fractions |
| 3000-µm sieve of 8 in diameter | 1 | Separate trash and larger particles |
| Taller Sieve Stand (PVC-made) | 1 | To hold sieve above water level |
| DI water or clean water source | | Wash the sediments off the sieve |
| Wash bottle | 1 | Wash the sediments off the sieve |
| Soft brush | 1 | To dislodge sand from bottom |
| Clean bucket | 1 | Hold sample and filtrate from sieving |
| Aluminum weighing dishes | 1 per each sample | Hold drying materials |
| Water bath | 1 | Heat source for evaporation |
| 105°C Drying oven | 1 | Heat source for drying |
| Desiccator | 1 | Cool off the dried sample |
| Laboratory balance (0.1 mg) | 1 | Measure weights |

### Wet Sieving

3.1.1 Determine the total volume of the sample by the markings on the carboy and measuring the cylinder or beaker. Otherwise, determine volume by measuring weight.

3.1.2 If stored in the refrigerator, let it come to room temperature.

3.1.3 Place the 32-µm sieve on a sieve stand over another clean and dry bucket. Place 3000-µm or similar sieve over the 32-µm sieve. Shake the sample and then pour it through the sieve. Use supernatant water which was separated before to clean up the little remaining sediment particles inside the carboy until no sediment is left inside.

*Note: Do not use extra water other than that obtained from the sample for the sieving process because the sample should be tested for fine fraction as well.*

3.1.4 Some sediments may require vigorous rinsing with water to disaggregate clumps retained on the sieve. Then, use the supernatant water which was left to complete the sieving process.

3.1.5 Utilize a soft brush to remove coarse particles attached to the bottom, which may be challenging to dislodge using water alone. Wash all the particles attached to the brush using DI water.

3.1.6 Take the tare weight of a clean and dry aluminum dish and record it. Wash the coarse sediments retained on the sieve into the aluminum dish. Use a wash bottle filled with DI water for this procedure.

*Aluminum pans should be dried in the oven for few minutes and then cooled in a desiccator before they can be measured.*

*Preserve the filtrate collected in the bucket to use for analysis of fine sediment.*

## Evaporation method

3.1.7 The sediment and water mixture (slurry) on aluminum dish is taken into a water bath with the temperature below boiling. Leave the evaporating dish on the water bath until visible traces of water have evaporated (around two hours). Then, transfer the crucible into an oven set at the temperature of 105 °C for about two hours.

3.1.8 Transfer the dish from the oven to the desiccator to allow it to cool (two minutes) without capturing moisture from the air.

3.1.9 Weigh the dish to the nearest 0.1 mg as quickly as possible. Record the total weight of the sediments and the dish in the lab sheet. Subtract the net tare weight from the gross to obtain the net weight.

*This dried sediment is used for wet sieving.*

*Note: Dissolved-solid correction (as mentioned in ASTM D3977) is not considered because most of the liquid was poured through the sieve.*

3.1.10 Calculation:

Coarse Suspended Sediment concentration ($SSC_{coarse}$) =

Net weight of dried sediment (mg) / Total volume of the sample (L)

### 3.2 Particle Size Distribution: Coarse Particles

To determine the particle size distribution of coarse fraction, we will use the dried sample obtained from 3.1. The wet sieving method will be done using six different sieve sizes.

Table H.2 Laboratory items required for sieve analysis

| Apparatus | Quantity | Purpose |
|---|---|---|
| Clean sieves of sizes (1000 µm 500 µm, 250 µm, 125 µm, 63 µm and 32 µm) and 8-in diameter | 1-each | Wet sieving |
| Water shower | 1 | Agitation during sieving |
| DI water or clean water source | 1 | Wash the sediments off the sieve |
| Wash bottle | 1 | Washing sediments into aluminum pan |
| Aluminum pans (dried overnight) | 6 for each sample | Hold drying materials |
| Water bath | 1 | Evaporation |
| 105°C Drying oven | 1 | Heat source for removing moisture |
| Desiccator | 1 | Cool off the dried sample |
| Laboratory balance (0.1 mg) | 1 | Measure weights |

**Wet Sieving**

3.2.1 Stack up sieves in order (1000, 500, 250, 125, 63 and 32 µm).

3.2.2 Take six clean aluminum dishes dried in the 105°C oven and cooled in the desiccator, mark them, and take the tare weight of each.

3.2.3 Take the dried coarse sediment left from the evaporation process and mix it with clean or distilled water.

3.2.4 Pass it through the sieves using a water shower. Properly wash the materials for every sieve starting from 1000 µm until you reach 32 µm.

3.2.5 For 125-, 63-, and 32-µm sieves, wash the retained solids using clean water into pre-weighted aluminum pans marked to identify the corresponding sizes.

3.2.6 Take these aluminum pans with solids and place them on a water bath until visible traces of water have evaporated (around two hours). Then, transfer those pans into an oven set at 105 °C for about two hours.

3.2.7 Measure the gross weight of each after they are cooled with the desiccator. Determine the net weight for each particle size range of the solid. Note it on the lab sheet.

3.2.8 It is hard to wash coarse sediments from 1000, 500, and 250 µm, so put them in the oven for few minutes until they are completely dry. Cool them in open air and transfer all particles into marked aluminum dishes with the help of a tray and brush.

The total weight will be compared to the total weight obtained from the SSC measurement. The data will be used to determine particle size distribution of the coarser particles.

### 3.3 Sediment concentration: Fine Particles

To characterize the fine fraction of our sample, we need to take representative aliquots of the whole sample. The filtrate obtained by wet sieving will be used in this process. A Teflon churn splitter will be used to take multiple sub-samples. Filtration and Evaporation will follow this step to determine suspended sediment concentration of fine particles. Similarly, one of the subsamples will be sent to an external lab for PSD analysis.

Table H.3 Laboratory items required for filtration method

| Apparatus | Quantity | Purpose |
|---|---|---|
| Teflon churn splitter | 1 | Divide the sample |
| Filtration apparatus | 1 | Filtration process |
| Vacuum pump | 1 | Filtration process |
| Volumetric flask 50ml, 25ml | 1 each | Measure volume accurately |
| Glass fiber filter (1.5um) | 3 for each sample | Filtration process |
| Aluminum pans | 3 for each sample | Hold drying materials |
| 105°C Drying oven | 1 | Heat source for evaporation |
| Desiccator | 1 | Cool off the dried sample |
| Laboratory balance (0.1 mg) | 1 | Measure weights |
| Plastic sample bottles (500 ml) | 1 for each sample | Backup sample for safety |
| Plastic sample bottles (250 ml) | 1 for each sample | Preserve sample for PSD analysis |

3.3.1 Transfer the filtrate obtained from the sieving method into the Teflon Churn Splitter. Churn should be operated in a careful way. The churner should be moved up and down at a speed of 9” per sec. The disc should touch the bottom during each stroke and should be just high enough not to break the water surface. Before taking out the aliquot from the splitter, 10 full strokes must be completed. The water level should be at least two inches above the spigot inlet. Sub samples are generally taken out in order of volume from largest to smallest. It would be more convenient with two individuals: one operating the churner and the other extracting the sample.

3.3.2 Use a volumetric flask to extract the sample. Take around three aliquots of the same volume (25 ml to 50 ml depending upon turbidity). These samples will be used in the filtration process to determine the suspended sediment concentration of the fine portion.

3.3.3 Store about 250 ml of the sample in a marked watertight sample bottle and store in a refrigerator. This will be sent to an external lab for particle size distribution of finer particles. Take another 500 ml of sample and store it as a backup.

### **Filtration**

3.3.4 Take three clean filter papers and aluminum dishes. Label each of the aluminum pans.

3.3.5 Take tare weights of all filter papers along with aluminum dishes. Note their weights on the lab data sheet in the proper order.

3.3.6 Setup the filtration apparatus. Decant the sub-sample which was obtained in 3.3.2 through the filter paper. Use all the liquid; do not pipette out a smaller volume of the sample for testing. Use a vacuum pump to speed up the process. Flush the inner surfaces of the sample bottle with distilled water to complete the transfer.

3.3.7 During the filtration process, check if the filtrate is clear or not. If it is turbid then pour the filtrate back through the filter paper a second or third time. If it is still turbid, the filter paper should be replaced.

3.3.8 When filtration is complete, place the filter paper on an aluminum dish and place them inside an oven set at 105°C for drying.

3.3.9 Repeat the same steps for other sub-samples.

3.3.10 Wait for at least two hours for them to dry. Then, transfer them to the desiccator for cooling. Weigh the filter paper with an aluminum dish and its content to the nearest 0.1 mg. Record them on lab sheet.

3.3.11 Calculate net weights of the fine sediment from these three results.

Net weight = Gross weight of filter paper, aluminum dish and content – Tare weight of filter paper and aluminum dish

3.3.12 Fine sediment concentration is calculated using these results and from the volume of each sub-sample.

$SSC_{fine}$ = Net weight (mg)/ Volume of aliquot (L)

3.3.13 Compare and take the average value of the three different results.

### 3.4 Suspended Sediment Concentration of the Sample

3.4.1 SSC (mg/L) = $SSC_{coarse} + SSC_{fine}$

3.4.2 After a certain number of sub samples are collected for the external lab, send only a select number of the samples for PSD analysis.

3.4.3 Samples should not be preserved for more than six months. Further, they should be shipped inside a cooler.

Table H.4 Worksheet for laboratory measurements

LAB SHEET FOR SEDIMENT CHARACTERIZATION IN WATER SAMPLE

|  |  |  |  |
|---|---|---|---|
| Sample Name: |  | Date: |  |
|  |  | Tested by: |  |

**A. Volume of whole sample**

|  |  |  |
|---|---|---|
| Wt. of empty bottle | ***g*** |  |
| Wt. of bottle + Sample | ***g*** |  |
| Volume of sample | ***ml*** |  |

**B. Coarse Sediment (>32 μm) Test Results**

*Wet Sieving Method by 32 μm sieve*

|  |  |  |
|---|---|---|
| Wt. of empty Aluminum pan | ***mg*** |  |
| Wt. of pan + sediments after drying | ***mg*** |  |
| Recovered Coarse sediment | ***mg*** |  |

| *Particle Size Determination (>32 μm)* |  | > 1000 μm | > 500 μm | > 250 μm | > 125 μm | > 63 μm | > 32 μm |
|---|---|---|---|---|---|---|---|
| Wt. of empty Aluminum pan | ***mg*** |  |  |  |  |  |  |
| Wt. of pan + sediments after drying | ***mg*** |  |  |  |  |  |  |
| Recovered sedmient wt. | ***mg*** |  |  |  |  |  |  |

**C. Fine Suspended Solids (<32 μm) Test Results**

*Filtration Method* *Min. 3 samples*

|  |  | I | II | III | IV | V |
|---|---|---|---|---|---|---|
| Volume of sub-sample | ***ml*** |  |  |  |  |  |
| Wt. of pan + clean filter paper | ***mg*** |  |  |  |  |  |
| Wt. of pan + f.paper + residue (dried) | ***mg*** |  |  |  |  |  |

**D. Remarks**

# Appendix I Laboratory measurements of samples analyzed

All laboratory measurement data for the analyzed samples are presented here. The results include total suspended solids (TSS) and particle size distribution (PSD) for particles larger than 32 µm. It also provides turbidity data for a few samples during the earlier phase of the study. All analyses were conducted at the Scott Engineering Center, University of Nebraska–Lincoln, following the procedures described in Appendix H.

Table I.1 Laboratory analysis results for Beal Slough samples

| Sample name | Sample volume [ml] | TSS [mg/L] | Coarse fraction [mg/L] | Fine fraction [mg/L] | Turbidity of sample [NTU] | Turbidity of filtrate [NTU] | Mass of samples retained on sieves [mg] | | | | | |
|---|---|---|---|---|---|---|---|---|---|---|---|---|
| | | | | | | | **1000 µm** | **500 µm** | **250 µm** | **125 µm** | **63 µm** | **32 µm** |
| BS-240324 | 455 | 406 | 222 | 184 | 88 | 0 | 41.5 | 65.1 | 61.8 | 24 | 27.3 | 24 |
| BS-240416 | 9235 | 877 | 432 | 445 | 160 | 5 | 51.4 | 46.2 | 95.3 | 73.3 | 53.9 | 78.6 |
| BS-240426 | 2745 | 846 | 727 | 119 | 33 | 7 | 160.5 | 94.9 | 256.9 | 125.5 | 29.7 | 38 |
| BS-240428 | 9245 | 495 | 373 | 122 | 28 | 2 | 48.9 | 39.1 | 131.3 | 67.8 | 27.6 | 38.7 |
| BS-240502 | 9205 | 386 | 304 | 82 | 32 | 2 | 39.7 | 59.6 | 109.4 | 40.8 | 18.4 | 25.7 |
| BS-240504 | 4095 | 324 | 272 | 52 | 18 | 3 | 60.5 | 42.8 | 94.9 | 46.6 | 14.7 | 15.7 |
| BS-240507 | 3680 | 557 | 507 | 49 | 16 | 2 | 66.7 | 72.6 | 83.3 | 73.3 | 50.2 | 81 |
| BS-240513 | 9000 | 467 | 390 | 77 | 22 | 1 | 93.9 | 77 | 133.9 | 43.2 | 15.9 | 18.6 |
| BS-240520 | 7365 | 482 | 392 | 90 | 35 | 2 | 112.4 | 58.9 | 116.3 | 46.7 | 20.1 | 25.6 |
| BS-240524 | 9210 | 405 | 339 | 66 | 24 | 2 | 61.9 | 58.6 | 115.1 | 53.1 | 17.5 | 25.3 |
| BS-240531 | 1400 | 573 | 488 | 84 | 11 | 2 | 137.1 | 89.1 | 133.6 | 69.2 | 20.6 | 18.8 |
| BS-240608 | 9260 | 533 | 456 | 77 | 26 | 2 | 72.7 | 76.4 | 160.9 | 72.3 | 28.5 | 30.9 |
| BS-240616 | 9210 | 222 | 176 | 46 | 15 | 1 | 27.3 | 33.4 | 66.1 | 28.7 | 7.7 | 7.7 |
| BS-240626 | 1860 | 61 | 43 | 18 | 0 | 0 | 0 | 1.6 | 10.6 | 9.5 | 6.9 | 6.9 |
| BS-240701 | 8985 | 453 | 432 | 21 | 16 | 2 | 92.4 | 89.9 | 170.6 | 52.3 | 10.8 | 13.4 |
| BS-240706 | 2200 | 349 | 349 | 0 | 5 | 0 | 48.8 | 96.8 | 141.2 | 46.8 | 7.7 | 7 |
| BS-240707 | 9750 | 325 | 291 | 33 | - | - | 37.5 | 42.5 | 112.1 | 61.4 | 15.8 | 15.6 |
| BS-240721 | 4000 | 426 | 386 | 40 | - | - | 99.1 | 92 | 113.5 | 47.8 | 13.8 | 12.7 |
| BS-240801 | 10100 | 334 | 303 | 31 | - | - | 45 | 48.1 | 125.8 | 50.2 | 9.7 | 10.6 |
| BS-240814 | 9000 | 341 | 300 | 41 | - | - | 56.8 | 48.7 | 102.5 | 51.8 | 15.1 | 17.7 |
| BS-240830 | 6000 | 321 | 260 | 61 | - | - | 41.8 | 43.2 | 73 | 47.6 | 20.9 | 19.9 |
| BS-241022 | 500 | 346 | 300 | 45 | - | - | 97.4 | 86.6 | 57.8 | 17.8 | 4.8 | 9.4 |
| BS-241031 | 8460 | 159 | 148 | 11 | - | - | 45.5 | 17.8 | 30.2 | 19.6 | 10 | 15.2 |
| BS-241109 | 1400 | 466 | 451 | 15 | - | - | 180 | 57.9 | 122 | 47.6 | 12.9 | 18.4 |
| BS-241113 | 3600 | 132 | 122 | 11 | - | - | 17.2 | 12.9 | 41.6 | 24.3 | 9.2 | 11.4 |
| BS-241119 | 9000 | 169 | 125 | 44 | - | - | 8.2 | 15.4 | 45.9 | 26.4 | 9 | 13 |
| BS-250425 | 5100 | 1111 | 489 | 622 | - | - | 39.3 | 34.9 | 148.6 | 91.8 | 57.9 | 79.1 |
| BS-250520 | 9100 | 772 | 505 | 267 | - | - | 65.2 | 59.9 | 161.2 | 89.1 | 45.7 | 73.2 |
| BS-250602 | 1450 | 655 | 492 | 163 | - | - | 91 | 71 | 139 | 87.9 | 35.9 | 44.5 |
| BS-250604 | 9000 | 459 | 342 | 117 | - | - | 27.4 | 49 | 107.3 | 61.8 | 34 | 43.6 |

Table I.2 Laboratory analysis results for Beatrice West samples

| Sample name | Sample volume [ml] | TSS [mg/L] | Coarse fraction [mg/L] | Fine fraction [mg/L] | Turbidity of sample [NTU] | Turbidity of filtrate [NTU] | Mass of samples retained on sieves [mg] | | | | | |
|---|---|---|---|---|---|---|---|---|---|---|---|---|
| | | | | | | | 1000 µm | 500 µm | 250 µm | 125 µm | 63 µm | 32 µm |
| BTW-240426 | 2795 | 348 | 194 | 155 | 51 | 7 | 41.3 | 10.7 | 14 | 22.4 | 28.5 | 41.8 |
| BTW-240428 | 7990 | 340 | 188 | 153 | 103 | 19 | 38.8 | 27.4 | 24.7 | 52.8 | 33.2 | 44.1 |
| BTW-240502 | 9325 | 226 | 76 | 150 | 107 | 16 | 6.1 | 2.1 | 4.4 | 8.6 | 16.2 | 26.7 |
| BTW-240504 | 9540 | 2066 | 1197 | 869 | 470 | 38 | 60.3 | 44.9 | 113.8 | 195.7 | 218.5 | 349.4 |
| BTW-240507 | 4635 | 159 | 87 | 71 | 49 | 12 | 21.2 | 9.2 | 7 | 10.9 | 15.4 | 3.4 |
| BTW-240524 | 3735 | 157 | 70 | 87 | 49 | 7 | 14.6 | 3.5 | 8.1 | 11.2 | 14.5 | 16.4 |
| BTW-240531 | 9575 | 2860 | 1974 | 886 | 373 | 19 | 47.6 | 120.3 | 365.6 | 334.6 | 369.5 | 472.9 |
| BTW-240603 | 6570 | 55 | 26 | 29 | 37 | 12 | 1.9 | 3.1 | 6.5 | 4.4 | 4.1 | 4.5 |
| BTW-240616 | 9410 | 109 | 66 | 43 | 21 | 3 | 2.3 | 4 | 9.5 | 12.4 | 14.9 | 16.5 |
| BTW-240701 | 9450 | 91 | 49 | 42 | 36 | 8 | 1.1 | 2.2 | 8 | 12.6 | 9.6 | 9.6 |
| BTW-240706 | 9420 | 99 | 44 | 55 | 44 | 8 | 0 | 1.9 | 6.5 | 6.1 | 8.6 | 13.2 |
| BTW-240707 | 10000 | 304 | 200 | 103 | - | - | 3.4 | 8.7 | 21.3 | 31.1 | 44.3 | 53.3 |
| BTW-241031 | 9500 | 209 | 168 | 41 | - | - | 8.6 | 21.3 | 43.4 | 40.6 | 21.6 | 16.2 |
| BTW-241104 | 9600 | 87 | 42 | 45 | - | - | 3.6 | 3.7 | 5.8 | 6.6 | 6.8 | 8.9 |
| BTW-241109 | 9400 | 20 | 1 | 19 | - | - | 0 | 0 | 0 | 0 | 0 | 0 |
| BTW-241113 | 9500 | 15 | 2 | 13 | - | - | 0 | 0.3 | 0.3 | 0.4 | 0.6 | 0.8 |
| BTW-241119 | 9600 | 37 | 6 | 31 | - | - | 0 | 2.3 | 2.4 | 1 | 1 | 1.2 |
| BTW-250402 | 7500 | 685 | 330 | 355 | - | - | 16.9 | 47.6 | 46.8 | 63.4 | 56.2 | 38.2 |
| BTW-250520 | 9500 | 245 | 166 | 79 | - | - | 14.4 | 20 | 23.4 | 18.3 | 23 | 27.8 |
| BTW-250527 | 2300 | 7 | 7 | 0 | - | - | 0 | 0 | 0 | 0 | 0 | 0 |
| BTW-250602 | 3500 | 231 | 154 | 77 | - | - | 1.9 | 8.1 | 19.4 | 46.2 | 41.2 | 28.3 |
| BTW-250604 | 9500 | 73 | 41 | 32 | - | - | 3.3 | 2.5 | 6.3 | 8.1 | 8.7 | 6.7 |

Table I.3 Laboratory analysis results for Cornhusker samples

| Sample name | Sample volume [ml] | TSS [mg/L] | Coarse fraction [mg/L] | Fine fraction [mg/L] | Turbidity of sample [NTU] | Turbidity of filtrate [NTU] | Mass of samples retained on sieves [mg] | | | | | |
|---|---|---|---|---|---|---|---|---|---|---|---|---|
| | | | | | | | 1000 µm | 500 µm | 250 µm | 125 µm | 63 µm | 32 µm |
| CH-240324 | 950 | 981 | 358 | 623 | 316 | 0 | 61.7 | 43.5 | 38.8 | 59.8 | 55.3 | 58.6 |
| CH-240407 | 280 | 742 | 120 | 623 | 316 | 0 | 12.9 | 16.1 | 33.6 | 30 | 20 | 15 |
| CH-240416 | 10040 | 1235 | 531 | 703 | 378 | 5 | 54.2 | 63.4 | 85.1 | 89.1 | 80.5 | 103.9 |
| CH-240426 | 10790 | 510 | 110 | 400 | 284 | 14 | 32.7 | 20.5 | 16.9 | 8.2 | 9.6 | 13.8 |
| CH-240428 | 10715 | 484 | 119 | 365 | 249 | 9 | 26.2 | 52.6 | 22.5 | 10.1 | 2.9 | 5.6 |
| CH-240502 | 4560 | 244 | 157 | 87 | 35 | 3 | 31.3 | 55.1 | 29.1 | 11.8 | 11.1 | 13.9 |
| CH-240504 | 9865 | 381 | 196 | 185 | 84 | 6 | 30.2 | 45.3 | 37.2 | 21.9 | 18.8 | 31.7 |
| CH-240507 | 8785 | 221 | 102 | 119 | 65 | 5 | 34.4 | 23.5 | 15.4 | 7.2 | 7.1 | 9.3 |
| CH-240513 | 10690 | 178 | 46 | 133 | 75 | 5 | 14.1 | 10.3 | 8.6 | 3.1 | 3.3 | 4 |
| CH-240520 | 10705 | 262 | 57 | 205 | 114 | 4 | 2.6 | 5.2 | 8 | 8.4 | 9.9 | 13.3 |
| CH-240524 | 9450 | 317 | 153 | 164 | 56 | 2 | 15.4 | 23.4 | 28.5 | 20.9 | 22.6 | 34.6 |
| CH-240531 | 9460 | 641 | 332 | 309 | 111 | 6 | 34.1 | 42.6 | 50.6 | 51.9 | 56.1 | 83 |
| CH-240603 | 2885 | 51 | 15 | 35 | 34 | 5 | 1.8 | 1.8 | 2.7 | 2.1 | 2.1 | 2.2 |
| CH-240608 | 7135 | 711 | 479 | 231 | 76 | 4 | 61.3 | 84.8 | 93.2 | 73.8 | 67.6 | 77.6 |
| CH-240616 | 9435 | 224 | 165 | 59 | 23 | 1 | 47.2 | 41.3 | 38.1 | 17.4 | 9.3 | 8.8 |
| CH-240619 | 3660 | 217 | 79 | 138 | 92 | 8 | 8.4 | 17.9 | 18.3 | 10.7 | 6.4 | 6.8 |
| CH-240626 | 10665 | 163 | 107 | 57 | 26 | 2 | 13.8 | 34.5 | 27.5 | 12.7 | 5.9 | 5.5 |
| CH-240628 | 3470 | 230 | 56 | 174 | 126 | 7 | 11.1 | 11.9 | 12.1 | 5.8 | 3.8 | 3.2 |
| CH-240701 | 7250 | 166 | 73 | 93 | - | - | 0.2 | 2.3 | 11.7 | 13.7 | 15.4 | 20.3 |
| CH-240808 | 2900 | 311 | 232 | 79 | - | - | 48.3 | 40 | 57.9 | 30.9 | 18.4 | 21.9 |
| CH-240812 | 1980 | 101 | 40 | 61 | - | - | 12.7 | 11.2 | 3.6 | 3 | 3 | 3.7 |
| CH-240814 | 9500 | 417 | 367 | 49 | - | - | 78 | 87.8 | 153.9 | 22.6 | 10.1 | 9.9 |
| CH-240819 | 10800 | 404 | 298 | 106 | - | - | 62.2 | 180.2 | 48.5 | 1.1 | 0.9 | 1.3 |
| CH-240830 | 10800 | 407 | 252 | 155 | - | - | 67.6 | 122.1 | 46.8 | 3.5 | 3.7 | 4.3 |
| CH-241022 | 11800 | 585 | 202 | 383 | - | - | 26.7 | 57.9 | 39.6 | 26 | 17 | 16.7 |
| CH-241104 | 9000 | 423 | 288 | 135 | - | - | 60.5 | 94 | 60.7 | 17.7 | 18.9 | 26.8 |
| CH-250315 | 1450 | 2356 | 631 | 1725 | - | - | 81.9 | 55.2 | 72.2 | 84.2 | 93 | 164.1 |
| CH-250425 | 2700 | 595 | 104 | 491 | - | - | 4.4 | 2.5 | 12.5 | 18.6 | 20.6 | 27.4 |
| CH-250520 | 2050 | 495 | 178 | 317 | - | - | 14.5 | 39.7 | 33.2 | 19.9 | 23.6 | 40.5 |
| CH-250527 | 3000 | 65 | 54 | 11 | - | - | 8.6 | 13.4 | 19.3 | 3.7 | 2.8 | 2.4 |
| CH-250602 | 9700 | 725 | 390 | 334 | - | - | 60.8 | 86.4 | 73.3 | 36.1 | 42.4 | 70.5 |

Table I.4 Laboratory analysis results for Beatrice North samples

| Sample name | Sample volume [ml] | TSS [mg/L] | Coarse fraction [mg/L] | Fine fraction [mg/L] | Turbidity of sample [NTU] | Turbidity of filtrate [NTU] | Mass of samples retained on sieves [mg] | | | | | |
|---|---|---|---|---|---|---|---|---|---|---|---|---|
| | | | | | | | 1000 µm | 500 µm | 250 µm | 125 µm | 63 µm | 32 µm |
| BTN-240426 | 9410 | 918 | 241 | 677 | 443 | 6 | 29.9 | 28.5 | 45.7 | 37.5 | 28.1 | 41.6 |
| BTN-240428 | 7960 | 1079 | 73 | 1006 | 1267 | 24 | 14 | 8.2 | 12.2 | 15.9 | 9.6 | 12.9 |
| BTN-240502 | 1000 | 1590 | 351 | 1239 | 788 | 8 | 42.3 | 23.6 | 34.6 | 36 | 53.9 | 112.8 |
| BTN-240504 | 9875 | 2625 | 1195 | 1430 | 986 | 25 | 274 | 191.4 | 305.4 | 165.9 | 95.5 | 112.5 |
| BTN-240507 | 9430 | 495 | 97 | 397 | 279 | 12 | 25.8 | 1.1 | 19.4 | 24 | 11.4 | 7.8 |
| BTN-240513 | 4210 | 180 | 16 | 164 | 167 | 16 | 4.3 | 3.2 | 2.3 | 3.7 | 0.9 | 1.4 |
| BTN-240524 | 9745 | 750 | 368 | 382 | 225 | 6 | 54.3 | 73.6 | 109.2 | 55 | 29.3 | 34.9 |
| BTN-240531 | 9780 | 2548 | 1311 | 1237 | 653 | 9 | 172.1 | 212.9 | 318.2 | 207.4 | 141.4 | 197.3 |
| BTN-240608 | 6265 | 179 | 30 | 149 | 128 | 13 | 0.8 | 3.9 | 6.8 | 6.5 | 4.8 | 4.4 |
| BTN-240616 | 9685 | 408 | 121 | 287 | 171 | 4 | 5.3 | 14.6 | 38.4 | 26.3 | 13 | 16.1 |
| BTN-240626 | 9730 | 881 | 342 | 539 | 294 | 5 | 48.8 | 65.2 | 98.7 | 44.7 | 28.2 | 40.1 |
| BTN-240721 | 6760 | 101 | 28 | 73 | - | - | 1 | 3.6 | 6 | 5.3 | 3.7 | 2.9 |
| BTN-240814 | 1870 | 118 | 39 | 79 | - | - | 0 | 2.6 | 6.5 | 6.1 | 7.4 | 7.3 |
| BTN-240830 | 10540 | 476 | 124 | 352 | - | - | 32.9 | 13.5 | 21.8 | 15.9 | 12.1 | 17.3 |
| BTN-240923 | 2500 | 132 | 35 | 98 | - | - | 1.3 | 2.8 | 4 | 4.8 | 3.5 | 4 |
| BTN-241022 | 3780 | 662 | 145 | 517 | - | - | 22.1 | 23.7 | 35.1 | 21.9 | 11.1 | 9.3 |
| BTN-241031 | 9600 | 1041 | 349 | 692 | - | - | 64.8 | 72.5 | 74.4 | 33.4 | 29.2 | 43.3 |
| BTN-241104 | 11250 | 393 | 73 | 321 | - | - | 4.8 | 8.2 | 15.3 | 11.8 | 8.7 | 16.4 |
| BTN-241109 | 9500 | 185 | 24 | 161 | - | - | 1.5 | 2.3 | 5.3 | 3.9 | 3 | 4.3 |
| BTN-241113 | 9500 | 334 | 38 | 297 | - | - | 5 | 3.3 | 5.2 | 5.7 | 5 | 8.9 |
| BTN-241119 | 10600 | 564 | 16 | 549 | - | - | 3.2 | -0.7 | -0.3 | 2.6 | 2.6 | 3.8 |
| BTN-241214 | 8000 | 103 | 19 | 83 | - | - | 0.8 | 1.8 | 3.6 | 4.2 | 2.7 | 3.2 |
| BTN-250306 | 11000 | 1669 | 44 | 1625 | - | - | 0.2 | 2.2 | 7.9 | 8.4 | 7.5 | 9.6 |
| BTN-250320 | 11000 | 1125 | 60 | 1065 | - | - | 0.6 | 2.4 | 9.1 | 8.1 | 10.6 | 16 |
| BTN-250402 | 8000 | 3530 | 1423 | 2107 | - | - | 207.5 | 347 | 410.5 | 181.5 | 95.1 | 120.8 |
| BTN-250404 | 11000 | 465 | 18 | 447 | - | - | 1 | 3.2 | 4.5 | 2.4 | 1.5 | 1.6 |
| BTN-250520 | 9500 | 970 | 307 | 662 | - | - | 35.6 | 38.6 | 69.1 | 54.1 | 39.6 | 51.2 |
| BTN-250527 | 11400 | 72 | 13 | 59 | - | - | 0.1 | 1 | 2.1 | 2.6 | 2.2 | 2.8 |
| BTN-250602 | 11000 | 769 | 111 | 658 | - | - | 7.4 | 14 | 23.2 | 17 | 15.5 | 25.2 |
| BTN-250604 | 9000 | 595 | 61 | 534 | - | - | 4.6 | 7.1 | 11.6 | 9.5 | 7.5 | 12.5 |

# Appendix J Data of extended Particle size distribution samples

This appendix presents data from an external laboratory related to the fine particle size distribution (PSD) of the extended PSD samples. This analysis focuses on particles smaller than 32 μm. The reported values represent the differential volume percentage for each particle size range. The standard operating procedure and lab methods used for these samples are described in Appendix N.

## Table J.1 Extended PSD Data from External Lab – Beal Slough (Part 1 of 3)

| Channel Number | Lower diameter (μm) | 240324 | 240416 | 240426 | 240428 | 240504 | 240524 | 240531 | Channel Number | Lower diameter (μm) | 240324 | 240416 | 240426 | 240428 | 240504 | 240524 | 240531 |
|---|---|---|---|---|---|---|---|---|---|---|---|---|---|---|---|---|---|
| | | Differential volume (%) | | | | | | | | | Differential volume (%) | | | | | | |
| 1 | 0.04 | 0.00 | 0.00 | 0.00 | 0.00 | 0.00 | 0.00 | 0.00 | 37 | 1.15 | 0.28 | 0.39 | 0.47 | 0.42 | 0.51 | 0.13 | 0.26 |
| 2 | 0.04 | 0.00 | 0.00 | 0.00 | 0.00 | 0.00 | 0.00 | 0.00 | 38 | 1.26 | 0.29 | 0.40 | 0.55 | 0.43 | 0.56 | 0.15 | 0.28 |
| 3 | 0.05 | 0.00 | 0.00 | 0.00 | 0.00 | 0.00 | 0.00 | 0.00 | 39 | 1.39 | 0.31 | 0.41 | 0.64 | 0.45 | 0.62 | 0.17 | 0.30 |
| 4 | 0.05 | 0.00 | 0.01 | 0.00 | 0.00 | 0.00 | 0.00 | 0.00 | 40 | 1.52 | 0.33 | 0.41 | 0.73 | 0.47 | 0.68 | 0.20 | 0.32 |
| 5 | 0.06 | 0.01 | 0.01 | 0.00 | 0.01 | 0.00 | 0.00 | 0.00 | 41 | 1.67 | 0.35 | 0.42 | 0.82 | 0.49 | 0.74 | 0.23 | 0.35 |
| 6 | 0.06 | 0.02 | 0.02 | 0.00 | 0.02 | 0.00 | 0.00 | 0.00 | 42 | 1.83 | 0.38 | 0.43 | 0.91 | 0.51 | 0.80 | 0.26 | 0.37 |
| 7 | 0.07 | 0.03 | 0.03 | 0.00 | 0.03 | 0.00 | 0.00 | 0.00 | 43 | 2.01 | 0.41 | 0.44 | 0.98 | 0.54 | 0.86 | 0.30 | 0.39 |
| 8 | 0.08 | 0.03 | 0.04 | 0.00 | 0.04 | 0.00 | 0.00 | 0.00 | 44 | 2.21 | 0.45 | 0.45 | 1.04 | 0.57 | 0.91 | 0.35 | 0.41 |
| 9 | 0.08 | 0.04 | 0.05 | 0.00 | 0.05 | 0.00 | 0.00 | 0.00 | 45 | 2.42 | 0.50 | 0.48 | 1.09 | 0.61 | 0.95 | 0.40 | 0.43 |
| 10 | 0.09 | 0.05 | 0.06 | 0.00 | 0.06 | 0.00 | 0.00 | 0.00 | 46 | 2.66 | 0.56 | 0.50 | 1.11 | 0.66 | 0.99 | 0.45 | 0.45 |
| 11 | 0.10 | 0.06 | 0.07 | 0.00 | 0.07 | 0.00 | 0.00 | 0.00 | 47 | 2.92 | 0.63 | 0.54 | 1.12 | 0.73 | 1.03 | 0.50 | 0.47 |
| 12 | 0.11 | 0.07 | 0.08 | 0.00 | 0.08 | 0.00 | 0.00 | 0.00 | 48 | 3.21 | 0.71 | 0.59 | 1.12 | 0.80 | 1.08 | 0.56 | 0.48 |
| 13 | 0.12 | 0.08 | 0.09 | 0.00 | 0.09 | 0.00 | 0.00 | 0.00 | 49 | 3.52 | 0.81 | 0.66 | 1.12 | 0.89 | 1.13 | 0.61 | 0.50 |
| 14 | 0.13 | 0.08 | 0.11 | 0.01 | 0.10 | 0.00 | 0.00 | 0.00 | 50 | 3.86 | 0.92 | 0.75 | 1.14 | 0.99 | 1.20 | 0.66 | 0.52 |
| 15 | 0.15 | 0.09 | 0.12 | 0.01 | 0.11 | 0.01 | 0.00 | 0.00 | 51 | 4.24 | 1.04 | 0.85 | 1.19 | 1.11 | 1.29 | 0.70 | 0.55 |
| 16 | 0.16 | 0.10 | 0.13 | 0.01 | 0.12 | 0.01 | 0.00 | 0.01 | 52 | 4.66 | 1.18 | 0.97 | 1.27 | 1.25 | 1.40 | 0.73 | 0.58 |
| 17 | 0.18 | 0.10 | 0.14 | 0.02 | 0.13 | 0.01 | 0.00 | 0.01 | 53 | 5.11 | 1.34 | 1.11 | 1.38 | 1.41 | 1.55 | 0.75 | 0.61 |
| 18 | 0.20 | 0.11 | 0.15 | 0.02 | 0.14 | 0.02 | 0.01 | 0.01 | 54 | 5.61 | 1.51 | 1.28 | 1.53 | 1.58 | 1.72 | 0.77 | 0.65 |
| 19 | 0.21 | 0.12 | 0.16 | 0.03 | 0.15 | 0.03 | 0.01 | 0.02 | 55 | 6.16 | 1.69 | 1.47 | 1.72 | 1.77 | 1.91 | 0.77 | 0.71 |
| 20 | 0.24 | 0.13 | 0.17 | 0.04 | 0.16 | 0.03 | 0.01 | 0.02 | 56 | 6.76 | 1.88 | 1.67 | 1.92 | 1.97 | 2.13 | 0.78 | 0.77 |
| 21 | 0.26 | 0.14 | 0.19 | 0.05 | 0.18 | 0.04 | 0.01 | 0.03 | 57 | 7.42 | 2.09 | 1.90 | 2.14 | 2.19 | 2.37 | 0.78 | 0.85 |
| 22 | 0.28 | 0.14 | 0.20 | 0.06 | 0.19 | 0.06 | 0.01 | 0.03 | 58 | 8.15 | 2.31 | 2.17 | 2.35 | 2.44 | 2.62 | 0.80 | 0.95 |
| 23 | 0.31 | 0.15 | 0.22 | 0.07 | 0.21 | 0.07 | 0.01 | 0.04 | 59 | 8.94 | 2.54 | 2.47 | 2.56 | 2.70 | 2.88 | 0.83 | 1.05 |
| 24 | 0.34 | 0.16 | 0.23 | 0.08 | 0.22 | 0.09 | 0.02 | 0.05 | 60 | 9.82 | 2.77 | 2.80 | 2.79 | 2.98 | 3.15 | 0.89 | 1.18 |
| 25 | 0.38 | 0.17 | 0.24 | 0.09 | 0.23 | 0.10 | 0.02 | 0.06 | 61 | 10.78 | 3.02 | 3.14 | 3.04 | 3.27 | 3.43 | 0.97 | 1.32 |
| 26 | 0.41 | 0.17 | 0.26 | 0.11 | 0.25 | 0.12 | 0.02 | 0.07 | 62 | 11.83 | 3.27 | 3.52 | 3.34 | 3.59 | 3.74 | 1.08 | 1.47 |
| 27 | 0.45 | 0.18 | 0.27 | 0.12 | 0.26 | 0.14 | 0.03 | 0.08 | 63 | 12.99 | 3.50 | 3.97 | 3.65 | 3.91 | 4.03 | 1.20 | 1.65 |
| 28 | 0.50 | 0.19 | 0.29 | 0.14 | 0.28 | 0.16 | 0.03 | 0.09 | 64 | 14.26 | 3.72 | 4.45 | 3.92 | 4.23 | 4.27 | 1.35 | 1.83 |
| 29 | 0.55 | 0.20 | 0.30 | 0.15 | 0.29 | 0.19 | 0.04 | 0.10 | 65 | 15.65 | 3.91 | 4.92 | 4.07 | 4.52 | 4.40 | 1.52 | 2.04 |
| 30 | 0.60 | 0.21 | 0.31 | 0.17 | 0.31 | 0.21 | 0.05 | 0.12 | 66 | 17.18 | 4.03 | 5.36 | 4.10 | 4.77 | 4.40 | 1.70 | 2.26 |
| 31 | 0.66 | 0.21 | 0.33 | 0.19 | 0.33 | 0.24 | 0.06 | 0.14 | 67 | 18.86 | 4.08 | 5.77 | 4.07 | 4.95 | 4.30 | 1.89 | 2.51 |
| 32 | 0.72 | 0.22 | 0.34 | 0.22 | 0.34 | 0.28 | 0.07 | 0.16 | 68 | 20.71 | 4.06 | 6.19 | 4.04 | 5.03 | 4.17 | 2.10 | 2.78 |
| 33 | 0.79 | 0.23 | 0.35 | 0.25 | 0.36 | 0.31 | 0.08 | 0.17 | 69 | 22.73 | 3.96 | 6.60 | 4.10 | 5.01 | 4.08 | 2.35 | 3.08 |
| 34 | 0.87 | 0.24 | 0.37 | 0.29 | 0.37 | 0.36 | 0.09 | 0.19 | 70 | 24.95 | 3.79 | 6.81 | 4.23 | 4.86 | 4.03 | 2.63 | 3.40 |
| 35 | 0.95 | 0.25 | 0.38 | 0.34 | 0.39 | 0.40 | 0.10 | 0.21 | 71 | 27.39 | 3.57 | 6.54 | 4.35 | 4.57 | 3.98 | 2.94 | 3.74 |
| 36 | 1.05 | 0.26 | 0.39 | 0.40 | 0.40 | 0.45 | 0.11 | 0.24 | 72 | 30.07 | 3.29 | 5.62 | 4.35 | 4.14 | 3.84 | 3.28 | 4.09 |

## Table J.2 Extended PSD Data from External Lab – Beal Slough (Part 2 of 3)

| Channel Number | Lower diameter (µm) | 240616 | 240701 | 240707 | 240721 | 240814 | 240830 | 241031 | Channel Number | Lower diameter (µm) | 240616 | 240701 | 240707 | 240721 | 240814 | 240830 | 241031 |
|---|---|---|---|---|---|---|---|---|---|---|---|---|---|---|---|---|---|
| | | Differential volume (%) | | | | | | | | | Differential volume (%) | | | | | | |
| 1 | 0.04 | 0.00 | 0.00 | 0.00 | 0.00 | 0.00 | 0.00 | 0.00 | 37 | 1.15 | 0.17 | 0.21 | 0.43 | 0.22 | 0.17 | 0.18 | 0.32 |
| 2 | 0.04 | 0.00 | 0.00 | 0.00 | 0.00 | 0.00 | 0.00 | 0.00 | 38 | 1.26 | 0.18 | 0.22 | 0.53 | 0.30 | 0.17 | 0.19 | 0.33 |
| 3 | 0.05 | 0.00 | 0.00 | 0.00 | 0.00 | 0.00 | 0.00 | 0.00 | 39 | 1.39 | 0.19 | 0.24 | 0.63 | 0.39 | 0.18 | 0.20 | 0.34 |
| 4 | 0.05 | 0.00 | 0.00 | 0.00 | 0.00 | 0.00 | 0.00 | 0.00 | 40 | 1.52 | 0.20 | 0.25 | 0.74 | 0.48 | 0.19 | 0.21 | 0.35 |
| 5 | 0.06 | 0.00 | 0.00 | 0.01 | 0.00 | 0.00 | 0.00 | 0.00 | 41 | 1.67 | 0.20 | 0.26 | 0.85 | 0.59 | 0.19 | 0.21 | 0.36 |
| 6 | 0.06 | 0.00 | 0.00 | 0.01 | 0.00 | 0.00 | 0.00 | 0.00 | 42 | 1.83 | 0.21 | 0.27 | 0.96 | 0.69 | 0.20 | 0.22 | 0.36 |
| 7 | 0.07 | 0.00 | 0.00 | 0.02 | 0.00 | 0.00 | 0.00 | 0.00 | 43 | 2.01 | 0.22 | 0.29 | 1.04 | 0.77 | 0.21 | 0.23 | 0.37 |
| 8 | 0.08 | 0.00 | 0.00 | 0.02 | 0.01 | 0.00 | 0.00 | 0.00 | 44 | 2.21 | 0.23 | 0.30 | 1.11 | 0.83 | 0.21 | 0.24 | 0.38 |
| 9 | 0.08 | 0.00 | 0.00 | 0.03 | 0.01 | 0.00 | 0.00 | 0.00 | 45 | 2.42 | 0.24 | 0.31 | 1.15 | 0.86 | 0.21 | 0.24 | 0.39 |
| 10 | 0.09 | 0.00 | 0.00 | 0.03 | 0.01 | 0.00 | 0.00 | 0.00 | 46 | 2.66 | 0.25 | 0.32 | 1.16 | 0.85 | 0.22 | 0.25 | 0.41 |
| 11 | 0.10 | 0.00 | 0.00 | 0.04 | 0.02 | 0.00 | 0.00 | 0.00 | 47 | 2.92 | 0.26 | 0.34 | 1.14 | 0.81 | 0.22 | 0.26 | 0.43 |
| 12 | 0.11 | 0.00 | 0.00 | 0.04 | 0.02 | 0.00 | 0.00 | 0.01 | 48 | 3.21 | 0.28 | 0.35 | 1.11 | 0.74 | 0.22 | 0.27 | 0.46 |
| 13 | 0.12 | 0.01 | 0.01 | 0.05 | 0.03 | 0.01 | 0.01 | 0.01 | 49 | 3.52 | 0.30 | 0.37 | 1.08 | 0.66 | 0.23 | 0.28 | 0.50 |
| 14 | 0.13 | 0.01 | 0.01 | 0.05 | 0.03 | 0.01 | 0.02 | 0.01 | 50 | 3.86 | 0.32 | 0.38 | 1.06 | 0.60 | 0.23 | 0.29 | 0.55 |
| 15 | 0.15 | 0.02 | 0.02 | 0.06 | 0.04 | 0.02 | 0.02 | 0.02 | 51 | 4.24 | 0.34 | 0.40 | 1.07 | 0.56 | 0.24 | 0.31 | 0.61 |
| 16 | 0.16 | 0.02 | 0.02 | 0.06 | 0.05 | 0.02 | 0.03 | 0.02 | 52 | 4.66 | 0.37 | 0.43 | 1.13 | 0.55 | 0.25 | 0.33 | 0.68 |
| 17 | 0.18 | 0.03 | 0.03 | 0.07 | 0.06 | 0.03 | 0.04 | 0.03 | 53 | 5.11 | 0.41 | 0.46 | 1.24 | 0.60 | 0.26 | 0.35 | 0.76 |
| 18 | 0.20 | 0.04 | 0.04 | 0.08 | 0.07 | 0.04 | 0.04 | 0.04 | 54 | 5.61 | 0.45 | 0.49 | 1.41 | 0.69 | 0.28 | 0.37 | 0.85 |
| 19 | 0.21 | 0.04 | 0.04 | 0.08 | 0.08 | 0.04 | 0.05 | 0.04 | 55 | 6.16 | 0.50 | 0.53 | 1.63 | 0.82 | 0.30 | 0.40 | 0.96 |
| 20 | 0.24 | 0.05 | 0.05 | 0.09 | 0.09 | 0.05 | 0.06 | 0.05 | 56 | 6.76 | 0.56 | 0.57 | 1.89 | 0.97 | 0.33 | 0.43 | 1.08 |
| 21 | 0.26 | 0.06 | 0.06 | 0.09 | 0.10 | 0.05 | 0.06 | 0.07 | 57 | 7.42 | 0.63 | 0.62 | 2.17 | 1.13 | 0.36 | 0.47 | 1.22 |
| 22 | 0.28 | 0.06 | 0.06 | 0.10 | 0.10 | 0.06 | 0.07 | 0.08 | 58 | 8.15 | 0.71 | 0.68 | 2.46 | 1.28 | 0.41 | 0.52 | 1.37 |
| 23 | 0.31 | 0.07 | 0.07 | 0.10 | 0.11 | 0.06 | 0.08 | 0.09 | 59 | 8.94 | 0.80 | 0.75 | 2.75 | 1.42 | 0.46 | 0.58 | 1.55 |
| 24 | 0.34 | 0.07 | 0.08 | 0.10 | 0.11 | 0.07 | 0.08 | 0.11 | 60 | 9.82 | 0.89 | 0.83 | 3.05 | 1.57 | 0.52 | 0.64 | 1.75 |
| 25 | 0.38 | 0.08 | 0.08 | 0.11 | 0.11 | 0.08 | 0.09 | 0.12 | 61 | 10.78 | 1.00 | 0.91 | 3.34 | 1.74 | 0.59 | 0.71 | 1.98 |
| 26 | 0.41 | 0.09 | 0.09 | 0.11 | 0.11 | 0.08 | 0.10 | 0.14 | 62 | 11.83 | 1.11 | 1.01 | 3.59 | 1.95 | 0.67 | 0.80 | 2.23 |
| 27 | 0.45 | 0.09 | 0.10 | 0.11 | 0.11 | 0.09 | 0.11 | 0.16 | 63 | 12.99 | 1.23 | 1.12 | 3.77 | 2.18 | 0.76 | 0.89 | 2.50 |
| 28 | 0.50 | 0.10 | 0.11 | 0.12 | 0.10 | 0.10 | 0.11 | 0.17 | 64 | 14.26 | 1.36 | 1.24 | 3.88 | 2.43 | 0.86 | 1.00 | 2.78 |
| 29 | 0.55 | 0.11 | 0.12 | 0.12 | 0.09 | 0.10 | 0.12 | 0.19 | 65 | 15.65 | 1.49 | 1.37 | 3.95 | 2.66 | 0.97 | 1.12 | 3.05 |
| 30 | 0.60 | 0.12 | 0.13 | 0.13 | 0.09 | 0.11 | 0.13 | 0.21 | 66 | 17.18 | 1.64 | 1.52 | 4.06 | 2.89 | 1.09 | 1.26 | 3.29 |
| 31 | 0.66 | 0.13 | 0.14 | 0.15 | 0.08 | 0.12 | 0.14 | 0.23 | 67 | 18.86 | 1.80 | 1.69 | 4.23 | 3.14 | 1.23 | 1.42 | 3.48 |
| 32 | 0.72 | 0.13 | 0.15 | 0.17 | 0.08 | 0.13 | 0.14 | 0.25 | 68 | 20.71 | 1.97 | 1.90 | 4.42 | 3.45 | 1.37 | 1.60 | 3.65 |
| 33 | 0.79 | 0.14 | 0.16 | 0.19 | 0.08 | 0.13 | 0.15 | 0.26 | 69 | 22.73 | 2.17 | 2.13 | 4.54 | 3.82 | 1.53 | 1.82 | 3.81 |
| 34 | 0.87 | 0.15 | 0.17 | 0.23 | 0.10 | 0.14 | 0.16 | 0.28 | 70 | 24.95 | 2.39 | 2.41 | 4.46 | 4.25 | 1.70 | 2.08 | 3.97 |
| 35 | 0.95 | 0.16 | 0.19 | 0.28 | 0.12 | 0.15 | 0.17 | 0.30 | 71 | 27.39 | 2.64 | 2.74 | 4.17 | 4.66 | 1.90 | 2.39 | 4.13 |
| 36 | 1.05 | 0.17 | 0.20 | 0.35 | 0.16 | 0.16 | 0.17 | 0.31 | 72 | 30.07 | 2.93 | 3.11 | 3.73 | 4.97 | 2.11 | 2.74 | 4.23 |

## Table J.3 Extended PSD Data from External Lab – Beal Slough (Part 3 of 3)

| Channel Number | Lower diameter (µm) | 241109 | 241119 | 240425 | 250520 | 250602 | 250604 | Channel Number | Lower diameter (µm) | 241109 | 241119 | 240425 | 250520 | 250602 | 250604 |
|---|---|---|---|---|---|---|---|---|---|---|---|---|---|---|---|
| | | Differential volume (%) | | | | | | | | Differential volume (%) | | | | | |
| 1 | 0.04 | 0.00 | 0.00 | 0.00 | 0.00 | 0.00 | 0.00 | 37 | 1.15 | 0.36 | 0.35 | 0.63 | 0.45 | 0.36 | 0.21 |
| 2 | 0.04 | 0.00 | 0.00 | 0.00 | 0.00 | 0.00 | 0.00 | 38 | 1.26 | 0.39 | 0.37 | 0.66 | 0.51 | 0.37 | 0.20 |
| 3 | 0.05 | 0.00 | 0.00 | 0.00 | 0.00 | 0.00 | 0.00 | 39 | 1.39 | 0.42 | 0.38 | 0.69 | 0.58 | 0.38 | 0.19 |
| 4 | 0.05 | 0.00 | 0.00 | 0.00 | 0.00 | 0.01 | 0.01 | 40 | 1.52 | 0.45 | 0.40 | 0.72 | 0.65 | 0.39 | 0.18 |
| 5 | 0.06 | 0.00 | 0.01 | 0.00 | 0.01 | 0.02 | 0.02 | 41 | 1.67 | 0.48 | 0.42 | 0.75 | 0.71 | 0.40 | 0.18 |
| 6 | 0.06 | 0.00 | 0.01 | 0.00 | 0.01 | 0.03 | 0.04 | 42 | 1.83 | 0.52 | 0.44 | 0.78 | 0.77 | 0.42 | 0.18 |
| 7 | 0.07 | 0.00 | 0.01 | 0.00 | 0.02 | 0.05 | 0.06 | 43 | 2.01 | 0.55 | 0.46 | 0.81 | 0.81 | 0.45 | 0.19 |
| 8 | 0.08 | 0.00 | 0.02 | 0.01 | 0.02 | 0.06 | 0.07 | 44 | 2.21 | 0.59 | 0.49 | 0.84 | 0.85 | 0.48 | 0.20 |
| 9 | 0.08 | 0.00 | 0.02 | 0.01 | 0.03 | 0.08 | 0.09 | 45 | 2.42 | 0.64 | 0.52 | 0.89 | 0.86 | 0.52 | 0.22 |
| 10 | 0.09 | 0.00 | 0.03 | 0.01 | 0.03 | 0.09 | 0.11 | 46 | 2.66 | 0.69 | 0.56 | 0.94 | 0.87 | 0.57 | 0.25 |
| 11 | 0.10 | 0.00 | 0.04 | 0.01 | 0.04 | 0.11 | 0.12 | 47 | 2.92 | 0.75 | 0.61 | 1.01 | 0.86 | 0.64 | 0.28 |
| 12 | 0.11 | 0.00 | 0.04 | 0.02 | 0.04 | 0.12 | 0.14 | 48 | 3.21 | 0.81 | 0.67 | 1.09 | 0.85 | 0.72 | 0.33 |
| 13 | 0.12 | 0.01 | 0.05 | 0.02 | 0.05 | 0.13 | 0.15 | 49 | 3.52 | 0.88 | 0.74 | 1.19 | 0.85 | 0.82 | 0.40 |
| 14 | 0.13 | 0.01 | 0.06 | 0.03 | 0.05 | 0.15 | 0.17 | 50 | 3.86 | 0.95 | 0.81 | 1.32 | 0.86 | 0.93 | 0.47 |
| 15 | 0.15 | 0.01 | 0.06 | 0.03 | 0.06 | 0.16 | 0.18 | 51 | 4.24 | 1.03 | 0.90 | 1.46 | 0.90 | 1.06 | 0.56 |
| 16 | 0.16 | 0.02 | 0.07 | 0.04 | 0.06 | 0.17 | 0.19 | 52 | 4.66 | 1.12 | 1.00 | 1.62 | 0.98 | 1.21 | 0.66 |
| 17 | 0.18 | 0.02 | 0.08 | 0.05 | 0.07 | 0.19 | 0.20 | 53 | 5.11 | 1.21 | 1.11 | 1.80 | 1.09 | 1.38 | 0.77 |
| 18 | 0.20 | 0.03 | 0.09 | 0.06 | 0.07 | 0.20 | 0.22 | 54 | 5.61 | 1.31 | 1.23 | 2.00 | 1.24 | 1.57 | 0.90 |
| 19 | 0.21 | 0.04 | 0.10 | 0.08 | 0.08 | 0.21 | 0.23 | 55 | 6.16 | 1.41 | 1.36 | 2.20 | 1.42 | 1.78 | 1.05 |
| 20 | 0.24 | 0.04 | 0.11 | 0.09 | 0.08 | 0.22 | 0.24 | 56 | 6.76 | 1.51 | 1.51 | 2.42 | 1.62 | 2.01 | 1.21 |
| 21 | 0.26 | 0.05 | 0.12 | 0.11 | 0.09 | 0.24 | 0.25 | 57 | 7.42 | 1.62 | 1.66 | 2.66 | 1.84 | 2.26 | 1.39 |
| 22 | 0.28 | 0.06 | 0.13 | 0.13 | 0.09 | 0.25 | 0.25 | 58 | 8.15 | 1.73 | 1.82 | 2.90 | 2.06 | 2.52 | 1.60 |
| 23 | 0.31 | 0.08 | 0.14 | 0.15 | 0.10 | 0.26 | 0.26 | 59 | 8.94 | 1.85 | 2.01 | 3.14 | 2.28 | 2.82 | 1.83 |
| 24 | 0.34 | 0.09 | 0.16 | 0.18 | 0.11 | 0.27 | 0.27 | 60 | 9.82 | 1.98 | 2.20 | 3.39 | 2.52 | 3.13 | 2.09 |
| 25 | 0.38 | 0.10 | 0.17 | 0.20 | 0.12 | 0.28 | 0.27 | 61 | 10.78 | 2.12 | 2.41 | 3.63 | 2.80 | 3.46 | 2.39 |
| 26 | 0.41 | 0.12 | 0.19 | 0.23 | 0.13 | 0.29 | 0.27 | 62 | 11.83 | 2.28 | 2.64 | 3.87 | 3.12 | 3.80 | 2.73 |
| 27 | 0.45 | 0.13 | 0.20 | 0.26 | 0.14 | 0.30 | 0.27 | 63 | 12.99 | 2.46 | 2.89 | 4.10 | 3.45 | 4.15 | 3.11 |
| 28 | 0.50 | 0.15 | 0.22 | 0.29 | 0.15 | 0.31 | 0.27 | 64 | 14.26 | 2.67 | 3.14 | 4.28 | 3.74 | 4.48 | 3.52 |
| 29 | 0.55 | 0.17 | 0.23 | 0.33 | 0.16 | 0.32 | 0.27 | 65 | 15.65 | 2.87 | 3.37 | 4.39 | 3.97 | 4.78 | 3.96 |
| 30 | 0.60 | 0.19 | 0.25 | 0.37 | 0.18 | 0.32 | 0.27 | 66 | 17.18 | 3.07 | 3.57 | 4.41 | 4.12 | 5.01 | 4.39 |
| 31 | 0.66 | 0.21 | 0.26 | 0.40 | 0.20 | 0.33 | 0.26 | 67 | 18.86 | 3.23 | 3.72 | 4.31 | 4.22 | 5.15 | 4.78 |
| 32 | 0.72 | 0.24 | 0.28 | 0.44 | 0.23 | 0.34 | 0.26 | 68 | 20.71 | 3.35 | 3.80 | 4.14 | 4.33 | 5.16 | 5.10 |
| 33 | 0.79 | 0.26 | 0.29 | 0.48 | 0.26 | 0.34 | 0.25 | 69 | 22.73 | 3.44 | 3.80 | 3.92 | 4.44 | 5.04 | 5.31 |
| 34 | 0.87 | 0.28 | 0.31 | 0.52 | 0.30 | 0.35 | 0.24 | 70 | 24.95 | 3.49 | 3.73 | 3.67 | 4.51 | 4.78 | 5.36 |
| 35 | 0.95 | 0.31 | 0.33 | 0.56 | 0.34 | 0.35 | 0.23 | 71 | 27.39 | 3.51 | 3.59 | 3.38 | 4.46 | 4.39 | 5.22 |
| 36 | 1.05 | 0.33 | 0.34 | 0.59 | 0.39 | 0.36 | 0.22 | 72 | 30.07 | 3.46 | 3.36 | 3.03 | 4.19 | 3.87 | 4.88 |

Table J.4 Extended PSD Data from External Lab – Beatrice West (Part 1 of 3)

| Channel Number | Lower diameter (µm) | 240428 | 240502 | 240504 | 240507 | 240524 | 240531 | 240616 | Channel Number | Lower diameter (µm) | 240428 | 240502 | 240504 | 240507 | 240524 | 240531 | 240616 |
|---|---|---|---|---|---|---|---|---|---|---|---|---|---|---|---|---|---|
| | | Differential volume (%) | | | | | | | | | Differential volume (%) | | | | | | |
| 1 | 0.04 | 0.00 | 0.00 | 0.00 | 0.02 | 0.00 | 0.00 | 0.00 | 37 | 1.15 | 0.93 | 1.09 | 0.82 | 0.55 | 0.38 | 0.38 | 0.24 |
| 2 | 0.04 | 0.00 | 0.00 | 0.00 | 0.02 | 0.00 | 0.00 | 0.00 | 38 | 1.26 | 0.97 | 1.15 | 0.87 | 0.60 | 0.42 | 0.43 | 0.27 |
| 3 | 0.05 | 0.00 | 0.00 | 0.00 | 0.02 | 0.00 | 0.00 | 0.00 | 39 | 1.39 | 1.01 | 1.21 | 0.93 | 0.66 | 0.46 | 0.47 | 0.29 |
| 4 | 0.05 | 0.00 | 0.00 | 0.00 | 0.02 | 0.00 | 0.00 | 0.00 | 40 | 1.52 | 1.05 | 1.26 | 1.00 | 0.72 | 0.50 | 0.51 | 0.32 |
| 5 | 0.06 | 0.00 | 0.00 | 0.00 | 0.03 | 0.00 | 0.00 | 0.00 | 41 | 1.67 | 1.09 | 1.32 | 1.07 | 0.79 | 0.53 | 0.56 | 0.35 |
| 6 | 0.06 | 0.00 | 0.00 | 0.00 | 0.03 | 0.00 | 0.00 | 0.00 | 42 | 1.83 | 1.14 | 1.39 | 1.14 | 0.87 | 0.57 | 0.61 | 0.38 |
| 7 | 0.07 | 0.00 | 0.00 | 0.00 | 0.03 | 0.00 | 0.00 | 0.00 | 43 | 2.01 | 1.20 | 1.46 | 1.23 | 0.95 | 0.61 | 0.67 | 0.40 |
| 8 | 0.08 | 0.00 | 0.00 | 0.00 | 0.04 | 0.00 | 0.00 | 0.00 | 44 | 2.21 | 1.27 | 1.55 | 1.33 | 1.05 | 0.64 | 0.72 | 0.43 |
| 9 | 0.08 | 0.00 | 0.00 | 0.00 | 0.04 | 0.00 | 0.00 | 0.00 | 45 | 2.42 | 1.36 | 1.65 | 1.44 | 1.15 | 0.68 | 0.78 | 0.46 |
| 10 | 0.09 | 0.00 | 0.00 | 0.00 | 0.04 | 0.00 | 0.00 | 0.00 | 46 | 2.66 | 1.46 | 1.76 | 1.57 | 1.26 | 0.72 | 0.83 | 0.48 |
| 11 | 0.10 | 0.00 | 0.00 | 0.01 | 0.05 | 0.00 | 0.00 | 0.00 | 47 | 2.92 | 1.59 | 1.90 | 1.71 | 1.39 | 0.75 | 0.89 | 0.51 |
| 12 | 0.11 | 0.00 | 0.00 | 0.01 | 0.05 | 0.00 | 0.00 | 0.00 | 48 | 3.21 | 1.73 | 2.06 | 1.87 | 1.52 | 0.79 | 0.96 | 0.53 |
| 13 | 0.12 | 0.00 | 0.00 | 0.02 | 0.06 | 0.00 | 0.00 | 0.00 | 49 | 3.52 | 1.88 | 2.23 | 2.04 | 1.67 | 0.84 | 1.02 | 0.56 |
| 14 | 0.13 | 0.00 | 0.00 | 0.03 | 0.06 | 0.00 | 0.00 | 0.00 | 50 | 3.86 | 2.05 | 2.41 | 2.22 | 1.83 | 0.89 | 1.10 | 0.60 |
| 15 | 0.15 | 0.00 | 0.00 | 0.04 | 0.07 | 0.00 | 0.00 | 0.00 | 51 | 4.24 | 2.23 | 2.61 | 2.41 | 2.01 | 0.94 | 1.17 | 0.63 |
| 16 | 0.16 | 0.01 | 0.01 | 0.05 | 0.08 | 0.00 | 0.00 | 0.00 | 52 | 4.66 | 2.40 | 2.80 | 2.61 | 2.21 | 1.01 | 1.25 | 0.68 |
| 17 | 0.18 | 0.02 | 0.01 | 0.06 | 0.08 | 0.00 | 0.01 | 0.00 | 53 | 5.11 | 2.58 | 2.99 | 2.81 | 2.42 | 1.09 | 1.34 | 0.73 |
| 18 | 0.20 | 0.04 | 0.03 | 0.08 | 0.09 | 0.00 | 0.01 | 0.00 | 54 | 5.61 | 2.74 | 3.17 | 3.01 | 2.66 | 1.18 | 1.44 | 0.79 |
| 19 | 0.21 | 0.06 | 0.05 | 0.10 | 0.10 | 0.00 | 0.01 | 0.00 | 55 | 6.16 | 2.88 | 3.33 | 3.19 | 2.92 | 1.29 | 1.55 | 0.86 |
| 20 | 0.24 | 0.09 | 0.07 | 0.12 | 0.11 | 0.01 | 0.02 | 0.00 | 56 | 6.76 | 3.01 | 3.46 | 3.37 | 3.21 | 1.41 | 1.66 | 0.95 |
| 21 | 0.26 | 0.12 | 0.10 | 0.15 | 0.12 | 0.01 | 0.02 | 0.00 | 57 | 7.42 | 3.12 | 3.56 | 3.53 | 3.52 | 1.55 | 1.79 | 1.05 |
| 22 | 0.28 | 0.16 | 0.14 | 0.18 | 0.13 | 0.02 | 0.03 | 0.01 | 58 | 8.15 | 3.20 | 3.63 | 3.67 | 3.86 | 1.71 | 1.92 | 1.17 |
| 23 | 0.31 | 0.20 | 0.18 | 0.21 | 0.15 | 0.03 | 0.04 | 0.01 | 59 | 8.94 | 3.27 | 3.66 | 3.78 | 4.24 | 1.88 | 2.06 | 1.30 |
| 24 | 0.34 | 0.25 | 0.23 | 0.24 | 0.16 | 0.04 | 0.05 | 0.01 | 60 | 9.82 | 3.30 | 3.64 | 3.85 | 4.66 | 2.07 | 2.21 | 1.45 |
| 25 | 0.38 | 0.30 | 0.28 | 0.28 | 0.18 | 0.05 | 0.06 | 0.02 | 61 | 10.78 | 3.32 | 3.58 | 3.88 | 5.11 | 2.26 | 2.35 | 1.62 |
| 26 | 0.41 | 0.35 | 0.34 | 0.31 | 0.20 | 0.06 | 0.08 | 0.03 | 62 | 11.83 | 3.33 | 3.50 | 3.87 | 5.61 | 2.47 | 2.50 | 1.80 |
| 27 | 0.45 | 0.41 | 0.40 | 0.35 | 0.21 | 0.08 | 0.09 | 0.04 | 63 | 12.99 | 3.35 | 3.40 | 3.83 | 6.16 | 2.69 | 2.64 | 1.99 |
| 28 | 0.50 | 0.47 | 0.47 | 0.39 | 0.24 | 0.10 | 0.11 | 0.05 | 64 | 14.26 | 3.37 | 3.27 | 3.74 | 6.76 | 2.90 | 2.78 | 2.19 |
| 29 | 0.55 | 0.53 | 0.54 | 0.44 | 0.26 | 0.12 | 0.13 | 0.07 | 65 | 15.65 | 3.36 | 3.09 | 3.58 | 7.42 | 3.12 | 2.91 | 2.41 |
| 30 | 0.60 | 0.59 | 0.61 | 0.48 | 0.28 | 0.15 | 0.16 | 0.08 | 66 | 17.18 | 3.30 | 2.87 | 3.35 | 8.15 | 3.33 | 3.04 | 2.64 |
| 31 | 0.66 | 0.65 | 0.69 | 0.52 | 0.31 | 0.18 | 0.18 | 0.10 | 67 | 18.86 | 3.18 | 2.62 | 3.11 | 8.94 | 3.54 | 3.16 | 2.87 |
| 32 | 0.72 | 0.70 | 0.76 | 0.57 | 0.34 | 0.21 | 0.21 | 0.12 | 68 | 20.71 | 3.03 | 2.39 | 2.91 | 9.82 | 3.73 | 3.27 | 3.12 |
| 33 | 0.79 | 0.76 | 0.83 | 0.62 | 0.38 | 0.24 | 0.24 | 0.14 | 69 | 22.73 | 2.89 | 2.20 | 2.77 | 10.78 | 3.90 | 3.36 | 3.37 |
| 34 | 0.87 | 0.81 | 0.90 | 0.66 | 0.41 | 0.27 | 0.27 | 0.16 | 70 | 24.95 | 2.80 | 2.06 | 2.66 | 11.83 | 4.03 | 3.45 | 3.63 |
| 35 | 0.95 | 0.85 | 0.97 | 0.71 | 0.45 | 0.31 | 0.31 | 0.19 | 71 | 27.39 | 2.73 | 1.92 | 2.45 | 12.99 | 4.14 | 3.53 | 3.88 |
| 36 | 1.05 | 0.89 | 1.03 | 0.77 | 0.50 | 0.34 | 0.34 | 0.21 | 72 | 30.07 | 2.61 | 1.71 | 2.07 | 14.26 | 4.19 | 3.59 | 4.11 |

Table J.5 Extended PSD Data from External Lab – Beatrice West (Part 2 of 3)

| Channel Number | Lower diameter (µm) | 240701 | 240707 | 241031 | 241104 | 241109 | 241113 | 241119 | Channel Number | Lower diameter (µm) | 240701 | 240707 | 241031 | 241104 | 241109 | 241113 | 241119 |
|---|---|---|---|---|---|---|---|---|---|---|---|---|---|---|---|---|---|
| | | Differential volume (%) | | | | | | | | | Differential volume (%) | | | | | | |
| 1 | 0.04 | 0.00 | 0.00 | 0.00 | 0.00 | 0.00 | 0.00 | 0.00 | 37 | 1.15 | 0.28 | 0.78 | 0.46 | 0.51 | 0.55 | 0.42 | 0.60 |
| 2 | 0.04 | 0.00 | 0.00 | 0.00 | 0.00 | 0.00 | 0.00 | 0.00 | 38 | 1.26 | 0.32 | 0.82 | 0.48 | 0.55 | 0.56 | 0.43 | 0.61 |
| 3 | 0.05 | 0.00 | 0.00 | 0.00 | 0.00 | 0.00 | 0.00 | 0.00 | 39 | 1.39 | 0.37 | 0.87 | 0.50 | 0.58 | 0.57 | 0.44 | 0.62 |
| 4 | 0.05 | 0.00 | 0.00 | 0.00 | 0.00 | 0.00 | 0.00 | 0.00 | 40 | 1.52 | 0.41 | 0.92 | 0.53 | 0.62 | 0.58 | 0.46 | 0.64 |
| 5 | 0.06 | 0.00 | 0.00 | 0.01 | 0.00 | 0.00 | 0.01 | 0.00 | 41 | 1.67 | 0.46 | 0.97 | 0.57 | 0.66 | 0.59 | 0.49 | 0.66 |
| 6 | 0.06 | 0.00 | 0.00 | 0.01 | 0.00 | 0.00 | 0.01 | 0.00 | 42 | 1.83 | 0.52 | 1.03 | 0.62 | 0.71 | 0.61 | 0.52 | 0.69 |
| 7 | 0.07 | 0.00 | 0.00 | 0.02 | 0.00 | 0.00 | 0.02 | 0.00 | 43 | 2.01 | 0.57 | 1.10 | 0.68 | 0.76 | 0.64 | 0.57 | 0.73 |
| 8 | 0.08 | 0.00 | 0.00 | 0.03 | 0.00 | 0.00 | 0.03 | 0.00 | 44 | 2.21 | 0.62 | 1.17 | 0.76 | 0.82 | 0.67 | 0.63 | 0.78 |
| 9 | 0.08 | 0.00 | 0.00 | 0.03 | 0.01 | 0.00 | 0.03 | 0.00 | 45 | 2.42 | 0.68 | 1.26 | 0.85 | 0.88 | 0.71 | 0.71 | 0.84 |
| 10 | 0.09 | 0.00 | 0.00 | 0.04 | 0.01 | 0.00 | 0.04 | 0.00 | 46 | 2.66 | 0.73 | 1.36 | 0.97 | 0.96 | 0.77 | 0.81 | 0.92 |
| 11 | 0.10 | 0.00 | 0.01 | 0.05 | 0.01 | 0.00 | 0.05 | 0.00 | 47 | 2.92 | 0.78 | 1.48 | 1.11 | 1.04 | 0.83 | 0.92 | 1.02 |
| 12 | 0.11 | 0.00 | 0.01 | 0.06 | 0.02 | 0.00 | 0.06 | 0.00 | 48 | 3.21 | 0.83 | 1.61 | 1.26 | 1.13 | 0.92 | 1.06 | 1.14 |
| 13 | 0.12 | 0.00 | 0.02 | 0.07 | 0.02 | 0.01 | 0.07 | 0.00 | 49 | 3.52 | 0.87 | 1.76 | 1.43 | 1.23 | 1.02 | 1.21 | 1.28 |
| 14 | 0.13 | 0.00 | 0.02 | 0.08 | 0.03 | 0.01 | 0.09 | 0.01 | 50 | 3.86 | 0.91 | 1.92 | 1.63 | 1.34 | 1.13 | 1.39 | 1.44 |
| 15 | 0.15 | 0.00 | 0.03 | 0.09 | 0.04 | 0.02 | 0.10 | 0.01 | 51 | 4.24 | 0.94 | 2.10 | 1.85 | 1.46 | 1.26 | 1.59 | 1.61 |
| 16 | 0.16 | 0.00 | 0.04 | 0.11 | 0.04 | 0.03 | 0.11 | 0.02 | 52 | 4.66 | 0.97 | 2.29 | 2.08 | 1.58 | 1.41 | 1.81 | 1.80 |
| 17 | 0.18 | 0.00 | 0.06 | 0.12 | 0.05 | 0.04 | 0.13 | 0.03 | 53 | 5.11 | 0.99 | 2.50 | 2.31 | 1.72 | 1.56 | 2.04 | 2.00 |
| 18 | 0.20 | 0.00 | 0.07 | 0.14 | 0.06 | 0.05 | 0.14 | 0.05 | 54 | 5.61 | 1.01 | 2.71 | 2.56 | 1.86 | 1.73 | 2.29 | 2.20 |
| 19 | 0.21 | 0.00 | 0.09 | 0.16 | 0.08 | 0.07 | 0.16 | 0.07 | 55 | 6.16 | 1.03 | 2.92 | 2.82 | 2.00 | 1.90 | 2.54 | 2.40 |
| 20 | 0.24 | 0.00 | 0.12 | 0.18 | 0.09 | 0.09 | 0.18 | 0.09 | 56 | 6.76 | 1.07 | 3.13 | 3.10 | 2.15 | 2.08 | 2.80 | 2.61 |
| 21 | 0.26 | 0.00 | 0.14 | 0.20 | 0.11 | 0.11 | 0.20 | 0.11 | 57 | 7.42 | 1.11 | 3.34 | 3.36 | 2.30 | 2.26 | 3.07 | 2.80 |
| 22 | 0.28 | 0.00 | 0.17 | 0.22 | 0.13 | 0.14 | 0.22 | 0.14 | 58 | 8.15 | 1.18 | 3.55 | 3.62 | 2.46 | 2.46 | 3.33 | 2.99 |
| 23 | 0.31 | 0.00 | 0.20 | 0.24 | 0.15 | 0.17 | 0.24 | 0.18 | 59 | 8.94 | 1.28 | 3.74 | 3.90 | 2.63 | 2.66 | 3.60 | 3.15 |
| 24 | 0.34 | 0.00 | 0.23 | 0.26 | 0.17 | 0.20 | 0.26 | 0.21 | 60 | 9.82 | 1.41 | 3.91 | 4.21 | 2.79 | 2.86 | 3.85 | 3.30 |
| 25 | 0.38 | 0.00 | 0.27 | 0.28 | 0.19 | 0.23 | 0.28 | 0.24 | 61 | 10.78 | 1.58 | 4.05 | 4.53 | 2.96 | 3.07 | 4.08 | 3.42 |
| 26 | 0.41 | 0.01 | 0.30 | 0.30 | 0.21 | 0.26 | 0.30 | 0.28 | 62 | 11.83 | 1.77 | 4.15 | 4.82 | 3.13 | 3.27 | 4.28 | 3.52 |
| 27 | 0.45 | 0.01 | 0.34 | 0.32 | 0.23 | 0.29 | 0.32 | 0.32 | 63 | 12.99 | 2.00 | 4.20 | 5.10 | 3.31 | 3.47 | 4.43 | 3.59 |
| 28 | 0.50 | 0.03 | 0.38 | 0.34 | 0.26 | 0.32 | 0.33 | 0.35 | 64 | 14.26 | 2.24 | 4.18 | 5.39 | 3.47 | 3.64 | 4.53 | 3.62 |
| 29 | 0.55 | 0.04 | 0.42 | 0.36 | 0.28 | 0.36 | 0.35 | 0.39 | 65 | 15.65 | 2.51 | 4.09 | 5.73 | 3.60 | 3.75 | 4.56 | 3.60 |
| 30 | 0.60 | 0.06 | 0.47 | 0.37 | 0.31 | 0.39 | 0.36 | 0.42 | 66 | 17.18 | 2.78 | 3.89 | 5.99 | 3.70 | 3.75 | 4.48 | 3.54 |
| 31 | 0.66 | 0.08 | 0.51 | 0.39 | 0.33 | 0.42 | 0.37 | 0.46 | 67 | 18.86 | 3.04 | 3.60 | 5.94 | 3.74 | 3.61 | 4.29 | 3.44 |
| 32 | 0.72 | 0.10 | 0.55 | 0.40 | 0.36 | 0.45 | 0.38 | 0.49 | 68 | 20.71 | 3.30 | 3.24 | 5.35 | 3.72 | 3.31 | 4.03 | 3.31 |
| 33 | 0.79 | 0.13 | 0.60 | 0.42 | 0.39 | 0.47 | 0.39 | 0.52 | 69 | 22.73 | 3.55 | 2.85 | 4.20 | 3.63 | 2.90 | 3.75 | 3.14 |
| 34 | 0.87 | 0.16 | 0.64 | 0.43 | 0.42 | 0.50 | 0.40 | 0.54 | 70 | 24.95 | 3.79 | 2.46 | 2.69 | 3.47 | 2.47 | 3.48 | 2.90 |
| 35 | 0.95 | 0.20 | 0.69 | 0.44 | 0.45 | 0.52 | 0.41 | 0.56 | 71 | 27.39 | 4.00 | 2.11 | 1.34 | 3.23 | 2.11 | 3.24 | 2.58 |
| 36 | 1.05 | 0.24 | 0.73 | 0.45 | 0.48 | 0.53 | 0.41 | 0.58 | 72 | 30.07 | 4.16 | 1.79 | 0.48 | 2.94 | 1.87 | 2.97 | 2.22 |

Table J.6 Extended PSD Data from External Lab – Beatrice West (Part 3 of 3)

| Channel Number | Lower diameter (µm) | 250402 | 250520 | 250527 | 250602 | 250604 | Channel Number | Lower diameter (µm) | 250402 | 250520 | 250527 | 250602 | 250604 |
|---|---|---|---|---|---|---|---|---|---|---|---|---|---|
| | | Differential volume (%) | | | | | | | Differential volume (%) | | | | |
| 1 | 0.04 | 0.00 | 0.00 | 0.00 | 0.00 | 0.00 | 37 | 1.15 | 0.00 | 0.00 | 0.00 | 0.00 | 0.00 |
| 2 | 0.04 | 0.00 | 0.00 | 0.00 | 0.00 | 0.00 | 38 | 1.26 | 0.00 | 0.00 | 0.00 | 0.00 | 0.00 |
| 3 | 0.05 | 0.00 | 0.00 | 0.00 | 0.00 | 0.00 | 39 | 1.39 | 0.00 | 0.00 | 0.00 | 0.00 | 0.00 |
| 4 | 0.05 | 0.00 | 0.00 | 0.00 | 0.00 | 0.00 | 40 | 1.52 | 0.00 | 0.00 | 0.00 | 0.00 | 0.00 |
| 5 | 0.06 | 0.00 | 0.00 | 0.00 | 0.00 | 0.00 | 41 | 1.67 | 0.00 | 0.00 | 0.00 | 0.00 | 0.00 |
| 6 | 0.06 | 0.00 | 0.01 | 0.00 | 0.00 | 0.00 | 42 | 1.83 | 0.00 | 0.01 | 0.00 | 0.00 | 0.00 |
| 7 | 0.07 | 0.00 | 0.01 | 0.00 | 0.00 | 0.00 | 43 | 2.01 | 0.00 | 0.01 | 0.00 | 0.00 | 0.00 |
| 8 | 0.08 | 0.00 | 0.01 | 0.01 | 0.00 | 0.00 | 44 | 2.21 | 0.00 | 0.01 | 0.01 | 0.00 | 0.00 |
| 9 | 0.08 | 0.00 | 0.02 | 0.01 | 0.00 | 0.00 | 45 | 2.42 | 0.00 | 0.02 | 0.01 | 0.00 | 0.00 |
| 10 | 0.09 | 0.00 | 0.02 | 0.01 | 0.00 | 0.00 | 46 | 2.66 | 0.00 | 0.02 | 0.01 | 0.00 | 0.00 |
| 11 | 0.10 | 0.01 | 0.03 | 0.01 | 0.00 | 0.01 | 47 | 2.92 | 0.01 | 0.03 | 0.01 | 0.00 | 0.01 |
| 12 | 0.11 | 0.02 | 0.04 | 0.01 | 0.00 | 0.01 | 48 | 3.21 | 0.02 | 0.04 | 0.01 | 0.00 | 0.01 |
| 13 | 0.12 | 0.02 | 0.05 | 0.01 | 0.00 | 0.02 | 49 | 3.52 | 0.02 | 0.05 | 0.01 | 0.00 | 0.02 |
| 14 | 0.13 | 0.03 | 0.06 | 0.01 | 0.00 | 0.03 | 50 | 3.86 | 0.03 | 0.06 | 0.01 | 0.00 | 0.03 |
| 15 | 0.15 | 0.05 | 0.07 | 0.02 | 0.01 | 0.04 | 51 | 4.24 | 0.05 | 0.07 | 0.02 | 0.01 | 0.04 |
| 16 | 0.16 | 0.06 | 0.09 | 0.02 | 0.02 | 0.05 | 52 | 4.66 | 0.06 | 0.09 | 0.02 | 0.02 | 0.05 |
| 17 | 0.18 | 0.08 | 0.10 | 0.02 | 0.03 | 0.07 | 53 | 5.11 | 0.08 | 0.10 | 0.02 | 0.03 | 0.07 |
| 18 | 0.20 | 0.10 | 0.12 | 0.02 | 0.05 | 0.09 | 54 | 5.61 | 0.10 | 0.12 | 0.02 | 0.05 | 0.09 |
| 19 | 0.21 | 0.13 | 0.14 | 0.03 | 0.08 | 0.12 | 55 | 6.16 | 0.13 | 0.14 | 0.03 | 0.08 | 0.12 |
| 20 | 0.24 | 0.16 | 0.16 | 0.03 | 0.11 | 0.15 | 56 | 6.76 | 0.16 | 0.16 | 0.03 | 0.11 | 0.15 |
| 21 | 0.26 | 0.20 | 0.19 | 0.04 | 0.14 | 0.18 | 57 | 7.42 | 0.20 | 0.19 | 0.04 | 0.14 | 0.18 |
| 22 | 0.28 | 0.24 | 0.22 | 0.04 | 0.19 | 0.22 | 58 | 8.15 | 0.24 | 0.22 | 0.04 | 0.19 | 0.22 |
| 23 | 0.31 | 0.28 | 0.24 | 0.05 | 0.23 | 0.25 | 59 | 8.94 | 0.28 | 0.24 | 0.05 | 0.23 | 0.25 |
| 24 | 0.34 | 0.32 | 0.27 | 0.06 | 0.28 | 0.29 | 60 | 9.82 | 0.32 | 0.27 | 0.06 | 0.28 | 0.29 |
| 25 | 0.38 | 0.37 | 0.30 | 0.06 | 0.34 | 0.33 | 61 | 10.78 | 0.37 | 0.30 | 0.06 | 0.34 | 0.33 |
| 26 | 0.41 | 0.42 | 0.32 | 0.07 | 0.39 | 0.36 | 62 | 11.83 | 0.42 | 0.32 | 0.07 | 0.39 | 0.36 |
| 27 | 0.45 | 0.48 | 0.35 | 0.08 | 0.45 | 0.40 | 63 | 12.99 | 0.48 | 0.35 | 0.08 | 0.45 | 0.40 |
| 28 | 0.50 | 0.54 | 0.37 | 0.09 | 0.52 | 0.43 | 64 | 14.26 | 0.54 | 0.37 | 0.09 | 0.52 | 0.43 |
| 29 | 0.55 | 0.60 | 0.40 | 0.10 | 0.58 | 0.46 | 65 | 15.65 | 0.60 | 0.40 | 0.10 | 0.58 | 0.46 |
| 30 | 0.60 | 0.66 | 0.42 | 0.12 | 0.64 | 0.48 | 66 | 17.18 | 0.66 | 0.42 | 0.12 | 0.64 | 0.48 |
| 31 | 0.66 | 0.73 | 0.44 | 0.13 | 0.71 | 0.50 | 67 | 18.86 | 0.73 | 0.44 | 0.13 | 0.71 | 0.50 |
| 32 | 0.72 | 0.80 | 0.46 | 0.14 | 0.77 | 0.51 | 68 | 20.71 | 0.80 | 0.46 | 0.14 | 0.77 | 0.51 |
| 33 | 0.79 | 0.87 | 0.48 | 0.15 | 0.83 | 0.51 | 69 | 22.73 | 0.87 | 0.48 | 0.15 | 0.83 | 0.51 |
| 34 | 0.87 | 0.95 | 0.50 | 0.17 | 0.89 | 0.51 | 70 | 24.95 | 0.95 | 0.50 | 0.17 | 0.89 | 0.51 |
| 35 | 0.95 | 1.03 | 0.51 | 0.18 | 0.94 | 0.50 | 71 | 27.39 | 1.03 | 0.51 | 0.18 | 0.94 | 0.50 |
| 36 | 1.05 | 1.11 | 0.53 | 0.19 | 1.00 | 0.48 | 72 | 30.07 | 1.11 | 0.53 | 0.19 | 1.00 | 0.48 |

## Table J.7 Extended PSD Data from External Lab – Cornhusker (Part 1 of 2)

| Channel Number | Lower diameter (µm) | 240324 | 240407 | 240416 | 240428 | 240502 | 240504 | 240524 | Channel Number | Lower diameter (µm) | 240324 | 240407 | 240416 | 240428 | 240502 | 240504 | 240524 |
|---|---|---|---|---|---|---|---|---|---|---|---|---|---|---|---|---|---|
| | | Differential volume (%) | | | | | | | | | Differential volume (%) | | | | | | |
| 1 | 0.04 | 0.00 | 0.00 | 0.00 | 0.00 | 0.00 | 0.00 | 0.00 | 37 | 1.15 | 0.42 | 0.56 | 0.39 | 0.81 | 0.59 | 0.46 | 0.21 |
| 2 | 0.04 | 0.00 | 0.00 | 0.00 | 0.00 | 0.00 | 0.00 | 0.00 | 38 | 1.26 | 0.43 | 0.58 | 0.39 | 0.87 | 0.62 | 0.48 | 0.22 |
| 3 | 0.05 | 0.00 | 0.00 | 0.00 | 0.00 | 0.00 | 0.00 | 0.00 | 39 | 1.39 | 0.44 | 0.61 | 0.39 | 0.92 | 0.66 | 0.50 | 0.24 |
| 4 | 0.05 | 0.01 | 0.00 | 0.01 | 0.00 | 0.00 | 0.00 | 0.00 | 40 | 1.52 | 0.45 | 0.63 | 0.38 | 0.99 | 0.70 | 0.53 | 0.25 |
| 5 | 0.06 | 0.01 | 0.00 | 0.02 | 0.00 | 0.00 | 0.01 | 0.00 | 41 | 1.67 | 0.46 | 0.66 | 0.38 | 1.06 | 0.75 | 0.55 | 0.26 |
| 6 | 0.06 | 0.02 | 0.00 | 0.03 | 0.00 | 0.00 | 0.02 | 0.00 | 42 | 1.83 | 0.48 | 0.70 | 0.38 | 1.14 | 0.80 | 0.59 | 0.27 |
| 7 | 0.07 | 0.04 | 0.00 | 0.04 | 0.01 | 0.01 | 0.03 | 0.00 | 43 | 2.01 | 0.50 | 0.74 | 0.38 | 1.23 | 0.86 | 0.62 | 0.28 |
| 8 | 0.08 | 0.05 | 0.00 | 0.06 | 0.01 | 0.01 | 0.04 | 0.00 | 44 | 2.21 | 0.53 | 0.80 | 0.39 | 1.34 | 0.93 | 0.67 | 0.29 |
| 9 | 0.08 | 0.06 | 0.00 | 0.07 | 0.01 | 0.01 | 0.05 | 0.00 | 45 | 2.42 | 0.56 | 0.87 | 0.41 | 1.46 | 1.01 | 0.73 | 0.31 |
| 10 | 0.09 | 0.07 | 0.00 | 0.08 | 0.02 | 0.02 | 0.06 | 0.00 | 46 | 2.66 | 0.61 | 0.96 | 0.45 | 1.60 | 1.10 | 0.79 | 0.32 |
| 11 | 0.10 | 0.08 | 0.00 | 0.10 | 0.03 | 0.02 | 0.07 | 0.00 | 47 | 2.92 | 0.66 | 1.06 | 0.49 | 1.76 | 1.21 | 0.88 | 0.33 |
| 12 | 0.11 | 0.09 | 0.01 | 0.11 | 0.03 | 0.03 | 0.08 | 0.00 | 48 | 3.21 | 0.74 | 1.19 | 0.56 | 1.93 | 1.33 | 0.97 | 0.34 |
| 13 | 0.12 | 0.10 | 0.01 | 0.12 | 0.04 | 0.04 | 0.09 | 0.01 | 49 | 3.52 | 0.82 | 1.34 | 0.64 | 2.12 | 1.47 | 1.08 | 0.35 |
| 14 | 0.13 | 0.12 | 0.02 | 0.14 | 0.05 | 0.04 | 0.10 | 0.01 | 50 | 3.86 | 0.93 | 1.51 | 0.75 | 2.32 | 1.63 | 1.21 | 0.37 |
| 15 | 0.15 | 0.13 | 0.03 | 0.15 | 0.06 | 0.05 | 0.11 | 0.02 | 51 | 4.24 | 1.05 | 1.69 | 0.88 | 2.53 | 1.79 | 1.36 | 0.38 |
| 16 | 0.16 | 0.14 | 0.04 | 0.16 | 0.08 | 0.07 | 0.12 | 0.02 | 52 | 4.66 | 1.19 | 1.90 | 1.04 | 2.74 | 1.98 | 1.52 | 0.41 |
| 17 | 0.18 | 0.15 | 0.05 | 0.18 | 0.10 | 0.08 | 0.13 | 0.03 | 53 | 5.11 | 1.35 | 2.13 | 1.23 | 2.95 | 2.17 | 1.70 | 0.43 |
| 18 | 0.20 | 0.16 | 0.07 | 0.19 | 0.11 | 0.09 | 0.14 | 0.03 | 54 | 5.61 | 1.52 | 2.37 | 1.45 | 3.16 | 2.37 | 1.90 | 0.47 |
| 19 | 0.21 | 0.18 | 0.08 | 0.20 | 0.14 | 0.11 | 0.16 | 0.04 | 55 | 6.16 | 1.70 | 2.63 | 1.70 | 3.34 | 2.57 | 2.11 | 0.51 |
| 20 | 0.24 | 0.19 | 0.10 | 0.22 | 0.16 | 0.13 | 0.17 | 0.05 | 56 | 6.76 | 1.90 | 2.89 | 1.97 | 3.51 | 2.78 | 2.33 | 0.56 |
| 21 | 0.26 | 0.21 | 0.13 | 0.23 | 0.19 | 0.15 | 0.18 | 0.05 | 57 | 7.42 | 2.12 | 3.16 | 2.28 | 3.66 | 2.99 | 2.57 | 0.62 |
| 22 | 0.28 | 0.22 | 0.15 | 0.25 | 0.22 | 0.17 | 0.20 | 0.06 | 58 | 8.15 | 2.34 | 3.43 | 2.61 | 3.79 | 3.20 | 2.82 | 0.70 |
| 23 | 0.31 | 0.23 | 0.18 | 0.26 | 0.25 | 0.19 | 0.22 | 0.07 | 59 | 8.94 | 2.58 | 3.70 | 2.98 | 3.87 | 3.41 | 3.08 | 0.78 |
| 24 | 0.34 | 0.25 | 0.21 | 0.28 | 0.28 | 0.21 | 0.23 | 0.07 | 60 | 9.82 | 2.83 | 3.96 | 3.37 | 3.92 | 3.61 | 3.34 | 0.88 |
| 25 | 0.38 | 0.26 | 0.23 | 0.29 | 0.32 | 0.24 | 0.25 | 0.08 | 61 | 10.78 | 3.08 | 4.19 | 3.78 | 3.91 | 3.79 | 3.61 | 1.00 |
| 26 | 0.41 | 0.28 | 0.26 | 0.31 | 0.35 | 0.26 | 0.27 | 0.09 | 62 | 11.83 | 3.35 | 4.37 | 4.20 | 3.87 | 3.95 | 3.88 | 1.13 |
| 27 | 0.45 | 0.29 | 0.30 | 0.32 | 0.39 | 0.29 | 0.28 | 0.10 | 63 | 12.99 | 3.60 | 4.50 | 4.61 | 3.78 | 4.08 | 4.13 | 1.27 |
| 28 | 0.50 | 0.31 | 0.33 | 0.33 | 0.43 | 0.32 | 0.30 | 0.11 | 64 | 14.26 | 3.83 | 4.58 | 4.97 | 3.64 | 4.17 | 4.36 | 1.43 |
| 29 | 0.55 | 0.32 | 0.36 | 0.34 | 0.47 | 0.35 | 0.32 | 0.12 | 65 | 15.65 | 4.02 | 4.55 | 5.26 | 3.44 | 4.20 | 4.54 | 1.60 |
| 30 | 0.60 | 0.34 | 0.39 | 0.36 | 0.51 | 0.37 | 0.33 | 0.13 | 66 | 17.18 | 4.17 | 4.40 | 5.43 | 3.18 | 4.15 | 4.65 | 1.79 |
| 31 | 0.66 | 0.35 | 0.42 | 0.37 | 0.55 | 0.40 | 0.35 | 0.14 | 67 | 18.86 | 4.25 | 4.11 | 5.45 | 2.85 | 4.02 | 4.67 | 2.01 |
| 32 | 0.72 | 0.36 | 0.44 | 0.38 | 0.59 | 0.43 | 0.37 | 0.15 | 68 | 20.71 | 4.25 | 3.75 | 5.30 | 2.50 | 3.83 | 4.58 | 2.24 |
| 33 | 0.79 | 0.38 | 0.47 | 0.38 | 0.63 | 0.46 | 0.39 | 0.16 | 69 | 22.73 | 4.17 | 3.41 | 4.97 | 2.14 | 3.58 | 4.41 | 2.50 |
| 34 | 0.87 | 0.39 | 0.50 | 0.39 | 0.67 | 0.49 | 0.41 | 0.18 | 70 | 24.95 | 4.00 | 3.17 | 4.50 | 1.83 | 3.32 | 4.18 | 2.78 |
| 35 | 0.95 | 0.40 | 0.52 | 0.39 | 0.72 | 0.52 | 0.42 | 0.19 | 71 | 27.39 | 3.77 | 3.02 | 3.96 | 1.58 | 3.04 | 3.89 | 3.09 |
| 36 | 1.05 | 0.41 | 0.54 | 0.39 | 0.76 | 0.55 | 0.44 | 0.20 | 72 | 30.07 | 3.55 | 2.88 | 3.10 | 1.38 | 2.73 | 3.55 | 3.41 |

Table J.8 Extended PSD Data from External Lab – Cornhusker (Part 2 of 3)

| Channel Number | Lower diameter (μm) | 240531 | 240608 | 240616 | 240701 | 240814 | 240830 | 241022 | Channel Number | Lower diameter (μm) | 240531 | 240608 | 240616 | 240701 | 240814 | 240830 | 241022 |
|---|---|---|---|---|---|---|---|---|---|---|---|---|---|---|---|---|---|
| | | Differential volume (%) | | | | | | | | | Differential volume (%) | | | | | | |
| 1 | 0.04 | 0.00 | 0.00 | 0.00 | 0.00 | 0.00 | 0.00 | 0.00 | 37 | 1.15 | 0.30 | 0.57 | 0.21 | 0.32 | 0.25 | 0.21 | 0.57 |
| 2 | 0.04 | 0.00 | 0.00 | 0.00 | 0.00 | 0.00 | 0.00 | 0.00 | 38 | 1.26 | 0.32 | 0.60 | 0.22 | 0.34 | 0.27 | 0.23 | 0.60 |
| 3 | 0.05 | 0.00 | 0.00 | 0.00 | 0.00 | 0.00 | 0.00 | 0.00 | 39 | 1.39 | 0.33 | 0.62 | 0.24 | 0.35 | 0.30 | 0.26 | 0.64 |
| 4 | 0.05 | 0.00 | 0.00 | 0.00 | 0.00 | 0.00 | 0.00 | 0.00 | 40 | 1.52 | 0.35 | 0.66 | 0.25 | 0.37 | 0.32 | 0.28 | 0.69 |
| 5 | 0.06 | 0.00 | 0.01 | 0.00 | 0.00 | 0.00 | 0.00 | 0.00 | 41 | 1.67 | 0.36 | 0.69 | 0.26 | 0.38 | 0.35 | 0.31 | 0.76 |
| 6 | 0.06 | 0.00 | 0.01 | 0.00 | 0.00 | 0.00 | 0.00 | 0.00 | 42 | 1.83 | 0.37 | 0.73 | 0.27 | 0.40 | 0.37 | 0.34 | 0.83 |
| 7 | 0.07 | 0.00 | 0.01 | 0.00 | 0.00 | 0.00 | 0.00 | 0.01 | 43 | 2.01 | 0.39 | 0.78 | 0.28 | 0.41 | 0.40 | 0.36 | 0.92 |
| 8 | 0.08 | 0.00 | 0.02 | 0.00 | 0.00 | 0.00 | 0.00 | 0.01 | 44 | 2.21 | 0.40 | 0.83 | 0.29 | 0.42 | 0.42 | 0.39 | 1.02 |
| 9 | 0.08 | 0.00 | 0.03 | 0.00 | 0.00 | 0.00 | 0.00 | 0.01 | 45 | 2.42 | 0.41 | 0.90 | 0.31 | 0.43 | 0.45 | 0.41 | 1.15 |
| 10 | 0.09 | 0.00 | 0.03 | 0.00 | 0.00 | 0.00 | 0.00 | 0.02 | 46 | 2.66 | 0.42 | 0.97 | 0.32 | 0.44 | 0.47 | 0.43 | 1.29 |
| 11 | 0.10 | 0.00 | 0.04 | 0.00 | 0.00 | 0.00 | 0.00 | 0.02 | 47 | 2.92 | 0.43 | 1.07 | 0.33 | 0.45 | 0.50 | 0.45 | 1.45 |
| 12 | 0.11 | 0.01 | 0.05 | 0.00 | 0.01 | 0.00 | 0.00 | 0.03 | 48 | 3.21 | 0.45 | 1.18 | 0.34 | 0.47 | 0.52 | 0.47 | 1.62 |
| 13 | 0.12 | 0.01 | 0.06 | 0.01 | 0.01 | 0.00 | 0.00 | 0.04 | 49 | 3.52 | 0.46 | 1.30 | 0.35 | 0.48 | 0.55 | 0.49 | 1.82 |
| 14 | 0.13 | 0.02 | 0.06 | 0.01 | 0.02 | 0.00 | 0.00 | 0.05 | 50 | 3.86 | 0.48 | 1.45 | 0.37 | 0.50 | 0.58 | 0.50 | 2.02 |
| 15 | 0.15 | 0.03 | 0.07 | 0.02 | 0.03 | 0.00 | 0.00 | 0.06 | 51 | 4.24 | 0.51 | 1.61 | 0.38 | 0.53 | 0.61 | 0.52 | 2.23 |
| 16 | 0.16 | 0.04 | 0.09 | 0.02 | 0.04 | 0.00 | 0.00 | 0.07 | 52 | 4.66 | 0.54 | 1.78 | 0.41 | 0.56 | 0.65 | 0.54 | 2.44 |
| 17 | 0.18 | 0.05 | 0.10 | 0.03 | 0.05 | 0.00 | 0.00 | 0.09 | 53 | 5.11 | 0.58 | 1.97 | 0.43 | 0.60 | 0.69 | 0.56 | 2.65 |
| 18 | 0.20 | 0.06 | 0.11 | 0.03 | 0.06 | 0.01 | 0.00 | 0.10 | 54 | 5.61 | 0.63 | 2.16 | 0.47 | 0.65 | 0.74 | 0.59 | 2.85 |
| 19 | 0.21 | 0.07 | 0.13 | 0.04 | 0.08 | 0.01 | 0.00 | 0.12 | 55 | 6.16 | 0.69 | 2.37 | 0.51 | 0.71 | 0.80 | 0.63 | 3.04 |
| 20 | 0.24 | 0.08 | 0.14 | 0.05 | 0.09 | 0.01 | 0.00 | 0.14 | 56 | 6.76 | 0.77 | 2.58 | 0.56 | 0.78 | 0.88 | 0.68 | 3.21 |
| 21 | 0.26 | 0.09 | 0.16 | 0.05 | 0.10 | 0.02 | 0.00 | 0.17 | 57 | 7.42 | 0.86 | 2.79 | 0.62 | 0.88 | 0.96 | 0.75 | 3.36 |
| 22 | 0.28 | 0.10 | 0.18 | 0.06 | 0.11 | 0.02 | 0.01 | 0.19 | 58 | 8.15 | 0.97 | 3.00 | 0.70 | 0.99 | 1.06 | 0.84 | 3.49 |
| 23 | 0.31 | 0.11 | 0.20 | 0.07 | 0.12 | 0.03 | 0.01 | 0.22 | 59 | 8.94 | 1.10 | 3.21 | 0.78 | 1.12 | 1.18 | 0.96 | 3.59 |
| 24 | 0.34 | 0.12 | 0.23 | 0.07 | 0.13 | 0.04 | 0.01 | 0.24 | 60 | 9.82 | 1.24 | 3.41 | 0.88 | 1.26 | 1.31 | 1.10 | 3.66 |
| 25 | 0.38 | 0.13 | 0.25 | 0.08 | 0.14 | 0.04 | 0.02 | 0.27 | 61 | 10.78 | 1.41 | 3.59 | 1.00 | 1.43 | 1.45 | 1.27 | 3.69 |
| 26 | 0.41 | 0.15 | 0.27 | 0.09 | 0.16 | 0.05 | 0.02 | 0.29 | 62 | 11.83 | 1.59 | 3.75 | 1.13 | 1.62 | 1.61 | 1.47 | 3.69 |
| 27 | 0.45 | 0.16 | 0.30 | 0.10 | 0.17 | 0.06 | 0.03 | 0.32 | 63 | 12.99 | 1.79 | 3.89 | 1.27 | 1.82 | 1.77 | 1.70 | 3.67 |
| 28 | 0.50 | 0.17 | 0.32 | 0.11 | 0.18 | 0.08 | 0.04 | 0.34 | 64 | 14.26 | 2.01 | 3.99 | 1.43 | 2.05 | 1.95 | 1.95 | 3.62 |
| 29 | 0.55 | 0.19 | 0.35 | 0.12 | 0.20 | 0.09 | 0.05 | 0.37 | 65 | 15.65 | 2.24 | 4.05 | 1.60 | 2.29 | 2.14 | 2.23 | 3.53 |
| 30 | 0.60 | 0.20 | 0.38 | 0.13 | 0.21 | 0.11 | 0.07 | 0.39 | 66 | 17.18 | 2.49 | 4.05 | 1.79 | 2.55 | 2.35 | 2.55 | 3.38 |
| 31 | 0.66 | 0.22 | 0.40 | 0.14 | 0.23 | 0.12 | 0.08 | 0.41 | 67 | 18.86 | 2.76 | 3.97 | 2.01 | 2.84 | 2.55 | 2.89 | 3.18 |
| 32 | 0.72 | 0.23 | 0.43 | 0.15 | 0.25 | 0.14 | 0.10 | 0.44 | 68 | 20.71 | 3.04 | 3.85 | 2.24 | 3.15 | 2.77 | 3.26 | 2.95 |
| 33 | 0.79 | 0.24 | 0.46 | 0.16 | 0.26 | 0.16 | 0.12 | 0.46 | 69 | 22.73 | 3.33 | 3.70 | 2.50 | 3.48 | 2.98 | 3.64 | 2.71 |
| 34 | 0.87 | 0.26 | 0.49 | 0.18 | 0.28 | 0.18 | 0.14 | 0.48 | 70 | 24.95 | 3.63 | 3.56 | 2.78 | 3.81 | 3.20 | 4.04 | 2.50 |
| 35 | 0.95 | 0.27 | 0.51 | 0.19 | 0.29 | 0.20 | 0.16 | 0.51 | 71 | 27.39 | 3.93 | 3.44 | 3.09 | 4.15 | 3.42 | 4.42 | 2.31 |
| 36 | 1.05 | 0.29 | 0.54 | 0.20 | 0.31 | 0.22 | 0.18 | 0.53 | 72 | 30.07 | 4.21 | 3.29 | 3.41 | 4.49 | 3.62 | 4.75 | 2.13 |

Table J.9 Extended PSD Data from External Lab – Cornhusker (Part 3 of 3)

| Channel Number | Lower diameter (µm) | 241104 | 250315 | 250425 | 250520 | 250527 | 250602 | Channel Number | Lower diameter (µm) | 241104 | 250315 | 250425 | 250520 | 250527 | 250602 |
|---|---|---|---|---|---|---|---|---|---|---|---|---|---|---|---|
| | | Differential volume (%) | | | | | | | | Differential volume (%) | | | | | |
| 1 | 0.04 | 0.00 | 0.00 | 0.00 | 0.00 | 0.00 | 0.00 | 37 | 1.15 | 0.56 | 0.54 | 0.72 | 0.50 | 0.54 | 0.39 |
| 2 | 0.04 | 0.00 | 0.00 | 0.00 | 0.00 | 0.00 | 0.00 | 38 | 1.26 | 0.59 | 0.56 | 0.76 | 0.52 | 0.56 | 0.40 |
| 3 | 0.05 | 0.00 | 0.00 | 0.00 | 0.00 | 0.00 | 0.00 | 39 | 1.39 | 0.63 | 0.58 | 0.80 | 0.54 | 0.58 | 0.41 |
| 4 | 0.05 | 0.00 | 0.01 | 0.00 | 0.01 | 0.01 | 0.01 | 40 | 1.52 | 0.66 | 0.60 | 0.85 | 0.57 | 0.60 | 0.43 |
| 5 | 0.06 | 0.00 | 0.01 | 0.00 | 0.02 | 0.01 | 0.01 | 41 | 1.67 | 0.69 | 0.63 | 0.91 | 0.61 | 0.63 | 0.44 |
| 6 | 0.06 | 0.00 | 0.02 | 0.00 | 0.03 | 0.02 | 0.02 | 42 | 1.83 | 0.72 | 0.66 | 0.97 | 0.65 | 0.66 | 0.46 |
| 7 | 0.07 | 0.00 | 0.04 | 0.01 | 0.04 | 0.04 | 0.03 | 43 | 2.01 | 0.75 | 0.70 | 1.04 | 0.71 | 0.70 | 0.48 |
| 8 | 0.08 | 0.00 | 0.05 | 0.01 | 0.06 | 0.05 | 0.05 | 44 | 2.21 | 0.79 | 0.74 | 1.13 | 0.77 | 0.74 | 0.51 |
| 9 | 0.08 | 0.01 | 0.06 | 0.02 | 0.07 | 0.06 | 0.06 | 45 | 2.42 | 0.83 | 0.80 | 1.23 | 0.84 | 0.80 | 0.54 |
| 10 | 0.09 | 0.01 | 0.07 | 0.02 | 0.08 | 0.07 | 0.07 | 46 | 2.66 | 0.88 | 0.86 | 1.34 | 0.93 | 0.86 | 0.59 |
| 11 | 0.10 | 0.01 | 0.09 | 0.03 | 0.10 | 0.09 | 0.08 | 47 | 2.92 | 0.94 | 0.95 | 1.47 | 1.03 | 0.95 | 0.65 |
| 12 | 0.11 | 0.01 | 0.10 | 0.04 | 0.11 | 0.10 | 0.09 | 48 | 3.21 | 1.01 | 1.04 | 1.62 | 1.15 | 1.04 | 0.72 |
| 13 | 0.12 | 0.02 | 0.11 | 0.04 | 0.12 | 0.11 | 0.10 | 49 | 3.52 | 1.10 | 1.16 | 1.78 | 1.29 | 1.16 | 0.80 |
| 14 | 0.13 | 0.02 | 0.13 | 0.05 | 0.14 | 0.13 | 0.11 | 50 | 3.86 | 1.20 | 1.29 | 1.96 | 1.44 | 1.29 | 0.90 |
| 15 | 0.15 | 0.03 | 0.14 | 0.06 | 0.15 | 0.14 | 0.12 | 51 | 4.24 | 1.32 | 1.44 | 2.15 | 1.62 | 1.44 | 1.02 |
| 16 | 0.16 | 0.04 | 0.15 | 0.08 | 0.16 | 0.15 | 0.13 | 52 | 4.66 | 1.46 | 1.60 | 2.34 | 1.80 | 1.60 | 1.16 |
| 17 | 0.18 | 0.04 | 0.17 | 0.09 | 0.18 | 0.17 | 0.14 | 53 | 5.11 | 1.61 | 1.79 | 2.55 | 2.01 | 1.79 | 1.31 |
| 18 | 0.20 | 0.05 | 0.18 | 0.11 | 0.19 | 0.18 | 0.16 | 54 | 5.61 | 1.77 | 1.98 | 2.74 | 2.23 | 1.98 | 1.49 |
| 19 | 0.21 | 0.07 | 0.20 | 0.13 | 0.21 | 0.20 | 0.17 | 55 | 6.16 | 1.94 | 2.19 | 2.94 | 2.45 | 2.19 | 1.68 |
| 20 | 0.24 | 0.08 | 0.21 | 0.15 | 0.22 | 0.21 | 0.18 | 56 | 6.76 | 2.13 | 2.41 | 3.12 | 2.69 | 2.41 | 1.89 |
| 21 | 0.26 | 0.10 | 0.23 | 0.18 | 0.24 | 0.23 | 0.19 | 57 | 7.42 | 2.32 | 2.64 | 3.29 | 2.94 | 2.64 | 2.12 |
| 22 | 0.28 | 0.12 | 0.25 | 0.20 | 0.26 | 0.25 | 0.21 | 58 | 8.15 | 2.54 | 2.88 | 3.45 | 3.19 | 2.88 | 2.37 |
| 23 | 0.31 | 0.14 | 0.27 | 0.23 | 0.27 | 0.27 | 0.22 | 59 | 8.94 | 2.76 | 3.13 | 3.58 | 3.45 | 3.13 | 2.65 |
| 24 | 0.34 | 0.16 | 0.29 | 0.26 | 0.29 | 0.29 | 0.23 | 60 | 9.82 | 2.98 | 3.38 | 3.69 | 3.71 | 3.38 | 2.94 |
| 25 | 0.38 | 0.18 | 0.31 | 0.29 | 0.30 | 0.31 | 0.25 | 61 | 10.78 | 3.21 | 3.63 | 3.76 | 3.95 | 3.63 | 3.26 |
| 26 | 0.41 | 0.21 | 0.32 | 0.32 | 0.32 | 0.32 | 0.26 | 62 | 11.83 | 3.45 | 3.88 | 3.80 | 4.17 | 3.88 | 3.60 |
| 27 | 0.45 | 0.23 | 0.34 | 0.35 | 0.33 | 0.34 | 0.27 | 63 | 12.99 | 3.68 | 4.12 | 3.81 | 4.36 | 4.12 | 3.94 |
| 28 | 0.50 | 0.26 | 0.36 | 0.39 | 0.35 | 0.36 | 0.29 | 64 | 14.26 | 3.88 | 4.32 | 3.78 | 4.51 | 4.32 | 4.29 |
| 29 | 0.55 | 0.29 | 0.38 | 0.42 | 0.36 | 0.38 | 0.30 | 65 | 15.65 | 4.02 | 4.47 | 3.69 | 4.58 | 4.47 | 4.61 |
| 30 | 0.60 | 0.33 | 0.40 | 0.46 | 0.38 | 0.40 | 0.31 | 66 | 17.18 | 4.07 | 4.54 | 3.53 | 4.56 | 4.54 | 4.89 |
| 31 | 0.66 | 0.36 | 0.42 | 0.49 | 0.39 | 0.42 | 0.32 | 67 | 18.86 | 4.03 | 4.52 | 3.32 | 4.43 | 4.52 | 5.09 |
| 32 | 0.72 | 0.39 | 0.44 | 0.53 | 0.41 | 0.44 | 0.34 | 68 | 20.71 | 3.93 | 4.39 | 3.06 | 4.18 | 4.39 | 5.20 |
| 33 | 0.79 | 0.43 | 0.46 | 0.56 | 0.43 | 0.46 | 0.35 | 69 | 22.73 | 3.82 | 4.17 | 2.79 | 3.86 | 4.17 | 5.20 |
| 34 | 0.87 | 0.46 | 0.48 | 0.60 | 0.44 | 0.48 | 0.36 | 70 | 24.95 | 3.73 | 3.85 | 2.51 | 3.50 | 3.85 | 5.09 |
| 35 | 0.95 | 0.50 | 0.50 | 0.64 | 0.46 | 0.50 | 0.37 | 71 | 27.39 | 3.65 | 3.45 | 2.23 | 3.14 | 3.45 | 4.83 |
| 36 | 1.05 | 0.53 | 0.52 | 0.68 | 0.48 | 0.52 | 0.38 | 72 | 30.07 | 3.53 | 2.99 | 1.95 | 2.77 | 2.99 | 4.41 |

## Table J.10 Extended PSD Data from External Lab – Beatrice North (Part 1 of 2)

| Channel Number | Lower diameter (µm) | 240426 | 240428 | 240504 | 240507 | 240524 | 240531 | 240608 | 240616 | Channel Number | Lower diameter (µm) | 240426 | 240428 | 240504 | 240507 | 240524 | 240531 | 240608 | 240616 |
|---|---|---|---|---|---|---|---|---|---|---|---|---|---|---|---|---|---|---|---|
| | | Differential volume (%) | | | | | | | | | | Differential volume (%) | | | | | | | |
| 1 | 0.04 | 0.00 | 0.00 | 0.00 | 0.00 | 0.00 | 0.00 | 0.00 | 0.00 | 37 | 1.15 | 0.85 | 1.53 | 0.83 | 1.19 | 0.47 | 0.51 | 0.66 | 0.53 |
| 2 | 0.04 | 0.00 | 0.00 | 0.00 | 0.00 | 0.00 | 0.00 | 0.00 | 0.00 | 38 | 1.26 | 0.90 | 1.61 | 0.86 | 1.27 | 0.49 | 0.53 | 0.68 | 0.54 |
| 3 | 0.05 | 0.00 | 0.00 | 0.00 | 0.00 | 0.00 | 0.00 | 0.00 | 0.00 | 39 | 1.39 | 0.96 | 1.69 | 0.90 | 1.35 | 0.51 | 0.55 | 0.70 | 0.56 |
| 4 | 0.05 | 0.01 | 0.00 | 0.01 | 0.00 | 0.00 | 0.00 | 0.00 | 0.00 | 40 | 1.52 | 1.02 | 1.77 | 0.93 | 1.42 | 0.53 | 0.57 | 0.73 | 0.57 |
| 5 | 0.06 | 0.01 | 0.00 | 0.02 | 0.00 | 0.00 | 0.00 | 0.00 | 0.00 | 41 | 1.67 | 1.09 | 1.84 | 0.97 | 1.50 | 0.54 | 0.59 | 0.78 | 0.58 |
| 6 | 0.06 | 0.03 | 0.00 | 0.03 | 0.00 | 0.00 | 0.00 | 0.00 | 0.00 | 42 | 1.83 | 1.17 | 1.92 | 1.01 | 1.59 | 0.56 | 0.60 | 0.83 | 0.60 |
| 7 | 0.07 | 0.04 | 0.00 | 0.05 | 0.00 | 0.00 | 0.00 | 0.00 | 0.00 | 43 | 2.01 | 1.26 | 2.01 | 1.07 | 1.69 | 0.58 | 0.62 | 0.90 | 0.61 |
| 8 | 0.08 | 0.05 | 0.01 | 0.06 | 0.00 | 0.00 | 0.00 | 0.00 | 0.00 | 44 | 2.21 | 1.37 | 2.10 | 1.13 | 1.79 | 0.60 | 0.64 | 1.00 | 0.63 |
| 9 | 0.08 | 0.07 | 0.01 | 0.08 | 0.01 | 0.00 | 0.00 | 0.00 | 0.00 | 45 | 2.42 | 1.49 | 2.20 | 1.21 | 1.89 | 0.62 | 0.66 | 1.12 | 0.64 |
| 10 | 0.09 | 0.08 | 0.02 | 0.10 | 0.01 | 0.00 | 0.00 | 0.01 | 0.00 | 46 | 2.66 | 1.63 | 2.32 | 1.31 | 2.02 | 0.64 | 0.68 | 1.26 | 0.66 |
| 11 | 0.10 | 0.10 | 0.02 | 0.11 | 0.02 | 0.00 | 0.01 | 0.02 | 0.01 | 47 | 2.92 | 1.78 | 2.45 | 1.43 | 2.18 | 0.66 | 0.71 | 1.44 | 0.69 |
| 12 | 0.11 | 0.11 | 0.03 | 0.13 | 0.03 | 0.01 | 0.01 | 0.02 | 0.01 | 48 | 3.21 | 1.95 | 2.60 | 1.57 | 2.34 | 0.68 | 0.74 | 1.65 | 0.72 |
| 13 | 0.12 | 0.13 | 0.04 | 0.15 | 0.04 | 0.02 | 0.02 | 0.03 | 0.03 | 49 | 3.52 | 2.15 | 2.76 | 1.73 | 2.52 | 0.72 | 0.77 | 1.89 | 0.77 |
| 14 | 0.13 | 0.15 | 0.06 | 0.17 | 0.05 | 0.04 | 0.04 | 0.04 | 0.05 | 50 | 3.86 | 2.35 | 2.93 | 1.91 | 2.71 | 0.76 | 0.81 | 2.16 | 0.82 |
| 15 | 0.15 | 0.16 | 0.07 | 0.18 | 0.06 | 0.05 | 0.06 | 0.06 | 0.08 | 51 | 4.24 | 2.57 | 3.10 | 2.10 | 2.93 | 0.80 | 0.87 | 2.46 | 0.88 |
| 16 | 0.16 | 0.18 | 0.09 | 0.20 | 0.08 | 0.07 | 0.08 | 0.07 | 0.10 | 52 | 4.66 | 2.78 | 3.26 | 2.32 | 3.18 | 0.87 | 0.93 | 2.77 | 0.97 |
| 17 | 0.18 | 0.20 | 0.12 | 0.22 | 0.10 | 0.09 | 0.10 | 0.09 | 0.12 | 53 | 5.11 | 3.00 | 3.41 | 2.53 | 3.42 | 0.94 | 1.02 | 3.10 | 1.07 |
| 18 | 0.20 | 0.22 | 0.15 | 0.24 | 0.12 | 0.10 | 0.12 | 0.11 | 0.15 | 54 | 5.61 | 3.23 | 3.52 | 2.76 | 3.65 | 1.04 | 1.12 | 3.43 | 1.19 |
| 19 | 0.21 | 0.24 | 0.18 | 0.27 | 0.15 | 0.12 | 0.14 | 0.14 | 0.17 | 55 | 6.16 | 3.44 | 3.60 | 2.97 | 3.89 | 1.15 | 1.24 | 3.75 | 1.33 |
| 20 | 0.24 | 0.26 | 0.22 | 0.29 | 0.18 | 0.14 | 0.16 | 0.16 | 0.19 | 56 | 6.76 | 3.64 | 3.64 | 3.18 | 4.16 | 1.29 | 1.38 | 4.06 | 1.50 |
| 21 | 0.26 | 0.29 | 0.27 | 0.32 | 0.22 | 0.16 | 0.18 | 0.20 | 0.22 | 57 | 7.42 | 3.81 | 3.64 | 3.38 | 4.43 | 1.45 | 1.55 | 4.34 | 1.70 |
| 22 | 0.28 | 0.31 | 0.32 | 0.35 | 0.26 | 0.18 | 0.20 | 0.23 | 0.24 | 58 | 8.15 | 3.98 | 3.60 | 3.57 | 4.65 | 1.64 | 1.74 | 4.59 | 1.92 |
| 23 | 0.31 | 0.34 | 0.38 | 0.38 | 0.30 | 0.19 | 0.22 | 0.26 | 0.26 | 59 | 8.94 | 4.14 | 3.50 | 3.72 | 4.81 | 1.84 | 1.95 | 4.79 | 2.16 |
| 24 | 0.34 | 0.37 | 0.44 | 0.41 | 0.35 | 0.21 | 0.24 | 0.29 | 0.28 | 60 | 9.82 | 4.27 | 3.34 | 3.84 | 4.93 | 2.07 | 2.18 | 4.91 | 2.41 |
| 25 | 0.38 | 0.40 | 0.51 | 0.44 | 0.40 | 0.23 | 0.26 | 0.33 | 0.30 | 61 | 10.78 | 4.35 | 3.14 | 3.92 | 5.03 | 2.31 | 2.42 | 4.94 | 2.69 |

| Channel Number | Lower diameter (µm) | 240426 | 240428 | 240504 | 240507 | 240524 | 240531 | 240608 | 240616 | Channel Number | Lower diameter (µm) | 240426 | 240428 | 240504 | 240507 | 240524 | 240531 | 240608 | 240616 |
|---|---|---|---|---|---|---|---|---|---|---|---|---|---|---|---|---|---|---|---|
| | | Differential volume (%) | | | | | | | | | | Differential volume (%) | | | | | | | |
| 26 | 0.41 | 0.43 | 0.58 | 0.47 | 0.45 | 0.24 | 0.28 | 0.36 | 0.32 | 62 | 11.83 | 4.39 | 2.92 | 3.95 | 5.02 | 2.56 | 2.66 | 4.86 | 2.97 |
| 27 | 0.45 | 0.46 | 0.65 | 0.50 | 0.50 | 0.26 | 0.30 | 0.40 | 0.34 | 63 | 12.99 | 4.43 | 2.69 | 3.94 | 4.71 | 2.81 | 2.91 | 4.67 | 3.25 |
| 28 | 0.50 | 0.49 | 0.73 | 0.53 | 0.56 | 0.28 | 0.32 | 0.43 | 0.36 | 64 | 14.26 | 4.46 | 2.44 | 3.87 | 3.95 | 3.07 | 3.16 | 4.35 | 3.53 |
| 29 | 0.55 | 0.52 | 0.81 | 0.56 | 0.63 | 0.31 | 0.34 | 0.46 | 0.39 | 65 | 15.65 | 4.40 | 2.14 | 3.72 | 2.76 | 3.33 | 3.40 | 3.89 | 3.81 |
| 30 | 0.60 | 0.56 | 0.90 | 0.60 | 0.69 | 0.33 | 0.36 | 0.50 | 0.41 | 66 | 17.18 | 4.10 | 1.81 | 3.49 | 1.48 | 3.58 | 3.63 | 3.32 | 4.06 |
| 31 | 0.66 | 0.59 | 0.99 | 0.63 | 0.75 | 0.35 | 0.38 | 0.53 | 0.43 | 67 | 18.86 | 3.47 | 1.47 | 3.19 | 0.55 | 3.82 | 3.84 | 2.68 | 4.29 |
| 32 | 0.72 | 0.63 | 1.08 | 0.67 | 0.82 | 0.37 | 0.41 | 0.55 | 0.44 | 68 | 20.71 | 2.54 | 1.18 | 2.86 | 0.13 | 4.02 | 4.02 | 2.09 | 4.48 |
| 33 | 0.79 | 0.67 | 1.17 | 0.70 | 0.90 | 0.39 | 0.43 | 0.58 | 0.46 | 69 | 22.73 | 1.54 | 0.97 | 2.54 | 0.02 | 4.19 | 4.15 | 1.64 | 4.60 |
| 34 | 0.87 | 0.71 | 1.27 | 0.73 | 0.97 | 0.41 | 0.45 | 0.60 | 0.48 | 70 | 24.95 | 0.75 | 0.83 | 2.25 | 0.00 | 4.31 | 4.23 | 1.35 | 4.66 |
| 35 | 0.95 | 0.75 | 1.36 | 0.77 | 1.04 | 0.43 | 0.47 | 0.62 | 0.50 | 71 | 27.39 | 0.29 | 0.73 | 1.97 | 0.00 | 4.36 | 4.26 | 1.20 | 4.62 |
| 36 | 1.05 | 0.80 | 1.44 | 0.80 | 1.11 | 0.45 | 0.49 | 0.64 | 0.51 | 72 | 30.07 | 0.08 | 0.61 | 1.69 | 0.00 | 4.34 | 4.20 | 1.08 | 4.47 |

## Table J.11 Extended PSD Data from External Lab – Beatrice North (Part 2 of 2)

| Channel Number | Lower diameter (µm) | 240626 | 240814 | 240830 | 241022 | 241031 | 241109 | 241119 | 241214 | Channel Number | Lower diameter (µm) | 240626 | 240814 | 240830 | 241022 | 241031 | 241109 | 241119 | 241214 |
|---|---|---|---|---|---|---|---|---|---|---|---|---|---|---|---|---|---|---|---|
| | | Differential volume (%) | | | | | | | | | | Differential volume (%) | | | | | | | |
| 1 | 0.04 | 0.00 | 0.00 | 0.00 | 0.00 | 0.00 | 0.00 | 0.00 | 0.00 | 37 | 1.15 | 0.44 | 0.12 | 0.41 | 1.07 | 0.86 | 1.35 | 2.01 | 1.33 |
| 2 | 0.04 | 0.00 | 0.00 | 0.00 | 0.00 | 0.00 | 0.00 | 0.00 | 0.00 | 38 | 1.26 | 0.46 | 0.14 | 0.42 | 1.13 | 0.92 | 1.47 | 2.11 | 1.37 |
| 3 | 0.05 | 0.00 | 0.00 | 0.00 | 0.00 | 0.00 | 0.00 | 0.00 | 0.00 | 39 | 1.39 | 0.47 | 0.16 | 0.43 | 1.18 | 0.97 | 1.59 | 2.20 | 1.40 |
| 4 | 0.05 | 0.00 | 0.00 | 0.00 | 0.00 | 0.00 | 0.00 | 0.00 | 0.00 | 40 | 1.52 | 0.49 | 0.17 | 0.44 | 1.23 | 1.02 | 1.70 | 2.27 | 1.44 |
| 5 | 0.06 | 0.00 | 0.00 | 0.00 | 0.00 | 0.00 | 0.00 | 0.00 | 0.00 | 41 | 1.67 | 0.50 | 0.19 | 0.45 | 1.28 | 1.06 | 1.81 | 2.34 | 1.47 |
| 6 | 0.06 | 0.00 | 0.00 | 0.00 | 0.00 | 0.00 | 0.00 | 0.00 | 0.00 | 42 | 1.83 | 0.51 | 0.22 | 0.46 | 1.33 | 1.11 | 1.91 | 2.40 | 1.51 |
| 7 | 0.07 | 0.00 | 0.00 | 0.00 | 0.00 | 0.00 | 0.00 | 0.00 | 0.00 | 43 | 2.01 | 0.52 | 0.25 | 0.46 | 1.38 | 1.15 | 1.99 | 2.46 | 1.56 |
| 8 | 0.08 | 0.00 | 0.00 | 0.00 | 0.00 | 0.01 | 0.00 | 0.00 | 0.00 | 44 | 2.21 | 0.52 | 0.28 | 0.47 | 1.43 | 1.19 | 2.06 | 2.53 | 1.62 |
| 9 | 0.08 | 0.00 | 0.00 | 0.00 | 0.01 | 0.01 | 0.00 | 0.00 | 0.00 | 45 | 2.42 | 0.53 | 0.31 | 0.47 | 1.49 | 1.24 | 2.11 | 2.59 | 1.70 |
| 10 | 0.09 | 0.00 | 0.00 | 0.00 | 0.01 | 0.01 | 0.00 | 0.00 | 0.01 | 46 | 2.66 | 0.53 | 0.35 | 0.47 | 1.56 | 1.29 | 2.16 | 2.67 | 1.81 |
| 11 | 0.10 | 0.00 | 0.00 | 0.00 | 0.01 | 0.02 | 0.00 | 0.00 | 0.01 | 47 | 2.92 | 0.54 | 0.39 | 0.48 | 1.65 | 1.36 | 2.20 | 2.77 | 1.93 |
| 12 | 0.11 | 0.01 | 0.00 | 0.01 | 0.02 | 0.02 | 0.00 | 0.00 | 0.02 | 48 | 3.21 | 0.55 | 0.43 | 0.48 | 1.75 | 1.44 | 2.25 | 2.87 | 2.08 |
| 13 | 0.12 | 0.02 | 0.00 | 0.02 | 0.02 | 0.03 | 0.00 | 0.00 | 0.03 | 49 | 3.52 | 0.55 | 0.47 | 0.49 | 1.87 | 1.54 | 2.31 | 2.99 | 2.25 |
| 14 | 0.13 | 0.04 | 0.00 | 0.03 | 0.03 | 0.04 | 0.00 | 0.00 | 0.05 | 50 | 3.86 | 0.57 | 0.50 | 0.51 | 2.01 | 1.66 | 2.40 | 3.11 | 2.43 |
| 15 | 0.15 | 0.06 | 0.00 | 0.05 | 0.04 | 0.05 | 0.00 | 0.01 | 0.07 | 51 | 4.24 | 0.59 | 0.53 | 0.53 | 2.17 | 1.81 | 2.52 | 3.23 | 2.63 |
| 16 | 0.16 | 0.07 | 0.00 | 0.07 | 0.05 | 0.06 | 0.00 | 0.03 | 0.09 | 52 | 4.66 | 0.62 | 0.56 | 0.57 | 2.34 | 1.99 | 2.66 | 3.34 | 2.83 |
| 17 | 0.18 | 0.09 | 0.00 | 0.08 | 0.06 | 0.07 | 0.00 | 0.05 | 0.12 | 53 | 5.11 | 0.66 | 0.57 | 0.61 | 2.52 | 2.18 | 2.79 | 3.42 | 3.03 |
| 18 | 0.20 | 0.11 | 0.00 | 0.10 | 0.08 | 0.09 | 0.01 | 0.07 | 0.15 | 54 | 5.61 | 0.72 | 0.59 | 0.68 | 2.70 | 2.38 | 2.92 | 3.47 | 3.21 |
| 19 | 0.21 | 0.13 | 0.00 | 0.12 | 0.11 | 0.10 | 0.03 | 0.11 | 0.20 | 55 | 6.16 | 0.80 | 0.59 | 0.76 | 2.88 | 2.58 | 3.04 | 3.48 | 3.37 |
| 20 | 0.24 | 0.15 | 0.00 | 0.14 | 0.13 | 0.12 | 0.05 | 0.16 | 0.24 | 56 | 6.76 | 0.90 | 0.60 | 0.87 | 3.05 | 2.79 | 3.13 | 3.44 | 3.51 |
| 21 | 0.26 | 0.16 | 0.01 | 0.15 | 0.17 | 0.15 | 0.08 | 0.21 | 0.30 | 57 | 7.42 | 1.02 | 0.60 | 1.00 | 3.21 | 2.99 | 3.18 | 3.37 | 3.62 |
| 22 | 0.28 | 0.18 | 0.01 | 0.17 | 0.21 | 0.17 | 0.11 | 0.28 | 0.36 | 58 | 8.15 | 1.17 | 0.62 | 1.16 | 3.35 | 3.18 | 3.15 | 3.25 | 3.69 |
| 23 | 0.31 | 0.20 | 0.01 | 0.18 | 0.25 | 0.20 | 0.16 | 0.36 | 0.42 | 59 | 8.94 | 1.34 | 0.65 | 1.34 | 3.47 | 3.35 | 3.07 | 3.07 | 3.71 |
| 24 | 0.34 | 0.21 | 0.01 | 0.20 | 0.29 | 0.23 | 0.21 | 0.44 | 0.48 | 60 | 9.82 | 1.54 | 0.70 | 1.55 | 3.55 | 3.49 | 2.96 | 2.85 | 3.70 |
| 25 | 0.38 | 0.23 | 0.02 | 0.21 | 0.34 | 0.27 | 0.26 | 0.53 | 0.55 | 61 | 10.78 | 1.77 | 0.77 | 1.78 | 3.60 | 3.62 | 2.87 | 2.60 | 3.64 |

| Channel Number | Lower diameter (µm) | 240626 | 240814 | 240830 | 241022 | 241031 | 241109 | 241119 | 241214 |
|---|---|---|---|---|---|---|---|---|---|
| | | Differential volume (%) | | | | | | | |
| 26 | 0.41 | 0.25 | 0.02 | 0.23 | 0.39 | 0.30 | 0.32 | 0.64 | 0.62 |
| 27 | 0.45 | 0.27 | 0.03 | 0.25 | 0.45 | 0.34 | 0.39 | 0.75 | 0.69 |
| 28 | 0.50 | 0.29 | 0.03 | 0.27 | 0.50 | 0.38 | 0.47 | 0.87 | 0.77 |
| 29 | 0.55 | 0.31 | 0.04 | 0.28 | 0.57 | 0.43 | 0.54 | 0.99 | 0.84 |
| 30 | 0.60 | 0.32 | 0.05 | 0.30 | 0.63 | 0.48 | 0.63 | 1.12 | 0.91 |
| 31 | 0.66 | 0.34 | 0.06 | 0.32 | 0.69 | 0.53 | 0.72 | 1.25 | 0.99 |
| 32 | 0.72 | 0.36 | 0.07 | 0.33 | 0.76 | 0.58 | 0.81 | 1.39 | 1.06 |
| 33 | 0.79 | 0.38 | 0.08 | 0.35 | 0.82 | 0.64 | 0.91 | 1.52 | 1.12 |
| 34 | 0.87 | 0.40 | 0.09 | 0.37 | 0.89 | 0.69 | 1.01 | 1.66 | 1.18 |
| 35 | 0.95 | 0.41 | 0.10 | 0.38 | 0.95 | 0.75 | 1.12 | 1.78 | 1.24 |
| 36 | 1.05 | 0.43 | 0.11 | 0.40 | 1.01 | 0.81 | 1.24 | 1.90 | 1.29 |
| 62 | 11.83 | 2.03 | 0.86 | 2.04 | 3.63 | 3.75 | 2.84 | 2.36 | 3.54 |
| 63 | 12.99 | 2.31 | 0.97 | 2.32 | 3.63 | 3.85 | 2.83 | 2.16 | 3.41 |
| 64 | 14.26 | 2.61 | 1.09 | 2.61 | 3.57 | 3.87 | 2.78 | 1.99 | 3.24 |
| 65 | 15.65 | 2.93 | 1.23 | 2.92 | 3.41 | 3.75 | 2.62 | 1.80 | 3.06 |
| 66 | 17.18 | 3.27 | 1.38 | 3.23 | 3.14 | 3.49 | 2.33 | 1.55 | 2.84 |
| 67 | 18.86 | 3.62 | 1.54 | 3.56 | 2.78 | 3.15 | 1.98 | 1.23 | 2.57 |
| 68 | 20.71 | 3.98 | 1.72 | 3.87 | 2.40 | 2.81 | 1.68 | 0.86 | 2.22 |
| 69 | 22.73 | 4.33 | 1.93 | 4.17 | 2.09 | 2.57 | 1.51 | 0.52 | 1.78 |
| 70 | 24.95 | 4.65 | 2.17 | 4.43 | 1.87 | 2.42 | 1.50 | 0.28 | 1.29 |
| 71 | 27.39 | 4.93 | 2.44 | 4.64 | 1.73 | 2.33 | 1.59 | 0.15 | 0.80 |
| 72 | 30.07 | 5.12 | 2.73 | 4.78 | 1.62 | 2.22 | 1.70 | 0.07 | 0.41 |

## Table J.12 Extended PSD Data from External Lab – Beatrice North (Part 3 of 3)

| Channel Number | Lower diameter (µm) | 250306 | 250320 | 250402 | 250404 | 250520 | 250527 | 250602 | 250604 | Channel Number | Lower diameter (µm) | 250306 | 250320 | 250402 | 250404 | 250520 | 250527 | 250602 | 250604 |
|---|---|---|---|---|---|---|---|---|---|---|---|---|---|---|---|---|---|---|---|
| | | Differential volume (%) | | | | | | | | | | Differential volume (%) | | | | | | | |
| 1 | 0.04 | 0.00 | 0.00 | 0.00 | 0.00 | 0.00 | 0.00 | 0.00 | 0.00 | 37 | 1.15 | 0.00 | 0.00 | 0.00 | 0.00 | 0.00 | 0.00 | 0.00 | 0.00 |
| 2 | 0.04 | 0.00 | 0.00 | 0.00 | 0.00 | 0.00 | 0.00 | 0.00 | 0.00 | 38 | 1.26 | 0.00 | 0.00 | 0.00 | 0.00 | 0.00 | 0.00 | 0.00 | 0.00 |
| 3 | 0.05 | 0.00 | 0.00 | 0.00 | 0.00 | 0.00 | 0.00 | 0.00 | 0.00 | 39 | 1.39 | 0.00 | 0.00 | 0.00 | 0.00 | 0.00 | 0.00 | 0.00 | 0.00 |
| 4 | 0.05 | 0.00 | 0.00 | 0.01 | 0.00 | 0.01 | 0.00 | 0.00 | 0.01 | 40 | 1.52 | 0.00 | 0.00 | 0.01 | 0.00 | 0.01 | 0.00 | 0.00 | 0.01 |
| 5 | 0.06 | 0.00 | 0.00 | 0.01 | 0.00 | 0.02 | 0.00 | 0.00 | 0.02 | 41 | 1.67 | 0.00 | 0.00 | 0.01 | 0.00 | 0.02 | 0.00 | 0.00 | 0.02 |
| 6 | 0.06 | 0.00 | 0.00 | 0.03 | 0.00 | 0.03 | 0.00 | 0.00 | 0.03 | 42 | 1.83 | 0.00 | 0.00 | 0.03 | 0.00 | 0.03 | 0.00 | 0.00 | 0.03 |
| 7 | 0.07 | 0.00 | 0.00 | 0.04 | 0.00 | 0.05 | 0.00 | 0.00 | 0.05 | 43 | 2.01 | 0.00 | 0.00 | 0.04 | 0.00 | 0.05 | 0.00 | 0.00 | 0.05 |
| 8 | 0.08 | 0.00 | 0.00 | 0.05 | 0.00 | 0.07 | 0.00 | 0.00 | 0.06 | 44 | 2.21 | 0.00 | 0.00 | 0.05 | 0.00 | 0.07 | 0.00 | 0.00 | 0.06 |
| 9 | 0.08 | 0.00 | 0.00 | 0.07 | 0.00 | 0.09 | 0.00 | 0.01 | 0.08 | 45 | 2.42 | 0.00 | 0.00 | 0.07 | 0.00 | 0.09 | 0.00 | 0.01 | 0.08 |
| 10 | 0.09 | 0.00 | 0.00 | 0.08 | 0.00 | 0.10 | 0.00 | 0.01 | 0.10 | 46 | 2.66 | 0.00 | 0.00 | 0.08 | 0.00 | 0.10 | 0.00 | 0.01 | 0.10 |
| 11 | 0.10 | 0.00 | 0.00 | 0.10 | 0.00 | 0.12 | 0.00 | 0.02 | 0.12 | 47 | 2.92 | 0.00 | 0.00 | 0.10 | 0.00 | 0.12 | 0.00 | 0.02 | 0.12 |
| 12 | 0.11 | 0.00 | 0.00 | 0.11 | 0.00 | 0.14 | 0.00 | 0.03 | 0.14 | 48 | 3.21 | 0.00 | 0.00 | 0.11 | 0.00 | 0.14 | 0.00 | 0.03 | 0.14 |
| 13 | 0.12 | 0.00 | 0.00 | 0.13 | 0.00 | 0.16 | 0.00 | 0.04 | 0.16 | 49 | 3.52 | 0.00 | 0.00 | 0.13 | 0.00 | 0.16 | 0.00 | 0.04 | 0.16 |
| 14 | 0.13 | 0.01 | 0.01 | 0.15 | 0.00 | 0.17 | 0.01 | 0.05 | 0.18 | 50 | 3.86 | 0.01 | 0.01 | 0.15 | 0.00 | 0.17 | 0.01 | 0.05 | 0.18 |
| 15 | 0.15 | 0.02 | 0.02 | 0.16 | 0.00 | 0.19 | 0.01 | 0.07 | 0.20 | 51 | 4.24 | 0.02 | 0.02 | 0.16 | 0.00 | 0.19 | 0.01 | 0.07 | 0.20 |
| 16 | 0.16 | 0.04 | 0.04 | 0.18 | 0.01 | 0.21 | 0.02 | 0.09 | 0.23 | 52 | 4.66 | 0.04 | 0.04 | 0.18 | 0.01 | 0.21 | 0.02 | 0.09 | 0.23 |
| 17 | 0.18 | 0.06 | 0.06 | 0.20 | 0.02 | 0.23 | 0.03 | 0.12 | 0.25 | 53 | 5.11 | 0.06 | 0.06 | 0.20 | 0.02 | 0.23 | 0.03 | 0.12 | 0.25 |
| 18 | 0.20 | 0.08 | 0.08 | 0.22 | 0.04 | 0.24 | 0.04 | 0.15 | 0.28 | 54 | 5.61 | 0.08 | 0.08 | 0.22 | 0.04 | 0.24 | 0.04 | 0.15 | 0.28 |
| 19 | 0.21 | 0.11 | 0.12 | 0.24 | 0.07 | 0.26 | 0.06 | 0.18 | 0.31 | 55 | 6.16 | 0.11 | 0.12 | 0.24 | 0.07 | 0.26 | 0.06 | 0.18 | 0.31 |
| 20 | 0.24 | 0.15 | 0.16 | 0.27 | 0.11 | 0.29 | 0.08 | 0.22 | 0.34 | 56 | 6.76 | 0.15 | 0.16 | 0.27 | 0.11 | 0.29 | 0.08 | 0.22 | 0.34 |
| 21 | 0.26 | 0.20 | 0.21 | 0.29 | 0.16 | 0.31 | 0.10 | 0.27 | 0.38 | 57 | 7.42 | 0.20 | 0.21 | 0.29 | 0.16 | 0.31 | 0.10 | 0.27 | 0.38 |
| 22 | 0.28 | 0.26 | 0.26 | 0.32 | 0.23 | 0.33 | 0.13 | 0.32 | 0.41 | 58 | 8.15 | 0.26 | 0.26 | 0.32 | 0.23 | 0.33 | 0.13 | 0.32 | 0.41 |
| 23 | 0.31 | 0.32 | 0.33 | 0.35 | 0.29 | 0.35 | 0.16 | 0.37 | 0.45 | 59 | 8.94 | 0.32 | 0.33 | 0.35 | 0.29 | 0.35 | 0.16 | 0.37 | 0.45 |
| 24 | 0.34 | 0.39 | 0.40 | 0.37 | 0.37 | 0.37 | 0.20 | 0.43 | 0.48 | 60 | 9.82 | 0.39 | 0.40 | 0.37 | 0.37 | 0.37 | 0.20 | 0.43 | 0.48 |
| 25 | 0.38 | 0.46 | 0.47 | 0.40 | 0.46 | 0.39 | 0.24 | 0.49 | 0.52 | 61 | 10.78 | 0.46 | 0.47 | 0.40 | 0.46 | 0.39 | 0.24 | 0.49 | 0.52 |

| Channel Number | Lower diameter (µm) | 250306 | 250320 | 250402 | 250404 | 250520 | 250527 | 250602 | 250604 | Channel Number | Lower diameter (µm) | 250306 | 250320 | 250402 | 250404 | 250520 | 250527 | 250602 | 250604 |
|---|---|---|---|---|---|---|---|---|---|---|---|---|---|---|---|---|---|---|---|
| | | Differential volume (%) | | | | | | | | | | Differential volume (%) | | | | | | | |
| 26 | 0.41 | 0.55 | 0.55 | 0.43 | 0.55 | 0.42 | 0.27 | 0.55 | 0.55 | 62 | 11.83 | 0.55 | 0.55 | 0.43 | 0.55 | 0.42 | 0.27 | 0.55 | 0.55 |
| 27 | 0.45 | 0.63 | 0.64 | 0.46 | 0.65 | 0.44 | 0.32 | 0.62 | 0.59 | 63 | 12.99 | 0.63 | 0.64 | 0.46 | 0.65 | 0.44 | 0.32 | 0.62 | 0.59 |
| 28 | 0.50 | 0.73 | 0.73 | 0.50 | 0.75 | 0.46 | 0.36 | 0.69 | 0.62 | 64 | 14.26 | 0.73 | 0.73 | 0.50 | 0.75 | 0.46 | 0.36 | 0.69 | 0.62 |
| 29 | 0.55 | 0.83 | 0.83 | 0.53 | 0.86 | 0.48 | 0.41 | 0.76 | 0.66 | 65 | 15.65 | 0.83 | 0.83 | 0.53 | 0.86 | 0.48 | 0.41 | 0.76 | 0.66 |
| 30 | 0.60 | 0.94 | 0.93 | 0.56 | 0.97 | 0.50 | 0.46 | 0.84 | 0.69 | 66 | 17.18 | 0.94 | 0.93 | 0.56 | 0.97 | 0.50 | 0.46 | 0.84 | 0.69 |
| 31 | 0.66 | 1.05 | 1.03 | 0.59 | 1.08 | 0.53 | 0.51 | 0.92 | 0.73 | 67 | 18.86 | 1.05 | 1.03 | 0.59 | 1.08 | 0.53 | 0.51 | 0.92 | 0.73 |
| 32 | 0.72 | 1.16 | 1.13 | 0.63 | 1.19 | 0.55 | 0.56 | 1.00 | 0.76 | 68 | 20.71 | 1.16 | 1.13 | 0.63 | 1.19 | 0.55 | 0.56 | 1.00 | 0.76 |
| 33 | 0.79 | 1.27 | 1.23 | 0.66 | 1.31 | 0.57 | 0.61 | 1.07 | 0.79 | 69 | 22.73 | 1.27 | 1.23 | 0.66 | 1.31 | 0.57 | 0.61 | 1.07 | 0.79 |
| 34 | 0.87 | 1.39 | 1.34 | 0.69 | 1.41 | 0.59 | 0.66 | 1.15 | 0.81 | 70 | 24.95 | 1.39 | 1.34 | 0.69 | 1.41 | 0.59 | 0.66 | 1.15 | 0.81 |
| 35 | 0.95 | 1.51 | 1.43 | 0.72 | 1.52 | 0.61 | 0.72 | 1.23 | 0.84 | 71 | 27.39 | 1.51 | 1.43 | 0.72 | 1.52 | 0.61 | 0.72 | 1.23 | 0.84 |
| 36 | 1.05 | 1.62 | 1.53 | 0.75 | 1.62 | 0.63 | 0.77 | 1.31 | 0.86 | 72 | 30.07 | 1.62 | 1.53 | 0.75 | 1.62 | 0.63 | 0.77 | 1.31 | 0.86 |

### Laser diffraction analysis of PSD in duplicate samples

Some duplicate samples were re-tested for particle size distribution (PSD) using the laser diffraction method after different storage durations. A total of six samples from four sites were analyzed, as shown in Table J.13. Among them, four were collected in 2024 and two in 2025. The older tests were conducted a few weeks after collection, while all newer tests were done on 10/3/2025. This means the 2024 samples were stored for over a year, and the 2025 samples for about five months. Results showed that the proportion of fine particles increased notably in samples stored for more than a year, while the change was minor in those stored for about five months. The data suggest that samples should ideally be tested within five months of storage.

Table J.13 Comparison of PSD in duplicate samples by Laser diffraction (<32µm)

| Particle size (µm) | BS-240814 | | BS-250425 | | BTN-240626 | | BTN-250520 | | BTW-240524 | | CH-240524 | |
|---|---|---|---|---|---|---|---|---|---|---|---|---|
| | TSS<br>Coarse<br>Fine | 341<br>300<br>41 | TSS<br>Coarse<br>Fine | 1111<br>489<br>622 | TSS<br>Coarse<br>Fine | 881<br>342<br>539 | TSS<br>Coarse<br>Fine | 1125<br>60<br>1065 | TSS<br>Coarse<br>Fine | 157<br>70<br>87 | TSS<br>Coarse<br>Fine | 317<br>153<br>164 |
| | Old | New | Old | New | Old | New | Old | New | Old | New | Old | New |
| | Percent finer (%) | | | | | | | | | | | |
| 32 | 12 | 12 | 56 | 56 | 61 | 61 | 68 | 68 | 55 | 55 | 52 | 52 |
| 15.7 | 6 | 5 | 36 | 36 | 30 | 50 | 51 | 52 | 30 | 42 | 24 | 36 |
| 8.1 | 4 | 2 | 20 | 19 | 17 | 31 | 31 | 31 | 16 | 29 | 14 | 22 |
| 4.2 | 2 | 2 | 11 | 10 | 12 | 18 | 17 | 17 | 9 | 18 | 9 | 12 |
| 2.0 | 2 | 1 | 6 | 6 | 8 | 10 | 10 | 10 | 4 | 10 | 5 | 7 |
| 1.0 | 1 | 1 | 3 | 4 | 5 | 6 | 7 | 7 | 2 | 5 | 3 | 4 |
| Remarks | Small difference | | Small difference | | Significant difference | | Small difference | | Significant difference | | Significant difference | |

## Appendix K TSS and PSD estimation and SAFL Baffle selection

**Example K.1:** A short section (300 ft) of a busy concrete-paved highway, approximately 45 feet wide, drains laterally into a 3-ft-wide swale with dense vegetative cover. The contributing catchment has a gentle slope of less than 1% and shows no visible sources of erosion.

- Total area (ac): 48 ft x 300 ft (assumed length) = 0.33 ac
- Impervious area (ac): 45 ft x 300 ft = 0.31 ac
- Impervious %: 45 ft/ 48 ft *100 = 93.7 %
- Impervious area within right-of-way (ac): 0.31 ac
- Hydraulic length (ft): 345 ft (45 ft across roadway and 300 ft long swale)
- Average slope (%): 1%
- CN pervious surface: 75 (using NRCS method)

**TSS prediction:**

Based on the characteristics of the catchment, 1% slope, and majority of flow passes through the swale, TSS is predicted to be 220 – 30 – 60 = 130 mg/L.

The TSS of area within right-of-way = 130 mg/L (Same because all the area is within right-of-way)

**PSD prediction:**

For PSD, the average between the Winston PSD and Beatrice West PSD is selected because the majority of the catchment is roadway and passes through a swale.

Table K.1 PSD used for the SHSAM analysis

| **Size (µm)** | **Winston PSD** | **BTW PSD** | **Average of both (Selected PSD)** |
|---|---|---|---|
| 1000 | 100 | 100 | 100 |
| 250 | 95 | 86 | 90.5 |
| 125 | 85 | 75 | 80 |
| 32 | 30 | 47 | 38.5 |
| 8 | 10 | 17 | 13.5 |
| 0 | 0 | 0 | 0 |

*Value should be rounded down to zero decimals while using in SHSAM.

Table K.2 Results of SHSAM analysis

| **Model** | **Removal Efficiency (%)** |
|---|---|
| 42 | 43.9 |
| 44 | 52.2 |
| 55 | 62.2 |
| 63 | 66.1 |
| 66 | 74.5 |
| 86 | 82.8 |
| 106 | 88.1 |

Calculating the left hand side of Equation 5.1:

$$0.8\,.\frac{Area_{road}}{Area_{catchment}}.\frac{TSS_{road}}{TSS_{catchment}}$$

= 0.8 * (0.33/0.33) * (130/130) = 80%

The minimum removal efficiency needed to meet the permit requirements is 80%, so Model 86 with removal efficiency of 82.8 % is selected.

**Example K.2:** A 10-acre catchment includes approximately three acres of concrete-paved roadway within the ROW. Offsite areas consist of about one acre of gravel parking, 0.5 acres of rooftop coverage, and the remaining area is covered with well-maintained turfgrass. The average slope is around 2%, and the total flow path length is approximately 1,200 feet.

- Total area (ac): 10 ac
- Impervious area (ac): 3 ac of roadway + 1 ac of gravel parking + 0.5 acre of roof = 4.5 ac
- Impervious %: 4.5/10 * 100% = 45%
- Impervious area within right-of-way (ac): 3 ac
- Hydraulic length (ft): 1200 ft
- Average slope (%): 3%
- CN pervious surface: 75 (using NRCS method)

**TSS prediction (Refer to Table 6.1 and Figure 6.1)**

The base value of TSS is 220 mg/L. Two percent roadway slope will add coarse concentration which is calculated as: (2% - 1%)/(3% - 1%) * 250 mg/L = 125 mg/L. The presence of a gravel parking lot will increase coarse TSS by 30 mg/L and 280 mg/L. The estimated TSS from the catchment is: 220 + 125 + 30 + 280 = 655 mg/L

TSS of the roadway (within the ROW) = 220 + 125 = 345 mg/L. Here, gravel parking does not contribute to TSS as it is located outside the ROW.

**PSD prediction (Refer to Table 6.2 and Figure 6.1)**

We can see two site factors that affect the sediment runoff PSD. One is steep slope and the other is the presence of a gravel parking lot.

Table K.3 PSD used for the SHSAM analysis

| **Size (µm)** | **Beal Slough PSD** | **Beatrice North PSD** | **Average of both (Selected PSD)** |
|---|---|---|---|
| 1000 | 100 | 100 | 100 |
| 250 | 46 | 92 | 69 |
| 125 | 30 | 85 | 58 |
| 32 | 17 | 78 | 47 |
| 8 | 6 | 29 | 17 |
| 0 | 0 | 0 | 0 |

Table K.4 Results of SHSAM analysis

| **Model** | **Removal Efficiency (%)** |
|---|---|
| 42 | 9.2 |
| 44 | 16.8 |
| 55 | 24.8 |
| 63 | 27.2 |
| 66 | 33.9 |
| 86 | 40.8 |
| 106 | 46.3 |

Calculating left hand side of Equation 5.1:

$$0.8\,.\frac{Area_{road}}{Area_{catchment}}.\frac{TSS_{road}}{TSS_{catchment}}$$

= 0.8 * (3/10) * (345/655) = 12.6 %

The minimum removal efficiency needed to meet the permit requirements is 12.6%, so Model 44 with a removal efficiency of 16.8 % is selected.

# Appendix L Use of Charts to Estimate Required Removal and SAFL Baffle Efficiency

Note: These figures are limited in scope, offering only a narrow range of selectable values. They are created primarily to check sensitivity of certain site characteristics.

The following example shows how to use these charts for the Beatrice West site with the given characteristics:

- Area: 39.8 ac
- Impervious area: 34.23% of 39.8 ac = 13.6 ac
- Hydraulic length: 4388 ft
- Average slope of catchment: 0.75%
- Assuming Case 2 of ROW, Impervious area within ROW: 6.69 ac
- TSS of the catchment: 157 mg/L
- TSS of the roadway: 70 mg/L (Assuming Winston et al., 2023 data)
- $TSS_{road}/TSS_{catch}$: 70 mg/L / 157 mg/L = 0.45

**Estimating removal requirements using charts:**

Figure 6.3 has a $TSS_{road}/TSS_{catch} = 0.5$, which is closer to 0.45 as calculated above. The impervious area of the whole catchment is 13.6 ac and the impervious area within the ROW is 6.69 ac. The red dot in the chart shows the estimated removal requirement which is 23%. Using Equation 5.1 to calculate this value yields 18%, highlighting that the result is a rough estimate and should only be used to understand the sensitivity of required removal to certain variables.

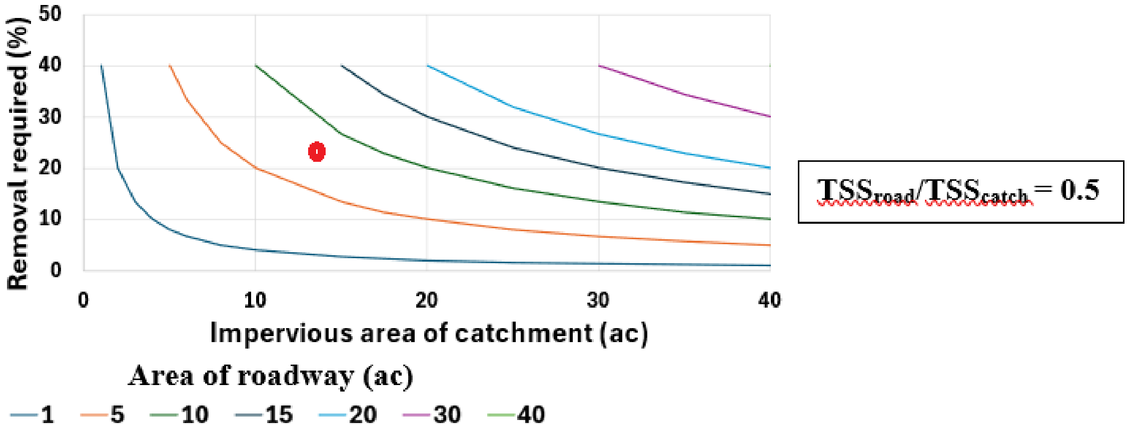

Figure L.1 The selected chart from Figure 6.3 (red marking indicates position used for this calculation)

**Estimating SAFL removal requirements using charts:**

The chart is made from the first row and first column in Figure 6.5 based on the following variables:

- PSD: Beatrice West PSD
- Impervious %: 34%
- √S/L: √(0.75%)/0.83miles = 1.04

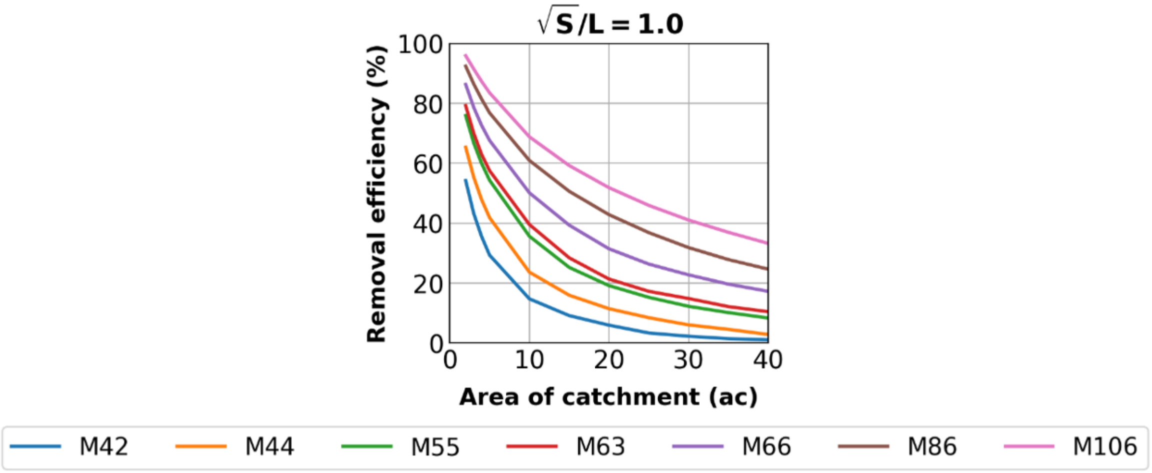

Figure L.2 The selected chart from Figure 6.5 for this calculation

The removal efficiency of SAFL Baffle is estimated using 39.8 ac.

## Appendix M List of equipment and supplies for sample collection and analysis

This appendix provides a detailed list of items, their quantities, and their purposes related to site setup, automatic sampling equipment, sample collection, laboratory methods, and shipping samples to an external lab for extended particle size distribution (PSD) analysis.

Table M.1 Equipment and supplies to establish a site

| Item name | Quantity | Purpose |
|---|---|---|
| Manhole opener | 1 | To access manhole and culvert |
| Flashlight | 1 | To access manhole and culvert |
| Safety glasses | 1 per person | For safety |
| Measuring tape | 1 | To measure layout for installation |
| Spray paint | 1 | To mark the layout for padding |
| Post hole digger | 1 | To dig a trench or pit |
| Shovel | 1 | To dig a trench or pit |
| Marking flags | Few | To mark layout or concrete padding |
| Core drill machine and bit | 1 | To drill holes on manhole or pipe |
| 4 in PVC and joints | Depends on site | To route sampling line and sensor cable |
| Reciprocating saw | 1 | To cut PVC pipe |
| Materials to build a concrete pad | (Usually taken care of by NDOT) | To hold enclosure |
| Ropes (longer than 10 ft) | Few | To phish sampling line and sensor cable |
| Hammar drill and accessories | 1 | To drill pilot holes in the concrete |
| Nut driver/screwdriver and accessories | 1 | To drill drive Tapcon screws |
| Tapcon screws 3/16 in | Many | To secure clamps and enclosure |
| Flat washer for screws | Few | To secure Tapcon screws |
| Rubber clamps | Many | To hold cable and sampling line |
| Components for Enclosure assembly | 1 set | To secure sampling equipment |
| Locks and keys | 1 | To protect enclosure contents |
| Hole saw (4 in) and accessories | 1 | To make a hole at the bottom of enclosure |

Table M.2 Equipment required for automatic sampling

| Item name | Quantity | Purpose |
|---|---|---|
| Enclosure | 1 per site | To secure monitoring station |
| ISCO automatic sample (6712 or 3700) | 1 per site | To collect water sample |
| ISCO AV flow module (750 or 2150) | 1 per site | To monitor flow |
| Flow meter sensor cable | 1 per site | To monitor flow |
| 12V deep cycle battery | 1 per site | To power automatic sampler |
| Mounting plate with 2 screws for sensor | 1 per site | To anchor sensor to the bottom of the culvert |
| Sampling carboy (10 L) | 1 per site | To collect water sample |
| Sampling line with strainer | 20 to 40 ft | To collect water sample |
| Manhole opener | 1 per site | To inspect inside manhole |
| Insulation foam board (2 in thick) | Enough to insulate top and vertical panels | Insulation during cold weather |
| Hose clamps | 2 per site | To secure sampling line |
| Pump tubes (different for each sampler typ) | 1 or 2 per site | To replace existing pump tubes |

Table M.3 Equipment required for sample collection

| Item name | Quantity | Purpose |
|---|---|---|
| Key to the enclosure | 1 | Open the enclosure |
| 2.5-gallon (9.4 L) carboys | 4 | For next samples |
| Laptop with Flowlink | 1 | Download data from sampler |
| USB communication cable for 2150 flow module | 1 | Connect laptop to flowmeter |
| USB communication cable for 750 flow module | 1 | Connect laptop to flowmeter |
| 12 V Battery | 2 | Replace the older battery |
| Voltmeter | 1 | Measure voltage of batteries |
| SOP to use sampler | 1 | Operate the sampler |
| Paper tape and Sharpie | 1 | Mark sample bottles |

Table M.4 Equipment and supplies required for laboratory analysis

| Item name | Quantity | Purpose |
|---|---|---|
| Clean sieves of sizes (500 µm, 250 µm, 125 µm, 63 µm and 37 µm) and 8-in diameter | 1 each | Wet sieving |
| 3000-µm sieve of 8 in diameter | 1 | Separate trash and larger particles |
| Taller Sieve Stand (PVC-made) | 1 | To hold sieve above water level |
| DI water or clean water source | | Wash the sediments off the sieve |
| Wash bottle | 1 | Wash the sediments off the sieve |
| Soft brush | 1 | To dislodge sand from bottom |
| Clean bucket | 1 | Hold sample and filtrate from sieving |
| Aluminum pans | 10 per sample | Hold drying materials |
| Water bath | 1 | Heat source for evaporation |
| 105°C Drying oven | 1 | Heat source for drying |
| Desiccator | 1 | Cool off the dried sample |
| Laboratory balance (0.1 mg) | 1 | Measure weights |
| Teflon churn splitter | 1 | Divide the sample |
| Filtration apparatus | 1 | For the filtration process |
| Vacuum pump | 1 | For the filtration process |
| Pipette | 1 | For the filtration process |
| Filter papers | 3 per sample | For the filtration process |
| Plastic bottle (250 ml and 500 ml) | 1 each per sample | To preserve fine sample |
| Tape and Sharpie | 1 each per sample | To label samples |
| Scrub and soap | 1 each | To clean dishes |

Table M.5 Supplies required for shipping extended samples for PSD

| Item name | Quantity | Purpose |
|---|---|---|
| Plastic sample bottles - 250ml | 1 per sample | To contain sample in liquid form |
| Cooler | 1 per batch | To keep samples, cool while shipping |
| Ice packs | Depends on the size of cooler | |
| Cardboard box - Cooler should fit inside | 1 per batch | For shipping |
| Packaging tape | 1 | To seal the package |
| Printed sample analysis request form | 1 | Sample identification |
| Weighing machine (optional) | 1 | To estimate package weight |

## Appendix N Information for submitting samples to External lab for Particle size distribution analysis

This appendix information can be useful in the future to help send samples to external labs for particle size distribution analysis of fine fraction of samples (< 32 µm).

### 1. External laboratory information:

- Lab Name: Independent Particle Labs
- Address: 4699 Pigeon Run Ave SW Laboratory B Navarre, OH 44662
- Email address: info@iparticlelabs.com
- Website: https://www.iparticlelabs.com/
- Analysis method: Laser diffraction method using Beckman Coulter LS13320 MW

### 2. Supplies and materials needed:

Table N.1 Supplies and materials required for sending samples

| Item name | Quantity | Purpose |
|---|---|---|
| Plastic sample bottles - 250ml | 1 per sample | To contain sample in liquid form |
| Cooler | 1 per batch | To keep samples, cool while shipping |
| Ice packs | Depending on the size of cooler | |
| Cardboard box - Cooler should fit inside | 1 per batch | For shipping |
| Packaging tape | 1 | To seal the package |
| Printed sample analysis request form | 1 | Sample identification |
| Weighing machine (optional) | 1 | To estimate package weight |

### 3. Sample preparation and holding time

Sample preparation involved taking an aliquot of the fine fraction during laboratory analysis and transferring approximately 200 to 250 mL into a 250 mL plastic container labeled with the sample name. The sample was then stored in a refrigerator to preserve its condition. The maximum recommended holding time for extended PSD analysis was six months from the date of preparation.

### 4. Sample packaging and shipping

For each batch, typically 6 to 16 samples were prepared for shipment. Based on cooling needs, a few ice packs were placed inside an insulated cooler. The external lab was contacted in advance to confirm sample acceptance and scheduling.

A sample analysis request form was completed and emailed to the lab, and a printed copy was included inside the package. A sturdy shipping box was prepared, and its approximate weight was estimated in pounds.

The package was shipped through FedEx, usually using overnight delivery. With assistance from the Civil and Environmental Engineering Department, a shipping label was generated, printed, and attached to the top of the box. Finally, the package was dropped off at the nearest FedEx drop-off location. The tracking ID was also shared with the external lab.

## Appendix O Street sweeping and regression analysis

This appendix provides dates of street sweeping done at Lincoln sites during monitoring period between March 2024 to June 2025. There was no street sweeping performed at the Beatrice sites.

Table O.1 Dates of street sweeping at Lincoln sites

| **Beal Slough** | **Cornhusker** |
|---|---|
| 3/7/2024 | 3/12/2024 |
| 4/10/2024 | 3/27/2024 |
| 5/7/2024 | 4/5/2024 |
| 7/9/2024 | 4/30/2024 |
| 7/25/2024 | 5/1/2024 |
| 8/20/2024 | 7/3/2024 |
| 9/9/2024 | 7/24/2024 |
| 9/24/2024 | 8/15/2024 |
| 10/14/2024 | 8/19/2024 |
| 11/6/2024 | 9/4/2024 |
| 12/27/2024 | 9/23/2024 |
| 4/3/2025 | 10/8/2024 |
| 5/14/2025 | 10/30/2024 |
|  | 12/19/2024 |
|  | 5/7/2025 |

The OLS method of linear regression was used for TSS, CSS (coarse part of TSS), and FSS (fine part of TSS) (Table O.2). Their log-transformed values were also tested. The results showed that the model explained only a small portion of the variation in the data. The in-sample $R^2$ values were 0.36, 0.26, and 0.28 for TSS, CSS, and FSS, respectively, showing weak relationships. The cross-validation $R^2$ values were negative for all except log-FSS (0.02), meaning the models did not perform well on new data. The variable "days since sweeping or rainfall" (**DSSR**) had small positive effects on TSS and FSS, suggesting that longer dry periods before a storm may slightly increase concentrations, although the relationship was not significant.

Table O.2 Results of regression analysis (Ordinary Least Squares)

<table>
<tr><th colspan="7">Beal Slough</th></tr>
<tr><th>Target variable</th><th>TSS</th><th>CSS</th><th>FSS</th><th>log_TSS</th><th>log_CSS</th><th>log_FSS</th></tr>
<tr><td>n</td><td>27</td><td>27</td><td>27</td><td>27</td><td>27</td><td>27</td></tr>
<tr><td>r2_in</td><td>0.36</td><td>0.26</td><td>0.28</td><td>0.31</td><td>0.20</td><td>0.56</td></tr>
<tr><td>rmse_in</td><td>186.58</td><td>126.14</td><td>114.96</td><td>0.22</td><td>0.22</td><td>0.28</td></tr>
<tr><td>mae_in</td><td>133.76</td><td>94.88</td><td>71.21</td><td>0.16</td><td>0.16</td><td>0.22</td></tr>
<tr><td>r2_cv</td><td>-0.32</td><td>-0.36</td><td>-4.75</td><td>-0.20</td><td>-0.59</td><td>0.02</td></tr>
<tr><td>rmse_cv</td><td>221.10</td><td>150.18</td><td>132.87</td><td>0.24</td><td>0.25</td><td>0.34</td></tr>
<tr><td>mae_cv</td><td>176.26</td><td>122.43</td><td>92.37</td><td>0.19</td><td>0.20</td><td>0.27</td></tr>
<tr><td>intercept</td><td>444.00</td><td>341.96</td><td>101.96</td><td>2.58</td><td>2.48</td><td>1.77</td></tr>
<tr><td>coef_Depth</td><td>9.23</td><td>-14.62</td><td>23.96</td><td>0.00</td><td>-0.02</td><td>0.07</td></tr>
<tr><td>coef_Intensity_20</td><td>-51.73</td><td>-18.21</td><td>-33.57</td><td>-0.02</td><td>0.00</td><td>-0.07</td></tr>
<tr><td>coef_DSSR</td><td>4.53</td><td>-13.85</td><td>18.46</td><td>-0.01</td><td>-0.03</td><td>0.08</td></tr>
<tr><td>coef_Week</td><td>-152.09</td><td>-74.98</td><td>-77.03</td><td>-0.15</td><td>-0.10</td><td>-0.34</td></tr>
<tr><th colspan="7">Cornhusker</th></tr>
<tr><th>Target variable</th><th>TSS</th><th>CSS</th><th>FSS</th><th>log_TSS</th><th>log_CSS</th><th>log_FSS</th></tr>
<tr><td>n</td><td>29</td><td>29</td><td>29</td><td>29</td><td>29</td><td>29</td></tr>
<tr><td>r2_in</td><td>0.37</td><td>0.36</td><td>0.41</td><td>0.34</td><td>0.37</td><td>0.34</td></tr>
<tr><td>rmse_in</td><td>352.76</td><td>123.16</td><td>254.19</td><td>0.29</td><td>0.29</td><td>0.37</td></tr>
<tr><td>mae_in</td><td>263.82</td><td>99.26</td><td>178.96</td><td>0.24</td><td>0.24</td><td>0.29</td></tr>
<tr><td>r2_cv</td><td>-7.59</td><td>-1.15</td><td>-7.58</td><td>-1.73</td><td>-0.44</td><td>-1.11</td></tr>
<tr><td>rmse_cv</td><td>406.62</td><td>144.97</td><td>294.46</td><td>0.35</td><td>0.35</td><td>0.45</td></tr>
<tr><td>mae_cv</td><td>312.12</td><td>120.81</td><td>217.35</td><td>0.30</td><td>0.29</td><td>0.37</td></tr>
<tr><td>intercept</td><td>472.76</td><td>194.79</td><td>277.93</td><td>2.53</td><td>2.15</td><td>2.22</td></tr>
<tr><td>coef_Depth</td><td>-200.30</td><td>-67.46</td><td>-132.77</td><td>-0.11</td><td>-0.07</td><td>-0.11</td></tr>
<tr><td>coef_Intensity_20</td><td>234.24</td><td>129.03</td><td>104.96</td><td>0.20</td><td>0.25</td><td>0.16</td></tr>
<tr><td>coef_DSSR</td><td>152.29</td><td>35.34</td><td>117.03</td><td>0.12</td><td>0.10</td><td>0.15</td></tr>
<tr><td>coef_Week</td><td>-182.45</td><td>-15.01</td><td>-167.49</td><td>-0.10</td><td>0.00</td><td>-0.20</td></tr>
</table>